

**Synthesis and Characterization of High Performance
Polybenzoxazoles**

by

William Dale Joseph

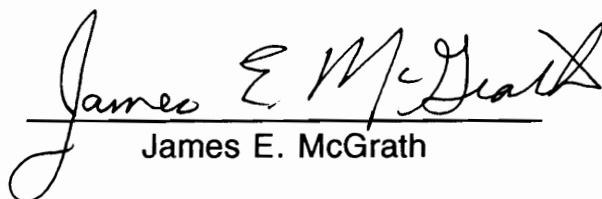
Dissertation submitted to the Faculty of the Virginia Polytechnic
Institute and State University in partial fulfillment of the
requirements for the degree of

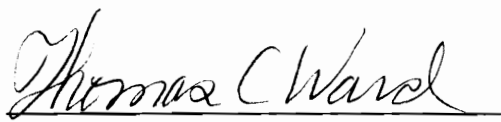
DOCTOR OF PHILOSOPHY


in


Chemistry

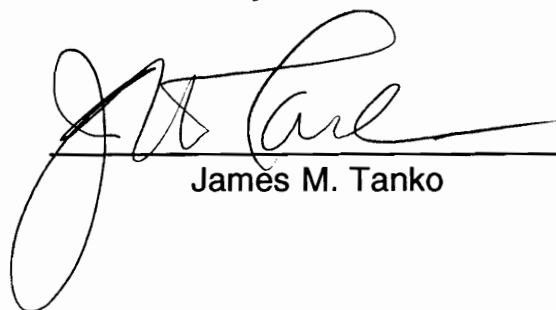
APPROVED:


James E. McGrath


Thomas C. Ward


Harry W. Gibson


Judy S. Riffle


James M. Tanko

August 1993

Blacksburg, Virginia

Synthesis and Characterization of High Performance Polybenzoxazoles

by

William Dale Joseph

Committee Chairman: Dr. James E. McGrath

Department of Chemistry

(ABSTRACT)

High molecular weight poly(hydroxy amide)s and polybenzoxazoles possessing a variety of backbone compositions have been synthesized via low temperature polycondensation and a novel catalytic cyclization reaction. Preliminary experiments involved the synthesis of poly(hydroxy amide)s and polybenzoxazoles based on a bisphenol-A aminophenol and isomeric acid chlorides. The polymers exhibited T_g 's around 280°C, limited solubilities and only fair thermo-oxidative stabilities. In an effort to improve these properties, fluorinated monomers were investigated. A number of novel fluorinated monomers and commercial monomers were incorporated into poly(hydroxy amide)s and polybenzoxazoles using the above mentioned polymerization/cyclization techniques. Enhanced solubilities, glass transition temperatures and thermo-oxidative stabilities were realized. Difficulties encountered during the polymerization of the fluorinated monomers prompted the study of polymerization conditions. Results of these studies indicate that the electronic environment about the bis(*o*-aminophenol)s and acid chlorides dictates the ability of these monomers to participate in an ester forming side reaction. Physical and spectroscopic evidence was presented to support this conclusion. Investigations were also

conducted to determine optimum cyclization conditions. It was shown that pyridine hydrochloride and *p*-toluenesulfonic acid monohydrate were active cyclization catalysts when used in conjunction with an azeotroping solvent, such as toluene or *o*-dichlorobenzene. In general, complete cyclization of the oxazole rings could be achieved in as little as 6 hours at 175°C. Unfortunately, generic cyclization conditions were not found. Additionally, phenylethynyl terminated polybenzoxazoles were successfully synthesized using the above techniques. Molecular weight control and phenylethynyl incorporation were confirmed by spectroscopic, thermal and mechanical analyses.

Acknowledgements

The results reported in this thesis are by no means a solo effort. Working together with my colleagues here at Virginia Tech has been an honor and I sincerely value the professional and social relationships forged during my tenure. Special thanks goes to Dr. Regis Mercier, who patiently listened to my theories and taught much about monomer and polymer synthesis. Thanks also goes to Drs. Herve' Marand, Matt Sheridan, Martin Rogers, Greg Lyle, Steve Liptak, Tae Ho Yoon, Jim Wescott and Mr. Dan Knauss, Mr. Gerry Meyer and Mr. Jean-Claude Abed. In addition, I would like to thank the intrinsics lab for their timely efforts and the secretarial staff, Bonnie, Laurie, Millie, Jeannie, Pat, Ester and Joyce for always having time to rush out a fax or a late Preprint.

On a personal note, I would like to thank my wife, Mary. A husband doesn't know how lucky he is until he looks back on four years of graduate school, broken promises, late night study groups, and weekends spent in the lab and realizes that all along a faithful partner has stood silently in the shadows offering support and comfort. For this and your undying support, I am in your debt.

To Dr. James McGrath, ever since I realized the magnitude of your job and the depth of your knowledge I've been amazed at the enormity of the task you've accepted and humbled by your talents and leadership. It has indeed been an honor and a privilege to have worked for a man of your stature. Finally, I would like to thank the members of my committee, Drs. Harry Gibson, Thomas Ward, Judy Riffle and James Tanko for their guidance and patience with my grammar.

Table of Contents

List of Figures	xii
List of Tables	xx
INTRODUCTION	1
LITERATURE REVIEW	5
2.1 Introduction	5
2.2 Polybenzoxazoles from Low Temperature Amidation Reactions and Thermal Cyclization	7
2.3 Melt Polymerizations	27
2.4 Synthesis of Polybenzoxazoles in Polyphosphoric Acid	33
2.5 PPSE Catalyzed Polybenzoxazole Formation	51
2.6 Polybenzoxazoles from Silylated Monomers	54
2.7 Polybenzoxazoles from Benzoxazole Monomer	61
2.7.1 Polybenzoxazoles via Nucleophilic Aromatic Substitution	61
2.7.2 Polybenzoxazoles via Acylation Reactions	68
2.7.3 Polybenzoxazoles via Oxidative Coupling	72
2.8 Polybenzoxazoles via Yamazaki Reaction	72
2.9 Polybenzoxazoles Containing Perfluoro Linkages	77

2.10 Thermal and Mechanical Properties of PBO's	85
EXPERIMENTAL	91
3.1 Introduction	91
3.2 Materials: Synthesis and Purification	94
3.2.1 Reagents and Monomers.	94
3.2.1.1 2,2-Bis(4-hydroxyphenyl)propane (Bisphenol-A)	94
3.2.1.2 2,2-Bis(4-hydroxy-3-nitrophenyl)propane (bANP)	95
3.2.1.3 2,2-Bis(3-amino-4-hydroxyphenyl)propane (bAAP)	96
3.2.1.4 Terephthaloyl Chloride (TC)	97
3.2.1.5 Isophthaloyl Chloride (IC)	98
3.2.1.6 2,2-Bis(3-amino-4-hydroxyphenyl)hexa- fluoropropane (6FAP)	98
3.2.1.7 2,2'-Dihydroxybenzidine (DHB)	99
3.2.1.8 α,α,α -Trifluoroacetophenone	101
3.2.1.9 1,1-Bis(4-hydroxyphenyl)-1-phenyl-2,2,2- trifluoroethane (3F-Bisphenol)	101
3.2.1.10 1,1-Bis(4-hydroxy-3-nitrophenyl)-1-phenyl- 2,2,2-trifluoroethane (3FNP)	102
3.2.1.11 1,1-Bis(3-amino-4-hydroxyphenyl)-1-phenyl- 2,2,2-trifluoroethane (3FAP)	104

3.2.1.12	4,4'-Oxydibenzoic Acid (ODBA)	105
3.2.1.13	4,4'-Oxydibenzoyl Chloride	106
3.2.1.14	2,2-Bis(4-carboxyphenyl)hexafluoropropane (6FDA)	107
3.2.1.15	2,2-Bis(4-chlorocarbonylphenyl)hexafluoropropane (6FAC)	107
3.3.1.16	1,1-Bis(4-methylphenyl)-1-phenyl-2,2,2-trifluoroethane	108
3.2.1.17	1,1-Bis(4-carboxyphenyl)-1-phenyl-2,2,2-trifluoroethane (3FDA)	109
3.2.1.18	1,1-Bis(4-chlorocarbonylphenyl)-1-phenyl-2,2,2-trifluoroethane (3FAC)	111
3.2.1.19	Phenylphosphine Sulfide Dichloride	112
3.2.1.20	Bis(4-methylphenyl)phenylphosphine Sulfide	113
3.2.1.21	Bis(4-methylphenyl)phenylphosphine Oxide	114
3.2.1.22	Bis(4-carboxyphenyl)phenylphosphine Oxide	115
3.2.1.23	Bis(4-chlorocarbonylphenyl)phenylphosphine Oxide (PPOAC)	116
3.2.1.24	4,6-Diaminoresorcinol Dihydrochloride (DAR•2HCl)	118
3.2.1.25	N,N',O,O'-Tetrakis(trimethylsilyl)-4,6-diaminoresorcinol (SDAR)	118
3.2.1.26	2,2-Bis(4-methoxyphenyl)propane	120
3.2.1.27	2,2-Bis(4-methoxy-3-nitrophenyl)propane	121

3.2.1.28	2,2-Bis(3-amino-4-methoxyphenyl)propane	122
3.2.1.29	2,2-Bis(4-methoxy-3-benzoylamino)propane	123
3.2.1.30	4-Iodobenzoic Acid	124
3.2.1.31	Methyl 4-Iodobenzoate	125
3.2.1.32	Phenylacetylene	126
3.2.1.33	Methyl 4-phenylethynylbenzoate	127
3.2.1.34	4-Phenylethynylbenzoic Acid	128
3.2.1.35	4-Phenylethynylbenzoyl Chloride	129
3.2.2	Solvents	130
3.2.2.1	N-Methylpyrrolidinone (NMP)	130
3.2.2.2	N,N-Dimethylacetamide (DMAc)	132
3.2.2.3	N-Cyclohexylpyrrolidinone (CHP)	132
3.2.2.4	<i>o</i> -Dichlorobenzene (DCB)	133
3.2.2.5	Toluene	134
3.2.2.6	Tetrahydrofuran (THF)	135
3.2.2.7	Triethylamine (TEA)	136
3.2.2.8	Pyridine	137
3.3	Synthesis of Polymers and Oligomers	138
3.3.1	General Poly(hydroxy amide) Synthesis	138
3.3.2	Phenylethynyl Terminated Poly(hydroxy amides)	140

3.3.3	General Polybenzoxazole Synthesis	142
3.4	Analysis of Oligomers and Polymers	145
3.4.1	Intrinsic Viscosity Determinations	145
3.4.2	Nuclear Magnetic Resonance Spectroscopy (NMR)	146
3.4.3	Fourier Transform Infrared Spectroscopy (FTIR)	147
3.4.4	Differential Scanning Calorimetry (DSC)	147
3.4.5	Dynamic Mechanical Thermal Analysis (DMTA)	148
3.4.6	Dynamic Thermal Gravimetric Analysis (TGA)	148
3.4.7	Isothermal Thermal Gravimetric Analysis (TGA)	149
3.4.8	Thermal Gravimetric Analysis - Mass Spectrometry (TGA-MS)	149
3.4.9	Hot Stage Optical Analysis	150
3.4.10	Stress-Strain Measurements	150
3.4.11	Titrations Methods	151
3.4.12	Melting Point Determinations	152
3.4.13	Gel Permeation Chromatography	152
	RESULTS AND DISCUSSION	153
4.1	Introduction	153
4.2	Synthesis of 2,2-Bis(3-amino-4-hydroxyphenyl)propane (bAAP)	156
4.3	Synthesis of 1,1,1-Triaryl-2,2,2-trifluoroethane	

Monomers	157
4.4 Synthesis of Bis(4-chlorocarbonylphenyl)phenylphosphine Oxide	170
4.5 Synthesis of Phenylethynylbenzoyl Chloride (PEBC).	183
4.6 Parameters Affecting the Formation of High Molecular Weight Poly(hydroxy amides)	186
4.6.1 Introduction	186
4.6.2 Effect of Base	194
4.6.3 Effect of Stirring Rate	198
4.6.4 Effect of Addition Method	199
4.6.5 Effect of Temperature	200
4.6.6 Effect of Linking Groups in the Aminophenols	202
4.6.7 Effect of Linking Groups in the Acid Chloride	206
4.6.8 Effect of Monomer Concentration	207
4.6.9 Effect of Solvent	208
4.6.10 Spectroscopic Evidence for an Ester Side Reaction	210
4.7 Methods of Cyclization	221
4.7.1 Poly(hydroxy amide)Cyclization Studies	221
4.7.2 Alternate Cyclization Techniques	237
4.8 Polymers Based on 2,2-Bis(3-amino-4-hydroxyphenyl)propane	243
4.9 Synthesis of Fluorinated Poly(hydroxy amides) and	

Polybenzoxazoles	258
4.10 Polymers Based on 4,6-Diaminoresorcinol	285
4.11 Phenylethynyl Terminated Polybenzoxazoles	295
4.12 Nonfluorinated Homopolymers and Fluorinated Copolymers	313
CONCLUSIONS	317
FUTURE WORK	322
References	323
Vitae	342

List of Figures

<u>Figure</u>	<u>Title</u>	<u>Page</u>
2.1	Low temperature polymerization of poly(hydroxy amide) and thermal cyclization to polybenzoxazole	8
2.2	Time dependence of the degree of cyclization of poly(hydroxy amide)s at various temperatures	11
2.3	Polybenzoxazole structures and linking groups reported by Korshak and Steinmann	18
2.4	Fluorinated bis(<i>o</i> -aminophenol)s	22
2.5	Structures of random poly(benzoxazole imide) copolymers	23
2.6	Structure of segmented poly(benzoxazole imide)	24
2.7	General polybenzoxazole melt polymerization scheme	28
2.8	Polybenzoxazole structures reported by Korshak	31
2.9	Monomers used in the synthesis of polybenzoxazoles	37
2.10	Isothermal aging curves of biphenyl modified cis PBO and cis PBT	43
2.11	Various substituted dicarboxylic acids	44
2.12	Monomers incorporated into fluorinated polybenzoxazoles via PPMA mediated polymerization	50
2.13	Silylated bis(<i>o</i> -aminophenol) monomers and polymerization, dehydration scheme	55
2.14	Activated dihalide benzoxazole monomers	63

2.15	SNAr2 polymerization scheme	63
2.16	Novel benzoxazole diamines	69
2.17	AB carboxylic acid/acetoxo monomers	70
2.18	AB monomers and Yamazaki polymerization scheme	73
2.19	Polybenzoxazole degradation and cyclodimerization mechanism	75
2.20	Polymerization of aliphatic and aromatic AA and BB Yamazaki reaction	76
2.21	Perfluoro- and perfluoro-ether bis(<i>o</i> -aminophenol)s	79
2.22	Thermomechanical spectrum of a perfluoro-polybenzoxazoles	81
2.23	Synthesis of fluorocarbon bridged polybenzoxazoles	84
2.24	Thermogravimetric analysis of polyheterocyclics	87
2.25	Isothermal weight loss of polyheterocyclics in air at 371°C	88
3.1	Graphical representation of fractional percent conversion versus number average degree of polymerization	93
3.2	Solvent distillation apparatus	131
3.3	Reaction vessel used to synthesis poly(hydroxy amide)s	139
3.4	Reaction vessel used in the cyclization of poly(hydroxy amide)s	144
4.1	Synthesis of 2,2-bis(3-amino-4-hydroxyphenyl)propane	158

4.2	FT-IR spectrum of 2,2-bis(3-amino-4-hydroxyphenyl)propane	159
4.3	¹ H NMR spectrum of 2,2-bis(3-amino-4-hydroxyphenyl)propane	161
4.4	Synthesis of 1,1-bis(3-amino-4-hydroxyphenyl)-1-phenyl-2,2,2-trifluoroethane	163
4.5	Synthesis of 1,1-bis(4-chlorocarbonylphenyl)-1-phenyl-2,2,2-trifluoroethane	164
4.6	¹ H NMR spectrum of 1,1-bis(3-amino-4-nitrophenyl)-1-phenyl-2,2,2-trifluoroethane	166
4.7	FT-IR spectrum of 1,1-bis(3-amino-4-hydroxyphenyl)-1-phenyl-2,2,2-trifluoroethane	167
4.8	¹ H NMR spectrum of 1,1-bis(3-amino-4-hydroxyphenyl)-1-phenyl-2,2,2-trifluoroethane	169
4.9	FT-IR spectrum of 1,1-bis(4-chlorocarbonylphenyl)-1-phenyl-2,2,2-trifluoroethane	171
4.10	¹ H NMR spectrum of 1,1-bis(4-chlorocarbonylphenyl)-1-phenyl-2,2,2-trifluoroethane	173
4.11	Synthesis of bis(4-chlorocarbonylphenyl)phenylphosphine oxide via Grignard chemistry	176
4.12	Synthesis of bis(4-chlorocarbonylphenyl)phenylphosphine oxide via Friedel-Crafts chemistry	177
4.13	FT-IR spectrum of PPOAc chlorination mixture	179
4.14	¹ H NMR spectrum of bis(4-chlorocarbonylphenyl)phenylphosphine oxide (PPOAc)	180
4.15	¹ H NMR spectra of PPOAc post-reaction as a function of time	181

4.16	Proposed mechanism for the chlorination of PPOAc	182
4.17	Synthesis of phenylethynylbenzoyl chloride	184
4.18	^1H NMR spectra of phenylethynylbenzoyl chloride and precursors involved in its synthesis	185
4.19	Polymerization of poly(hydroxy amide)s via low temperature, base-catalyzed solution techniques	187
4.20	Synthesis of 6FAP-6FDA polyimide using recently developed solution cyclization techniques	193
4.21	Effect of reaction temperature on intrinsic viscosity for 6FAP and TC polymerizations	201
4.22	Intrinsic viscosity as a function of time for 6FAP-TC polymerizations	201
4.23	Effect of solids content on intrinsic viscosity for a 6FAP-TC polymerization	208
4.24	Effect of cosolvent concentration on intrinsic viscosity for the polymerization of 6FAP-TC	209
4.25	^1H NMR spectra of various poly(hydroxy amide)s and 6FAP ester amide	211
4.26	2D ^1H NMR spectrum of base generated 6FAP-TC poly(hydroxy amide)	215
4.27	^1H NMR spectra of 6FAP-TC poly(hydroxy amide)s synthesized and analyzed under various conditions	216
4.28	FT-IR spectra of 6FAP-TC poly(hydroxy amide) and 6FAP model compounds	218
4.29	A proposed mechanism for the acid catalyzed hydrolysis of an amide bond in poly(hydroxy amide)s	223

4.30	A proposed mechanism for the acid catalyzed cyclization of poly(hydroxy amide)s to polybenzoxazoles	224
4.31	General poly(hydroxy amide) cyclization reaction	225
4.32	Change in ¹ H NMR spectra with time for conversion of 6FAP-ODBC PHA to polybenzoxazole at 185°C	227
4.33	Conversion of 6FAP-ODBC PHA to PBO as a function of reaction temperature with stoichiometric amounts of pyridine hydrochloride	229
4.34	Conversion of 6FAP-ODBC PHA to PBO as a function of reaction temperature and <i>p</i> -TSA concentration	231
4.25	Conversion of 6FAP-ODBC PHA to PBO as a function of catalyst composition and catalyst concentration	232
4.36	Synthesis of 2,2-bis(3-amino-4-methoxyphenyl)propane	238
4.37	Synthesis of 2,2-bis(4-methoxy-3-benzoylamino)propane	239
4.38	¹ H NMR spectra of methoxy cleavage reaction mixture at various times	241
4.39	Percent methoxy groups remaining as a function of time under various reaction conditions	242
4.40	Low temperature polymerization of bAAP based poly(hydroxy amide)s and polybenzoxazoles	245
4.41	Differential scanning calorimetry thermogram of bAAP-TC polybenzoxazoles	246
4.42	Wide angle X-ray scattering pattern of bAAP-TC polybenzoxazole	247

4.43	FT-IR spectra of bAAP poly(hydroxy amide) and polybenzoxazole	250
4.44	TGA thermogram of bAAP poly(hydroxy amide) and polybenzoxazole	251
4.45	Total ion and selective ion count TGA-MS spectra of bAAP polybenzoxazole	252
4.46	Acronyms and structures of various bis(<i>o</i> -aminophenol)s and acid chlorides	259
4.47	Low temperature polymerization of 6FAP-ODBC poly(hydroxy amide)	261
4.48	¹ H NMR spectra of 6FAP containing poly(hydroxy amide)s	262
4.49	¹ H NMR spectra of 3FAP containing poly(hydroxy amide)s	263
4.50	¹ H NMR spectra of DHB and DAR containing poly(hydroxy amide)s	264
4.51	Solution cyclization of 6FAP-ODBC poly(hydroxy amide) to polybenzoxazole	266
4.52	Dynamic thermogravimetric thermogram of 3FAP-6FAC poly benzoxazole	267
4.53	Total ion and selective ion count TGA-MS spectra of 3FAP-TC polybenzoxazole	268
4.54	FT-IR spectra of 3FAP-TC poly(hydroxy amide) and polybenzoxazole	269
4.55	FT-IR spectra of 6FAP containing polybenzoxazoles	271
4.56	FT-IR spectra of 3FAP containing polybenzoxazoles	272

4.57	FT-IR spectra of DHB and DAR containing polybenzoxazoles	273
4.58	Isothermal weight retention data for 3FAP-TC and 6FAP-TC poly benzoxazoles	276
4.59	Gel permeation chromatogram of 6FAP-3FAC polybenzoxazole	280
4.60	Optical micrographs of 6FAP-TC and 6FAP-IC polybenzoxazoles	283
4.61	Monomers and acronyms of high performance polymers	286
4.62	Synthesis of N,N',O,O'-tetrakis(trimethylsilyl)-diaminoresorcinol	287
4.63	Polymerization and cyclization of DAR-3FAC poly(hydroxy amide)	289
4.64	FT-IR spectrum of solution cyclized DAR-3FAC polybenzoxazole	292
4.65	TMA trace of solution cyclized DAR-3FAC polybenzoxazole film	294
4.66	Synthesis of 4-(phenylethynyl)benzoyl chloride	297
4.67	Synthesis of controlled molecular weight 6FAP-ODBC poly(hydroxy amide)s and polybenzoxazoles	298
4.68	¹ H NMR spectra of controlled and uncontrolled molecular weight 6FAP-ODBC poly(hydroxy amide)s	300
4.69	¹ H NMR spectra of controlled and uncontrolled molecular weight 6FAP-ODBC polybenzoxazoles	301
4.70	DSC thermogram of 5K, phenylethynyl terminated 6FAP-ODBC polybenzoxazole, before and after a 1 hour cure at 475°C	307

4.71	Gel permeation chromatogram of 5K 6FAP-ODBC polybenzoxazole	311
4.72	DSC thermogram of DHB-ODBC polybenzoxazole	316

List of Tables

<u>Table</u>	<u>Title</u>	<u>Page</u>
2.1	Structure and solution properties of sulfonyl, sulfide and oxygen containing poly(hydroxy amide)s and polybenzoxazoles	13
2.2	Structure, cyclization conditions and inherent viscosities of sulfonyl, oxygen and sulfide containing polybenzoxazoles	15
2.3	Mechanical properties of oxy-bis(3-amino-4-hydroxyphenyl) based polybenzoxazoles	20
2.4	Solution and thermal properties of carborane containing poly(hydroxy amide)s and polybenzoxazoles	21
2.5	Polybenzoxazoles derived from comonomers via melt polymerization	29
2.6	Properties of polybenzoxazoles reported by Korshak	31
2.7	Cis polybenzoxazole fiber properties	39
2.8	Mechanical properties of 2,5 PBO and cis PBO after various thermal and tension treatments	41
2.9	Structure and inherent viscosities of DHB polybenzoxazoles polymeized in PPMA	49
2.10	Solution properties of PPSE generated polybenzoxazoles	52
2.11	Thermal properties of PPSE generated polybenzoxazoles	53
2.12	Thermal properties of fluorinated polybenzoxazoles	56
2.13	Mechanical properties of fluorinated polybenzoxazoles	56

2.14	Permeability, diffusion, and solubility coefficients of polybenzoxazoles	56
2.15	Thermal and solution properties of poly(aryl ether benzoxazole)s	65
2.16	Poly(hydroxy amide) solution and optical properties	74
2.17	Properties of perfluoro-polybenzoxazoles	79
2.18	Properties of rubber-like fluorocarbon ether polybenzoxazoles	83
2.19	High performance fiber properties	90
4.1	FT-IR spectral assignments for 2,2-bis(3-amino-4-hydroxyphenyl)-propane	160
4.2	FT-IR spectral assignments for 1,1-bis(3-amino-4-hydroxyphenyl)-1-phenyl-2,2,2-trifluoroethane	168
4.3	FT-IR spectral assignments for 1,1-bis(4-chloro-carbonylphenyl)-1-phenyl-2,2,2-trifluoroethane	172
4.4	Effect of base on intrinsic viscosity	196
4.5	Effect of base concentration on intrinsic viscosity	198
4.6	Effect of acid chloride and aminophenol linking group on the inherent viscosity of various poly(hydroxy amide)s	203
4.7	¹ H NMR shifts of various bis(<i>o</i> -aminophenol)s	204
4.8	Summary of cyclization conditions for reactions catalyzed with pyridine hydrochloride	234
4.9	Summary of cyclization conditions and inherent viscosities for reactions catalyzed with <i>p</i> -toluene sulfonic acid and pyridine hydrochloride	235

4.10	Aromatic composition and solution properties of isomeric bAAP poly(hydroxy amide)s and polybenzoxazoles	249
4.11	Thermal and morphological properties of isomeric bAAP poly(hydroxy amide)s and polybenzoxazoles	254
4.12	Solubility of isomeric bAAP polybenzoxazoles in various solvents	256
4.13	Solution and thermal properties of various fluorine containing polybenzoxazoles	275
4.14	Solution properties of various fluorine containing poly(hydroxy amide)s and polybenzoxazoles	277
4.15	Solubility characteristics of various fluorinated polybenzoxazoles	279
4.16	Mechanical properties of various fluorinated polybenzoxazoles	282
4.17	Summary of SDAR polymerization conditions	290
4.18	Yields of controlled molecular weight poly(hydroxy amide)s and polybenzoxazoles	299
4.19	Molecular weight and intrinsic viscosity data for 6FAP-ODBC poly(hydroxy amide)s and polybenzoxazoles	303
4.20	Thermal transition data for uncured polybenzoxazoles	305
4.21	Thermal transition data for polybenzoxazoles cured at 350°C	305
4.22	Thin film tensile properties of cured and uncured polybenzoxazoles	309
4.23	Solution and thermal properties of various 2,2'-dihydroxybenzidine containing poly(hydroxy amide)s	314

Chapter 1

INTRODUCTION

High temperature, thermally stable polymers have been mentioned in the literature to a great extent due to their desirable thermal and mechanical properties, as well as their solvent resistance [1-4]. Some of the more notable materials include Ultem® and Kapton® polyimides, PMR-15 resins, Udel® polysulfones, PEEK® and PEK® poly(arylene ether ketones), polybenzimidazoles and a whole host of other experimental thermoplastic polymers and industrially important thermosets, such as epoxies, maleimides and cyanate esters. All these materials possess desirable properties as well as drawbacks. For example, Kapton® is an excellent high temperature polymer, but processing requires one to work with the poly(amic acid) stage of the polymer until the final shape has been achieved. Furthermore, thermal

cyclization of the poly(amic acid) to polyimide generates volatiles and causes shrinkage; consequently, the majority of Kapton®'s commercial applications are relegated to the area of thin films. Typical amorphous thermoplastic polymers generally lack solvent resistance, even though their strength and toughness properties are superior to most polymers. Thermosets on the other hand possess excellent solvent resistance, good mechanical properties and desirable processing characteristics, but lack toughness and moldability.

Other high performance polymers, such as polybenzoxazoles, have been mentioned with respect to excellent thermal and mechanical properties, but lack notoriety due to problems encountered during synthesis and processing. Polybenzoxazoles belong to the family of polymers characterized by a nitrogen containing heterocycle fused to a benzene ring in the polymer backbone. Consequently these polymers are extremely stable in thermo-oxidative environments. In addition, fibers spun from polybenzoxazole dopes and thermally treated, possess phenomenal mechanical properties as exemplified by tensile moduli and strengths exceeding 250 GPa and 3.5 GPa, respectively [5]. These exceptionally high mechanical properties can be directly related to the high degree of ordering found in these materials. Unfortunately, synthetic and processing drawbacks have hampered the development of these polymers into commercial products. Some of the major concerns include, low transverse mechanical properties, poor

solubility of the dicarboxylic acid in polyphosphoric acid and the use of environmentally unacceptable solvents.

Recent advances in the area of step-growth polymerizations have aided in pushing back the boundaries associated with synthesizing and processing heterocyclic polymers. Most notable is the incorporation of fluorine into the polymer backbone [6]. Reinhardt and Imai have demonstrated that by incorporating fluorinated moieties into polybenzoxazole backbones, solubility and processability were enhanced, while favorable thermal stability and glass transition temperatures were maintained [7,8]. Incorporation of flexible ether linkages into the polybenzoxazole backbone also improved processability. Poly(arylene ether benzoxazoles) possess desirable properties such as solubility, excellent mechanical and thermal properties and enhanced toughness relative to the parent polybenzoxazoles [9,10]. Unfortunately, the desirable improvements in processability and mechanical properties achieved with the above mentioned technologies have been offset by deteriorating material properties (e.g., solvent resistance, loss of ordering) and elaborate or expensive monomer syntheses. To overcome some of these drawbacks, the following chapters will outline efforts made to modify existing polybenzoxazole polymerization conditions using commercially available monomers.

The objectives of this dissertation research were to investigate alternate methods of synthesizing polybenzoxazoles using more favorable reaction conditions, in addition to generating novel

materials with improved properties; more specifically, to identify and correct, if possible, the reaction parameter (parameters) responsible for limiting molecular weight in the low temperature polymerization of bis(*o*-aminophenols) with diacid chlorides; secondly, to investigate the viability of acid-catalyzed solution cyclization with respect to conversion of poly(hydroxy amide)s to polybenzoxazole and amide hydrolysis. These investigations also served as a case study to establish the most efficient reaction conditions for the preparation of fully cyclized, soluble polybenzoxazoles. A third objective of the research was to synthesize novel unsymmetrical difunctional monomers, which when incorporated into polybenzoxazoles, enhance solubility. A final objective was to control the molecular weight of a soluble polybenzoxazole via the incorporation of a monofunctional reactive endcapper. The resulting oligomers can then be solution processed and thermally crosslinked into an insoluble, three dimensional network.

In Chapter 2 a review of the synthetic methods employed in the generation of aromatic polybenzoxazoles, as well as solution, thermal and mechanical properties of the resulting polymers will be presented. The purification and synthetic procedures used in the preparation of monomers and polymers are described in Chapter 3. A detailed discussion of the poly(hydroxy amide) polymerization, cyclization conditions and the resulting polymers will be presented in Chapter 4, followed with conclusions, future work and references.

Chapter 2

LITERATURE REVIEW

2.1 Introduction

Aliphatic polybenzoxazoles were first synthesized in the late 1950's via melt polymerizations [11], but it wasn't until 1964 that the synthesis of wholly aromatic polybenzoxazoles (PBO's) was reported [12]. Since that initial report, numerous polymerization methodologies have been developed to aid in the generation of aromatic polybenzoxazoles [13-17]. These techniques range from low temperature polymerization of bis(*o*-aminophenol)s with acid chlorides, followed by thermal cyclization to polyphosphoric acid mediated reactions between dihydrochloride salts of bis(*o*-aminophenol)s and dicarboxylic acids. Efforts to generate

polybenzoxazoles in the melt as well as incorporating preformed benzoxazole moieties into difunctional monomers have also been reported [9-11].

Interest in polybenzoxazoles can be directly attributed to their excellent thermo-oxidative stability, as well as their phenomenal mechanical properties. The wholly aromatic nature of the polybenzoxazole backbone affords it this superior thermal resistance [18]. Exceptional tensile properties can be attributed to the high degree of orientation achieved during the fiber spinning process, in addition to the para catenation of the exocyclic bonds, aromaticity and the development of three dimensional ordering [19,20]. Because of these highly desirable properties, many investigations have been conducted in an effort to optimize polymerization and processing conditions, as well as polymer properties.

The following section will outline these synthetic efforts, in addition to providing information regarding molecular weight, thermal stability and mechanical properties of the resulting polymers. The review has been divided into sections according to polybenzoxazole polymerization technique. At the end of the chapter, a few comments will be made regarding the thermal and mechanical properties of polybenzoxazoles with respect to other high performance systems.

2.2 Polybenzoxazoles from Low Temperature Amidation Reaction and Thermal Cyclization

The first successful synthesis of polybenzoxazoles made use of a low temperature polycondensation reaction in conjunction with a thermal cyclization reaction. Development of this method was prompted by the less than desirable results realized in melt polymerization attempts [21]. Kubota and Nakanishi [12,22] used low temperature, solution polymerization techniques to condense 3,3'-dihydroxybenzidine with aromatic diacid chlorides. Dissolving 3,3'-dihydroxybenzidine in DMAc with excess pyridine at 5°C and treating the solution slowly acid chlorides (in DMAc), followed by raising the temperature to 25°C for 12 hours, the authors were able to synthesize aromatic hydroxy substituted polyamides (Figure 2.1). High inherent viscosities (>1.00 dl/g, 0.5%, DMAc, 30°C) suggested that high molecular weights were achieved. Thermal treatment of these polymers at 200 °C, under inert reaction conditions, formed the oxazole ring structure and afforded polybenzoxazoles. Accordingly, tough, flexible, transparent films with excellent thermo-oxidative stabilities were obtained.

Kubota and Nakanishi's report [12,22] that poly(hydroxy amide)s could be generated at low temperatures and subsequently cyclized to wholly aromatic polybenzoxazoles initiated the search for alternate polybenzoxazoles with improved properties. The following

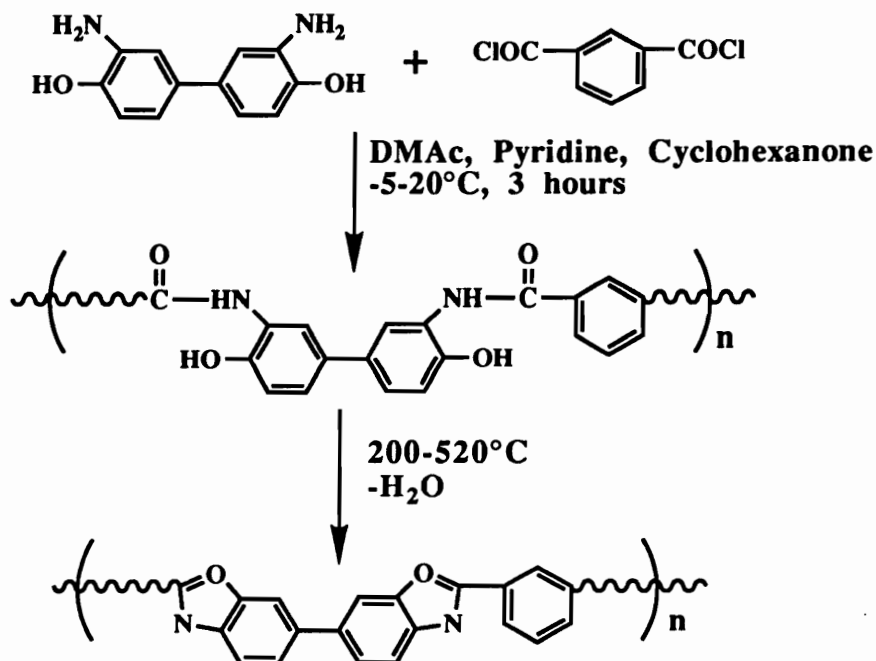
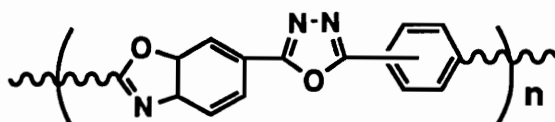
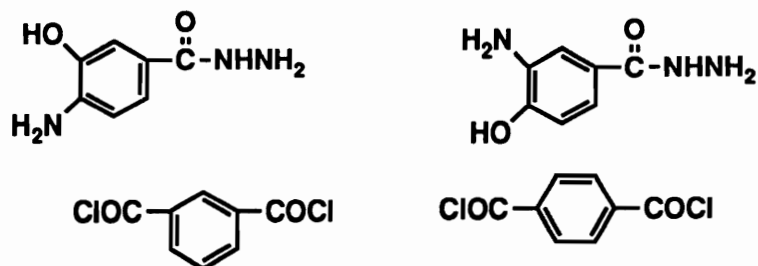


Figure 2.1. Low temperature polymerization of poly(hydroxy amide) and thermal cyclization to polybenzoxazole.

section will summarize these efforts and comment on some of the properties exhibited by these materials.

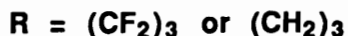
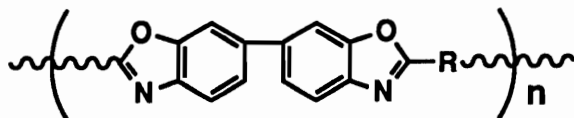
Culbertson [23,24] described the synthesis of poly(benzoxazole-oxadiazole)s by reacting aromatic hydrazides of aminohydroxy benzoic acids with diacid chlorides in NMP, without base. The resulting polymers were soluble in polar aprotic solvents and possessed inherent viscosities ranging from 0.6-2.17 dl/g (0.5%, 25°C , DMSO). Thermally treating the precursor polymers under reduced pressure resulted in cyclized material after 1 hour at 300°C . DSC analysis indicated no detectable glass transition



and isomers

temperatures and dynamic Thermogravimetric analysis (TGA) measured the onset of degradation at 520°C in air. Heat treated films were reported to be transparent and tough in nature. These materials, in addition to being novel polybenzoxazoles, represent the first synthesis of polybenzoxazoles containing heterocycles other than the oxazole heterocycle.

Russian investigators became very active in the area of high performance polybenzoxazoles in the mid 1960's and 70's, with a large portion of the research being reported from the laboratories of Yakubovich [25-33]. The earlier efforts revolved around the synthesis of polybenzoxazoles containing 3,3'-dihydroxybenzidine and aliphatic acid chlorides. Using diimidate derivatives of aliphatic dicarboxylic acids, Yakubovich [25] described the use of low temperature techniques to generate hydroxy substituted polyamides. Unfortunately the specific viscosities reported were all



less than 0.1 dl/g (*m*-cresol, 0.5%, 30°C). Repeating the experiments of Kubota and Nakanishi with an additional acid chlorides, Yakubovich [26,27] synthesized a number of polybenzoxazoles, some of which contained an oxygen linkage.

Solid state cyclization studies (thermogravimetric analysis) on these polymers suggested that incorporation of flexible linkages enhances the rate of cyclization and lowers the cyclization temperature (Figure 2.2). In general, it was found that cyclization temperatures greater than 300°C were required to achieve complete cyclization and the rate was directly dependent on the reaction temperature. Assuming unimolecular reaction kinetics, the authors observed that lower cyclization temperatures resulted in a sharper decrease in the cyclization rate at higher percent conversions. Reduction of the cyclization rate constants (k_c) was attributed to a decrease in backbone mobility with an increase in conversion to polybenzoxazole. Energies of activation for the process (17-55 kcal/mole) increased with elevated levels of rigidity in the polymer backbone (determined from $\log k_c - 1/T$ graphs).

Viscosity measurements made on the polymers, before, during and after cyclization indicated a loss of molecular weight (η_{inh} 's

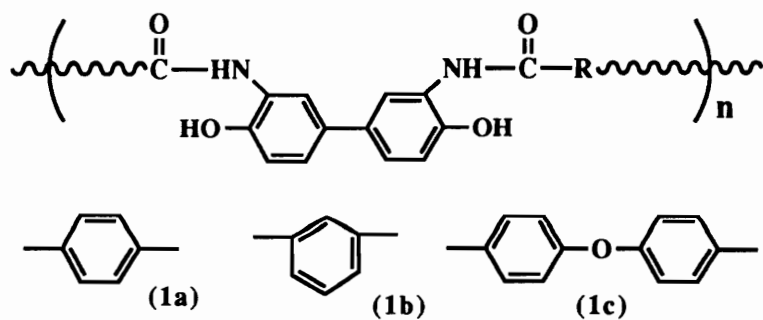
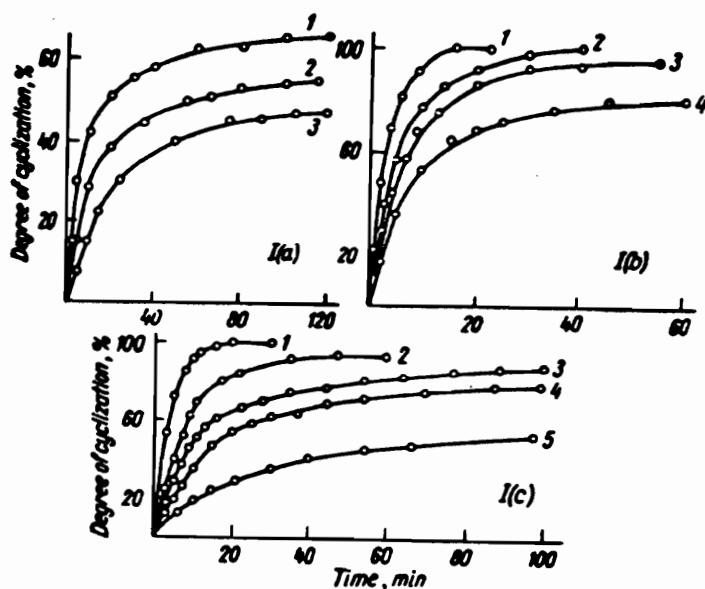
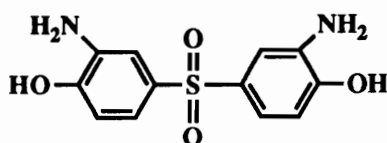


Figure 2.2. Time dependence of the degree of cyclization of poly(hydroxy amide)s at various temperatures. I(a): 1-330°C, 2-316°C, 3-296°C; I(b): 1-335°C, 2-319°C, 3-305°C, 4-291°C; I(c): 1-324°C, 2-286°C, 3-270°C, 4-260°C, 5-240°C [27].

decreased initially) during the initial stages of cyclization, but elevated viscosities towards the end of the process. The authors attributed the initial decrease in η_{inh} 's to chain degradation (amide hydrolysis) and the increases at the end of the cure process to incorporation of rigid oxazole units in the polymer backbone, as well as chain extension.

Changing the composition of the bis(*o*-aminophenol) bridging group from a single bond to a sulfonyl group and incorporating



sulfide, oxygen, pyridinyl and sulfonyl groups into the diacid chlorides, led to a series of polybenzoxazoles with enhanced solubility's, but decreased inherent viscosity's [28,29] (Table 2.1). This marked the first in a number of reports, where comment was made regarding the difficulty in achieving high molecular weight polymers when electron-withdrawing bridging groups were incorporated into the bis(*o*-aminophenol). Low amine basicity (poor amine nucleophiles) was credited for the inability to achieve high molecular weights. Polymers made from the sulfonyl bridged analog exhibited inferior thermal stabilities, but enhanced ductility relative to the biphenyl systems. Percent elongations for the biphenyl and sulfone systems were 3-5% and 5-13%, respectively. Polymers with an oxygen, sulfide or sulfonyl linkage in the diacid

Table 2.1. Structure and solution properties of sulfonyl, sulfide and oxygen containing poly(hydroxy amide)s and polybenzoxazoles [29].

Ar	Ar'	PHA η_{inh} (dl/g) ^a	Cyclization Conditions ^b Temperature (°C)/Time (hr)	Percentage of Theoretical Wt. Loss During Cyclization	PBO η_{inh} (dl/g) ^c
		1.8	350/0.5	100	1.03
		1.0	350/4	100	2.20
		1.15	300/1	100	1.32
		1.15	300/1+ 350/1	100	1.81
		1.12	310/1	100	1.21
		0.57	370/1	118	0.60
		0.57	310/1	110	0.73
		0.57	300/1.5	104	0.85

^aRun in H₂SO₄ at 25°C (0.5%).

^bCyclization carried out at $\sim 10^{-3}$ mm Hg.

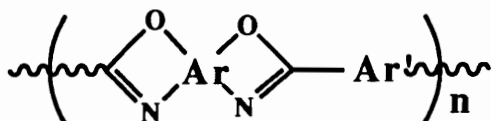
^cRun in H₂SO₄ at 25°C (0.5%).

chloride portion also showed enhanced elongations (5-9%). Tensile strengths decreased with incorporation of flexible linkages, but increased with an increase in draw ratio. Tensile moduli were reported to be around 3.9 GPa for the high molecular weight systems.

Yakubovich extended this work further by incorporating acid chlorides containing two sulfide or oxygen linkages [30,31]. Low to high molecular weight polymer was obtained depending on the nature of the bis(*o*-aminophenol) linkage (sulfonyl being lower) (Table 2.2). All the poly(hydroxy amide)s exhibited excellent solubility's in organic solvents, especially polar, aprotic solvents and were readily cyclized at temperatures between 300 and 370°C. No data was presented on PBO solubility. Addition of an extra sulfide or oxygen linkage into the polymer backbone increased percent elongation to 25%, while reducing tensile strengths, tensile moduli and glass transition temperatures. Glass transition temperatures for the biphenyl based systems ranged from 280-475°C (TMA) and X-ray analysis indicated the presence of crystallinity in the polymers supporting flexible linkages. Fortunately, the additional sulfide and oxygen linkages didn't detrimentally affect thermo-oxidative stability, at least dynamically.

Around 1970, Yakubovich and coworkers [32,33] published two contradictory papers related to the synthesis of high molecular weight poly(hydroxy amide)s containing both electron-withdrawing and electron-donating *o*-aminophenol bridging groups. The first

Table 2.2. Structure, cyclization conditions and inherent viscosity's of sulfonyl, oxygen and sulfide containing polybenzoxazoles. Inherent viscosity's measured in H₂SO₄ at 25°C (0.5%) [31].



Ar	Ar'	Cyclization Conditions ^a		η_{inh}^b
		Temp. (°C)	Time (hr)	
		350-370	2	1.74
		350	2	1.03
		350	2	0.67
		325	1	0.76
		300	1	0.62

^aCyclization carried out at 10^{-3} mm Hg.

^bRun in H₂SO₄ at 25°C (0.5%).

paper [32] reported the generation of high molecular weight polybenzoxazoles containing the sulfonyl bridging group when the polymerizations were carried out in N-methylpyrrolidinone (NMP), but low molecular weight polymer if N,N-dimethylacetamide (DMAc) was used. Reasons why NMP should give higher molecular weight polymer relative to DMAc were not given. They also noted very high inherent viscosity's (~2.0 dl/g) when the polymers was first dissolved in N,N-dimethylformamide (5% LiCl,0.5%, 25°C), but drastic reduction in the η_{inh} 's over a period of several days at room temperature (~0.6 dl/g). Extensive H-bonding was credited for the enormous viscosity's. The reduction in the η_{inh} 's with time was rationalized as a disruption in the H-bonding by LiCl. Higher inherent viscosity's were also reported with higher initial monomer concentrations, a trend also observed in our laboratory.

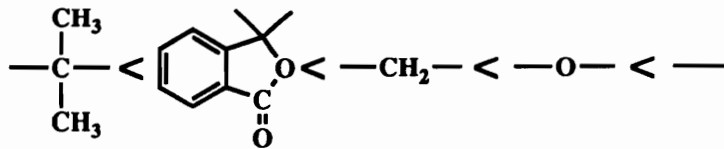
Eight months later, Yakubovich [33] published a paper on the chemistry of low temperature polycondensation reactions between diacid chlorides and bis(*o*-aminophenol)s in various amide solvents. Arguments were made to support the occurrence of transamidation reactions between amide solvents and the poly(hydroxy amide)s. It was proposed that these side reactions were inhibiting the formation of high molecular weight polymer. It was further suggested that by switch from an amide solvent to tetramethylene sulfone, the solvent induced transamidation side reactions could be suppressed and higher molecular weights achieved. Some of the results supported these claims, but in general the results were

inconclusive. Surprisingly, no mention was made of the earlier paper which claimed the synthesis of very high molecular weight poly(hydroxy amide)s containing electron-withdrawing bridging groups in amide solvents. This fact raises some suspicion as to whether or not high molecular weight polymer was ever achieved when electron-withdrawing bridging groups were incorporated. The authors also noted the appearance of an ester carbonyl stretch (1735 cm^{-1}) when pyridine or triethylamine (TEA) was used as an acid scavenger, but no carbonyl stretch when DMF, DMAc or NMP were used. Esterification of the hydroxyl groups during polymerization was credited for these stretches.

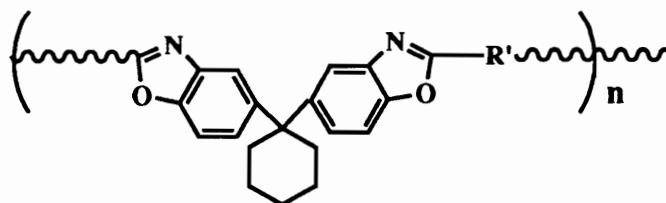
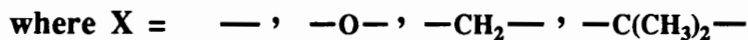
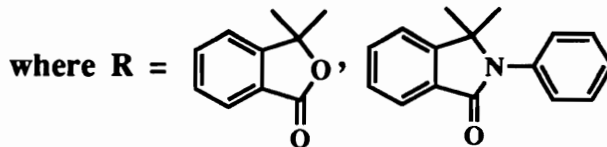
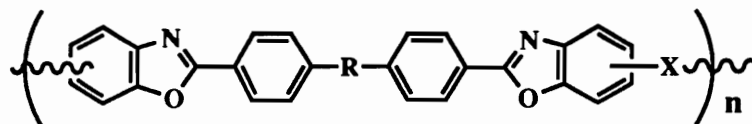
During this same period of time, a number of international patents [34-36] were awarded to Toyo Rayon Co., Ltd, regarding the synthesis of linear polybenzoxazoles and poly(benzoxazole imides) via low temperature polymerization techniques.

Polymerization of various other bis(*o*-aminophenol) monomers were reported by Korshak [37,38] and Steinmann [39] using similar techniques. Some of the linking groups are shown in Figure 2.3. Unfortunately, no data was supplied regarding the molecular weight of the poly(hydroxy amide)s, but according to the appreciable η_{inh} 's of the polybenzoxazoles (0.35-1.45 dl/g, H_2SO_4 , 0.5%, 25°C), molecular weights for the PHA's should have been appreciable. Dynamic weight loss studies indicated the lactone and lactam bridging groups to be less stable than the other linking groups investigated, with the lactams being less stable than the lactones.

The order of thermal stability for the polymers containing the lactone (phthalide) diacid is as follows:



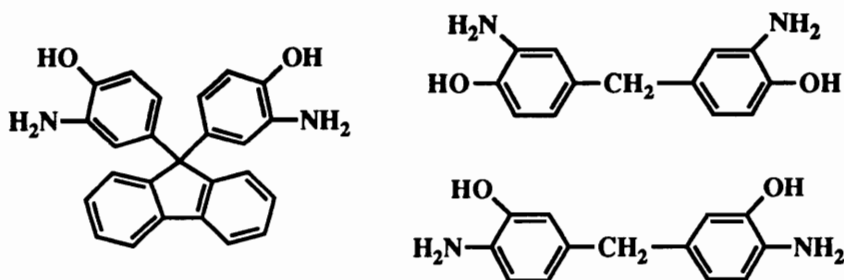
with the highest onset of degradation in air being recorded at ~430°C. No glass transition temperatures were reported.



where R' is an alkyl chain

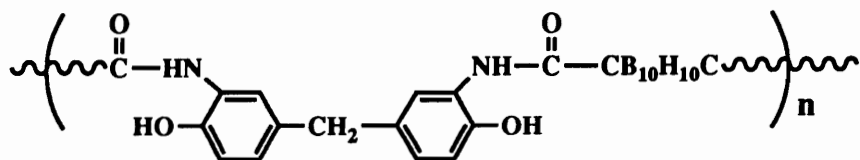
Figure 2.3. Polybenzoxazole structures and linking groups reported by Korshak and Steinmann [37,39].

Fluorene and methylene linked bis(*o*-aminophenol)s were also polymerized with iso- and terephthaloyl chloride (PBO η_{spec} 's = 0.60-1.34 dl/g, H₂SO₄, 20°C) [40]. Unfortunately the synthetic work was reported in a Russian patent [41] and little data has been found regarding the particulars of these polymers.



Replacement of the methylene linking group for an oxygen linking group results in a pair of isomeric bis(*o*-aminophenols) [42,43,]. Homopolymerizing or copolymerizing these monomers with various acid chlorides has resulted in fiber forming polybenzoxazoles (PHA η_{inh} 's ~0.8 dl/g, 0.5%, 25°C, DMF). Mechanical properties of the oxy-bis(3-amino-4-hydroxyphenyl) (4,4'-OAP) isomer polymerized with isophthaloyl chloride and oxydibenzoyl chloride are shown in Table 2.3. Notice the percent elongation increases with incorporation of flexible linkages.

Perhaps the most novel poly(hydroxy amide) introduced by the Russians was poly[4,4'-dihydroxy-3,3'-(carboranylneamido) diphenylmethane] [44,45]. This polymer is the condensation product of *para* and *m*-carboranedicarboxylic acid dichlorides with 4,4'-



dihydroxy-3,3'-diaminodiphenylmethane. Other bis(*o*-aminophenol)s were also incorporated into the polymer backbone (Table 2.4). No solution or thermal properties were reported for the *meta*-linked

Table 2.3. Mechanical properties (20°C) of 4,4'-OAP based polybenzoxazoles [42].

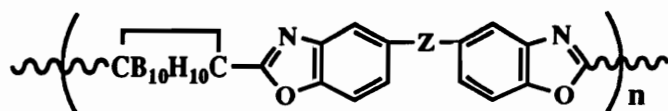
Acid Chloride	T _g (°C)	η _{inh} ^a (dl/g)	Tensile Strength (MPa)	Percent Elongation
Isophthaloyl	270	0.85	117.6	15%
Oxydibenzoyl	240	0.77	107.8	50%

^aPoly(hydroxy amide) η_{inh}'s run in DMF at 25°C (0.5%)

systems due to the inability to achieve high molecular weight. Attempts to thermally cyclize the *meta*-linked poly(hydroxy amide)s resulted in simultaneous cyclization and carborane chain cleavage, while the *para*-linked systems were reported to have cyclized without degradation. Efforts to cyclize both series of polymers in polyphosphoric acid failed.

Adamantane was incorporated into polybenzoxazoles through its 5,7-dicarboxylic acid chloride [46,47]. Films, melt pressed from the poly(hydroxy amide) were colorless and reportedly soluble in water. Mechanical properties were slightly lower than wholly aromatic,

Table 2.4. Solution and thermal properties of carborane containing poly(hydroxy amide)s and polybenzoxazoles [45].



Z	η_{red}^a (dl/g)	T_g^b (°C)	5% Wt. Loss ^c (°C)	Char Yield at 900°C
-CH ₂ -	1.1	320	550	80%
-C(CH ₃) ₂ -	0.4	290	400	88%
-SO ₂ -	- - -	470	470	98%
-O-	1.0	360	450	90%

^aRun in NMP at 25°C (0.5%)

^bBased on thermomechanical curves

^c5% weight loss in air (5°C/min.)

isotropic polybenzoxazoles. The use of bisorthoesters were reported in 1980 by Bansleben and Vogl [48] to generate PBO's. Unfortunately, the instability of the bisorthoesters resulted in low molecular weight materials.

More recently, a number of fluorinated bis(*o*-aminophenol)s have been introduced [49-54]. The characteristic common to all these monomers is the presence of a trifluoromethyl linkage. Monomer structures are illustrated in Figure 2.4. Attempts to polymerize these monomers via low temperature techniques resulted in low molecular weight materials in most cases [53-58]. Most of literature pertaining to these materials is related to the microelectronics industry, where highly fluorinated materials are

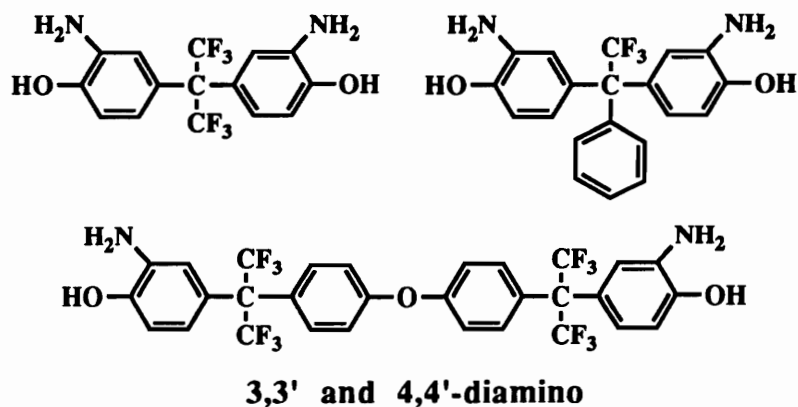


Figure 2.4. Fluorinated bis(*o*-aminophenols)

desired. Glass transition temperatures range from 200°C to greater than 400°C, solubility in general is enhanced and in some cases, thermoformable materials are realized. The thermo-oxidative stability of these materials are very similar to wholly aromatic materials, indicating incorporation of the hexafluoroisopropylidene group has a negligible effect on thermal stability.

It was mentioned previously that Culbertson [23,24] was the first to report the synthesis of polybenzoxazole containing alternate heterocyclic ring systems. Since that disclosure, numerous other heterocyclic ring systems have been incorporated into the polybenzoxazole backbone, in both a random and alternate fashion. The following section will review some of the efforts made in this area. It should be emphasized that only polybenzoxazole copolymers made via low temperature amidation reactions, with subsequent thermal cyclization will be discussed at

this time. Discussion of polybenzoxazole copolymers formed via preformed benzoxazole monomers will be delayed until Section 2.7.

Initial efforts to synthesize polybenzoxazole copolymers were made by Korshak and coworkers [59-61] in the late 1960's. Combining various ratios of bis(*o*-aminophenol)s, diamines, acid chlorides and PMDA in polar aprotic solvents at 20°C resulted in low to moderate molecular weight substituted polyamides. Subsequent cyclodehydration at elevated temperatures generated brown films of random poly(benzoxazole imide) copolymers. It was mentioned that high PMDA concentrations yielded higher viscosity's and superior films. The structures of some of the copolymers are illustrated in Figure 2.5.

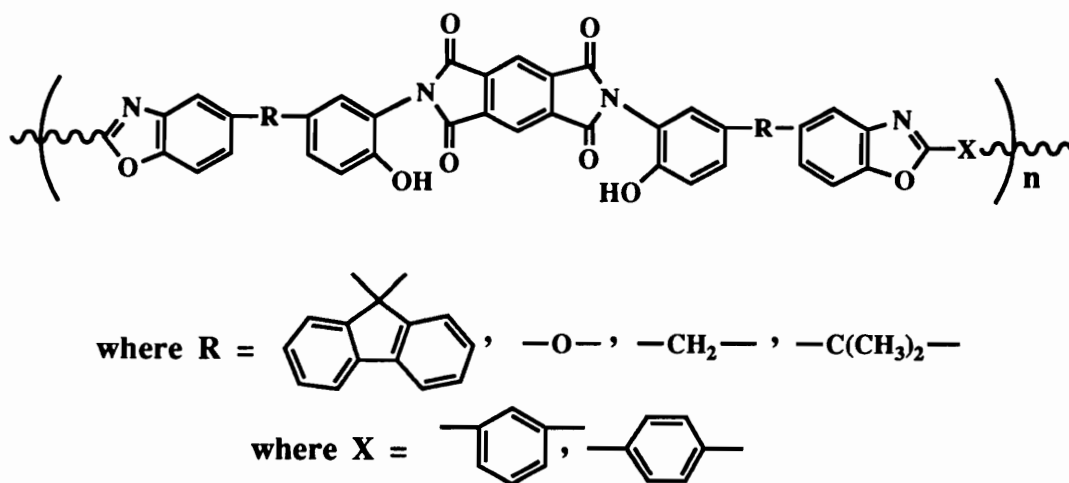


Figure 2.5. Structures of random poly(benzoxazole imide) copolymers [59].

Yakubovich [62] reported the synthesis of block copolymers containing benzoxazole and imide functionality's in the late 1960's.

Copolymerizing amine terminated oligomers of 3,3'-dihydroxybenzidine and terephthaloyl chloride with amine terminated oligomers of 4,4'-oxydianiline and pyromellitic dianhydride (PMDA) in the presence of excess PMDA reportedly resulted in carboxy and hydroxy substituted block polyamides. Subsequent cyclodehydration generated block poly(benzoxazoles imide) in good yields. It was found that higher molecular weights could be achieved with higher imide content and the presence of TEA or pyridine hampered the polymerization of PMDA. Thermal treatment of polymer films at 200°C resulted in imidization only and it wasn't until the films were exposed to 400°C, that benzoxazole formation was complete. The segmented poly(benzoxazole imide) copolymer structure is illustrated in Figure 2.6. Moderate to high molecular weights were achieved in nearly all cases. Tensile strengths varied from 127.4-166.6 MPa and elongation at break varied from 4-20%.

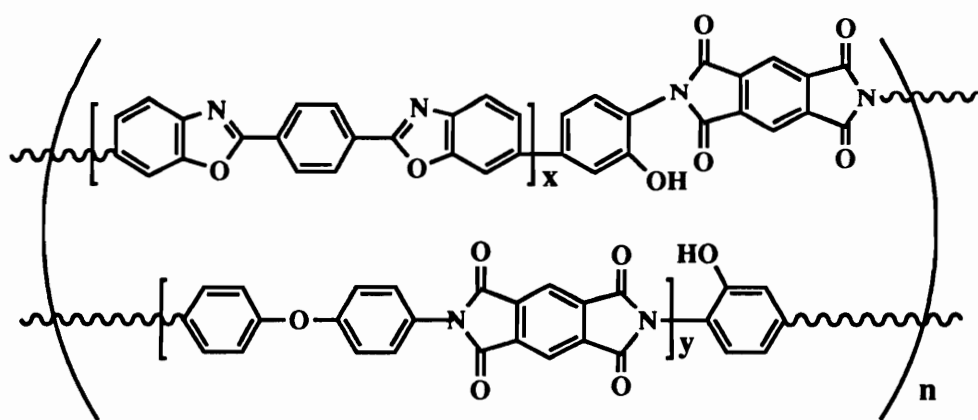


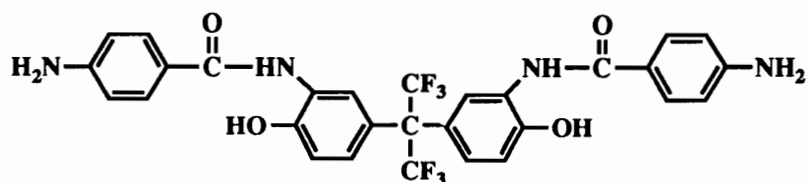
Figure 2.6. Structure of segmented poly(benzoxazole imide) [62].

Yoda and coworkers [63,64] generated hydroxy substituted dianhydrides by reacting trimellitic anhydride with various bis(*o*-aminophenols) and regenerating the anhydride functionality. Subsequent polymerization with diamines and cyclodehydration at elevated temperatures resulted in poly(benzoxazole imide) copolymers. Alternatively, polymerization of the acid chloride derivative of trimellitic anhydride with 3,3'-dihydroxybenzidine resulted in substituted polyamides of similar structure. Under these conditions, a 5% excess of trimellitic anhydride was required due to the proposed loss of acid chloride functionality in the presence of triethylamine or pyridine. Mechanical properties and thermal stabilities were very similar to the block copolymers reported by Yakobovich [62].

Reversing the order of addition, Preston [65] generated acid chlorides from 4,4'-oxydianiline and trimellitic anhydride. The acid chloride analog of the condensate of trimellitic anhydride and *p*-aminobenzoic acid was also reported. Polymerization of these monomers with 3,3'-dihydroxybenzidine followed by thermal treatment resulted in poly(benzoxazole imide) copolymers. Fibers spun from poly(hydroxy amide)/DMAc solutions and heat treated exhibited moderate mechanical properties at room temperature (tensile moduli = 36-64 g/den., tenacity = 1.4-2.2 g/den and elongation = 10-22%), but surprisingly good mechanical properties were observed after aging at 300°C for 35 days (tensile moduli =

37-79 g/den., tenacity = 1.5-1.8 g/den and % elongation = 2-11%). Thermo-oxidative stabilities were apparently excellent.

Adamantane containing poly(benzoxazole imide)s have been generated by coreacting 3,3'-dihydroxybenzidine and an adamantane containing diamine with trimellitic anhydride, followed by thermal cyclodehydration [66]. Stephenson and coworkers [67] generated poly(sulfone benzoxazole) resins by coreacting bis[4-(3-chloro-carbonylphenoxy)phenyl]sulfone, its nadic dicapped derivative and 3,3'-dihydroxybenzidine in DMAc. Application of heat resulted in the generation of 3-dimensional networks. Soluble, fluorinated poly(benzoxazole imide)s have been synthesized by condensing 2,2-bis[3-(4-amino)-benzoylamino-4-hydroxyphenyl]hexafluoropropane



with various dianhydrides and cyclizing via thermal treatment [68]. Poly(ester benzoxazole)s have also been synthesized by condensing 2-(4-hydroxyphenyl)-5-amino-4-hydroxybenzoxazole with isophthaloyl chloride followed by thermal cyclization at elevated temperatures [69].

In addition to the low temperature polymerization of acid chlorides with bis(*o*-aminophenols) to generate polybenzoxazoles, numerous other examples of low temperature polymerizations of alternate monomers have been reported. Shono and coworkers

[70,71] synthesized chloro-substituted polyamides, which upon exposure to ammonia/ KNH_2 or heat result in polybenzoxazoles. Polyesteroximes, synthesized from bis(carbohydroxamoyl chloride)s and bisphenates were reported to cyclize to polybenzoxazoles upon exposure to *p*-toluenesulfonic acid [72]. Costanza [73] and Korshak [74,75] were able to generate polybenzoxazoles via reductive cyclization of poly(*o*-nitro ester)s. Treatment of dicarboxylic acids with bis(*o*-methoxy isocyanate)s at 90°C, followed by thermal treatment, also yielded polybenzoxazoles [76]. Similarly bis(*o*-aminoanisole)s can be reacted with acid chlorides and thermally cyclized to polybenzoxazoles [79,80]. PBO films of monolayer thicknesses have been formed by reacting aromatic alkylaldimines with hydrochloride salts of bis(*o*-aminophenol)s, followed by thermal cyclization [79,80].

2.3. Melt Polymerizations

Simultaneous patents by Brinker and Stephens [11,82] reported the use of melt polymerizations to generate aliphatic polybenzoxazoles. Reacting bis(*o*-aminophenol)s with aliphatic dicarboxylic acids or self-condensation of ω -(*o*-aminohydroxy-

phenyl)aliphatic carboxylic acids resulted in melt processable materials with desirable mechanical properties.

In 1965, Moyer, Cole and Anyos [21] extended this work to include aromatic acid chlorides and wholly aromatic AB monomers.



A general polymerization scheme is outlined in Figure 2.7. The authors examined a variety of carboxylic acid derivatives and found that phenyl esters give superior results, but even with this functional group, loss of monomer due to sublimation was a problem.

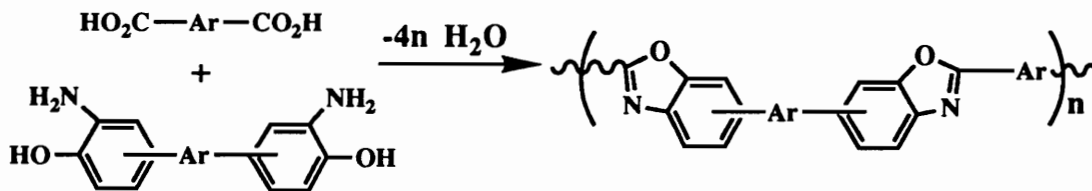
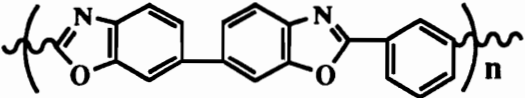
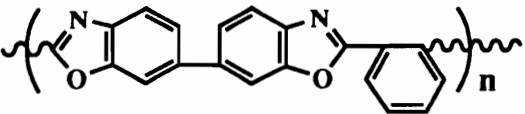
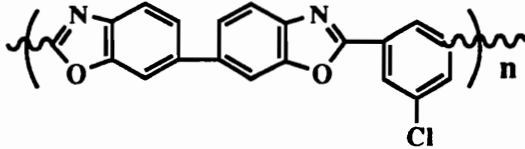
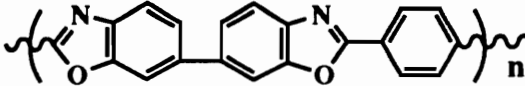


Figure 2.7. General polybenzoxazole melt polymerization scheme.

Reaction temperatures ranged from 220-330°C, depending on polymer structure. The reaction mixture typically went through a homogeneous solution stage followed by solid state polymerization. Application of vacuum at the end of the reactions to further drive the equilibrium towards poly(hydroxy amide) had little effect on

molecular weight. Representative polymers, reaction conditions and η_{inh} 's are outlined in Table 2.5.

Table 2.5. Polybenzoxazoles derived from comonomers via melt polymerization [21].

Polymer Repeat Unit	Reaction Time (hr)	Reaction Temp. (°C)	η_{inh}^a (dl/g)	Solubility in H ₂ SO ₄ %
	6	300-330	0.43	99%
	24	250-330	0.93	100%
	48	280-310	0.20	75%
	26	220-280	0.25	77%

^aRun in H₂SO₄ at 25°C (0.2%)

The AB monomers failed to form high molecular weight polymer using the above mentioned melt polymerization techniques and therefore were prepolymerized using an indirect SOCl₂ catalyzed polymerization technique. The phenyl ester/aminophenol endcapped oligomers prepared by this technique were subsequently chain extended and cyclized using the melt polymerization process. In general, the polymers were found to be infusible and insoluble in all organic solvents and, in some cases, crystallinity was observed.

Chemical and thermal stability tended to increase with molecular weight, but all polymers were reported to be very thermally stable.

At nearly the same time, Korshak and coworkers [60,61,83] reported on a series of aliphatic and aromatic polybenzoxazoles. Using similar polymerization techniques, the authors were able to generate polybenzoxazoles with enhanced solubility and good thermal stability. Figure 2.8 and Table 2.6 exhibit some of the structures and properties associated with these polymers. The majority of thermal characterization carried out on these polymers was limited to dynamic thermal gravimetric analysis. The polymers containing aliphatic or oxymethylene linkages started to degrade at temperatures as low as 200°C, while the polymers containing the fluorene or $-\text{C}(\text{CH}_3)_x(\text{Ph})_y-$ (where x or $y=0-2$) bridging groups showed enhanced thermal stability with degradation commencing at temperatures higher than 300°C.

In 1970, Kokelenberg and Marvel [84] reported the synthesis of poly(5,5'-bibenzoxazole-2,2'-diyl-1,5-anthrylene) via the melt polymerization of diphenyl 1,5-anthracenedicarboxylate and 3,3'-diaminobiphenol. Polymer structure was confirmed by IR spectroscopy and elemental analysis. Additionally, the polymer was only soluble in sulfuric acid and exhibited degradation onset around 420°C. Six years later, Breed and Wiley [85] synthesized siloxane modified polybenzoxazoles via melt polymerizations. Incorporation of the siloxane functionality was accomplished by polymerizing the 3,3'- and 4,4'- isomers of diphenyl(1,1,3,3,-tetraphenyldisiloxane)-

dibenzoate with 3,3'-dihydroxybenzidine. Final polymerization temperatures ranged from 300-325°C and the resulting polymers

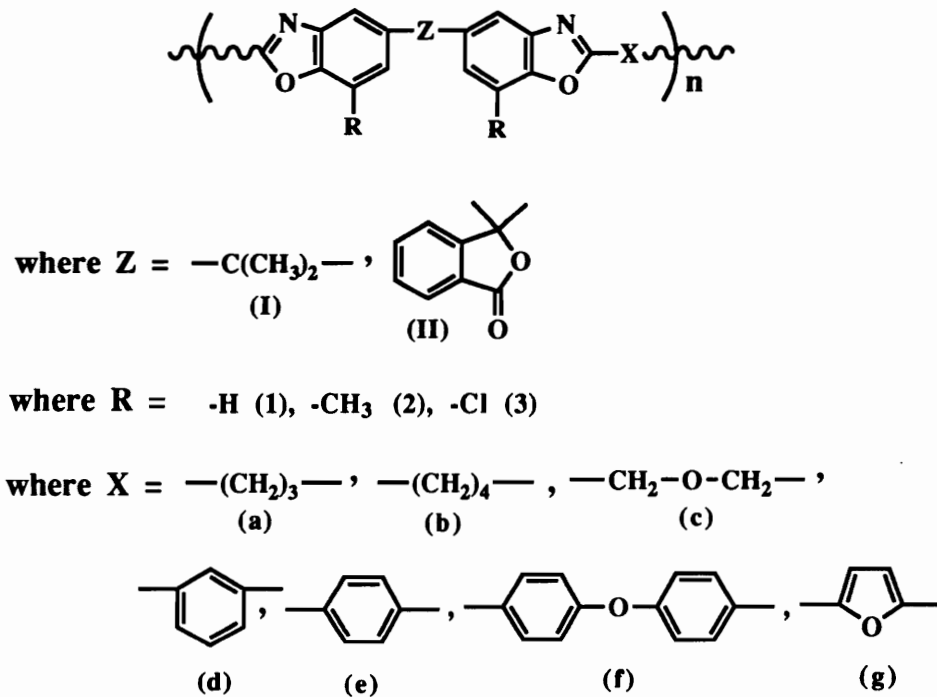


Figure 2.8. Polybenzoxazole structures reported by Korshak [60].

Table 2.6. Solution and thermal properties of the polybenzoxazoles displayed in Figure 2.8 [60].

Polymer Structure (Z-R-X)	η_{red}^a (dl/g)	Degradation Onset Temp. (°C)	Morphology
I-1-a	0.38	~420	Amorphous
I-1-b	0.32	~420	Amorphous
I-1-c	0.18 ^b	~250	Amorphous
I-1-d	0.15	~500	Amorphous
I-1-e	0.16	~500	Slightly Crystalline

(continued on next page)

(continued from the previous page)

I-1-f	0.21	~420	Amorphous
I-1-g	0.12	~450	Amorphous
I-2-a	0.34	~300	Slightly Crystalline
I-2-b	0.32	~400	Slightly Crystalline
I-2-c	---	~200	Amorphous
I-2-d	0.18	~400	Amorphous
I-2-e	0.17	~400	Amorphous
I-2-f	0.20	~300	Amorphous
I-2-g	0.15	~300	Amorphous
II-1-a	0.17 ^b	~330	Amorphous
II-3-a	---	~280	Amorphous
II-3-b	---	~220	Slightly Crystalline
II-3-c	---	~250	Amorphous
II-3-d	---	~180	Amorphous

^aRun in chloroform at 20°C (0.5%)

^bRun in sulfuric acid at 20°C (0.5%)

were soluble in pyridine and N-methylpyrrolidinone. Inherent viscosities, measured in pyridine (concentration and temperature not reported), ranged from 0.17-0.38 dl/g, T_g 's of the 3,3'- and 4,4'-PBO's were 160°C and 221°C respectively and both polymers showed less than 4% weight loss at 500°C in air (1.25°C/min).

More recently, Painter and coworkers [86,87] described the synthesis of polybenzoxazole-polybenzimidazole block copolymers via melt polymerization. Condensing 3,3'-dihydroxybenzidine with an excess diphenyl isophthalate resulted in phenyl ester terminated

polybenzoxazole oligomers which were subsequently condensed with polybenzimidazole oligomers in the melt. Reaction temperatures of 375°C or greater were required. The resulting materials were reported to be brittle solids which possessed 10% weight losses in N₂ of 627°C. Polybenzoxazoles from the melt polymerization of aromatic aminophenols and aromatic dialdehydes have also been reported [88].

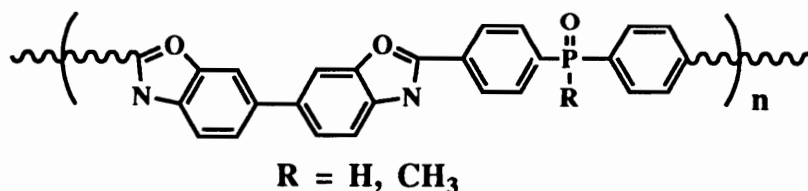
2.4. Synthesis of Polybenzoxazoles in Polyphosphoric Acid

The use of low temperature polymerizations for the synthesis of polybenzoxazoles has resulted in a large number of structural variations in the polymer backbone, as well as an interesting number of copolymers. Unfortunately, the drawbacks associated with this technology (e.g., high cyclization temperatures, inert cyclization atmospheres, shrinkage during cyclization) have hampered its widespread application. In an effort to circumvent these difficulties, Imai [89,90] implemented the use of polyphosphoric acid (PPA) as a condensation/cyclization media in the synthesis of polybenzoxazoles. Polyphosphoric acid was selected as a solvent because of its ability to catalyze carboxylic acylation reactions, in addition to its non-oxidizing nature and

ability to act as a dehydrating agent. In the synthesis of polybenzoxazoles, it has been proposed that PPA activates carboxylic acid groups toward nucleophilic substitution (hydroxyl groups being the nucleophile), as well as trapping the water formed during the condensation and cyclization process [89]. Additionally, polyphosphoric acid was shown to be an excellent solvent for the resulting polymers.

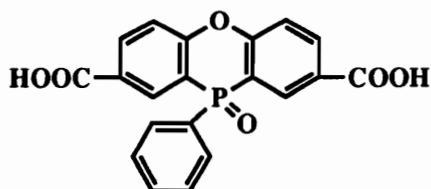
Imai chose 3-amino-4-hydroxy benzoic acid and its isomer, as well as 3,3'-dihydroxybenzidine and iso- or terephthalic acid as monomers in his initial work. The resulting polymers were only soluble in sulfuric acid, possessed inherent viscosities of 0.40-2.21 dl/g (H₂SO₄, 0.20%, 30°C) and exhibited some crystallinity. Onset of thermal decomposition in air was approximately 450°C.

Yokoyama and coworkers [91] reported using PPA as a polymerization solvent in the synthesis of phosphorus containing polybenzoxazoles of the following general structure:



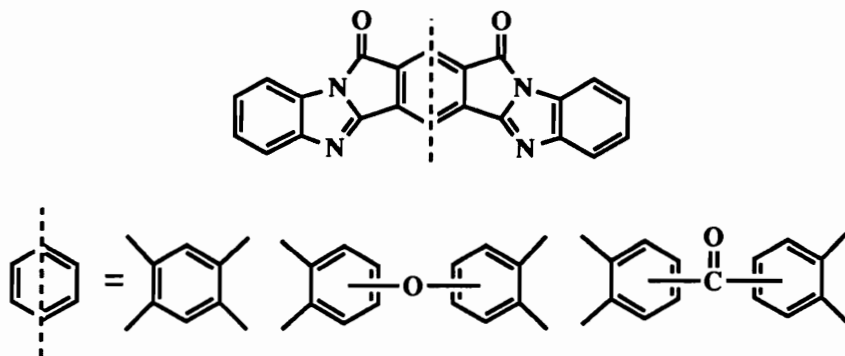
The solubility of these polymers was enhanced, but improvements in flame retardancy were negligible relative to the polymers reported by Imai. Thermo-oxidative stability also proved inferior. The

reason for the poor properties exhibited by these polymers may lie in the fact that only low molecular weight materials were obtained. Phenoxaphosphine oxide dicarboxylic acid has also been incorporated



into polybenzoxazoles using PPA [92,93], but like the above mentioned phosphorus containing polymers, low molecular weight material resulted. The thermo-oxidative stability of these polymers proved superior to the previously mentioned phosphorus containing polymers, but inferior to polyimides of analogous structure [94].

Korshak and coworkers [95] described the synthesis of benzimidazole substituted polybenzoxazoles via the ring opening polymerization of cyclic lactams. Bis(*o*-aminophenol) comonomers



containing oxygen, methylene and sulfonyl linking groups were polymerized in PPA with 3,3'-dihydroxybenzidine. Judging from the

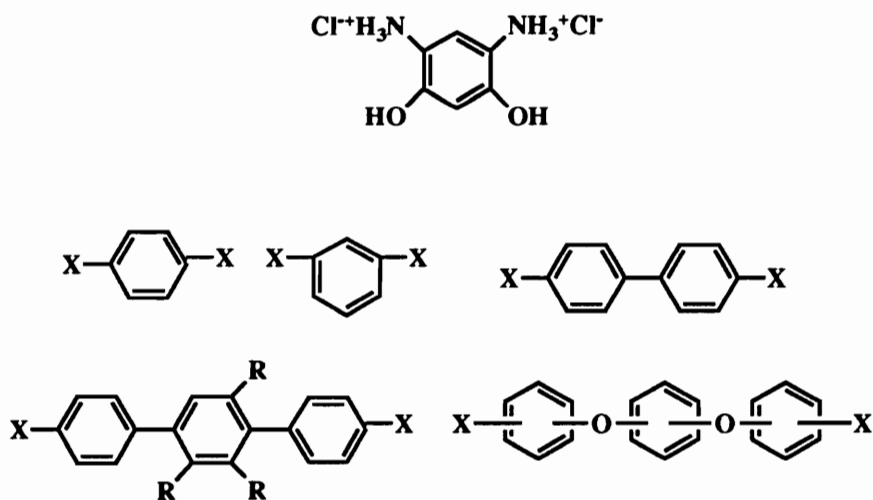
reduced viscosities and the low 10% weight loss values (in air), the polymers must have been of low molecular weight. Glass transition temperatures ranged from 290-370°C, with the PMDA based system being the highest. Surprisingly, the authors reported these materials to be soluble in DMAc, NMP, m-cresol and hexamethylphosphoramide (HMPA) at elevated temperatures.

Wolfe [96] attempted the polymerization of 2,5-diaminohydroquinone with various dicarboxylic acids in PPA, but due to the oxidative instability of 2,5-diaminohydroquinone's in the reaction mixture, only low molecular weight species were recovered.

The limited number of references cited above suggests that little research was conducted relative to the synthesis of polybenzoxazoles in polyphosphoric acid prior to the late 1970's. It should be mentioned that a number of workers reported using PPA as a cyclization media for polybenzoxazoles, but it wasn't used as a condensing or polymerization medium [12,37,84]. This trend of avoiding the use of PPA changed in the late 70's with the realization that wholly aromatic, rigid rod polymers could be synthesized in polyphosphoric acid [97-100].

In a series of papers which followed the original disclosures, Wolfe, Arnold and others [101-104] outlined in detail, the synthetic methodology required to generate high molecular weight polybenzoxazoles. Some of the monomers used are displayed in Figure 2.9. A typical reaction procedure consisted of first preparing a 1.52/1.0 (w/w) solution of phosphorus pentoxide and PPA, adding a

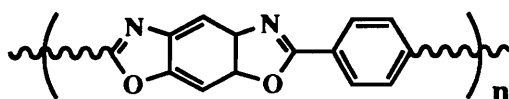
bis(*o*-aminophenol) dihydrochloride salt and diacid, dehydrochlorinating at $\sim 90^{\circ}\text{C}$ for an extended period of time and finally raising the temperature to $\sim 200^{\circ}\text{C}$ over the course of several days. Typical reaction concentrations ranged from 2-15% solids. The resulting polymers possessed intrinsic viscosities ranging from 0.60-12.7 dl/g in methanesulfonic acid at 30°C . The lower $[\eta]$'s were obtained on polymers with *meta* linked diphenoxy linkages and this was attributed to acylation side reactions. Two ether linkages *meta* to one another on the central phenyl ring provide the correct reaction geometry, as well as the enhanced electrophilic character to undergo Friedels-Craft acylation reactions with carboxylic acids.



where X = COOH, CN, COCl, CO₂CH₃
R = H or Phenyl

Figure 2.9. Monomers used in the synthesis of polybenzoxazoles.

It was found, in general, that phenylated and oxygen linked polymers were more soluble, but solubility was still limited to acidic solvents. Dynamic and isothermal thermal properties of these materials were excellent, with the least substituted polymer (cis PBO) out performing the substituted analogs (onset of degradation was greater than 550°C). It should be pointed out that only the



cis PBO

polymer synthesized with 100% terephthalic acid formed a liquid crystalline state when dissolved in methanesulfonic acid (5% solids). This observation will be further described in the following section. Mechanical properties obtained on dry-jet wet spun fibers are shown in Table 2.7 [105].

During these initial efforts to synthesis high molecular weight polybenzoxazoles, the critical importance of the P_2O_5 concentration in the polymerization mixture was recognized. It was observed that with higher P_2O_5 concentrations, a higher percentage of polymer could be dissolved in the polymerization mixture and higher molecular weights could be achieved. Unfortunately, higher concentrations of P_2O_5 at the beginning of the polymerization also meant monomer solubility, as well as dehydrochlorination, was hindered. Recognition of these facts resulted in the development of

Table 2.7. Cis polybenzoxazole fiber spinning parameters^a and fiber properties [105].

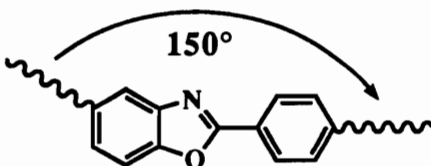
Coagulation Bath	Jet Velocity	Spin Draw Ratio	Elong. %	Tenacity g/den.	Mod. g/den.
MSA/H₂O	m/min	Ratio	%	g/den.	g/den.
30/70	4.5	1.4	1.4	4.2	502
40/60	6.3	1.1	2.4	3.4	340
40/60	6.3	1.0	6.6	2.3	132
50/50	6.3	<1.0	8.7	1.3	81

^aPolymer $[\eta]^{25^\circ\text{C}} = 2.8$ dl/g in MSA; dope concentration, 8.6% in 97.5% methanesulfonic acid and 2.5% chlorosulfonic acid; dope and coagulation bath temperatures, room temperature; spinneret, 10 X 100 μm . 1 g/den (gram/denier) = 12,800 ρ psi; 1 GPa = 145,000 psi.

an incremental addition technique for the P₂O₅, thereby maintaining monomer solubility, an adequate rate of dehydrochlorination and high polymer concentrations. This incremental addition of phosphorus pentoxide has become known as the "P₂O₅ adjustment method" [18,106]. The advent of the P₂O₅ adjustment method allowed for the generation of high molecular weight ($[\eta] \sim 10\text{-}30$ dl/g, 25°C, CH₃SO₃H) rigid rod polymers, as well as the synthesis of liquid crystalline polymerization mixtures; an important criteria for the preparation of high molecular weight polymers and high strength fibers [104].

AB monomers (3-amino-4-hydroxy benzoic acid and its isomers) could also be polymerized to high molecular weights, but required the use of higher monomer and P₂O₅ concentrations [107]. Higher

polymer concentrations (~14% solids) were required because poly-(2,5-benzoxazole) has a catenation angle of 150° (angle between the two exocyclic bonds in the monomer repeat unit) and therefore



assumes a variety of chain conformations in solution [108]. Increasing the polymer concentration, forces the polymer into its energetically favored extended or trans conformation and as a result, anisotropic reaction mixtures were achieved. Note that ~14% solids were required to achieve an anisotropic reaction mixture compared to only 5% solids for the rigid rod polymers. Higher P_2O_5 concentrations were also required to scavenge the extra water evolved. For a detailed review of the P_2O_5 adjustment method see references 18 and 106.

Processing these polymers usually involved dry-jet, wet extrusion of polymerization mixtures, followed by thermal treatments under tension. The extension and heat treatments were required in order to achieve optimal mechanical and thermal properties [109,110]. Polybenzoxazole ribbons and fibers generated by this process exhibited outstanding thermal and mechanical properties. Isothermal aging (371°C in air) of heat treated poly(2,5-benzoxazole) (2,5 PBO) and poly(benzobisoxazole-2,6-diyl-1,4-phenylene) (cis PBO) fibers resulted in weight losses of 8 and

12%, respectively, after an initial 12% weight loss due to water. Mechanical properties of fibers spun from anisotropic solutions are shown in Table 2.8. Note the extremely high tensile moduli and strengths of these fibers relative to previously reported mechanical properties (tensile moduli and strengths of 2-4 GPa and 120-160 MPa respectively).

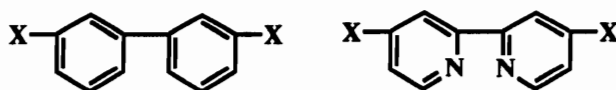
Table 2.8. Mechanical properties of 2,5 PBO and cis PBO after various thermal and tension treatments [18].

	AB PBO-1	AB PBO-2	AB PBO-2	PBO-3	PBO-4
<i>Spinning conditions</i>					
spin-draw ratio	6.6:1	145:1	100:1	6:1	53:1
spin temp, °C	65	90	90	63	70
air-gap distance, cm	32	21	21	21	20.3
jet dia, mm	0.38	0.25	0.25	0.38	0.25
<i>Spun-fiber properties</i>					
tensile strength, GPa ^c	2.34	3.6	2.83	3.0	3.12
tensile modulus, GPa ^c	41-96	133	61	90	303
strain at break, %	na	3.3	4.8	4.2-6	na
fiber dia, μm	na	na	21	33	na
<i>Heat-treatment conditions</i>					
temp, °C	500		400	500	450 500
time, s	60		30	60	30 30
stretch factor, %	7.5		4.4	na	2 2.5
atmosphere	nitrogen		nitrogen	nitrogen	air air
<i>Heat-treated fiber properties</i>					
tensile strength, GPa ^c	2.34		3.34	3.45	3.1 3.6
tensile modulus, GPa ^c	136		115	317	410 467
strain at break, %	na		3.6	1.8-2.4	na na
fiber dia, μm	na		na	31	na na

The phenomenal thermal and mechanical properties of the polybenzoxazoles discussed above have not gone unnoticed by industry. Currently there are 4 major efforts in this area, Dow Chemical Co., Wright Patterson Materials Laboratory, SRI Industries and the Research Development Corporation of Japan. Because of the industrial importance of these materials, external publications

regarding the effect of variations in polymer structure on physical behavior have been limited.

Structural modifications of these polymers have been conducted with the purpose of improving solubility and modifying the properties of fabricated articles. Altering the polymer backbone by incorporating a certain percentage of *meta* linked dicarboxylic acid



where X = COOH, CN, COCl

derivatives has resulted in ordered reaction mixtures, but hasn't produced an appreciable increase in solubility [111,112]. Using stoichiometric quantities of the *meta* linked monomers resulted in low molecular weight polymers as judged by their low inherent viscosities. Incorporation of a large quantities of terephthalic acid comonomer allowed for the preparation of high molecular weight polymer ($\eta_{inh} = 1.4-7.6$ dl/g (CH₃SO₃H, 0.2%, 25°C). Solution concentrations of 11% were required during these copolymerization in order to maintain stir opalescence throughout the polymerization. Unfortunately, the authors only reported the polymerization of the pyridinyl monomer with 2,5-diamino-1,4-benzenedithiol dihydrochloride and not with 2,6-diaminoresorcinol dihydrochloride. Isothermal aging of the copolymers at 300°C and 371°C gave results similar to those obtained on cis PBO (Figure 2.10). This should not be unexpected considering most of the polymer was cis PBO. Tensile

strength and moduli values obtained on films cast from methanesulfonic acid ranged from 5.8-6.9 ksi and 259-351 ksi respectively.

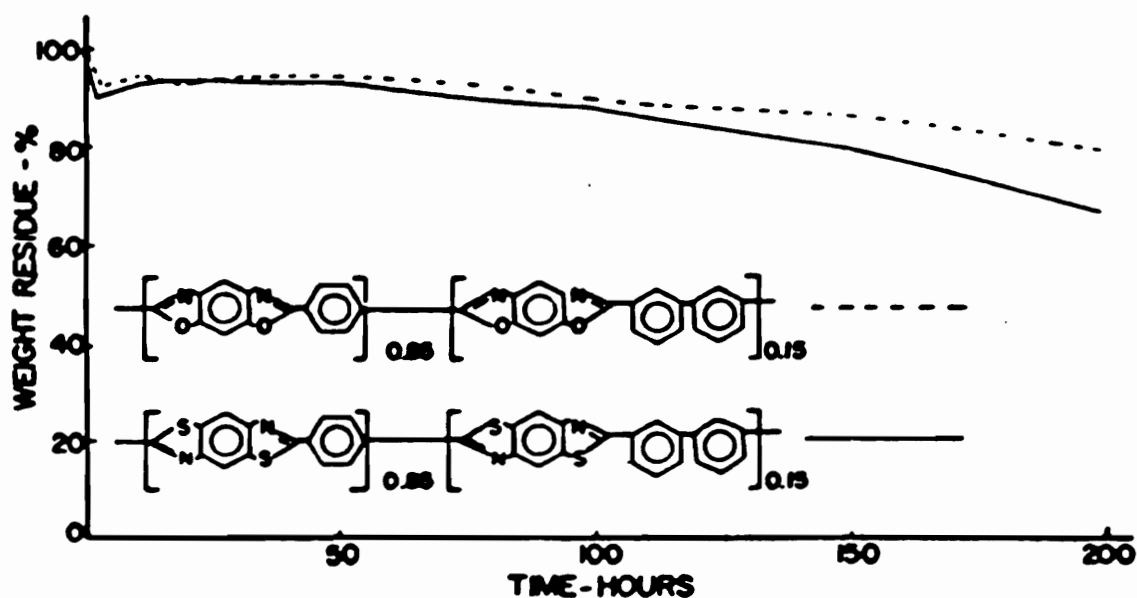


Figure 2.10. Isothermal aging curves for biphenyl modified cis PBO and cis PBT at 371°C in air [111].

A series of papers by Arnold and coworkers [113-117] have described the synthesis of monomers and polybenzoxazoles containing pendent aromatic moieties (Figure 2.11). Initial work with phenoxy phenyl substituted dicarboxylic acids was directed at synthesizing soluble *para* catenated polymers, but only low molecular weight species were recovered from the polymerizations. Initially it was thought that the pendent phenoxy moieties were

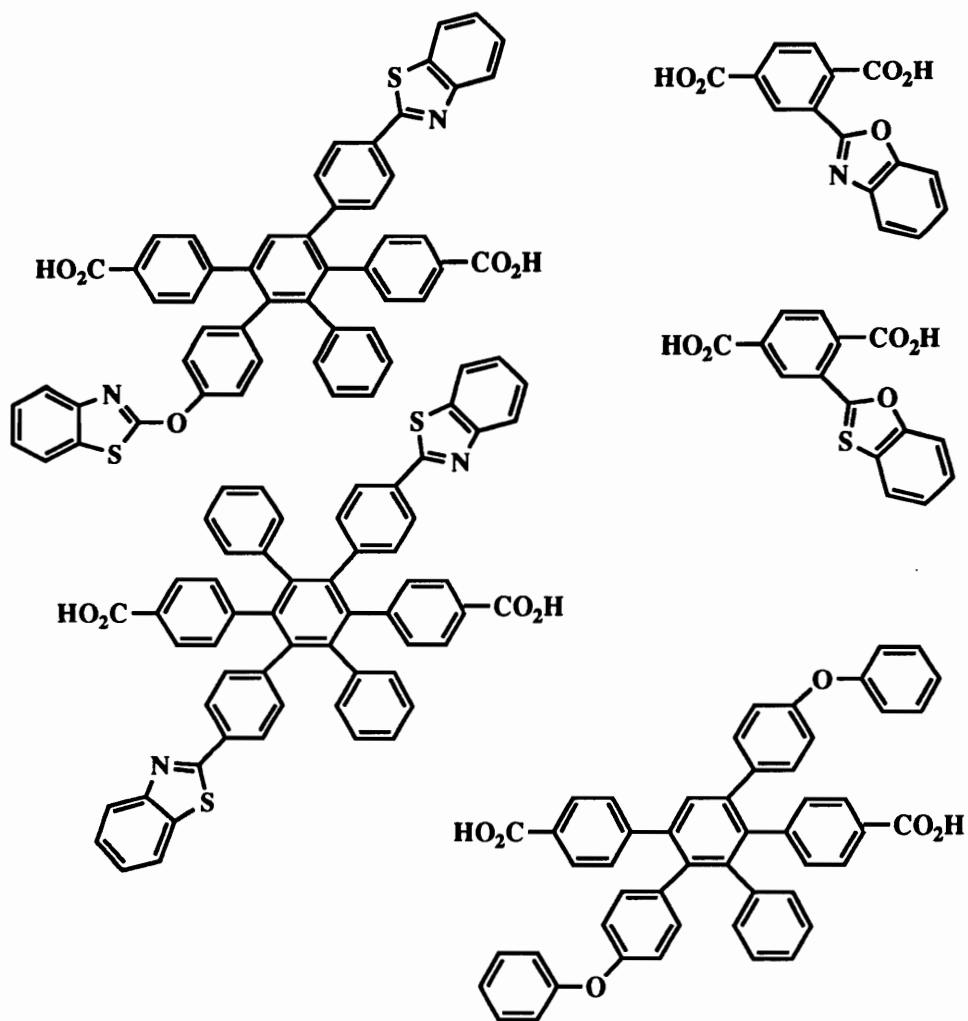


Figure 2.11. Various substituted dicarboxylic acids [113-117].

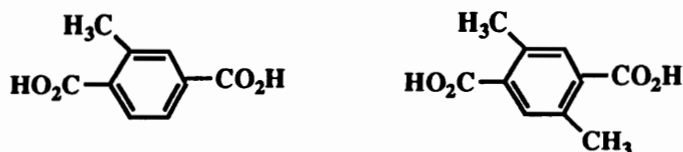
interfering with the condensation process, but subsequent investigations identified the insolubility of the phenoxyphenyl dicarboxylic acids as the limiting feature of the polymerization [115]. This led to the synthesis of polyphosphoric acid soluble benzoxazole and benzothiazole substituted dicarboxylic acid

monomers. Polymerizations carried out using the dicarboxylic acid with one pendent benzothiazole and 2,6-diaminoresorcinol dihydrochloride resulted in anisotropic reaction mixtures at 10-18% solids. The polymer ($[\eta]^{23^{\circ}\text{C}} = 4.5 \text{ dl/g}$, $\text{CH}_3\text{SO}_3\text{H}$) exhibited solubility in protic solvents, possessed no glass transition temperature (DSC or TMA) and showed inferior thermal properties relative to cis PBO. The premature thermal degradation was attributed to the loss of pendent benzothiazole linkages.

In contrast, polymerizations conducted with dicarboxylic acids bearing two benzothiazolyl phenyl substituents and 2,6-diaminoresorcinol dihydrochloride afforded high molecular weight polymer ($[\eta]^{25^{\circ}\text{C}} = 7.7 \text{ dl/g}$, $\text{CH}_3\text{SO}_3\text{H}$). Low reaction concentrations (~1%) were required to keep the polymers in solution and attempts to promote anisotropy in the reaction mixture by increasing percent solids resulted in premature precipitation of low molecular weight material. It was postulated that the long benzothiazolyl pendent groups prevented alignment of the polymers in solution and resulted in isotropic polymerization mixtures. Thermal properties of these materials were similar to the previously mentioned benzothiazole and phenoxy substituted polymers.

Dicarboxylic acids supporting pendent methyl groups were also investigated by Arnold [118,119]. The rationale behind using pendent methyl groups was to enhance mechanical properties, especially the transverse and compressive properties via network

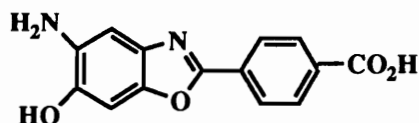
forming post-reactions in the solid state. Both the mono and dimethylated derivatives of terephthalic acid were polymerized



where X = COOH, CN, COCl

with 2,6-diaminoresorcinol dihydrochloride in PPA at solids concentrations of 12% (anisotropic reaction mixtures obtained). The resulting polymers ($[\eta]^{25^\circ\text{C}} \sim 10 \text{ dl/g (CH}_3\text{SO}_3\text{H)}$) exhibited solubility only in protic solvents. Exposure to elevated temperatures (300-350°C) in air for 30 to 40 seconds rendered the polymers insoluble. The same results could be obtained in a N₂ atmosphere, but only at temperatures of 500-550°C. Radiation crosslinking was also reported. TGA-MS analysis indicated methane loss initiated at 420°C and maximized at 580°C.

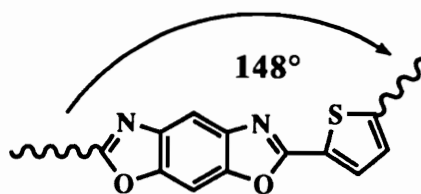
Chen and Feld [120] reported polymerizing an oxazole containing



AB monomer to moderate molecular weight ($[\eta]^{30^\circ\text{C}} = 6.5\text{-}12.5 \text{ dl/g, CH}_3\text{SO}_3\text{H}$). The final polymer structure was identical to the cis PBO polymers generated by Arnold. No thermal or mechanical data was reported. Adamantane dicarboxylic acid derivatives were

incorporated into polybenzoxazole backbones in an effort to obtain colorless, transparent films [121]. Polymerization of the 4,9-dimethyl ester with 2,6-diaminoresorcinol dihydrochloride generated light yellow, anisotropic reaction mixtures at 14% solids. Upon precipitation into water, white fibrous material was obtained ($[\eta]^{30^\circ\text{C}} = 9.8 \text{ dl/g}$, $\text{CH}_3\text{SO}_3\text{H}$). No thermal, optical or mechanical data were reported, but incorporation of adamantane moieties into the backbone of polybenzothiazoles eliminated all absorbances in the visible and near-infrared regions, in addition to rendering the polymer more thermo-oxidatively unstable.

It was previously mentioned that poly(2,5-benzoxazole) required solids concentrations greater than 14% to achieve lyotropic reaction mixtures due to the reduced exocyclic bond angle in the polymer repeat unit. Analogously, Preston and coworkers [122] reasoned that incorporation of 2,5-thiophene dicarbonyl chloride would generate lyotropic reaction mixtures, albeit at higher polymer concentrations. The overall exocyclic bond angle for a thiophene modified cis PBO repeat unit is 148° . Polymerizing 2,5-thiophene dicarbonyl chloride with 2,6-diaminoresorcinol dihydrochloride at a



solids concentration of 20% generated a birefringent (cross polars) reaction mixture, but only low molecular weight ($[\eta]^{30^\circ\text{C}} = 1.8 \text{ dl/g}$,

CH₃SO₃H) material resulted. Thermogravimetric analysis of the resulting polymer indicated no appreciable weight loss up to 500°C in helium.

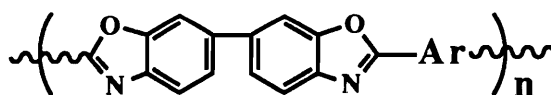
Isotropic reaction mixtures (10% solids) were achieved when 2,2'-bis(4-carboxyphenyl)hexafluoropropane was substituted for terephthalic acid in the synthesis of modified cis PBO [123]. As expected, the inherent viscosities were reduced with the incorporation of the hexafluoropropane linkage ($\eta_{inh}^{30^\circ\text{C}} = 0.72$ dl/g, 2.0%, CH₃SO₃H), while solubility was slightly enhanced. The 10% weight loss in argon was ~550°C and after isothermal aging at 350°C (air) for 300 hours a 6.6% weight loss was recorded. No glass transition temperature was identified via calorimetry.

Sakaguchi and Kato [124] reported the copolymerization of 3,3'-dihydroxybenzidine with 4-aminobenzoic and 3,3',4,4'-biphenyl dianhydride in PPA. The resulting benzoxazole imide copolymers were only soluble in acidic solvents, possessed an inherent viscosity of 0.59 dl/g (30°C, 0.5%, H₂SO₄) and showed a 5% weight loss in air of 478°C.

A modification of the P₂O₅ adjustment method was recently reported by Sato and coworkers [125]. Replacing polyphosphoric acid with methanesulfonic acid afforded a condensation/dehydration reaction medium (PPMA) very similar to PPA. Use of PPMA as a polymerization solvent allows for the added benefit of shorter reaction times and lower temperatures. The milder reaction conditions were attributed to the enhanced reactivity of PPMA

relative to PPA. One drawback associated with PMAA is its ability to acylate electron rich aromatic nuclei (in a Freidel-Crafts manner) at higher reaction temperatures due to increased acidity. Optimum polymerization conditions for the polymerization of 3,3'-dihydroxybenzidine and a series of ether linked dicarboxylic acids consisted of 5 molar monomer concentrations and heating at 140°C for ~4 hours. The structure of the repeat unit and inherent viscosities of the polymers synthesized are shown in Table 2.9. Ten percent weight losses in air were reported to be ~495°C.

Table 2.9. Structure, reaction time and inherent viscosities of DHB polybenzoxazoles polymerized in PPMA at 140°C [125].



Ar	Reaction Time (hr)	η_{inh}^a (dl/g)
	5	4.7
	3	1.3
	3	3.0

^aMeasured at a concentration of 0.2 g/dl in CH₃SO₃H at 30°C.

The PPMA polymerization technique was also used to synthesize fluorinated polybenzoxazoles based on 2,2-bis(3-amino-4-hydroxyphenyl)hexafluoropropane (Figure 2.12) [126,127]. Higher reaction temperatures (160°C) and 10-15% solids were found to be optimal for these particular systems. Much like Sato, the authors reported acylation side reactions when electron rich unhindered aromatic centers were incorporated into monomers. Intrinsic viscosities (30°C, CH₃SO₃H) ranged from 0.3 to 7.9 dl/g. Glass transition temperatures and thermal stabilities are described in section 2.5 (Table 2.10).

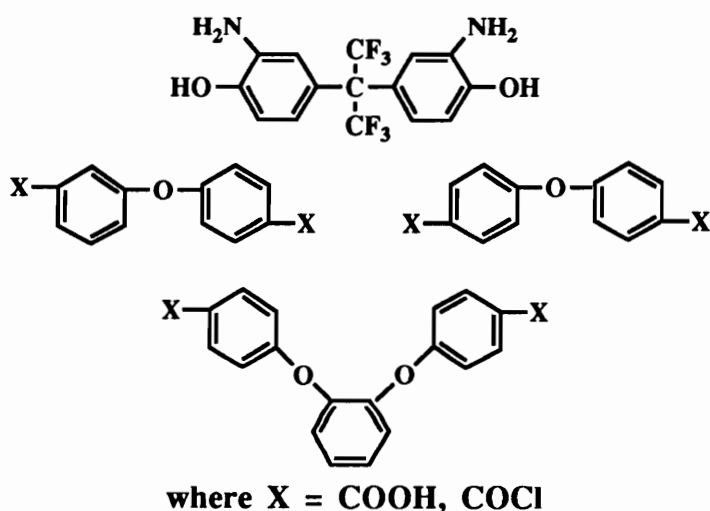
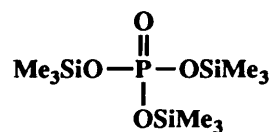


Figure 2.12. Monomers incorporated into fluorinated polybenzoxazoles via PPMA mediated polymerizations.

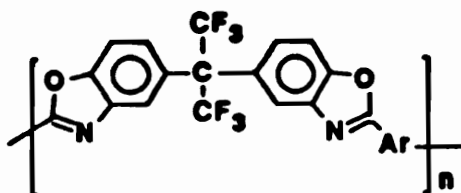
2.5. PPSE Catalyzed Polybenzoxazole Formation

An alternate approach to using polyphosphoric acid/P₂O₅ as a condensing media in the generation of fully cyclized polybenzoxazoles is the use of stoichiometric quantities of tris(trimethylsilyl) phosphate (PPSE). Reinhardt [8,127,128] pioneered the work in this area with the synthesis of fluorinated,



thermoplastic polybenzoxazoles containing the hexafluoroisopropylidene bridging group. A typical polymerization consists of dissolving stoichiometric amounts of bis(*o*-aminophenol), aromatic dicarboxylic acid and PPSE in *o*-dichlorobenzene (~25% solids) and heating at 135° and 165°C for 24 hours. As indicated, 4 moles of PPSE are required [129,130], presumably two moles for the condensation and 2 moles for dehydration. Some of the solution and thermal properties of the polymers are shown in Tables 2.10 and 2.11. Mechanical properties for these polymers were similar to those obtained by Imai using silylated monomers [7].

Table 2.10. Solution properties of PPSE generated PBO's [127]



Polymer	Ar Spacer	Analysis Calc. (Found)	$\eta_{inh}^{a, d, f}$ or $[\eta]$ (dL/g) ^b	Solubility
1 ^c		C, 60.01 (59.68) H, 2.19 (2.38) N, 6.09 (5.79) F, 24.77 (23.60)	2.82 ^a	MSA TCE-phenol H ₂ SO ₄
2 ^c		C, 60.01 (59.55) H, 2.19 (2.53) N, 6.09 (5.80) F, 24.77 (23.60)	2.23 ^a	MSA
3 ^c		C, 57.28 (56.75) H, 1.97 (2.13) N, 9.11 (8.93) F, 24.71 (23.59)	1.82 ^a	MSA H ₂ SO ₄
4 ^c		C, 57.28 (56.00) H, 1.97 (2.29) N, 9.11 (8.54) F, 24.71 (23.40)	2.18 ^a	MSA H ₂ SO ₄
5 ^c		C, 66.82 (66.14) H, 6.52 (6.56) N, 3.63 (3.37) F, 14.75 (14.27)	0.92 ^a 0.52 ^d	MSA CHCl ₃ THF
6 ^{c, e}		C, 63.05 (62.82) H, 2.55 (2.68) N, 5.07 (5.20) F, 20.64 (20.72)	1.43 ^{a, c} 0.75 ^{c, f} 7.9 ^{b, e}	MSA H ₂ SO ₄ CHCl ₃ , THF
7 ^c		C, 63.05 (62.83) H, 2.55 (2.53) N, 5.07 (4.35) F, 20.64 (20.70)	4.1 ^b	MSA H ₂ SO ₄ CHCl ₃ , THF
8 ^e		C, 65.22 (63.15) H, 2.81 (2.83) N, 4.34 (4.14)	6.0 ^b	MSA H ₂ SO ₄ CHCl ₃ , THF

- (a) Inherent viscosity in methanesulfonic acid (0.15 g/dL) at 30°C (403K).
 (b) Intrinsic viscosity in methanesulfonic acid at 30°C (403K).
 (c) Prepared in PPSE/ ρ -dichlorobenzene.
 (d) Inherent viscosity in ρ -dichlorobenzene (0.15 g/dL) at 30°C (403K).
 (e) Prepared in phosphorus pentoxide/methanesulfonic acid.
 (f) Inherent viscosity in 1,1,2,2-tetrachloroethane (0.15 g/dL) at 30°C (403K).
 (g) Prepared in 83% PPA.

Table 2.11. Thermal properties of PPSE generated PBO's [127].

Polymer	T _g ^a (°C), (K)	TGA ^b (°C), (K)	ITA ^c (%)
1	300 (573)	532 (805) air 524 (797) He	95
2	382 (655)	533 (806) air 525 (798) He	94
3	329 (602)	539 (812) air 528 (801) He	92
4	352 (625)	530 (803) air 547 (820) He	59
5	94 (367)	414 (687) air 426 (699) He	50 ^d
6	301 (574)	564 (837) air	---
7	266 (539)	535 (800) air	---
8	245 (518)	545 (818) air	---

- (a) Glass transition temperature determined by DSC ($\Delta T = 10^\circ\text{C}$ (10K)/min).
 (b) Extrapolated onset of major decomposition determined in air and/or helium.
 (c) Isothermal aging, weight retention after 200 h at 346°C (619K) in circulating air.
 (d) Weight retention after 50 h at 346°C (619K) in circulating air.

2.6. Polybenzoxazoles from Silylated Monomers

The first reported use of silylated monomers in the synthesis of polybenzoxazoles was made by Korshak and coworkers in a Russian patent [131]. Silylated 2,5-diaminohydroquinone was treated with various acid chlorides and thermally cyclized to form polybenzoxazoles. More recently, Imai and coworkers [7,132,133] have synthesized a series of silylated bis(*o*-aminophenol)s and successfully polymerized them with various acid chlorides. Some representative monomers and the polymerization scheme are shown in Figure 2.13. Silylation of the amine and hydroxyl groups activates the amines toward acylation reactions and deactivates the hydroxyl groups.

Condensation of these monomers with acid chlorides at low temperatures produces trimethylsilyl substituted poly(hydroxy amide)s and the byproduct, trimethylsilyl chloride. Polymer films could be cast directly from the reaction mixture due to the volatile nature of trimethylsilyl chloride and the absence of amine salts. Alternatively, the polymers could be precipitated and deprotected with dilute acid to generate the precursor poly(hydroxy amide)s. Polybenzoxazole films could also be obtained by thermally treating these polymers. Inherent viscosities for the poly(hydroxy amide)s ranged from 0.62-2.23 dl/g (5%, 30°C, H₂SO₄). Because Imai used

bis(*o*-aminophenol)s with flexible bridging groups, the PBO's exhibited enhanced solubility in common organic solvents.

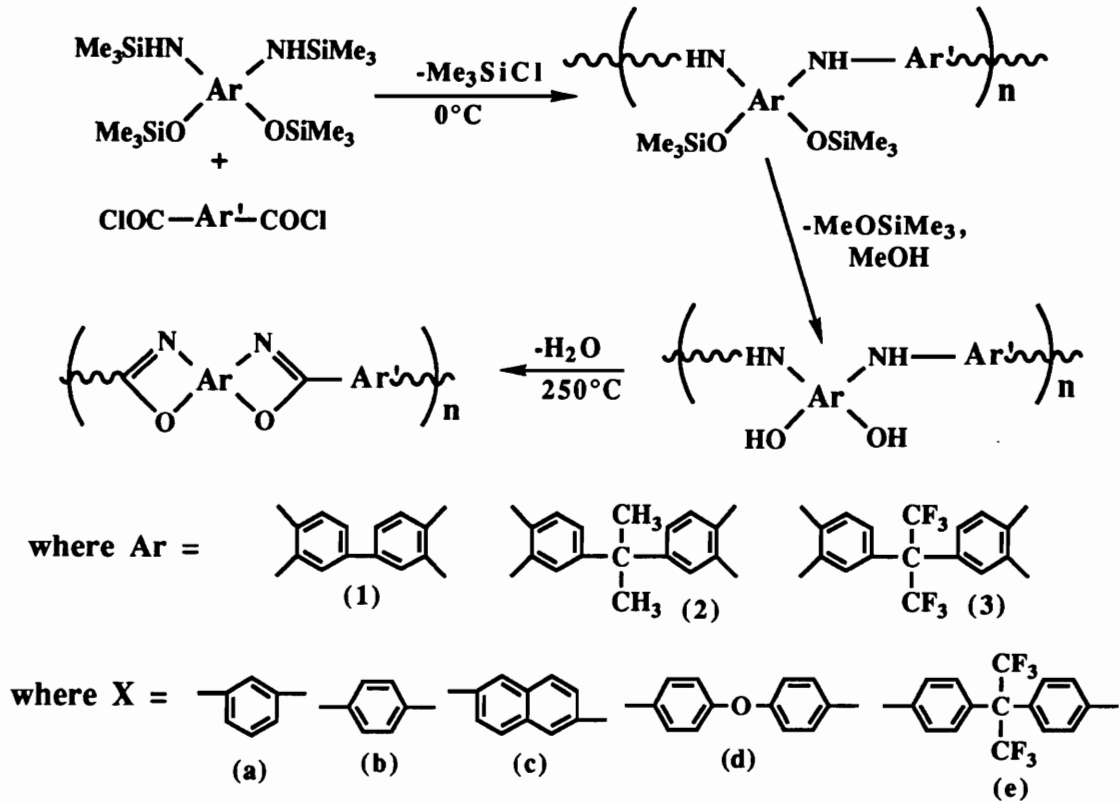


Figure 2.13. Silylated bis(*o*-aminophenol) monomers and polymerization, dehydration scheme [7].

Unfortunately, most of the polymers were still only soluble in sulfuric acid. Glass transition temperatures ranged from 240-325°C and 10% weight loss temperatures varied from 500-570°C (10°C/min, Table 2.12). The tensile strengths, elongations at break and tensile moduli of the films were 43-198 MPa, 2-7% and 2.1-4.5 GPa, respectively (Table 2.13). Due to the low tensile strengths and

low percent elongations, residual solvent or film imperfections are suspected.

Table 2.12. Thermal properties of fluorinated Polybenzoxazoles synthesized via the trimethylsilyl monomers [7].

Polymer	Tg^a (°C)	Decomposition Temp^b (°C)	
		in air	in nitrogen
1a	290	570	620
2a	240	500	530
3a	260	530	545
3b	310	545	555
3c	325	540	560
3d	300	545	560
3e	295	525	530

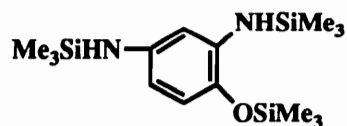
^aDetermined by TMA in air (10°C/min.).

^b10% weight loss (10°C/min.)

Table 2.13. Mechanical properties of fluorinated polybenzoxazoles synthesized with silylated monomers [7].

Polymer	Tensile Strength (MPa)	Elongation at break Percent	Tensile Modulus (GPa)
1a	198	7	4.5
2a	53	2	2.9
3c	93	6	2.4
3d	96	6	2.4
3e	43	2	2.1

Imai extended the silylated monomer technology to include the synthesis of poly(amide-benzoxazole)s [134]. Silylation of 2,4-diaminophenol, followed by low temperature polyamidation and



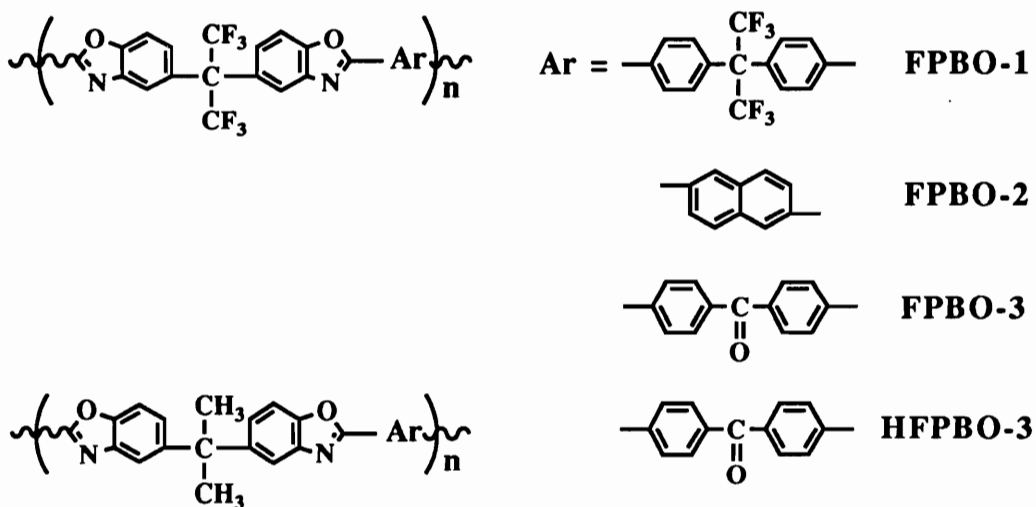
Silylated 2,4-diaminophenol

thermal cyclodehydration resulted in a series of poly(amide benzoxazole)s of moderate molecular weight ($\eta_{inh}^{30^\circ\text{C}} = 0.62\text{-}2.23$ dl/g (0.5 g/dl in DMAc)) and fairly good solubilities in common organic solvents. Glass transition temperatures ranged from 260-300°C (increasing with acid chloride rigidity), and 10% weight loss temperatures of 490-535°C in air and 495-590°C in nitrogen (10°C/min) were reported. Mechanical properties proved to be superior to analogous polybenzoxazoles with tensile strengths, elongations to break and tensile moduli of 104-120 MPa, 7-40% and 2.1-3.5 GPa, respectively.

Permeability and permselectivity investigations [135] were also determined for some of the above mentioned polybenzoxazoles and in general, the PBO's performed similarly to analogous polyimides. Fractional free volume measurements revealed that the poly(hydroxy amide)s possessed less free volume than fully cyclized PBO's and that free volume increased with incorporation of fluorine. This increase was rationalized on the bases of increased steric effects

and reduced molecular interactions. Selected permeability, diffusion and solubility coefficients are presented in Table 2.14. Because of the great variety in permeability and permselectivity between the various polymers and gases the interested reader is referred to reference 135 for details.

Table 2.14. Permeability (P), diffusion (D) and solubility (S) coefficients for polybenzoxazoles at 35°C and 10 atm [135].^a



Gases		FPBO-1	FPBO-2	FPBO-3	HPBO-3
H ₂	P	120	24	37	12.5
	D	550	140	230	86
	S	0.22	0.17	0.16	0.14
CO ₂	P	61	4.7	11.4	2.7
	D	5.9	0.70	1.8	0.51
	S	10	6.7	6.3	5.2
O ₂ ^b	P	16.4	1.44	3.3	0.78
	D	12	1.6	3.7	1.0

(continued on the next page)

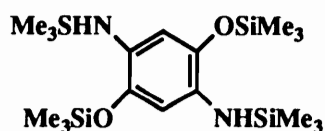
(continued from the previous page)

Gases		FPBO-1	FPBO-2	FPBO-3	HPBO-3
CO	S	1.3	0.92	0.88	0.76
	P	4.8	0.34	0.87	0.22
	D	3.7	0.38	1.0	0.31
N ₂ ^b	S	1.3	0.89	0.86	0.69
	P	3.4	0.21	0.55	0.12
	D	3.3	0.35	0.93	0.24
CH ₄	S	1.0	0.61	0.59	0.52
	P	1.60	0.097	0.28	0.086
	D	0.72	0.054	0.17	0.053
	S	2.2	1.8	1.6	1.6

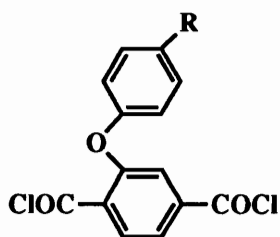
^aP is in $10^{-10} \text{ cm}^3 \text{ (STP) cm}^{-1} \text{ s}^{-1} \text{ cm Hg}^{-1}$, D is in $10^{-8} \text{ cm}^2 \text{ s}^{-1}$, and S is in $10^{-2} \text{ cm}^3 \text{ (STP) cm}^{-3} \text{ cm Hg}^{-1}$.

^bAt 2 atm.

Kricheldorf also investigated the use of silylated monomers in the synthesis of polybenzoxazoles [136]. Utilizing silylated 2,5-diaminohydroquinone (A) and various phenyl ether substituted terephthaloyl chlorides (B) or 2,6-naphthaloyl chloride, dichloro-



(A)



(B)

methane/trifluoroacetic acid soluble polymers were generated using a one-pot polymerization technique. The reaction medium consisted

of a mixture of terphenyl isomers (Marlotherm-S®) and all cyclization reactions were conducted as suspensions at 350°C. Initial polycondensation reactions were carried out at low temperatures in NMP, DMAc or Marlotherm. Inherent viscosities of the poly(hydroxy amide)s ranged from 0.55-1.77 dl/g (2 g/dl, 25°C, CH₂Cl₂/CH₃SO₃H (4:1 v/v)), while the polybenzoxazoles possessed η_{inh} 's of 0.66-1.19 dl/g (2.0 g/dl, 25°C, CH₂Cl₂/CH₃SO₃H (4:1 v/v)). No thermal transitions were detected by calorimetry experiments and degradation onsets were around 400°C (10°C/min).

Crosslinkable polybenzoxazole resins have been prepared by condensing silylated 2,2-bis(3-amino-4-hydroxyphenyl)hexafluoropropane with *p*-phenylenediacryloyl chloride and benzophenone dicarbonyl chloride [81]. Irradiation of the precursor resins with 365 nm light resulted in crosslinked polybenzoxazole systems.

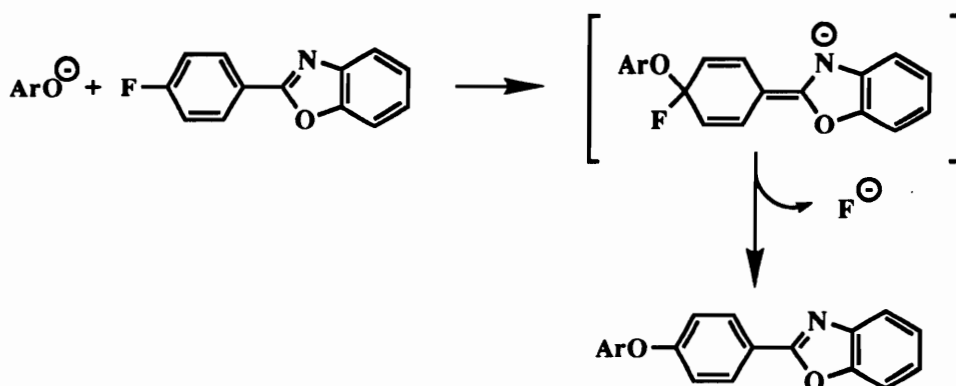
2.7. Polybenzoxazoles from Benzoxazole Monomers

To circumvent the problems associated with using undesirable solvents such as polyphosphoric acid or methanesulfonic acid and thermal cyclization techniques, a number of researchers have opted to preform the benzoxazole moiety in the monomers and subsequently conduct the polymerizations. As one would imagine, a large variation in monomer structure, as well as polymerization methodologies are possible depending on the nature of the functional groups attached to the benzoxazole heterocycle. The following sections will summarize these efforts with respect to monomer type and polymerization methodology, in addition to commenting on polymer properties.

2.7.1. Polybenzoxazoles via Nucleophilic Aromatic Substitution

Formation of polybenzoxazoles via nucleophilic aromatic substitution reactions is analogous to typical poly(arylene ether) syntheses [2], except for one notable exception, the nature of the activating group. Usually the activating group is an electron-withdrawing bridging group such as a carbonyl, sulfone or phosphine oxide, but Hedrick and coworkers [9,137,138] successfully demonstrated that an electron-deficient oxazole rings could mediate nucleophilic aromatic substitution reactions. The rationale

for facile nucleophilic aromatic substitution from a benzoxazole substituted benzene ring was 2-fold: (1) The electron-deficient oxazole ring has the effect on S_NAr2 reactions as an electron-withdrawing group and (2) a Meisenheimer complex is formed in the transition state and stabilizes the transition state via delocalization of the negative charge into the oxazole ring.



To take advantage of the electron-withdrawing nature of the oxazole ring system, the activated halide must be bound to the oxazole ring or reside on a phenyl ring directly attached to the 2 position of the oxazole ring. If the halide is attached to a phenyl ring, it must occupy the *para* position to be sufficiently activated towards nucleophiles. Some of the monomers reported by Hedrick and Maier [138-140] are shown in Figure 2.14

Polymerization of these monomers followed along the lines of now standard poly(arylene ether) methods [141], that being formation of the phenate with weak base (K_2CO_3), dehydration with various azeotroping solvents, followed by activation and further

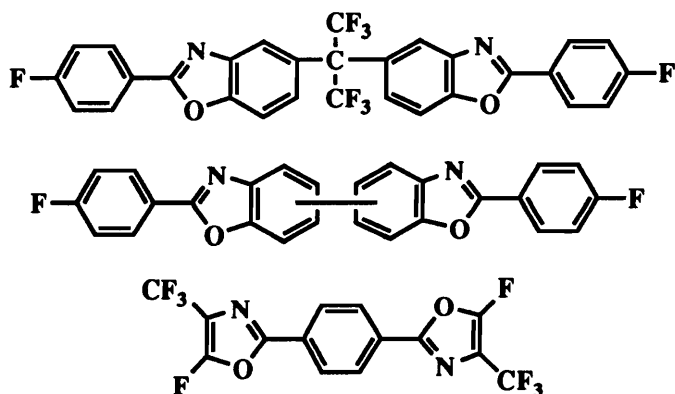


Figure 2.14. Activated dihalide benzoxazole monomers.

polymerization at elevated temperatures (Figure 2.15). N-methylpyrrolidinone and N-cyclohexylpyrrolidinone were solvents of choice, while toluene was chosen as the azeotroping solvent in Hedricks work. Maier reported using triethylamine in DMAc or NMP due to potential hydrolysis side reactions of the highly activated, trifluoromethyl substituted oxazole nuclei. In general, all the polymers stayed in solution during the polymerization process, viscosity increases were mentioned and the resulting polymers

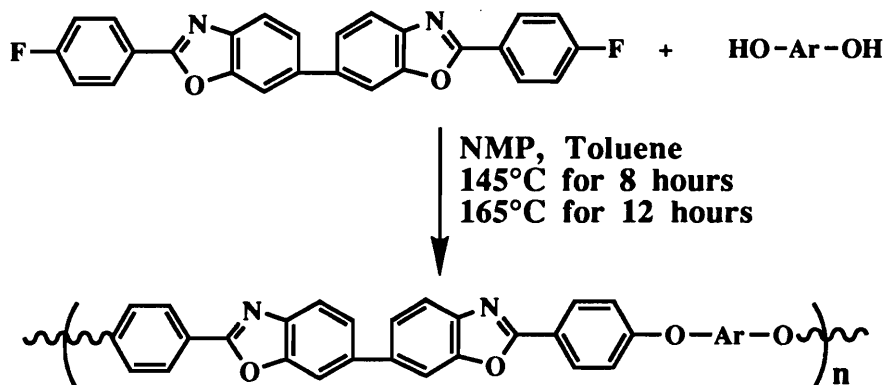


Figure 2.15. S_NAr2 polymerization scheme.

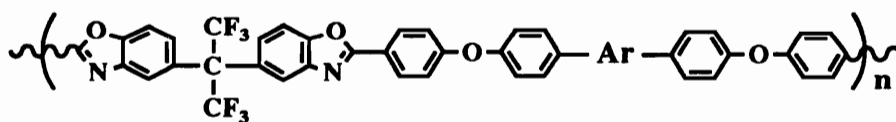
displayed $[\eta]$'s (0.51-1.05 dl/g in NMP at 25°C) and $\langle M_n \rangle$ (9,000-26,000 g/mole) representative of high molecular weight polymer.

Both groups reported improvements in solubility relative to traditional polybenzoxazoles, but only Hedrick's PBO's maintained superior thermo-oxidative stability (decomposition around 500°C). Maier reported decomposition beginning at 300°C and proposed that the trifluoromethyl substituent activates the oxazole ring to undergo a thermally induced, reverse cycloaddition reaction; the products being a nitrile and a ketocarbene. Glass transition temperatures ranged from 136-191°C for Maier's materials and 213-300°C for Hedrick's. Mechanical properties on Hedrick's polymers approached those of polybenzoxazoles more than poly(arylene ether)s (moduli~2.2 GPa, tensile strength ~70-80MPa, elongation.~4-25%) Unfortunately, all the polymers exhibited stress cracking when exposed to certain solvents.

Rather than incorporating the halide functionality into the benzoxazole and polymerizing with various bisphenols, Smith et al. [142] reversed the functionality's and utilized bisphenols containing the benzoxazole moiety. Thermal and mechanical properties (Table 2.15) were similar to those reported by Hedrick.

Reacting the above mentioned biphenyl based dihalides with *meta* and *p*-aminophenol under S_NAr2 conditions, Hedrick and coworkers [143,144] synthesized two novel benzoxazole containing diamines. Copolymerization of these diamines with pyromellitic dianhydride and varying percentages of 4,4'-oxydianiline afforded

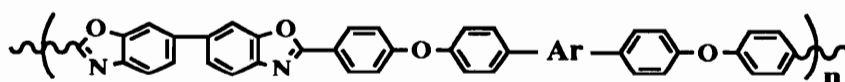
Tables 2.15. Thermal and solution properties of various poly(aryl ether benzoxazole)s [142].



Ar	η_{inh}^a (dl/g)	T_g (°C)	Percent Wt. Loss at 450°C	
			air	N ₂
	0.86	285	0.78	0.71
	0.67 ^b	254	0.89	0.52
	0.40	227	3.13	2.06
	0.922	249	2.13	0.68

^aInherent viscosity measured in DMAc at 25°C (0.5%).

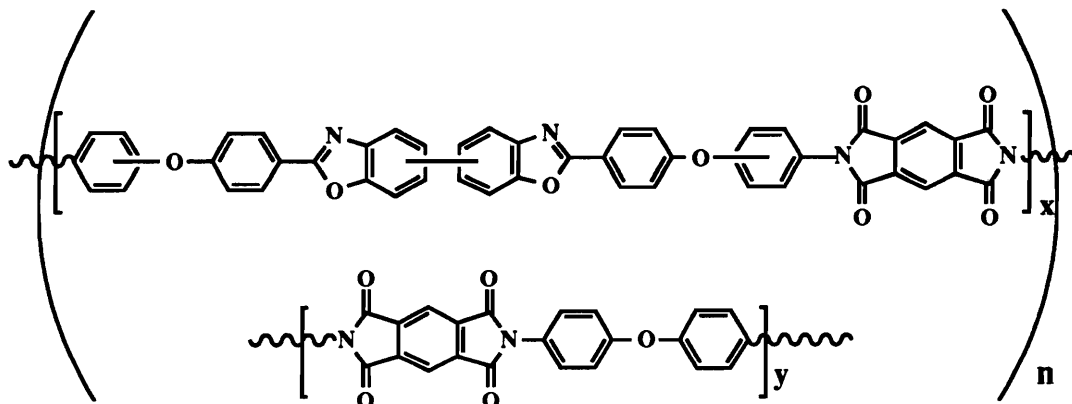
^bInherent viscosity measured in NMP at 25°C (0.5%).



Ar	η_{inh}^a (dl/g)	T_g (°C)	Percent Wt. Loss at 450°C	
			air	N ₂
	0.50	249 (425)	5.30	1.03
	0.40	247	3.45	3.60
	1.04	215 (373)	2.52	0.76
	0.40	237 (405,446)	5.53	2.56

¹Inherent viscosity measured in DMAc at 25°C (0.5%).

poly(amic acid)s. Poly(imide benzoxazole)s were formed by casting the poly(amic acid) solutions onto suitable substrates and thermally

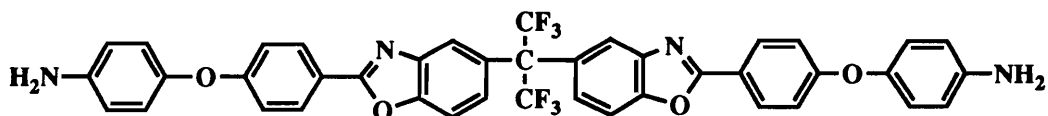


cyclizing at 400°C. Copolymer were prepared with both diamines and benzoxazole diamine compositions ranged from 10%-74%. Judging from the increase in solution viscosities and favorable mechanical properties, high molecular weight polymer was achieved. In general, the 3,3'-diamine containing polymers exhibited less thermal stability and higher rates of weight loss at 400°C, but surprisingly lower thermal expansion coefficients (TEC ~20-42 ppm) than the 4,4' analogs (TEC~40 ppm, PMDA-ODA polyimide has a TEC of 40 ppm). The 3,3' polymers showed glass transitions around 300°C for the higher PBO composition, but polyimides containing lower polybenzoxazole content exhibited no observable Tg's, much like the 4,4' polymers. Mechanical properties were very similar to the PMDA-ODA polyimide except for the enhanced elongation displayed by the 3,3' polymers (elongation.~80-110%). Perhaps the

most interesting feature of these materials was their superior adhesion in laminate form.

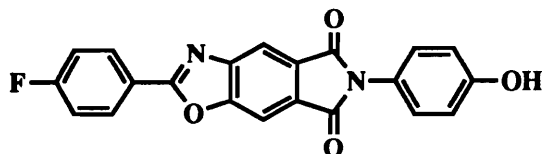
Using *m*-aminophenol as an endcapper, Hedrick and coworkers [10, 145,146] also synthesized a number of amine terminated poly(aryl ether benzoxazole)s of various molecular weights. Copolymerization of these oligomers with various compositions of ODA and PMDA diethyl ester diacyl chloride afforded a series of imide-aryl ether benzoxazole block copolymers. Thermal imidization at 350°C yielded clear tough films; indicating no appreciable homopolymer contamination or gross phase separation. Dynamic mechanical analysis of the copolymers displayed two transitions, one corresponding to the aryl ether benzoxazole and the other to the polyimide, characteristic of microphase separated materials. Incorporation of aryl ether benzoxazoles enhanced the moduli and tensile strengths slightly, but significantly increased elongations (50-80%) and self-adhesion

Mercer and McKenzie [147] generated a novel diamine by reacting *p*-aminophenol with 2,2-bis[2-(4-fluorophenyl)benzoxazol-6-yl]hexafluoropropane. This novel diamine was subsequently



polymerized with a number of dianhydrides to form novel polyimides. Glass transition temperatures ranged from 292-337°C.

Sundar and Mathias [148] incorporated a preformed benzoxazole and imide moiety into a novel AB monomer. Unfortunately, the



monomers rigidity and susceptibility to base resulted in low molecular weight materials upon polymerization.

2.7.2. Polybenzoxazoles via Acylation Reactions

Rodia, Preston and coworkers [149-152] were the first to demonstrate the utility of preformed benzoxazole monomers by synthesizing a number of diamines (Figure 2.16) and subsequently polymerizing them with various dianhydrides. Low temperature polycondensation of these monomers in DMAc followed by thermal cyclization in air at 300°C resulted in flexible, clear, yellow films. In general, the films showed excellent thermal stability, as judged by their flexibility after 14 weeks at 300°C and 10% weight losses in N₂ greater than 565°C. Fibers spun from these materials exhibited tenacities as high as 9 gpd. For a review and comparison of these fibers with other aromatic fibers see reference 153. Commenting on the thermal transition data is difficult due to the manner in which it was presented, but it could be said that glass

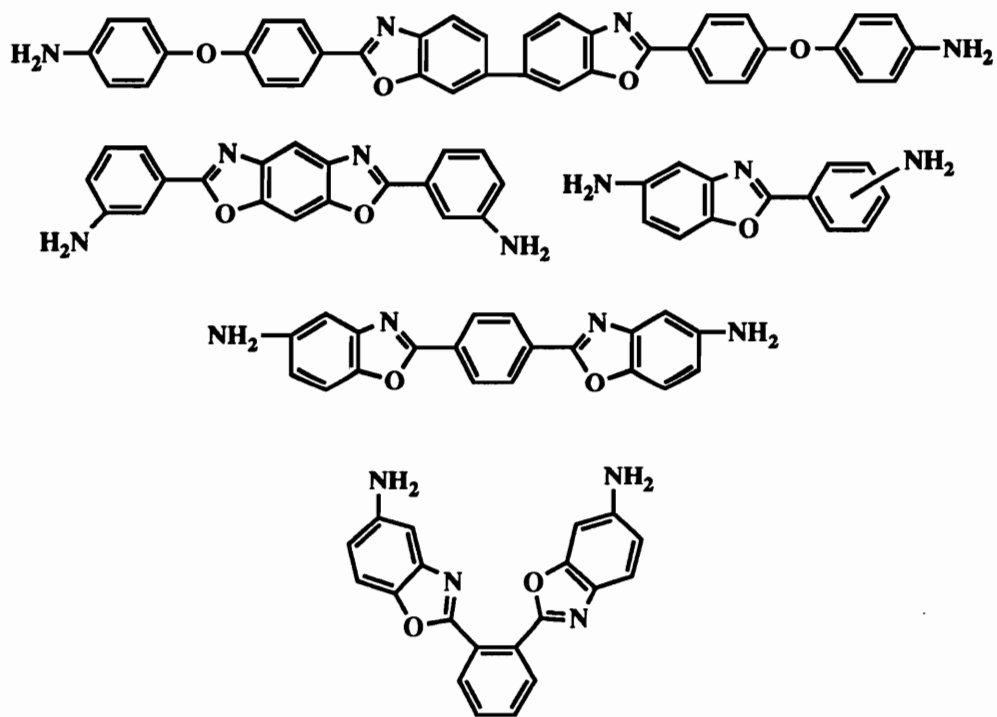
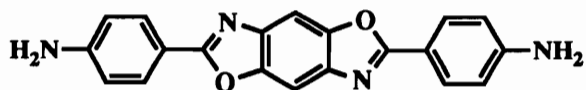


Figure 2.16. Novel benzoxazole diamines [149-152].

transition temperatures were apparently very high (~500°C) and some melt transitions may have been observed.

Preston has recently published on the synthesis of polyamides containing pendent benzoxazoles linkages [154]. Bonding a benzoxazole moiety to the 5 position of isophthaloyl chloride generated a suitable bulky monomer. Improved solubility as well as acceptable mechanical and thermal properties were noted.

Hirohashi, Hishiki and Ishikawa [155] reported the synthesis of 2,6-diaminophenylene benzbisoxazole (DBO) and its subsequent polymerization with a variety of functional groups (e.g., carboxylic



acids, acid chlorides, benzyl bromides, aldehydes) to form a series of polybenzoxazoles. Most of the polymers were synthesized in DMF or HMPA with the aid of a base catalyst (e.g., pyridine or triethylamine) at elevated temperatures. Inherent viscosity results ($\eta_{inh} \sim 0.10-0.43$ dl/g, sulfuric acid) suggest only low molecular weight polymer was generated. Due to the rigid nature of these materials, none of the polymers were soluble in common solvents and precipitation was observed during the polymerizations. Onsets of degradation were low (190-390°C); thermal transition data was again limited and specific resistivities at room temperature ranged from $10^{12}-10^{14}$ ohm cm.

Kricheldorf and Thomsen [156] employed an elaborate synthetic scheme to synthesize a variety of difunctional benzoxazole containing AB monomers (Figure 2.17) which were suspension

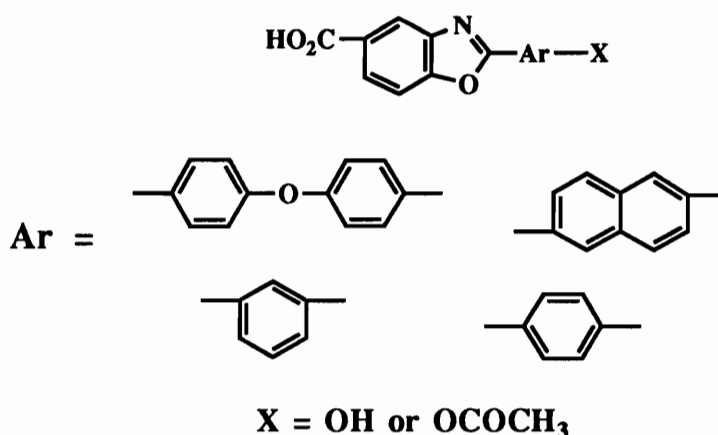
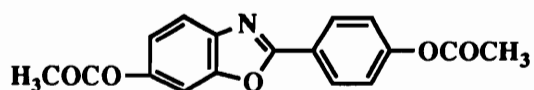


Figure 2.17. AB carboxylic acid/acetoxymonomers [156].

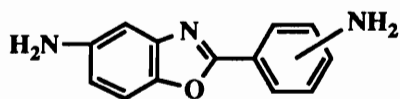
polymerized in Marlotherm-S® at 350°C. In all cases, the polymers precipitated from solution and showed high levels of crystallinity (>80%) by WAXS. Inherent viscosities in sulfuric acid ranged from 0.4-1.2 dl/g (2 g/L), T_g's were undetectable by DSC and 5% weight losses ranged from 350-518°C in air.

Caruso and coworkers [157] synthesized a diacetoxymonomer similar to Kricheldorf's monomers and polymerized it with terephthalic acid under acidolysis conditions. The resulting polymer



was soluble only in concentrated sulfuric acid and exhibited a T_g of 181°C. A liquid crystalline melt was reported at 408°C (nematic) and degradation occurred at 510°C.

Functionalizing Preston's simplest benzoxazole containing diamines with itaconic or nadic anhydride resulted in a series of



thermosets containing the benzoxazole moiety [158]. Unfortunately the melting points of these materials were high, and as a result, cure onsets and melt transitions occur simultaneously. Melt temperatures ranged from 190 to 245°C.

2.7.3. Polybenzoxazoles via Oxidative Coupling

Bach and coworkers [159-161] described the synthesis of aromatic azo monomers and azopolymers containing benzoxazole moieties. Diamines were synthesized using the method of Preston [162] or via selective oxidative coupling of diamines to form a number diamines containing one azo linkage. Polymerization of these diamines consisted of dissolving CuCl_2 in pyridine or DMAc in an oxygen environment, allowing oxidation and formation of the active catalyst ($\text{DMAc}_2\text{Cu}(\text{OH})\text{Cl}$ or $\text{Pyr}_2\text{Cu}(\text{OH})\text{Cl}$), addition of monomer and oxidation until O_2 absorption ceases. The resulting benzoxazole azopolymer exhibited solubility only in sulfuric acid and possessed an η_{inh} of 0.81 dl/g (sulfuric acid, 0.5%, 30°C). Benzoxazole containing azoaromatic polyamides were polymerized to high molecular weight as evident by an η_{inh} of 1.7 dl/g (DMAc, 5% LiCl, 0.1%, 30°C).

2.8. Polybenzoxazoles via Yamazaki Reaction

The two-step, polycondensation, cyclization methodology discussed in previous sections is related to the polycondensation of ω -(*o*-aminophenyl)carboxylic acid (AB) monomers under Yamazaki conditions. Traditionally, the Yamazaki reaction finds its utility in

the synthesis of aromatic polyamides, but Mathias and coworkers [163-167] demonstrated that under the right conditions, aliphatic and alkenyl poly(hydroxy amide)s could be generated using the Yamazaki reaction. While the resulting poly(hydroxy amide)s exhibited low molecular weights, it nonetheless demonstrates another synthetic route to PBO's. The polymerization scheme and monomers employed in the research are depicted in Figure 2.18. In a

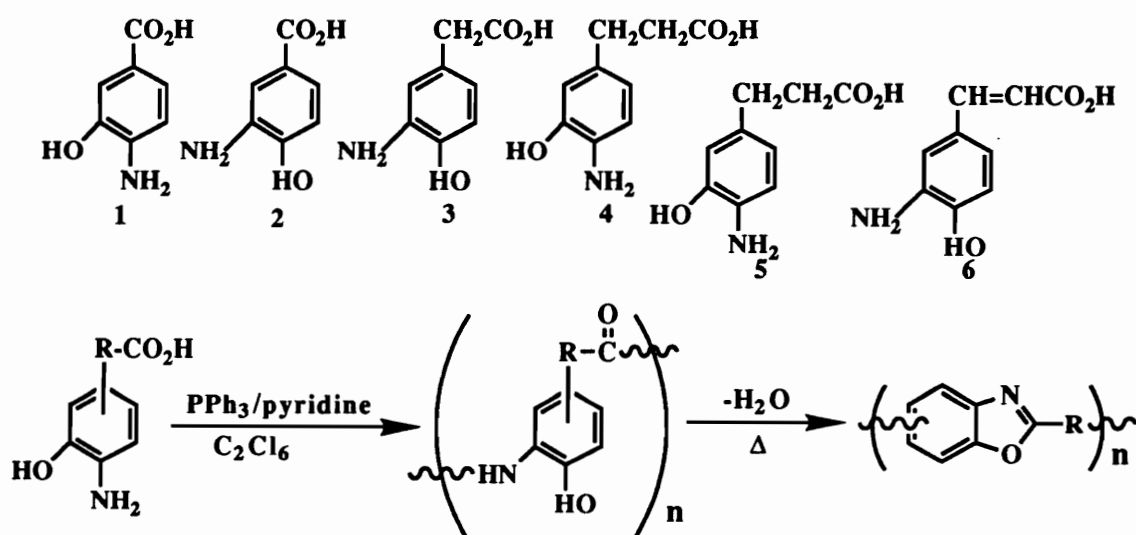


Figure 2.18. AB monomers and Yamazaki polymerization scheme used to synthesize aromatic and aliphatic polybenzoxazoles [163].

separate cyclodehydration step, the poly(hydroxy amide)s were converted to polybenzoxazoles in the melt. Enhanced inherent viscosities (η_{inh} 's = 0.01-2.25 dl/g, 0.2%, 25°C, H₂SO₄) were noted relative to the precursor poly(hydroxy amide)s, but unfortunately the materials were insoluble in all common solvents. The chain mobility of the aliphatic backbone was credited for the ability of

these polymers to chain extend under melt conditions. Inherent viscosities of the poly(hydroxy amide)s are shown in Table 2.16.

Table 2.16. Optical and solution properties of poly(hydroxy amide)s synthesized using Yamazaki conditions [163].

Monomer	Color	η_{inh} (dl/g) ^a
1	brown	0.18
2	light brown	0.20
3	pale yellow	0.13
4	brown	0.25
5	bright yellow	0.14
6	orange-yellow	0.49

^aMeasured in H₂SO₄ at 30°C on 0.2% solutions.

Regardless of the cyclization method, incomplete ring closure was detected by both FT-IR and TGA in most cases. Thermal characterization was limited to dynamic weight loss data and in general, the wholly aromatic polymers performed better than the aliphatic polymers. A particularly interesting result of these studies was the identification of a depolymerization/cyclodimerization process occurring in the methylene substituted polybenzoxazoles (Figure 2.19). Apparently, at 450°C, adjacent polymer chains decompose by way of a diradical and subsequently cyclodimerize. Alternatively, a mechanism of chain cleavage and backbiting was postulated.

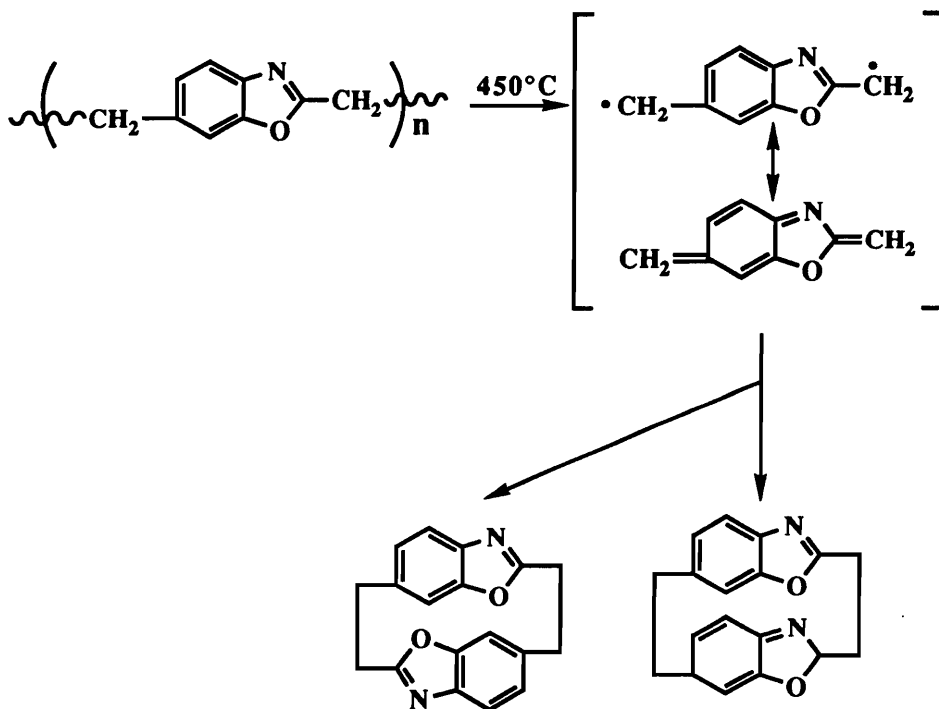
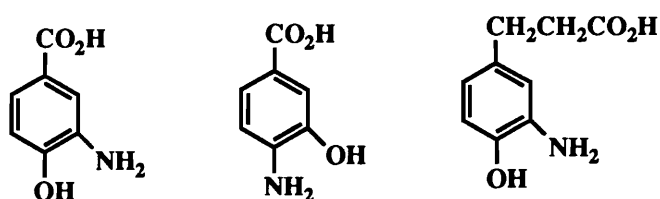


Figure 2.19. Polybenzoxazole degradation and cyclodimerization mechanism [165].

In an effort to avoid decomposition via dimerization and enhance thermal stability, copolymers were synthesized using various compositions of the aliphatic and aromatic AB monomers [168].



As before, low inherent viscosities (~ 0.20 dl/g, H_2SO_4 , 30°C , 0.2 g/dL) were achieved for the poly(hydroxy amide)s, but upon thermal conversion to the PBO's, inherent viscosities increased accordingly.

While a slight increase in thermal stability was noted for the 50/50 copolymers, no general conclusion could be reached regarding enhancement of thermal stability with incorporation of aromatic monomers.

Mathias [169] also polymerized a number of methylene substituted AA and BB monomers (Figure 2.20) using similar chemistry. Low inherent viscosities were once again obtained

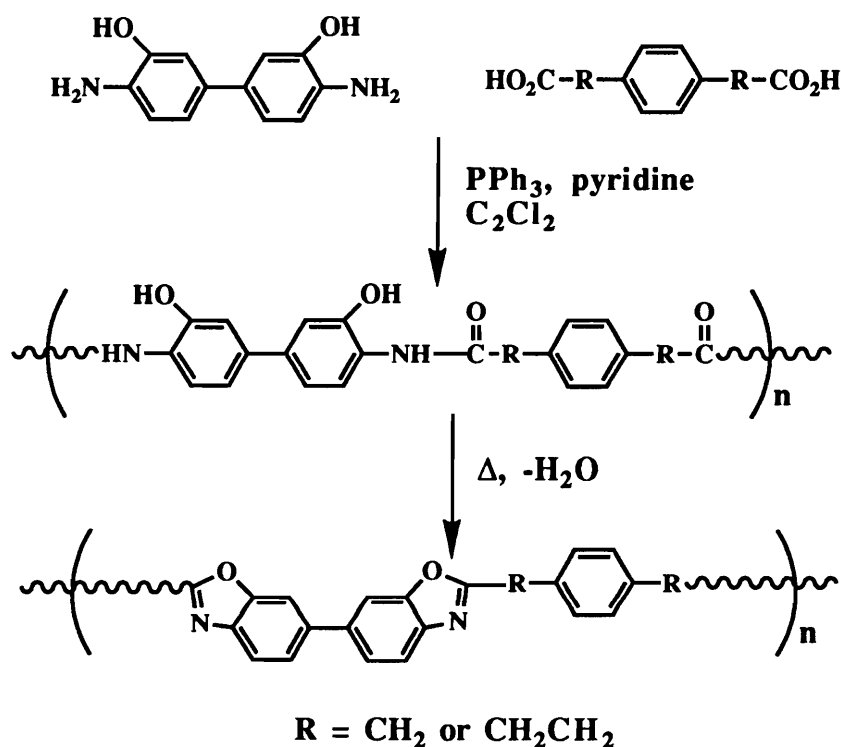
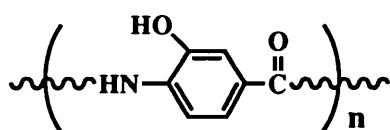


Figure 2.20. Polymerization of aliphatic and aromatic AA and BB monomers by Yamazaki reaction [169].

(0.18-0.24 dl/g in H₂SO₄) for the poly(hydroxy amide)s, but upon thermal cyclization, an increase in the η_{inh} 's of several fold were observed. Glass transition temperatures were greater than 270°C

and the ethylene derivative exhibited a melting endotherm at 384°C. Thermal decomposition was initiated at 480°C (N₂) for both polymers.

Preston [170] also reported the use of Yamazaki conditions to synthesis poly(hydroxy amide)s, but like Mathias, the polymers were of low molecular weight. No effort was made to cyclize these materials.



2.9. Polybenzoxazoles Containing Perfluoro Linkages

Previous review sections have demonstrated quite clearly that the majority of research pertaining to polybenzoxazoles revolves around the synthesis of high T_g , thermo-oxidatively stable materials. In the following section, research efforts focused on the generation of low T_g , thermally stable elastomers will be presented. Unlike their wholly aromatic counterparts, these materials exhibit glass transition temperatures from -30°C to 150°C, excellent solubility in common solvents and melt processability. In order to achieve these highly desirable properties, perfluoro linkages were

incorporated into bis(*o*-aminophenol)s and diimidate ester monomers.

The first reported synthesis of these materials took advantage of an acetic acid promoted polycondensation of 3,3'-dihydroxybenzidine or 3,3'-diamino-4,4'-dihydroxybenzophenone with a series of perfluoro and perfluoro ether-diimidate esters [171]. Moderate to high molecular weight polymers with excellent thermal stability resulted, but unfortunately the polymers exhibited little, if any, rubber-like character in the low temperature regime. This lack of appreciable elastomeric properties at lower temperatures was credited to insufficient backbone mobility resulting from crystallinity and bis(*o*-aminophenol) rigidity. Attempts to eliminate crystallinity in the polymer and lower glass transition temperatures were frustrated by the unavailability of the requisite long-chain fluorocarbon ether-diimidate esters.

Evers [172,173] circumvented the crystallinity, rigidity problem by synthesizing novel perfluoro and perfluoro ether bridged bis(*o*-aminophenol)s (Figure 2.21). Acetic acid promoted polymerization of these monomers with the fluorinated diimidate esters reported by Burton and Madison [171] in hexafluoroisopropanol (HFIP) at 50°C for ~200 hours resulted in a series of elastomeric polybenzoxazoles. Larger fluorocarbon linkages tended to form cyclics at lower monomer concentrations, but with increased percent solids, high molecular weight materials were realized. Table 2.17 summarizes the structures, as well as the solution and thermal properties of

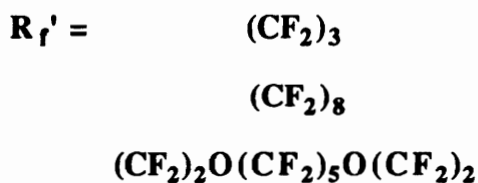
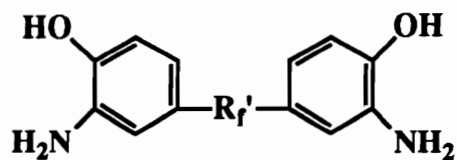
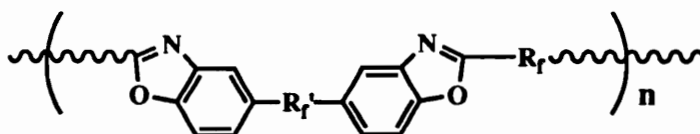


Figure 2.21. Perfluoro and perfluoro ether bis(*o*-aminophenol)s [172].

Table 2.17. Properties of perfluoro polybenzoxazoles. [173].



Trial No.	R _f	R _f	η _{inh} ^a (dl g ⁻¹)	T _m ^b (°C)	T _g ^b (°C)
3	(CF ₂) ₃	(CF ₂) ₃	0.45	187	106
6	(CF ₂) ₃	CF ₂ O(CF ₂) ₂ OCF ₂	0.94		29
7	(CF ₂) ₃	0.33 (CF ₂) ₃ 0.67 CF ₂ O(CF ₂) ₂ OCF ₂	0.52	112	45
8	(CF ₂) ₃	(CF ₂) ₄ O(CF ₂) ₂ OCF ₂	0.51		9
9	(CF ₂) ₃	CF ₂ O(CF ₂ CF ₂ O) _m (CF ₂) ₃ - (OCF ₂ CF ₂) _n OCF ₂ m + n = 5	0.72		-31
10	(CF ₂) ₃	(CF ₂) ₃	0.21	179	
11	(CF ₂) ₃	CF ₂ O(CF ₂) ₂ OCF ₂	0.30	93	
12	(CF ₂) ₃	(CF ₂) ₄ O(CF ₂) ₂ OCF ₂	0.32	106	19
13	(CF ₂) ₃	CF ₂ O(CF ₂ CF ₂ O) _m (CF ₂) ₃ - (OCF ₂ CF ₂) _n OCF ₂ m + n = 5	0.30	63	-28

^a 0.2 g dl⁻¹, 25°C, HFIP.

^b Determined by differential scanning calorimetry, ΔT = 20°C min⁻¹.

these materials. As expected, T_g 's decreased with increasing fluorocarbon ether linkages and in general ranged from -22°C to 106°C .

Gilham and coworkers [174-177] investigated the relationship between various physical properties and the molecular structure of these materials. Torsional braid analysis (TBA) (~ 1 Hz) and dynamic TGA were used to determine the effect of fluorocarbon structure and molecular position on thermal transitions and thermal stability. HFIP polymer solutions were applied to heat-cleaned glass braids, dried at 200°C and cycled under nitrogen through various schedules (e.g., $200^\circ\text{C} \rightarrow -180^\circ \rightarrow 200^\circ\text{C}$). A representative thermomechanical spectrum is displayed in Figure 2.22. It should be noted that the spectrum exhibits two secondary transitions in addition to a glass transition temperature. The lowest damping peak was attributed to the perfluoro linkages between the oxazole rings and the higher temperature secondary transition was attributed to the perfluoro bridge between the benzene rings. These two damping peaks decreased with an increase in fluorocarbon length and ether incorporation. Glass transition temperatures also followed this trend (Table 2.17). It was concluded that the linkage between the oxazole groups exhibits a greater degree of flexibility than the linking group between the benzene rings, indicating placement of fluorocarbon linkage also plays a role in the viscoelastic behavior.

TGA data indicates incorporation of fluorocarbon linkages in the bis(o-aminophenol) decreases thermal stability by $\sim 50^\circ\text{C}$ and ether

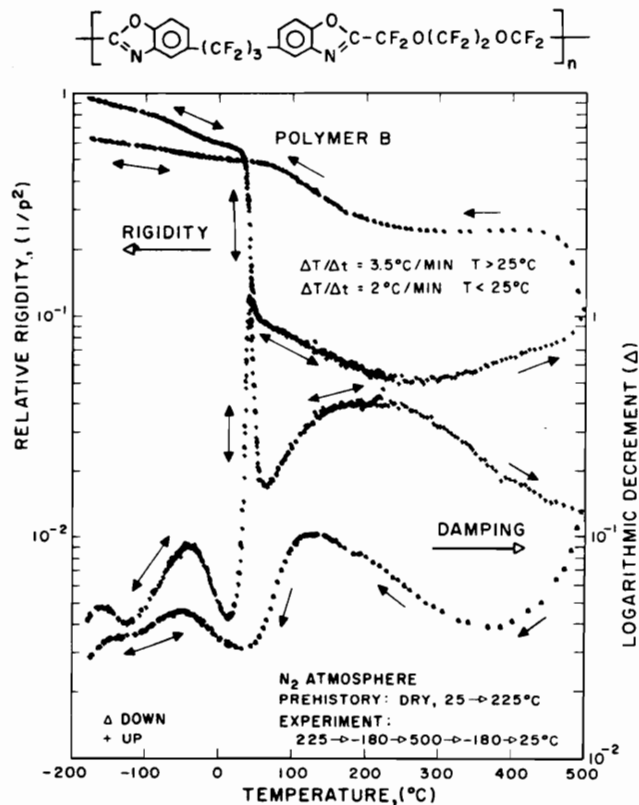


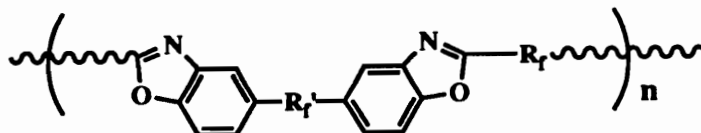
Figure 2.22. Thermomechanical spectrum of a perfluoro PBO [176].

linkages decrease it even further relative to unsubstituted bis(*o*-aminophenols). The onsets of degradation were ~260°C for all the polymers, but a weight loss of only 2-3% was observed up to 400°C, followed by rapid degradation at 450°C (N₂). Cycling experiments carried out with progressively higher maximum cycle temperatures revealed that crosslinking occurs when the polymers are exposed to

elevated temperatures for prolonged periods of time. At temperatures below 470°C, minimal increases in T_g were noticed, but after cycling to 525°C, the polymer displayed no glass transition temperature by TBA, indicating network formation. Evers and Abraham [178,179] attempted to further reduce glass transition temperatures and improve hydrolytic stability by synthesizing bis(*o*-aminophenols) with enhanced fluorocarbon ether content and diimidate esters with pendent trifluoromethyl groups. Polymerization techniques analogous to the above mentioned acetic acid catalyzed route produced polymers of moderate to high molecular weight. Inherent viscosities varied from 0.07 to 0.79 dl/g and T_g 's ranged from -58 to -5°C (Tables 2.18). None of the polymers exhibited crystalline melt temperatures and thermo-oxidative stability of the polymers tended to decrease with an increase in fluorocarbon ether content. Onset of degradation in air occurred in the 350-400°C range, while isothermal aging of representative polymers at 260°C for 200 hours resulted in weight losses of 5-7%. Pendent trifluoromethyl groups tended to enhance thermo-oxidative stability and improve hydrolytic stability.

Pyrolysis mass spectroscopic analysis on a number of these polymers [180] indicated that the fluorocarbon ether linkages were less stable than fluorocarbon linkages by ~50°. Additionally, it was found that polymers containing ether linkages *beta* to an oxazole ring decomposed at a lower temperature (500-540°C) and the major decomposition product was carbonyl difluoride. An intramolecular

Table 2.18 Properties of rubber-like fluorocarbon ether polybenzoxazoles [182].



R_f'	R_f	Time (hr)	Concentration [% monomer (w/v)]	η_{inh} (dl/g) ^a	T_g (°C) ^b
$(CF_2)_2O(CF_2)_2O(CF_2)_2$	$\begin{array}{c} CF(O CF_2 CF_2)_x O(CF_2)_y O(CF_2 CF_2 O)_z CF \\ \quad \quad \quad \\ CF_2 \quad CF_2 \quad CF_2 \quad CF_2 \end{array}$	252	26	0.20	-15
$(CF_2)_2O(CF_2)_2O(CF_2)_2$	$x + y = 4$ $x + y = 5$	192	37	0.20	-18
$(CF_2)_2O(CF_2)_3O(CF_2)_2$	$x + y = 4$	252	46	0.23	-19
$(CF_2)_2O(CF_2)_3O(CF_2)_2$	$x + y = 5$	240	36	0.25	-23
$(CF_2CF_2O)_3(CF_2)_6O(CF_2)_2$	$x + y = 5$	288	40	0.35	-34
$(CF_2)_2O(CF_2)_2O(CF_2)_2$	$\begin{array}{c} CF(O CF_2 CF_2)_x OCF \\ \quad \\ CF_2 \quad CF_2 \end{array}$	456	36.0	0.27	-39
$(CF_2)_2O(CF_2)_6O(CF_2)_2$	$\begin{array}{c} CF(O CF_2 CF_2)_x O(CF_2)_y O(CF_2 CF_2 O)_z CF \\ \quad \quad \\ CF_2 \quad \quad \quad CF_2 \end{array}$ $x + y = 5$	312	96.5	0.27	-35
$(CF_2)_2O(CF_2)_6O(CF_2)_2$	$\begin{array}{c} CF(O CF_2 CF_2)_x O(CF_2)_y O(CF_2 CF_2 O)_z CF \\ \quad \quad \\ CF_2 \quad \quad \quad CF_2 \end{array}$ $x + y = 6$	336	60.0	0.41	-38
$(CF_2)_2O(CF_2)_6O(CF_2)_2$	$\begin{array}{c} CF(O CF_2 CF_2)_x OCF_2 \\ \quad \\ CF_2 \quad CF_2 \end{array}$	288	50.5	0.30	-37
$(CF_2)_2O(CF_2)_6O(CF_2)_2$	$\begin{array}{c} CF(O CF_2 CF_2)_x O(CF_2)_y O(CF_2 CF_2 O)_z CF \\ \quad \quad \\ CF_2 \quad \quad \quad CF_2 \end{array}$	672	49.1	0.29	-45
$(CF_2CF_2O)_3(CF_2)_6O(CF_2)_2$	$\begin{array}{c} CF(O CF_2 CF_2)_x O(CF_2)_y O(CF_2 CF_2 O)_z CF \\ \quad \quad \\ CF_2 \quad \quad \quad CF_2 \end{array}$ $x + y = 6$	264	38.5	0.25	-44
$(CF_2CF_2O)_3(CF_2)_6O(CF_2)_2$	$\begin{array}{c} CF(O CF_2 CF_2)_x OCF_2 \\ \quad \\ CF_2 \quad CF_2 \end{array}$	384	56.5	0.40	-47
$(CF_2CF_2O)_3(CF_2)_6O(CF_2)_2$	$\begin{array}{c} CF(O CF_2 CF_2)_x O(CF_2)_y O(CF_2 CF_2 O)_z CF \\ \quad \quad \\ CF_2 \quad \quad \quad CF_2 \end{array}$	336	15.5	0.21	-48

^a 0.2 g/dl, 25°C, HFIP.

^b Differential scanning calorimetry ($\Delta T = 20^\circ C/min$).

ring opening rearrangement reaction was postulated to explain this observaion. At temperatures higher than 550°C, rapid cleavage of the fluorocarbon and fluorocarbon ether linkages occurred, as well as oxazole degradation.

Yakubovich and coworkers [181,182] utilized perfluoro bridged diacid chlorides under low temperature polycondensation conditions to prepare a series of fluorocarbon containing poly(hydroxy amide)s (Figure 2.23). Cyclization of the polymers, either thermally or in polyphosphoric acid, resulted in PBO's of moderate to high molecular weight. The poly(hydroxy amide)s exhibited good solubilities in polar solvents, while the polybenzoxazoles were only soluble in H₂SO₄. In general, the solution cyclized polymers were more

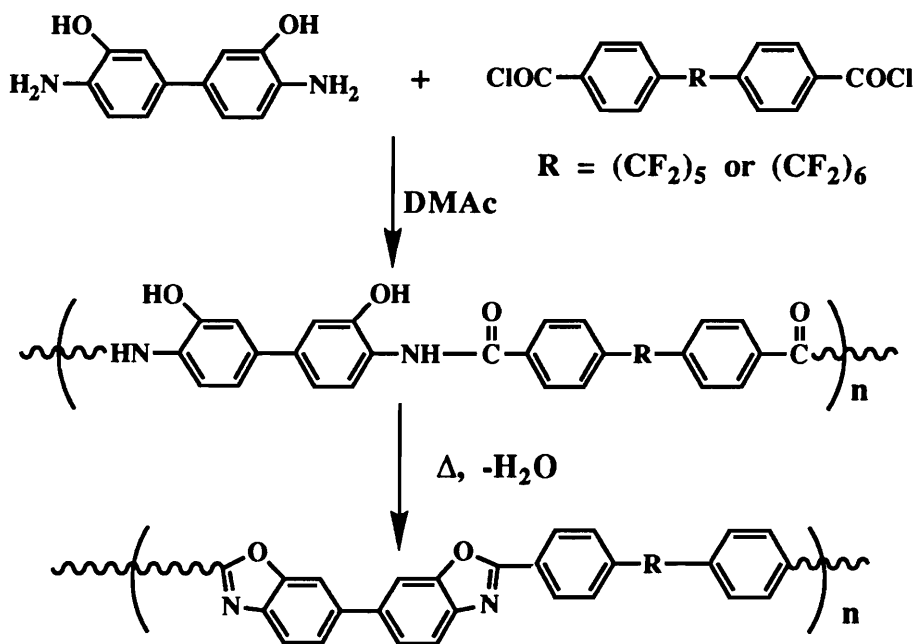


Figure 2.23. Synthesis of fluorocarbon bridged polybenzoxazoles [182].

soluble than the thermally cyclized materials. All the polybenzoxazoles possessed some form of crystallinity, initiated decomposition at $\sim 450^{\circ}\text{C}$, and exhibited elongations of 7-8% and tensile strengths of ~ 83.3 MPa.

2.10. Thermal and Mechanical Properties of PBO's

The requirements necessary for a polymer to be considered a high performance material are not well defined, but they usually encompass end uses that involve high temperatures, high tensile or compressive loads, hostile environments, dimensional stability, light weight, and high electrical conductivity. With these requirements in mind, high performance polymers can be discussed relative to two important material properties, thermal stability and mechanical properties. Its important to separate these two material properties because polymers can exhibit excellent mechanical properties, while possessing unfavorable thermo-oxidative stability. For example, Spectra[®], a highly crystalline polyethylene fiber, possesses tenacities and moduli of 30 gpd and 1400 gpd, respectively, but undergoes catastrophic failure at temperatures greater than 150°C [183]. Alternatively, polymers can display both excellent thermal stability and superior mechanical properties; polybenzoxazoles are a class of polymers which exhibit

this phenomenon. The following two sections will attempt to compare the thermal and mechanical properties of cis PBO and poly(2,5-benzoxazole) with a number of high performance materials.

The thermal stability of a material can be explained in terms of two sets of factors, namely chemical and physical. Chemical factors are determined by the choice of monomers used in the polymerization and include, primary bond strength, secondary or van der Waals forces (e.g., H-bonding, dipole-dipole, etc.), resonance stabilization, mechanism of cleavage, molecular symmetry, chain rigidity and topology. The most important factor being primary bond strength. The bond dissociation energy for a single carbon-carbon bond is ~350 kJ/mol, while that of a carbon-carbon double is ~610 kJ/mol. In aromatic or heterocyclic systems, resonance stabilization can add an additional 164-287 kJ/mol to the bond dissociation energy [184]. Hence, it is apparent that highly aromatic polymers possess much higher thermal stabilities relative to aliphatic polymers. The other chemical factors relate more to the cohesive energy density between polymer chains, in other words, the more closely chains can be packed together and the greater the intermolecular interaction between polymer chains, the greater the thermal stability of the polymer. Physical factors, such as molecular weight, molecular weight distribution and crystallinity, work in much the same manner.

In light of the above mentioned chemical and physical factors, it's obvious that aromatic heterocyclic polymers, such as

polybenzoxazoles, are prime candidates for applications requiring high thermal stability. Several of these polymers have recently been compared with regard to thermal stability. Dynamic thermogravimetric analysis (Figure 2.24) suggests that polybenzothiazoles

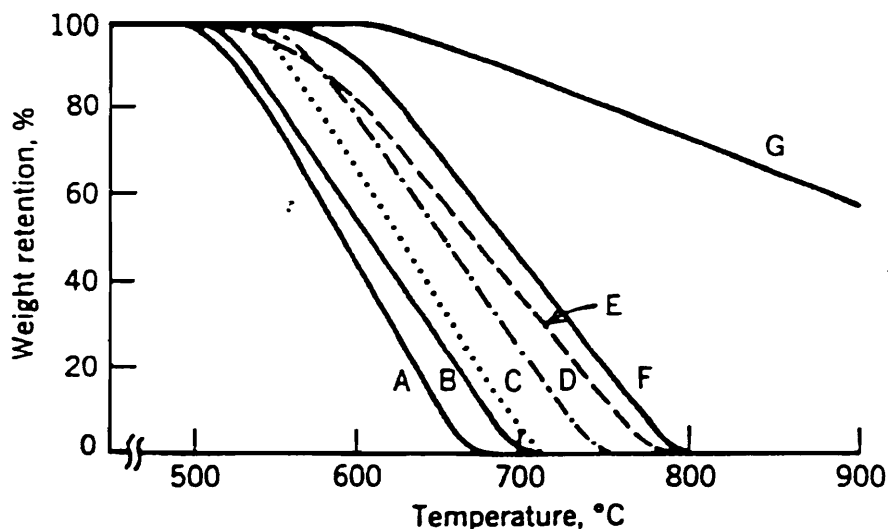


Figure 2.24. Thermogravimetric analysis of polyheterocyclics [185]. A, Polybenzimidazole; B, polyquinoxaline; C, polyimide; D, polybenzoxazole; E, poly(N-phenylbenzimidazole); F, polybenzothiazole; G, pyrolytic graphite. Atmosphere: static air; heating rate: 6.67°C/min.

are the most thermo-oxidatively stable of the polymers studied, while isothermal gravimetric analysis (Figure 2.25) indicates polyimides to be the most thermally stable. Regardless of which is considered the most stable, it's obvious from Figures 2.24 and 2.25, that all these polymers, excluding polybenzimidazoles, can be considered as high performance materials, polybenzoxazoles

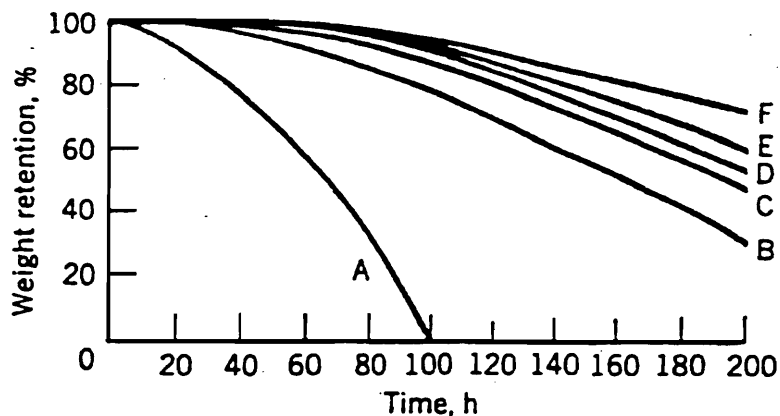


Figure 2.25. Isothermal weight loss of polyheterocyclics in air at 371°C [185]. A, Polybenzimidazole; B, poly(N-phenylbenzimidazole); C, polybenzothiazole; D, polyquinoxaline; E, polybenzoxazole; F, polyimide. Atmosphere: circulating air; sample form: >0.1 mm (<140 mesh) powder.

included. In many respects it is unfair to rank these polymers relative to thermal stability because a number of factors, unrelated to the intrinsic thermal stability of a material, dictate thermo-oxidative stability. Factors such as polymerization technique, monomer purity, draw ratio, crystallinity and others can dramatically alter thermal stability; therefore ranking similar backbone structures is relative.

Primary bond strengths, as alluded to previously, dictate the thermal stability of polymeric materials, but with respect to mechanical properties, intermolecular forces and physical factors dominate. Polyethylene illustrates this point quite clearly.

Polyethylene consists entirely of carbon-carbon single bonds, yet it possesses mechanical properties very similar to highly aromatic systems. A high degree of order in the draw direction and crystallinity (physical factors) are credited for these property enhancements [186]. Mechanical properties for a number of high performance polymers are compared in Table 2.20 [187]. It should be noted that the tenacity and moduli are similar for all the polymers, regardless of aromatic content.

Inspection of the thermal stability and fiber property data reflects the outstanding properties exhibited by polybenzoxazoles, more specifically, cis PBO. Unlike many of the other polymers which possess either excellent mechanical or thermal properties, cis-PBO exhibits both. This characteristic can be attributed to the wholly aromatic backbone structure, 180° catenation angles and the high degree of ordering achieved during the fiber spinning process [110].

Table 2.19. High performance fiber properties [187]

Fiber Type	Density (g/cc)	Melt Temperature (°C)	Tenacity (gpd)	Modulus (gpd)
<i>Aromatic Polyamides</i>				
Du Pont Kevlar 29	1.44	Not meltable	23 ^a	580 ^a
Kevlar 49	1.44	Not meltable	22 ^a	950 ^a
Kevlar 149	1.47	Not meltable	17 ^a	1100 ^a
Teijin Technora	1.39	485	25 ^a	550 ^a
<i>Aromatic Polyester</i>				
Dart Xydar		~350	18-20	1400
Sumitomo Ekonol	1.40	~350	31	1100
Kuraray Vectran	1.436	~350	22-25	600-700
<i>Aromatic Polyimides</i>				
Ube	~1.5		27	1500
Toray	~1.5		20	1300
<i>Aromatic Heterocyclic Polymers</i>				
PBT Aftech II	1.58	Not meltable	25	2200
PBO	1.5		26	2600
AB PBO			22	1000
<i>High-strength Polyethylene</i>				
Allied Spectra 900	0.97	150	30	1400
Spectra 1000	0.97	150	35	2000
<i>Carbon</i>				
Hercules IM-7	1.79	4000	35	1800
Toray	1.80		36	1740
<i>Inorganic Fibers</i>				
Du Pont Fiber FP	3.9	2045	4	1100
Silicone carbide	3.17	<2700	11	1200

^aContinuous filament yarn properties, 1GPa = 145,000 psi, 1 gpd (grams per denier) = 12800 ρ psi, where ρ is density

Chapter 3

EXPERIMENTAL

3.1. Introduction

The formation of poly(hydroxy amide)s can be characterized as a step-growth polymerization and like any step-growth polymerization, five important polymerization rules must be obeyed in order to achieve high molecular weight polymer:

- Monomer purity greater than 99.5%
- High conversion of functional groups (>99%)
- Accessibility of functional groups in the reaction mixture
- Balanced stoichiometry (total functionality = 2)
- No side reactions

Two of these parameters, monomer purity and high conversion, are intimately connected in many instances. For polymerizations to proceed to high conversion, stoichiometric amounts of monomers must be present if high molecular weight polymer is desired or a calculated offset in stoichiometry is required, if controlled molecular weight is desired. This relationship can be represented in mathematical terms by the Carothers equation [188,189]:

$$X_n = \frac{1+r}{1+r-2rp}$$

where X_n represents the number average degree of polymerization (directly related to molecular weight), r is the stoichiometric offset in monomer functionality and p is the fractional percent conversion. If perfect stoichiometry is achieved, r becomes 1, and the Carothers equation reduces to $X_n = 1/(1-p)$.

This relationship is graphically illustrated in Figure 2.1 and demonstrates the fact that high molecular weight (e.g., 100 units) polymer is not achieved until conversion reaches at least 99%. Monomer purity also has a dramatic affect on molecular weight through the terms r and p . The use of impure monomers will affect molecular weight similar to offsetting stoichiometry. Impure monomers will also manifest themselves in percent conversion. If one of the monomers is impure, the number of functional groups available to react will be in deficit, consequently complete

conversion of all functional groups will be impossible and percent conversion will be less than 100%.

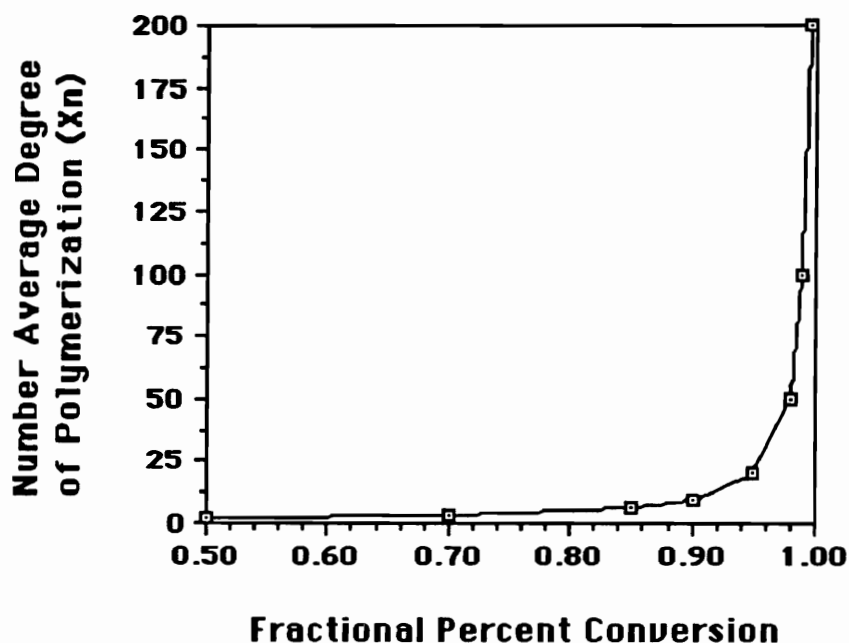


Figure 3.1. Graphical representation of fractional percent conversion versus number average degree of polymerization.

Due to the importance of monomer purity, extreme care must be taken during the purification of monomers, reagents and solvents. The following chapter will outline the synthesis and purification of monomers, monomer precursors, solvents, reagents and polymers used in this research. Information pertinent to each chemical, such as source, empirical formula, molecular weight, melting or boiling point and structure will be provided. Reagents used in the synthesis

of intermediates or monomers such as acetic acid, potassium permanganate, phenol, etc., were used as received without further purification or published purification procedures were followed. At the end of the chapter, the methods used to characterize the monomers and polymers will be described briefly.

3.2. Materials: Synthesis and Purification

3.2.1. Reagents and Monomers

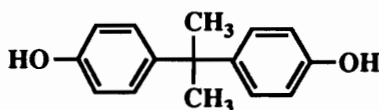
3.2.1.1. 2,2-Bis(4-hydroxyphenyl)propane (Bisphenol-A)

Source Dow Chemical Company

Empirical Formula $C_{15}H_{16}O_2$

Molecular Weight 228.27

Structure

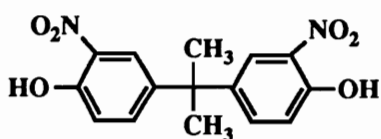


Purification procedure:

Bisphenol-A was used as received.

3.2.1.2. 2,2-Bis(4-hydroxy-3-nitrophenyl)propane (bANP)

Source	synthesized from Bisphenol-A
Empirical Formula	C ₁₅ H ₁₄ N ₂ O ₆
Molecular Weight	318.27
Molecular Structure	



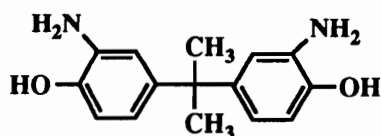
Synthesis procedure:

To a 2000 mL three neck flask equipped with a thermometer, reflux condenser and liquid addition funnel, 100.00 g (0.44 mol.) of Bisphenol-A was washed in with 500 mL of acetic acid. After 10 minutes, the slurry was cooled to 10-15°C and treated with 100 mL of a nitric acid/acetic acid solution (56 mL of 15.8 N nitric acid (0.88 mol.) in 44 mL of acetic acid) from the addition funnel. The addition took place over a 2 hour period and the temperature was maintained below 15°C. After complete addition, the reaction was held at 15°C for 1 hr and 23°C for 1 hr. The reaction mixture was cooled to 10°C, and the product precipitated by adding 700 mL of ice water over the course of 2 hr. The brownish yellow precipitate was filtered off, washed with copious amounts of distilled water and dried under reduced pressure at 80°C for 24 hr; crude yield ~ 75%.

Two recrystallizations from ethanol (one charcoal treatment) resulted in 88.88 g of yellow needles. M.p. = 133-135°C (lit. m.p. = 135°C [190]).

**3.2.1.3. 2,2-Bis(3-amino-4-hydroxyphenyl)propane
(bAAP)**

Source	synthesized from 2,2-bis(3-nitro-4-hydroxy)-propane
Empirical Formula	C ₁₅ H ₁₈ N ₂ O ₂
Molecular Weight	258.32
Molecular Structure	



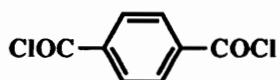
Synthesis procedure:

To a 500 mL pressure reactor equipped with heating coils and overhead stirrer, a homogeneous solution of 50.00 g (0.16 mol.) of 2,2-bis(4-hydroxy-3-nitrophenyl)propane, 350 mL of deoxygenated, deionized water and 15.87 g (0.40 mol.) of NaOH was added along with 2.50 g of 10% palladium on carbon (Aldrich) and 50 mL of water. After purging the reactor with H₂ for 20 minutes, the reactor was pressurized to 50 psi and warmed to 35°C. After 12 hours, the contents of the reactor were pressure filtered through

Celite® into an excess of aqueous acetic acid. The product was isolated via filtration, washed with water and 95% ethanol and dried under reduced pressure at 80°C for 24 hr. Yield~98%. The product was recrystallized by dissolving 50.00 g of bAAP in 1000 mL of refluxing THF and adding chloroform to the hot solution until turbid (~1000 mL of CHCl₃). After 12 hr in the refrigerator, 25.33 g of off white crystals were collected. M.p. = 247.6° (d) (lit. m.p. = 256°C (d) [191]).

3.2.1.4. Terephthaloyl Chloride (TC)

Source	Eastman Chemical Company
Empirical Formula	C ₈ H ₄ Cl ₂ O ₂
Molecular Weight	203.02
Molecular Structure	



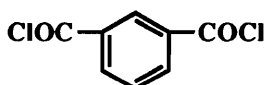
Purification procedure:

To a 500 mL, one neck, round bottom flask equipped with a reflux condenser and stir bar, 50.00 g (0.25 mol.) of terephthaloyl chloride and 100 mL of thionyl chloride were added. The mixture was warmed to reflux and maintained until a homogeneous solution was achieved (~3-4 hr). Filtration of the solution through a fritted funnel (medium porosity) with nitrogen pressure and evaporation of

the thionyl chloride via rotary evaporation followed by mechanical vacuum resulted in a light yellow solid. Two fractional distillations (80°C at 1 torr) resulted in 40.78 g of pure material. Yield~81%, m.p. = 81-82°C (lit. m.p. = 80-82°C [192]).

3.2.1.5. Isophthaloyl Chloride (IC)

Source	Eastman Chemical Company
Empirical Formula	C ₈ H ₄ Cl ₂ O ₂
Molecular Weight	203.02
Molecular Structure	



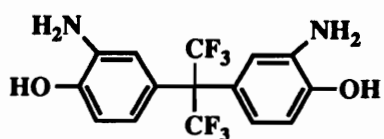
Purification procedure:

Purification of isophthaloyl chloride followed the same procedure as terephthaloyl chloride. Yield~85%, m.p. 43-44°C (lit. m.p. = 43-44°C [192]).

3.2.1.6. 2,2-Bis(3-amino-4-hydroxy)hexafluoropropane (6FAP)

Source	Central Glass Company of Japan
Empirical Formula	C ₁₅ H ₁₂ F ₆ N ₂ O ₂
Molecular Weight	366.26

Molecular Structure



Purification Procedure:

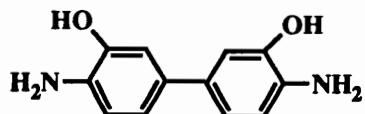
To a 1 liter, 2 neck, round bottom flask equipped with reflux condenser, magnetic stir bar and glass stopper, 100.00 g (0.27 mol.) of 2,2-bis(3-amino-4-hydroxyphenyl)hexafluoropropane and 150 mL of 95% ethanol were combined and heated to reflux. Upon dissolution of the 6FAP, chloroform (~150 mL) was added to the refluxing solution until turbidity was noticed. With continuous stirring, the solution was cooled and maintained at 23°C for 2 hours to allow for complete crystallization. After filtration, washing with chloroform and 50:50 (v/v) chloroform/diethyl ether and drying at 100°C for 24 hr, 87.33 g were recovered. Yield~87%, m.p. = 243-244°C (lit. m.p. = 244-245°C [193]). Evaporation of the recrystallization solvent from the filtrate will allow for the recovery of impure 2,2-bis(3-amino-4-hydroxyphenyl)hexafluoropropane.

3.2.1.7. 2,2'-Dihydroxybenzidine (DHB)

Source	Central Glass Company
Empirical Formula	C ₁₂ H ₁₂ N ₂ O ₂

Molecular Weight 216.24

Molecular Structure



Purification procedure:

To a 500 mL erlenmeyer flask containing 100 mL of 5M HCl at 80°C, 50.00 g (0.23 mol.) of 2,2'-dihydroxybenzidine was slowly added with stirring. Upon dissolution, the solution was filtered hot, treated with charcoal for 30 minutes, filtered through Celite® and precipitated by adding concentrated HCl. The HCl salt was collected via vacuum filtration and washed with 30% aqueous HCl, all in low light. The salt was recrystallized once from deionized water, collected and dried. The salt was redissolved in 80°C deionized water (treated with 1% SnCl₂), treated with charcoal for 30 minutes, filtered hot through Celite® and immediately treated with sodium acetate until a light pink precipitate appeared. Pressure filtration of the mixture with N₂ followed by pressure washings with 95% ethanol and diethyl ether resulted in a 70% yield (from the recrystallized salt) of pure 2,2'-dihydroxybenzidine. Determination of a melting point was hampered by gross decomposition which started around 265°C (lit. m.p. = 292°C, with decomposition [28]). The fact that DHB gave high molecular weight polymer and a very clean ¹H NMR spectra indicates high purity. NMR (d₆-DMSO) δ 4.44

(bs, 4H, NH₂), δ 6.56 (d, 2H, aromatic), δ 6.67 (d, 2H, aromatic) δ 6.78 (s, 2H, aromatic) δ 9.00 (bs, 2H, OH)

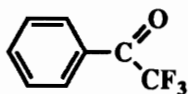
3.2.1.8. 2,2,2-Trifluoroacetophenone

Source H. J. Grubbs, Thesis 1993

Empirical Formula C₈H₅F₃O

Molecular Weight 174.12

Molecular Structure



Purification procedure:

2,2,2-Trifluoroacetophenone was used as received (b.p. = 165-166°C)

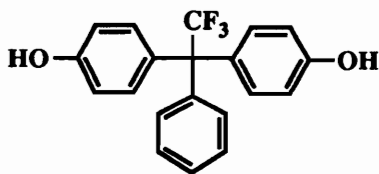
3.2.1.9. 1,1-Bis(4-hydroxyphenyl)-1-phenyl-2,2,2-trifluoroethane (3F-Bisphenol)

Source synthesized from trifluoroacetophenone

Empirical Formula C₂₀H₁₅F₃O₂

Molecular Weight 344.32

Molecular Structure



Synthesis procedure:

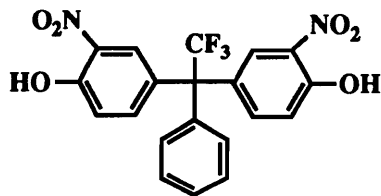
To 250 mL, three neck, flask equipped with a magnetic stir bar, N₂/thermometer inlet and an addition funnel fitted with a drying tube, 41.32 g (0.44 mol.) of phenol, 2.42 mL (2.7 X 10⁻² mol.) of 3-mercaptopropionic acid and 19.32 g (0.11 mol.) of 2,2,2-trifluoroacetophenone were added and heated to 45°C. Once a homogeneous solution was achieved, 2.45 mL (2.8 X 10⁻² mol.) of triflic acid was introduced dropwise while maintaining the temperature at 45°C. After 1 hr, the slurry was treated with 200 mL of hot deionized water and the product isolated by filtration. The pink solid was stirred in 200 mL of hot deionized water for 15 minutes, vacuum filtered, washed with hot water, methylene chloride and dried under reduced pressure at 80°C for 24 hr. Yield~75%, m.p. = 228-230°C (lit. m.p. = 225-226°C [194]).

3.2.1.10. 1,1-Bis(4-hydroxy-3-nitrophenyl)-1-phenyl-2,2,2-trifluoroethane (3FNP)

Source	synthesized from 1,1-bis(4-hydroxyphenyl)-1-phenyl-2,2,2-trifluoroethane
Empirical Formula	C ₂₀ H ₁₃ F ₃ N ₂ O ₆

Molecular Weight 434.32

Molecular Structure



Synthesis procedure:

To a 1 liter, 3 neck, round bottom flask equipped with reflux condenser, mechanical stirrer and liquid addition funnel, 50.00 g (0.15 mol.) of 3F-Bisphenol was slurried in 215 mL of acetic acid at 10°C. To the heterogeneous solution, 27.50 g of 70% nitric acid (0.31 mol.) diluted with 80 mL of acetic acid was added dropwise while maintaining the temperature below 15°C. After complete addition, the reaction was maintained at 15°C for an additional 1.5 hr and treated with 300 mL of ice water over the course of 2 hr. The yellow precipitate was filtered, washed with copious amounts of water and dried under reduced pressure at 80°C. After two recrystallizations from 95% ethanol, a 75% yield of product was obtained. M.p. = 150.9-152.0°C (lit. m.p. = 146-147°C [194])

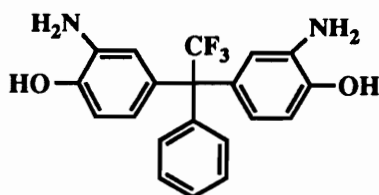
3.2.1.11. 1,1-Bis(3-amino-4-hydroxyphenyl)-1-phenyl-2,2,2-trifluoroethane (3FAP)

Source synthesized from 1,1-bis(4-hydroxy-3-nitrophenyl)-1-phenyl-2,2,2-trifluoroethane

Empirical Formula C₂₀H₁₇F₃N₂O₂

Molecular Weight 374.36

Molecular Structure



Synthesis procedure:

To a 500 mL pressure reactor equipped with heating coils and overhead stirrer, a homogeneous solution of 40.00 g (9.2 X10⁻² mol.) of 1,1-bis(4-hydroxy-3-nitrophenyl)-1-phenyl-2,2,2-trifluoroethane, 350 mL of deoxygenated, deionized water and 7.54 g (0.19 mol.) of NaOH was added along with 2.00 g of 10% palladium on carbon and 50 mL of water. After purging the reactor with H₂ for 20 minutes, the reactor was pressurized to 50 psi and warmed to 35°C. Ten hours later the reaction mixture was pressure filtered through Celite® into an excess of aqueous acetic acid. The product was isolated via filtration, washed with water and dried under reduced pressure at 80°C for 24 hr. Yield~98%. Multiple recrystallizations

were accomplished by dissolving 100.00 g (0.23 mol.) of 3FAP in 150 mL of boiling 95% ethanol and treating with chloroform (~150 mL) until turbidity was noticed. The solution was cooled to 23°C and maintain for 2 hours with stirring. After filtration, washing with chloroform, 50:50 (v/v) chloroform/diethyl ether and drying under reduced pressure at 100°C for 24 hr, a white crystalline solid was recovered. Yield~91% (1 recrystallization), m.p. = 216-217°C, NMR (d₆-DMSO) δ 4.51 (bs, 4H, NH₂), δ 5.97 (d, 2H, aromatic), δ 6.45 (s, 2H, aromatic) δ 6.56 (d, 2H, aromatic) δ 7.08 (d, 2H, aromatic) δ 7.33 (m, 3H, aromatic) δ 9.15 (bs, 2H, OH), *Elem. Anal.* Calcd. for C₂₀H₁₇F₃N₂O₂: C, 64.16; H, 4.58; N, 7.48. Found: C, 62.72; H, 4.98; N,7.31. Recovery of the impure 1,1-Bis(3-amino-4-hydroxyphenyl)-1-phenyl-2,2,2-trifluoroethane from the filtrate was achieved by simple evaporation.

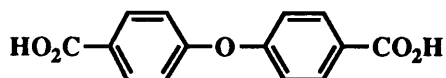
3.2.1.12. 4,4'-Oxydibenzoic Acid (ODBA)

Source Hoechst-A. G., Frankfurt, Germany

Empirical Formula C₁₄H₁₀O₅

Molecular Weight 258.22

Molecular Structure



Purification procedure:

4,4'-Oxydibenzoic acid was used as received.

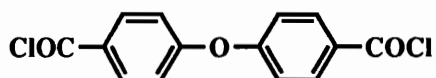
3.2.1.13. 4,4'-Oxydibenzoyl Chloride (ODBC)

Source synthesized from 4,4'-oxydibenzoic acid

Empirical Formula $C_{14}H_8Cl_2O_3$

Molecular Weight 295.10

Molecular Structure



Synthesis procedure:

To a 100 mL, two neck, round bottom flask equipped with a reflux condenser and N_2 inlet, 25.00 g (9.7×10^{-2} mol.) of 4,4'-oxydibenzoic acid, 35 mL of thionyl chloride and 3 drops of N,N-dimethylformamide were combined and warmed to $45^\circ C$. Upon dissolution of the acid (~3 hr), the contents were filtered through a medium porosity fritted funnel with N_2 pressure, reduced in volume via rotary evaporation and exposed to 500 mtorr of pressure for 1 hr. The resulting yellow solid was vacuum distilled twice at 300 mtorr with the fraction at $195^\circ C$ being collected. Yield~80%, m.p. = $88.2-89.4^\circ C$ (lit. m.p. = $88^\circ C$ [7]).

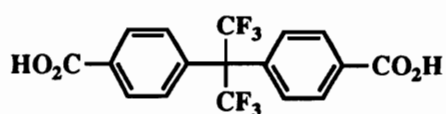
3.2.1.14. 2,2-Bis(4-carboxyphenyl)hexafluoropropane (6FDA)

Source Hoechst Celanese of Germany

Empirical Formula $C_{17}H_{10}F_6O_4$

Molecular Weight 392.25

Molecular Structure



Purification procedure:

2,2-Bis(4-carboxyphenyl)hexafluoropropane was used as received.

3.2.1.15. 2,2-Bis(4-chlorocarbonylphenyl)hexafluoropropane (6FAC)

Source synthesized from 2,2-bis(4-carboxyphenyl)-hexafluoropropane

Empirical Formula $C_{17}H_8Cl_2F_6O_2$

Molecular Weight 429.13

Molecular Structure

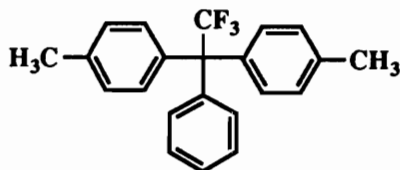


Synthesis procedure:

To a 100 mL, two neck, round bottom flask equipped with a reflux condenser and N₂ inlet, 25.00 g (6.4 X 10⁻² mol.) of 2,2-bis(4-carboxyphenyl)hexafluoropropane, 35 mL of thionyl chloride and 3 drops of N,N-dimethylformamide were combined and warmed to 45°C. Upon dissolution of the acid (~3 hr), the contents were filtered through a medium porosity fritted funnel under N₂ pressure, reduced in volume via rotary evaporation and exposed to 500 mtorr of pressure for 1 hr. The resulting yellow solid was vacuum distilled at 400 mtorr. Yield~87%, m.p. = 96.0-97.0°C (lit. m.p. = 94.5-95.5°C [7]).

3.2.1.16. 1,1-Bis(4-methylphenyl)-1-phenyl-2,2,2-trifluoroethane

Source	synthesized from 2,2,2-trifluoroacetophenone
Empirical Formula	C ₂₂ H ₁₉ F ₃
Molecular Weight	340.37
Molecular Structure	

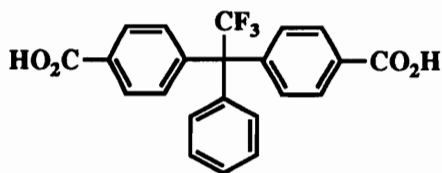


Synthesis procedure:

To a flame dried, one neck, 500 mL, round bottom flask equipped with a magnetic stir bar and septum, 52 mL (0.37 mol.) of 2,2,2-trifluoroacetophenone were syringed in along with 300 mL of toluene. Once a homogeneous solution was obtained, 33.00 mL (0.38 mol.) of triflic acid was added dropwise and the reaction maintained for 20 hours at 23°C. The reaction mixture was poured into 500 mL of water/methylene chloride (200 mL of water/300 mL of CH₂Cl₂) and extracted with methylene chloride. The organic layer was washed with two 300 mL aliquots of 5% K₂CO₃, water, a saturated sodium chloride solution, dried with MgSO₄ and evaporated to dryness. The resulting orange solid was washed with 95% ethanol until white and dried under reduced pressure at 80°C. Yield~83%, m.p. = 170-171.5°C (lit. m.p. = 168-169°C [194]).

3.2.1.17. 1,1-Bis(4-carboxyphenyl)-1-phenyl-2,2,2-trifluoroethane (3FDA)

Source	synthesized from 1,1-Bis(4-methylphenyl)-1-phenyl-2,2,2-trifluoroethane
Empirical Formula	C ₂₂ H ₁₅ F ₃ O ₄
Molecular Weight	400.34
Molecular Structure	



Synthesis procedure:

To a four neck, 2 liter, round bottom flask equipped with an overhead stirrer, reflux condenser, thermometer and glass stopper, 102.28 g (0.30 mol.) of 1,1-bis(4-methylphenyl)-1-phenyl-2,2,2-trifluoroethane was dissolved in 365 mL of pyridine and 100 mL of water. The contents of the flask were warmed to 60°C and 345.00 g (2.18 mol.) of KMnO₄ was added in 50.00 g aliquots. Thirty mL aliquots of water were used to wash in each KMnO₄ addition. After complete addition, the reaction temperature was raised to 95°C and maintained for 24 hr. The reaction mixture was cooled to 30°C, treated with 500 mL of water, filtered and neutralized with concentrated HCl. The off white product was stirred overnight in the acidic medium, filtered, washed with water, aspirator dried, redissolved in dilute aqueous KOH, filtered, cooled to 5°C and neutralized with 5% HCl. The resulting product was collected by filtration, washed with water and redissolved in 500 mL of aqueous KOH. The solution was returned to the reactor, treated with 50.00 g of KMnO₄ (0.32 mol.) at 80°C and then held at 95°C for 3 hours. After cooling to 30°C, the solution was filtered and neutralized with 1M HCl. The precipitate was collected by filtration, washed with copious amounts of water and dried under reduced pressure at 90°C

for 24 hours. Yield~89%. Purification of the acid was accomplished by chlorinating with thionyl chloride and hydrolyzing with dilute KOH. m.p. = 256-260°C, NMR (d₆-DMSO) δ 7.0 (d, 2H, aromatic), δ 7.11 (d, 4H, aromatic), δ 7.24-7.3 (m, 3H, aromatic) δ 7.89 (d, 4H, aromatic) δ 11.0 (bs, 2H, COOH), *Elem. Anal.* Calcd. for C₂₂H₁₅F₃O₄: C, 66.00; H, 3.78. Found: C, 65.21; H, 3.77.

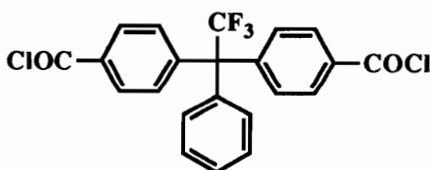
3.2.1.18. 1,1-Bis(4-chlorocarbonylphenyl)-1-phenyl-2,2,2-trifluoroethane (3FAC)

Source synthesized from 1,1-Bis(4-carboxyphenyl)-1-phenyl-2,2,2-trifluoroethane

Empirical Formula C₂₂H₁₃F₃Cl₂O₂

Molecular Weight 437.22

Molecular Structure



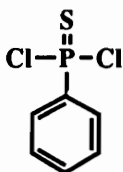
Synthesis procedure:

To a two neck, 500 mL, round bottom flask equipped with a reflux condenser, magnetic stir bar and N₂/thermometer inlet, 82.36 g (0.21 mol.) of 1,1-bis(4-carboxyphenyl)-1-phenyl-2,2,2-trifluoroethane, 150 mL of thionyl chloride and 4 drops of DMF were combined and warmed to 40°C for 12 hr. After filtration through a

medium porosity fritted funnel and evaporation of the thionyl chloride, a yellow solid resulted. The solid was slurried with hexanes, filtered, dissolved in hexanes (~100 mL), treated with charcoal for 30 minutes, filtered through Celite® and cooled to 23°C. Constant stirring of the solution resulted in the precipitation of a white solid. A second recrystallization from hexanes afforded a 73% yield of monomer grade material with a melting point of 67.2-69°C; *Elem. Anal.* Calcd. for C₂₂H₁₃Cl₂F₃O₂: C, 60.43; H, 3.00; Cl, 16.22. Found: C, 60.39; H, 3.01; Cl, 16.15, NMR (CDCl₃) δ 7.06 (d, 2H, aromatic), δ 7.30 (d, 4H, aromatic), δ 7.34-7.4 (m, 3H, aromatic) δ 8.09 (d, 4H, aromatic).

3.2.1.19. Phenylphosphine sulfide dichloride

Source	Janssen Chimica, Belgium
Empirical Formula	C ₆ H ₅ Cl ₂ PS
Molecular Weight	211.03
Molecular Structure	

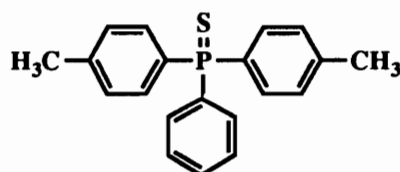


Purification procedure:

Phenylphosphine sulfide dichloride was used as received.

3.2.1.20. Bis(4-methylphenyl)phenylphosphine sulfide

Source	synthesized from phenylphosphine sulfide dichloride
Empirical Formula	C ₂₀ H ₁₉ PS
Molecular Weight	322.38
Molecular Structure	



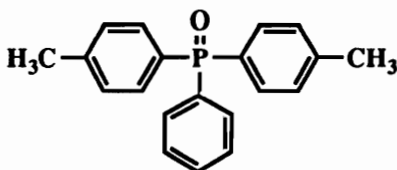
Synthesis procedure:

To a four neck, 2 liter, round bottom flask equipped with a reflux condenser, gas outlet, thermometer, glass stopper and magnetic stir bar, 100.00 g (0.47 mol.) of phenylphosphine sulfide dichloride and 260 mL (2.45 mol.) of toluene were added. After the solution temperature was raised to 70°C, 126.35 g (0.95 mol.) of AlCl₃ was added in 6 aliquots over the course of 1 hour. The reaction temperature was raised to 105°C and the extent of conversion monitored by TLC. After 7 hours, the contents were cooled to 25°C, poured into 600 mL of ice water and extracted with two 350 mL aliquots of chloroform. The chloroform extracts were combined, washed with 300 mL of 5% NaHCO₃, 1000 mL of water, dried with MgSO₄ and evaporated to a thick pink oil. Cooling the oil with agitation resulted in a pink solid. Slurring the solid in hexanes,

filtration and washing with hexanes resulted in a white solid. A second crop of crystals obtained from the hexanes filtrate afforded a total yield of 79% (m.p. = 150-153°C (lit. m.p. = 154°C [195])).

3.2.1.21. Bis(4-methylphenyl)phenylphosphine oxide

Source	synthesized from bis(4-methylphenyl)phenylphosphine sulfide
Empirical Formula	C ₂₀ H ₁₉ OP
Molecular Weight	306.32
Molecular Structure	



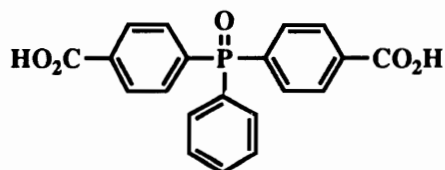
Synthesis procedure:

To a 500 mL, 4 neck, round bottom flask equipped with a reflux condenser, addition funnel, thermometer and glass stopper, 54.26 g (0.17 mol.) of bis(4-methylphenyl)phenylphosphine sulfide was added along with 250 mL of acetic acid. The solution temperature was raised to 60°C and 11.75 g (0.10 mol.) of 30% aqueous hydrogen peroxide was added dropwise. After complete addition of the hydrogen peroxide, the reaction temperature was raised to 85°C and maintained for 1 hour. Upon cooling the reaction mixture to 23°C, it was filtered through Celite[®], diluted with 500 mL of water and

extracted with two 250 mL aliquots of chloroform. The CHCl_3 extract was washed with water, 5% NaHCO_3 , water, dried with MgSO_4 and evaporated to a yellow viscous oil (Yield~95%). Repeated efforts to crystallize the product failed, therefore the product was confirmed by ^1H NMR and used without further purification. NMR (CDCl_3) δ 2.39 (s, 6H, CH_3), δ 7.25 (d, 4H, aromatic), δ 7.43 (m, 2H, aromatic) δ 7.54 (m, 5H, aromatic), δ 7.65 (m, 2H, aromatic). Morgan and Herr reported crystallizing the oxide from n-heptane with great difficulty (lit. m.p. = 79.5°C [195]).

3.2.1.22. Bis(4-carboxyphenyl)phenyl phosphine oxide

Source	synthesized from bis(4-methylphenyl)phenyl-phosphine oxide
Empirical Formula	$\text{C}_{20}\text{H}_{15}\text{O}_5\text{P}$
Molecular Weight	366.29
Molecular Structure	



Synthesis procedure:

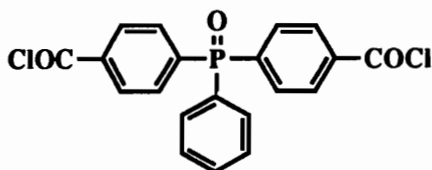
To a 1 liter, three neck, round bottom flask equipped with a thermometer, reflux condenser and glass stopper, 72.40 g (0.24 mol.) of bis(4-methylphenyl)phenylphosphine oxide, 285 mL of pyridine

and 140 mL of water were added. The mixture was heated to 70°C, 270.0 g (1.71 mol.) of KMnO_4 was added in 20.0 g aliquots over the course of 4 hours. After complete addition of the KMnO_4 , the reaction temperature was increased to 95°C and maintained for 12 hours. The reaction media was steam distilled to remove the pyridine, filtered and neutralization with 10% HCl to obtain a white precipitate. The precipitate was collected by filtration, washed with copious amounts of water, dissolved in 500 mL aqueous KOH and reintroduced into the reaction vessel. Two 25.00 g (0.32 mol.) aliquots of KMnO_4 were added to the flask and the reaction temperature increased to 90°C. After 5 hours, the reaction mixture was cooled to 30°C, filtered through Celite® and neutralized with 10% HCl. The resulting precipitate was collected via filtration, washed with copious amounts of water and dried under reduced pressure for 24 hours at 100°C. Yield~76%, m.p. = 344-347°C (lit. m.p. = 340-342°C [199]). Literature suggests it is desirable to derivatize to the methyl ester to purify [195].

**3.2.1.23. Bis(4-chlorocarbonylphenyl)phenylphosphine
oxide (PPOAc)**

Source	synthesized from bis(4-carboxyphenyl)- phenylphosphine oxide
Empirical Formula	$\text{C}_{20}\text{H}_{13}\text{Cl}_2\text{O}_3\text{P}$
Molecular Weight	403.17

Molecular Structure

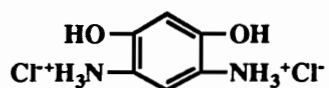


Synthesis procedure:

To a two neck, 125 mL, round bottom flask equipped with an N₂ inlet and reflux condenser, 5.00 g (1.4 X 10⁻² mol.) of bis(4-carboxyphenyl)-phenylphosphine oxide, 17 mL of 1,1-dichloroethane and 5.68 g (2.8 X 10⁻² mol.) of phosphorus pentachloride were added. The reaction temperature was raised to reflux and maintained until the reaction mixture became homogeneous. Infrared spectroscopy (COOH stretch at 3500-2800 cm⁻¹) indicated no carboxylic acid peaks, so the reaction mixture was cooled to 23°C, diluted with 10 mL of toluene and exposed to rotary evaporation until a viscous oil resulted. Diluting the oil with hexanes resulted in a light yellow solid. Quantitative yields were obtained prior to recrystallization. Purification methods consisted of dissolving the product in toluene, evaporating to a oil and precipitating with a 2:1 mixture of ethyl acetate/hexane. Two precipitations resulted in white material which exhibited the correct ¹H NMR. spectra and a melting point of 136-139°C (lit. m.p. = 128-129°C [196]). Similar results were obtained using SOCl₂ and previous mentioned methods.

**3.2.1.24. 4,6-Diaminoresorcinol Dihydrochloride
(DAR·2HCl)**

Source	Dow Chemical Company
Empirical Formula	C ₆ H ₁₀ Cl ₂ N ₂ O ₂
Molecular Weight	213.06
Molecular Structure	

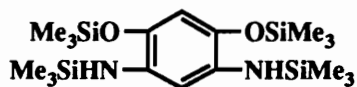


Purification procedure:

4,6-Diaminoresorcinol dihydrochloride was used as received.

**3.2.1.25. N,N',O,O'-Tetra(trimethylsilyl)-4,6-diamino-
resorcinol (SDAR)**

Source	synthesized from 4,6-diaminoresorcinol dihydrochloride
Empirical Formula	C ₁₈ H ₄₀ N ₂ O ₂ Si ₄
Molecular Weight	428.86
Molecular Structure	

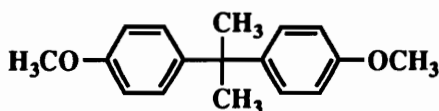


Synthesis procedure:

To a flame dried 250 mL, two neck, round bottom flask, 5.00 g (2.3×10^{-2} mol.) of 4,6-diaminoresorcinol dihydrochloride, 80 mL of tetrahydrofuran and 23.77 mL (0.17 mol.) of triethylamine were combined and cooled to 23°C. Immediately, 12.51 mL (9.9×10^{-2} mol.) of trimethylsilyl chloride (Aldrich) was added over a period of 10 minutes. The reaction was allowed to continue at 23°C for 3 hours and 14 hours at 60°C. After cooling to 23°C, the solution was pressure filtered with N₂ through pretreated Celite® (pretreated with triethylamine and tetrahydrofuran) twice and evaporated to dryness by rotary evaporation. The resulting brownish solid was vacuum distilled at 110-125°C (500 mtorr) twice with the fraction at 120-125°C being collected. Yield~61%, NMR (CDCl₃) δ 0.21 (s, 18H, NHSi(Me)₃), δ 0.24 (s, 18H, OSi(Me)₃), δ 3.51 (s, 2H, NH) δ 6.19 (s, 1H, aromatic), δ 6.25 (s, 1H, aromatic), *Elem. Anal.* Calcd. for C₁₈H₄₀N₂O₂Si₄: C, 50.41; H, 9.40; N, 6.53. Found: C, 48.81; H, 8.79; N, 8.77. N,N',O,O'-Tetra(trimethylsilyl)-4,6-diaminoresorcinol has been reported, but experimental data is unavailable in English [197]. A possible explanation for the difference in mass percentages could be the hydrolysis of trimethylsilyl groups during shipping and handling. Hydrolysis of trimethylsilyl groups would result in a higher percentage of nitrogen and lower percentages of carbon and hydrogen. The fact that high polymer could be generated from this material is indirect evidence of high monomer purity.

3.2.1.26. 2,2-Bis(4-methoxyphenyl)propane

Source	synthesized from 2,2-bis(4-hydroxyphenyl)propane
Empirical Formula	C ₁₇ H ₂₀ O ₂
Molecular Weight	256.33
Molecular Structure	



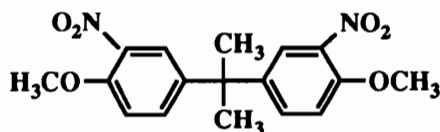
Synthesis procedure:

To a 500 mL, four neck, round bottom flask equipped with a reflux condenser, N₂ inlet, thermometer and glass stopper, 30.00 g (0.13 mol.) of 2,2-bis(4-hydroxyphenyl)propane, 60 mL of acetone, 36.79 g (0.27 mol.) of potassium carbonate and 38.22 g (0.27 mol.) of methyl iodide were combined and heated to reflux. After 24 hours, an additional 5.00 g (3.5 X 10⁻² mol.) of methyl iodide was added and the reaction allowed to continue for an additional 24 hours. The reaction mixture was cooled to 23°C, diluted with 300 mL of deionized water and extracted with 200 mL of chloroform. The organic extract was washed with water, 10% NaOH, water, saturated NaCl solution, dried with MgSO₄ and exposed to rotary evaporation to yield a clear viscous oil (Yield~72%). Trituration of the oil with deionized water afforded a white solid exhibiting a melting point of 50-52°C after exposure to vacuum for 24 hours. NMR (CDCl₃) δ 1.64

(s, 6H, CH₃), δ 3.78 (s, 6H, OCH₃), δ 6.80 (d, 4H, aromatic) δ 7.14 (d, 4H, aromatic), *Elem. Anal.* Calcd. for C₁₇H₂₀O₂: C, 79.65; H, 7.86. Found: C, 79.61; H, 7.84.

3.2.1.27. 2,2-Bis(4-methoxy-3-nitrophenyl)propane

Source	synthesized from 2,2-bis(4-methoxyphenyl)propane
Empirical Formula	C ₁₇ H ₁₈ N ₂ O ₆
Molecular Weight	346.33
Molecular Structure	



Synthesis procedure:

To a 500 mL, four neck, round bottom flask equipped with a reflux condenser, liquid addition funnel, N₂/thermometer inlet and glass stopper, 24.18 g (9.4 X 10⁻² mol.) of 2,2-bis(4-methoxyphenyl)propane and 50 mL of acetic anhydride were combined and cooled to 10°C. Over the course of 1.5 hours, a solution of 17.41 g (0.19 mol.) of 70% nitric acid in 8 mL of acetic acid was added slowly while maintaining the temperature between 10-15°C. The reaction mixture was treated with an additional 1.5 mL of 70% HNO₃ and warmed to 23°C for 2 hours. Finally the reaction

mixture was treated slowly with 300 mL of ice water and filtered. The yellow solid was washed with copious amounts of water and dried under reduced pressure for 20 hr at 85°C (Yield~90%).

Recrystallization from 95% ethanol afforded yellow crystals (104-105.6°C). NMR (CDCl₃) δ 1.67 (s, 6H, CH₃), δ 3.92 (s, 6H, OCH₃), δ 6.98 (d, 2H, aromatic) δ 7.28 (d, 2H, aromatic), δ 7.73 (s, 2H, aromatic), *Elem. Anal.* Calcd. for C₁₇H₁₈N₂O₆: C, 58.95; H, 5.24; N, 8.09. Found: C, 59.07; H, 5.23; N, 8.07.

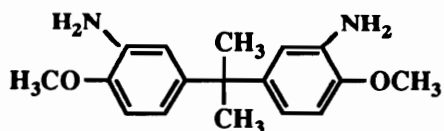
3.2.1.28. 2,2-Bis(3-amino-4-methoxyphenyl)propane

Source synthesized from 2,2-bis(4-methoxy-3-nitrophenyl)propane

Empirical Formula C₁₇H₂₂N₂O₂

Molecular Weight 286.37

Molecular Structure



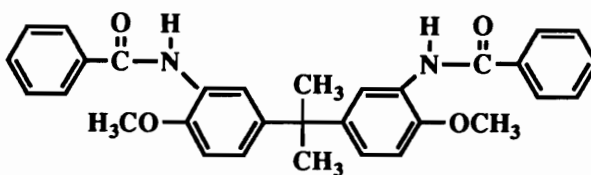
Synthesis procedure:

To a 500 mL pressure reactor, 23.61 g (6.8 X 10⁻² mol.) of 2,2-bis(4-methoxy-3-nitrophenyl)propane, 400 mL of methanol and 1.19 g of 10% palladium on charcoal were added. The system was purged with H₂ for 20 minutes, pressurized to 50 psi and heated to 30°C.

After 3 hours, the solution was pressure filtered through Celite® and stripped of methanol via rotary evaporation. The resulting brown viscous oil was put under vacuum (500 mtorr) for 24 hours at 45°C. Repeated efforts to purify the oil via distillation, crystallization and salt formation failed, so the product was confirmed by ¹H NMR and used without further purification. NMR (CDCl₃) δ 1.56 (s, 6H, CH₃), δ 3.66 (s, 4H, NH₂), δ 3.80 (s, 6H, OCH₃), δ 6.54 (s, 2H, aromatic) δ 6.62 (d, 2H, aromatic), δ 6.67 (d, 2H, aromatic), *Elem. Anal.* Calcd. for C₁₇H₂₂N₂O₂: C, 71.30; H, 7.74; N, 9.78. Found: C, 67.84; H, 7.36; N, 9.23. The difference in mass percentages could be attributed to impurities.

3.2.1.29. 2,2-Bis(4-methoxy-3-benzoylamino)propane

Source	synthesized from 2,2-bis(3-amino-4-hydroxyphenyl)propane
Empirical Formula	C ₃₁ H ₃₀ N ₂ O ₂
Molecular Weight	462.57
Molecular Structure	



Synthesis procedure:

To a two neck, 125 mL round bottom flask equipped with a N₂/thermometer inlet and drying tube, 3.08 g (1.1×10^{-2} mol.) of 2,2-bis(3-amino-4-methoxyphenyl)propane and 25 mL of N-methylpyrrolidinone were added, allowed to become homogeneous and cooled to 5-10°C. Immediately, 3.30 mL (2.6×10^{-2} mol.) of triethylamine was added followed by 2.74 mL (2.4×10^{-2} mol.) of benzoyl chloride (added dropwise over a period of 10 minutes). After 20 minutes the reaction temperature was increased to 23°C and maintained for 3 hours. The reaction mixture was filtered to remove the triethylamine hydrochloride salt and precipitated into 350 mL of water. The white precipitate was coagulated by adding NaCl, filtered and washed with copious amounts of water. The product was reprecipitated twice from methanol by slowly adding water. After filtration, washing with water and drying under reduced pressure at 100°C for 20 hours, a 87% yield was recovered m.p. = 179-182°C). NMR (d₆-DMSO) δ 1.61 (s, 6H, CH₃), δ 3.78 (s, 6H, OCH₃), δ 6.98 (d, 2H, aromatic), δ 7.4 (d, 2H, aromatic) δ 7.48 (t, 4H, aromatic), δ 7.55 (t, 2H, aromatic), δ 7.91 (d, 4H, aromatic), δ 9.37 (s, 2H NH), *Elem. Anal.* Calcd. for C₃₁H₃₀N₂O₄: C, 75.28; H, 6.11; N, 5.66. Found: C, 75.11; H, 6.16; N, 5.59.

3.2.1.30. 4-Iodobenzoic Acid

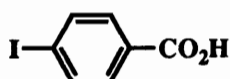
Source

Aldrich

Empirical Formula C₇H₅IO₂

Molecular Weight 248.02

Molecular Structure



Purification procedure:

4-Iodobenzoic acid was used as received.

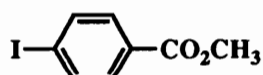
3.2.1.31. Methyl 4-iodobenzoate

Source synthesized from 4-iodobenzoic acid

Empirical Formula C₈H₇IO₂

Molecular Weight 262.05

Molecular Structure



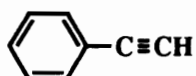
Synthesis procedure:

To a one neck, 500 mL, round bottom flask equipped with a stir bar and reflux condenser, 41.40 g (0.17 mol.) of 4-iodobenzoic acid, 400 mL of HPLC grade methanol and 3.00 g of concentrated sulfuric acid were added and heated to reflux. After 16 hours, 200 mL of methanol were removed from the reaction flask via rotary evaporation, 300 mL of deionized water added and the solution made

slightly basic with NaHCO_3 . The precipitate was filtered off, washed with copious amounts of water and aspirator dried. Sublimation of the solid resulted in white crystals (Yield~80%). M.p. = 112.7-114°C (lit. m.p. = 114°C [192]).

3.2.1.32. Phenylacetylene

Source	Aldrich
Empirical Formula	C_8H_6
Molecular Weight	102.13
Molecular Structure	



Purification procedure:

To a flame dried, one neck, 250 mL, round bottom flask containing pretreated 4Å molecular sieves, 100.00 g (0.98 mol.) of phenylacetylene was added, purged with N_2 , and fitted with a flame dried distillation apparatus. Immediately, 20 torr of vacuum was applied and flask heated to the distillation temperature. After discarding the first 5 mL, approximately 90 mL of water white phenylacetylene was collected between 45-47°C, sealed with a rubber septa, purged with nitrogen and stored in the freezer.

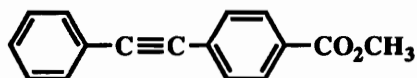
3.2.1.33. Methyl 4-phenylethynylbenzoate

Source synthesized from methyl 4-iodobenzoate

Empirical Formula $C_{16}H_{12}O_2$

Molecular Weight 236.26

Molecular Structure

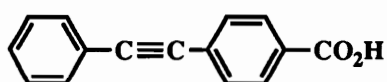


Synthesis procedure:

To a flame dried, three neck, 250 mL, round bottom flask equipped with a reflux condenser and 2 septa, 12.03 g (4.6×10^{-2} mol.) of methyl 4-iodobenzoate, 40 mL of triethylamine, 6.06 mL (5.5×10^{-2} mol.) of phenyl acetylene and 0.093 g (3.5×10^{-4} mol.) of triphenylphosphine were charged and warmed to 40°C. In the dark, 0.047 g (5.9×10^{-5} mol.) of $PdCl_2(PPh_3)_2$ was added with 20 mL of triethylamine and the solution warmed to 60°C. Copper iodide (0.019 g, 1.0×10^{-4} mol.)) was added and the reaction temperature further increased to 72°C. After 12 hours in the dark, the reaction mixture was cooled to 30°C, diluted with 100 mL of tetrahydrofuran, filtered and exposed to rotary evaporation. The resulting light brown solid was slurried with methanol, washed with methanol and aspirator dried. Yield~95%. The product was confirmed by ¹H NMR (Figure 4.18) and derivatization (acid and acid chloride). Methyl 4-phenylethynyl benzoate has been reported by Bumagin et al [198].

3.2.1.34. 4-Phenylethynylbenzoic Acid

Source	synthesized from methyl 4-phenylethynylbenzoate
Empirical Formula	C ₁₅ H ₁₀ O ₂
Molecular Weight	222.23
Molecular Structure	



Synthesis procedure:

In a one neck, 500 mL, round bottom flask equipped with a reflux condenser, 10.37 g (4.4×10^{-2} mol.) of methyl 4-phenylethynyl benzoate was slurried in 200 mL of methanol, 50 mL of deionized water and 20.00 g (0.50 mol.) of NaOH (NaOH was dissolved in water prior to addition). The reaction temperature was raised to reflux and maintained for 3 hours. After cooling to 5°C, the reaction mixture was diluted with 200 mL of water and neutralized with 5N HCl. The resulting off-white solid was collect by filtration, washed with an excess of water and dried under reduced pressure at 90°C for 24 hours (Yield~96%). The product was confirmed by ¹H NMR (Figure 4.18) and chlorinated without further purification (m.p. = 225-230°C (lit. m.p. = 221-222°C [199])).

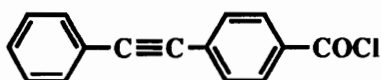
3.2.1.35. 4-Phenylethynylbenzoyl chloride

Source synthesized from 4-phenylethynylbenzoic acid

Empirical Formula $C_{15}H_9ClO$

Molecular Weight 240.68

Molecular Structure



Synthesis procedure:

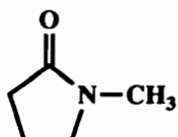
In a 100 mL, one neck, round bottom flask equipped with a reflux condenser, 5.00 g (2.2×10^{-2} mol.) of 4-phenylethynylbenzoic acid was slurried in 25 mL of thionyl chloride and 2 drops of N,N-dimethylformamide. The reaction temperature was raised to 55°C and maintained for 8 hours. After cooling the homogeneous solution to 40°C, it was filtered through a medium porosity fritted funnel with nitrogen into a flame dried flask. Subsequent evaporation of thionyl chloride resulted in a yellow solid which was slurried with hexanes, filtered and dried under reduced pressure at 23°C.

Fractional vacuum distillation of the product at 700 mtorr (fraction collected at 190-193°C) resulted in an off-white solid. Yield~66%, m.p. = 86.0-87.6°C (lit. m.p. = 88-89°C [200]).

3.2.2. Solvents

3.2.2.1. N-Methylpyrrolidinone (NMP)

Source	Fisher
Empirical Formula	C ₅ H ₉ ON
Molecular Weight	99.13
Boiling Point	78-79°C/10mm
Density at 25°C	1.033
Molecular Structure	



Purification procedure:

In a 2 liter, one neck, round bottom flask equipped with a Dririte® drying tube, 1500 mL of N-methylpyrrolidinone and 10.00 g of phosphorus pentoxide were combined and allowed to stir for 24 hours. The flask was fitted with a distillation apparatus (Figure 3.2) and heated to the reflux temperature of NMP at 10 torr. After 2 hours at reflux, 100 mL were collected and discarded. The remaining NMP, except for the last 100 mL, were collected, sealed with a rubber septum and purged with N₂ prior to storage.

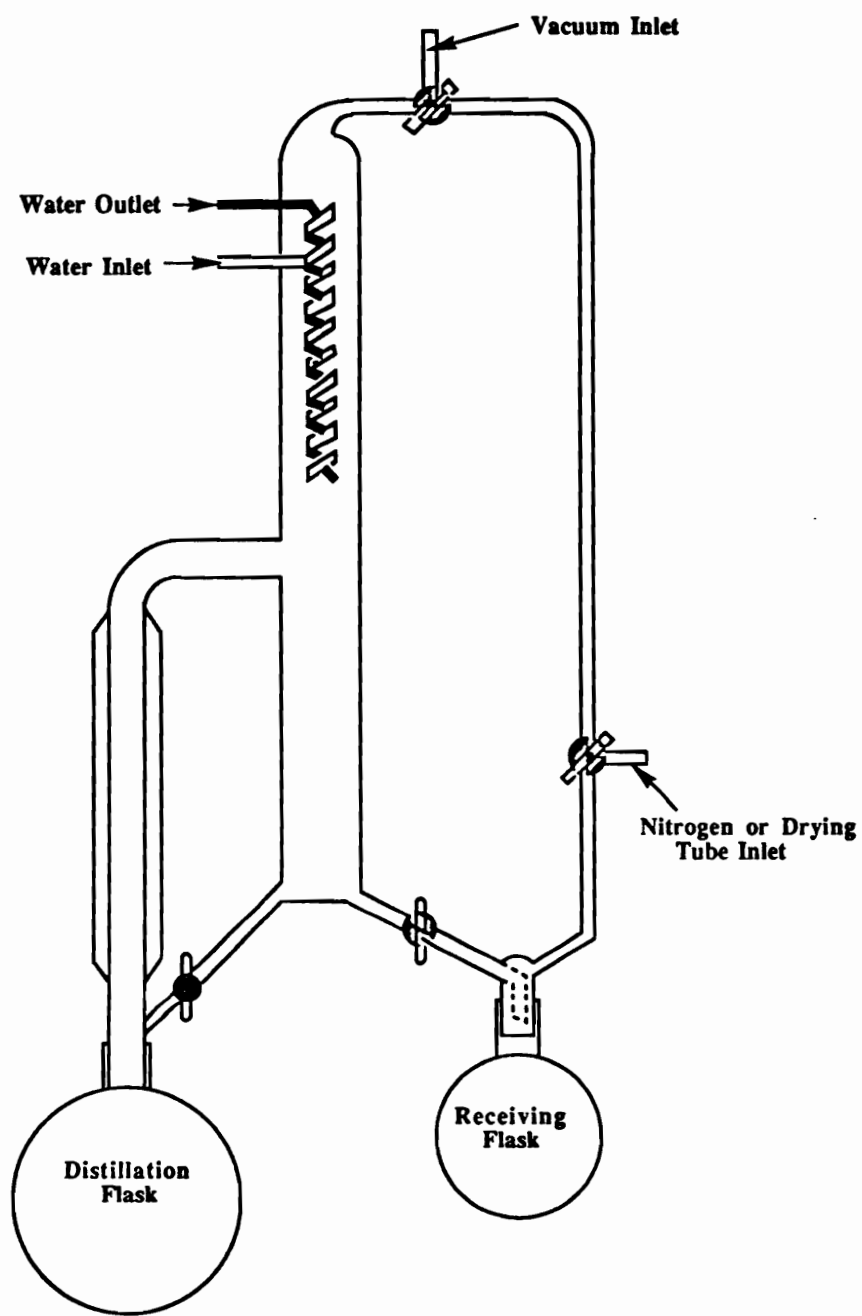
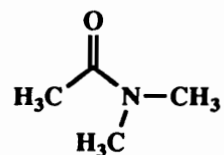


Figure 3.2. Solvent distillation apparatus.

3.2.2.2. N,N-Dimethylacetamide (DMAc)

Source	Fisher
Empirical Formula	C ₄ H ₉ ON
Molecular Weight	87.12
Boiling Point	164-166°C
Density at 25°C	0.938
Molecular Structure	



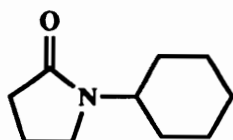
Purification procedure:

In a 2 liter, one neck, round bottom flask equipped with a Dririte® drying tube, 1500 mL of N,N-dimethylacetamide and 10.00 g of phosphorus pentoxide were combined and allowed to stir for 24 hours. The flask was fitted with a distillation apparatus (Figure 3.2) and heated to the reflux temperature of DMAc at 10 torr. After 2 hours at reflux, 100 mL were collected and discarded. The remaining DMAc, except for the last 100 mL, were collected, sealed with a rubber septum and purged with N₂ prior to storage.

3.2.2.3. N-Cyclohexylpyrrolidinone (CHP)

Source	Fisher
--------	--------

Empirical Formula	C ₁₀ H ₁₇ ON
Molecular Weight	167.25
Boiling Point	153-154°C/7mm
Density	1.007
Molecular Structure	



Purification procedure:

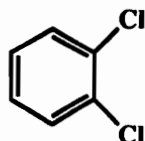
In a 1 liter, one neck, round bottom flask equipped with a Dririte® drying tube, 750 mL of N-cyclohexylpyrrolidinone and 5.00 g of phosphorus pentoxide were combined and allowed to stir for 24 hours. The flask was fitted with a distillation apparatus (Figure 3.2) and heated to the reflux temperature of CHP at 10 torr. After 2 hours at reflux, 25 mL were collected and discarded. The remaining CHP, except for the last 50 mL, were collected, sealed with a rubber septum and purged with N₂ prior to storage.

3.2.2.4. *o*-Dichlorobenzene (DCB)

Source	Fisher
Empirical Formula	C ₆ H ₄ Cl ₂
Molecular Weight	147.00
Boiling Point	178-180°C

Density 1.306

Molecular Structure

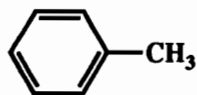


Purification procedure:

In a 2 liter, one neck, round bottom flask equipped with a Dririte® drying tube, 1500 mL of *o*-dichlorobenzene and 5.00 g of pulverized calcium hydride were combined and allowed to stir for 24 hours. The flask was fitted with a distillation apparatus (Figure 3.2) and heated to the reflux temperature of DCB at 10 torr. After 2 hours at reflux, 100 mL were collected and discarded. The remaining DCB, except for the last 100 mL, were collected, sealed with a rubber septum and purged with N₂ prior to storage.

3.2.2.5. Toluene

Source	Fisher
Empirical Formula	C ₇ H ₈
Molecular Weight	92.14
Boiling Point	110-111°C
Density	0.867
Molecular Structure	



Purification procedure:

In a 1 liter, one neck, round bottom flask, 750 mL of toluene and 5.00 g of pulverized calcium hydride were combined. The flask was fitted with a distillation apparatus (Figure 3.2) and heated to the reflux temperature of toluene. After 2 hours at reflux, 25 mL were collected and discarded. The remaining toluene, except for the last 50 mL, were collected, sealed with a rubber septum and purged with N₂ prior to storage.

3.2.2.6. Tetrahydrofuran (THF)

Source	Fisher
Empirical Formula	C ₄ H ₈ O
Molecular Weight	72.10
Boiling Point	67°C
Density at 25°C	0.866
Molecular Structure	

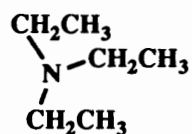


Purification procedure:

To a two liter, 1 neck, round bottom flask, 1500 mL of tetrahydrofuran, 10.0 g of sodium metal and 1 granule of benzophenone were added. The flask was equipped with a distillation apparatus (Figure 3.2) and purged with N₂. After heating to the reflux temperature of THF and allowing the solution to turn purple, desired aliquots of THF were removed via canula and stored in flame dried, septum sealed flasks under nitrogen.

3.2.2.7. Triethylamine (TEA)

Source	Fisher
Empirical Formula	C ₆ H ₁₅ N
Molecular Weight	101.19
Boiling Point	89-90°C
Density at 25°C	0.726
Molecular Structure	



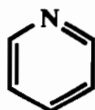
Purification procedure:

In a one neck, 500 mL, round bottom flask, 350 mL of triethylamine and 5.00 g of pulverized calcium hydride were combined and stirred for 2 hours. The flask was equipped with a

distillation apparatus, purged with N₂, heated to the reflux temperature of THF and distilled under a nitrogen blanket. After discarding the first 25 mL, the TEA was collected in a flame dried flask, sealed with a septum and purged with N₂ prior to storage.

3.2.2.8. Pyridine

Source	Fisher
Empirical Formula	C ₅ H ₅ N
Molecular Weight	79.10
Boiling Point	114-115°C
Density at 25°C	0.979
Molecular Structure	



Purification procedure:

In a one neck, 500 mL, round bottom flask, 350 mL of pyridine and 5.00 g of calcium hydride were combined and stirred for 2 hours. The flask was equipped with a distillation apparatus, purged with N₂ and the pyridine distilled under a nitrogen blanket. After discarding the first 25 mL, the pyridine was collected in a flame dried flask, sealed with a septum and purged with N₂ prior to storage.

3.3. Synthesis of Polymers and Oligomers

3.3.1. General Poly(hydroxy amide) Synthesis

Poly[imino-1,4-(2-hydroxyphenylene)[2,2,2-trifluoro-1-(trifluoromethyl)ethylidene]-1,4-(3-hydroxyphenylene)-iminocarbonyl-1,4-phenyleneoxy-1,4-phenylenecarbonyl] (6FAP-ODBC poly(hydroxy amide)) was synthesized using the following monomers and solvents. The reaction vessel used in the polymerization is shown in Figure 3.3.

6F Aminophenol (6FAP)	3.6626 g	10.0 mmoles
4,4'-Oxydibenzoyl Chloride	2.9512 g	10.0 mmoles
Pyridine	2.18 mL	27.0 mmoles
NMP	33 mL	

Polymerization procedure:

To a flame dried, three neck, 125 mL, round bottom flask equipped with an overhead stirrer, N₂/thermometer inlet and liquid addition funnel equipped with a drying tube, 3.6626 g of 2,2-bis(3-amino-4-hydroxyphenyl)hexafluoropropane (6FAP), 20 mL of N-methylpyrrolidinone (NMP) and 2.18 mL of pyridine were charged under N₂ purge. After the solution became homogeneous, it was cooled to 5°C and treated with an NMP/4,4'-oxydibenzoyl chloride solution (2.9512 g of 4,4'-oxydibenzoyl chloride dissolved in 5 mL of

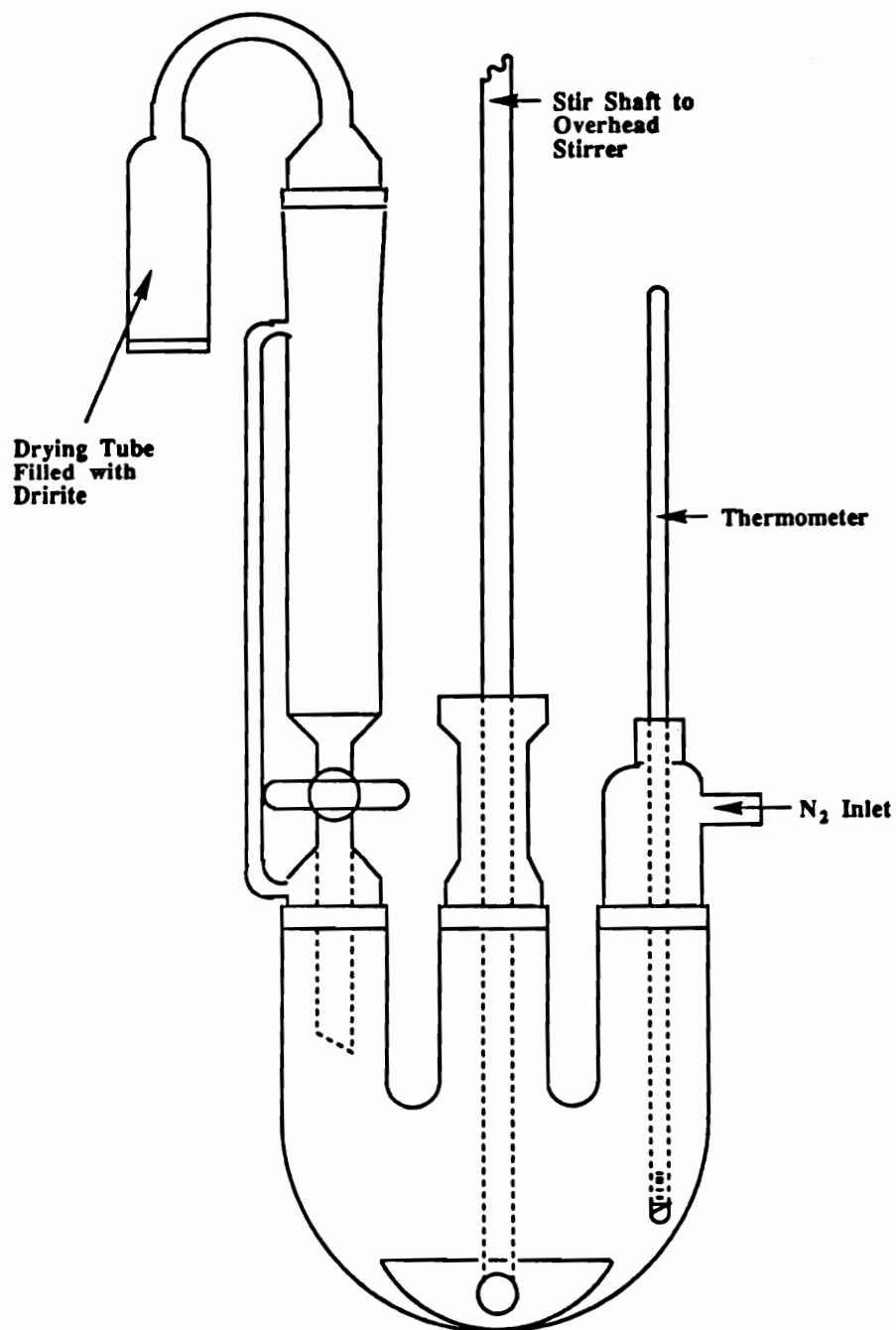


Figure 3.3. Reaction vessel used to synthesis poly(hydroxy amide)s

NMP) from the liquid addition funnel. Addition was made dropwise so as to maintain the reaction temperature below 10°C. After approximately half the acid chloride solution had been added, the stirring rate was continuously increased to avoid gelation of the reaction mixture. After all the acid chloride had been added, the addition funnel was washed twice with 4 mL aliquots of NMP and the reaction temperature increased to 23° by removing the ice water bath. After 12 hours at 23°C, the reaction mixture was precipitated into 500 mL of methanol/water (50:50) using a Waring blender. Fibrous, white polymer was collected, washed with 300 mL of 50:50 methanol/water, 300 mL of deionized water and dried under reduced pressure for 24 hours at 120°C. Nearly quantitative yields were achieved.

3.3.2. Phenylethynyl terminated poly(hydroxy amides)

A phenylethynyl terminated 6FAP-ODBC poly(hydroxy amide) ($M_n = 5000$ g/mol) was synthesized using the following monomers and reagents. The molar amounts of difunctional and monofunctional reagents used in the polymerization were determined using the Carothers equation [188,189].

6F Aminophenol (6FAP)	6.5927 g	18.0 mmoles
-----------------------	----------	-------------

4,4'-Oxydibenzoyl Chloride	4.7220 g	16.0 mmoles
4-Phenylethynylbenzoyl Chloride	0.9627 g	4.0 mmoles
Pyridine	3.90 mL	48.4 mmoles
NMP	45 mL	

Polymerization procedure:

To a flame dried three neck, 125 mL, round bottom flask equipped with an overhead stirrer, N₂/thermometer inlet and liquid addition funnel equipped with a drying tube, 6.5927 g of 2,2-bis(3-amino-4-hydroxyphenyl)-hexafluoropropane (6FAP), 30 mL of N-methyl-pyrrolidinone (NMP), 3.90 mL of pyridine and 0.9627 g of 4-phenylethynylbenzoyl chloride were charged under N₂ flow. After the solution became homogeneous, it was cooled to 5°C and treated with an NMP/4,4'-oxydibenzoyl chloride solution (4.7220 g of 4,4'-oxydibenzoyl chloride dissolved in 7 mL of NMP) from the liquid addition funnel. The addition was made dropwise so as to maintain the reaction temperature below 10°C. After approximately half the acid chloride solution had been added, the stirring rate was continually increased to avoid gelation of the reaction mixture. Once all the acid chloride had been added, the addition funnel was washed with two 4 mL aliquots of NMP and the reaction temperature raised to 23° by removing the ice water bath. After 12 hours at 23°C, the reaction mixture was precipitated into 1 liter of methanol/water (50:50) using a Waring blender. The white polymer was collected, washed with 300 mL of 50:50 methanol/water, 300

mL of deionized water and dried under reduced pressure for 24 hours at 120°C. The yield was nearly quantitative.

3.3.3. General Polybenzoxazole Synthesis

Poly[2,6-benzoxazolediy]l[2,2,2-trifluoro-1-(trifluoromethyl)ethylidene]-6,2-benzoxazolediy]l-1,4-phenyleneoxy-1,4-phenylene] (6FAP-ODBC polybenzoxazole) was synthesized using the following reagents. Phenylethynyl terminated polybenzoxazoles were generated in a similar fashion. The reaction vessel used for the cyclization reaction is shown in Figure 3.4.

6FAP-ODBC Poly(hydroxy amide)	5.00 g	85.0 mmoles
<i>p</i> -Toluenesulfonic acid monohydrate	0.16 g	8.5 mmoles
Toluene	5 mL	
NMP	20 mL	

Cyclization procedure:

To a 3 neck, 125 mL, round bottom flask equipped with an overhead stirrer, Dean-Stark trap fitted with a reflux condenser and a N₂/thermometer inlet, 0.160 g of *p*-toluenesulfonic acid monohydrate was added along with 5 mL of toluene and 5 mL of NMP. The Dean-Stark trap was filled with toluene and the reaction temperature raised to the azeotrope temperature of the system

(~130°C). After 2 hours, the reaction vessel was cooled to 50°C and 5.00 g of 6FAP-ODBC poly(hydroxy amide) was added along with 15 mL of NMP. The reaction system was purged with nitrogen and heated to 155-160°C. Immediately upon reaching the azeotrope temperature of the system, water was noticed collecting in the Dean-Stark trap. After 12 hours (reaction complete by ¹H NMR), the reaction mixture was cooled to 23°C and precipitated into 100 mL of methanol. The off-white polymer was collected by filtration, washed multiple times with water and methanol and finally dried under reduced pressure at 160°C for 24 hours. Nearly quantitative yields of polymer were recovered.

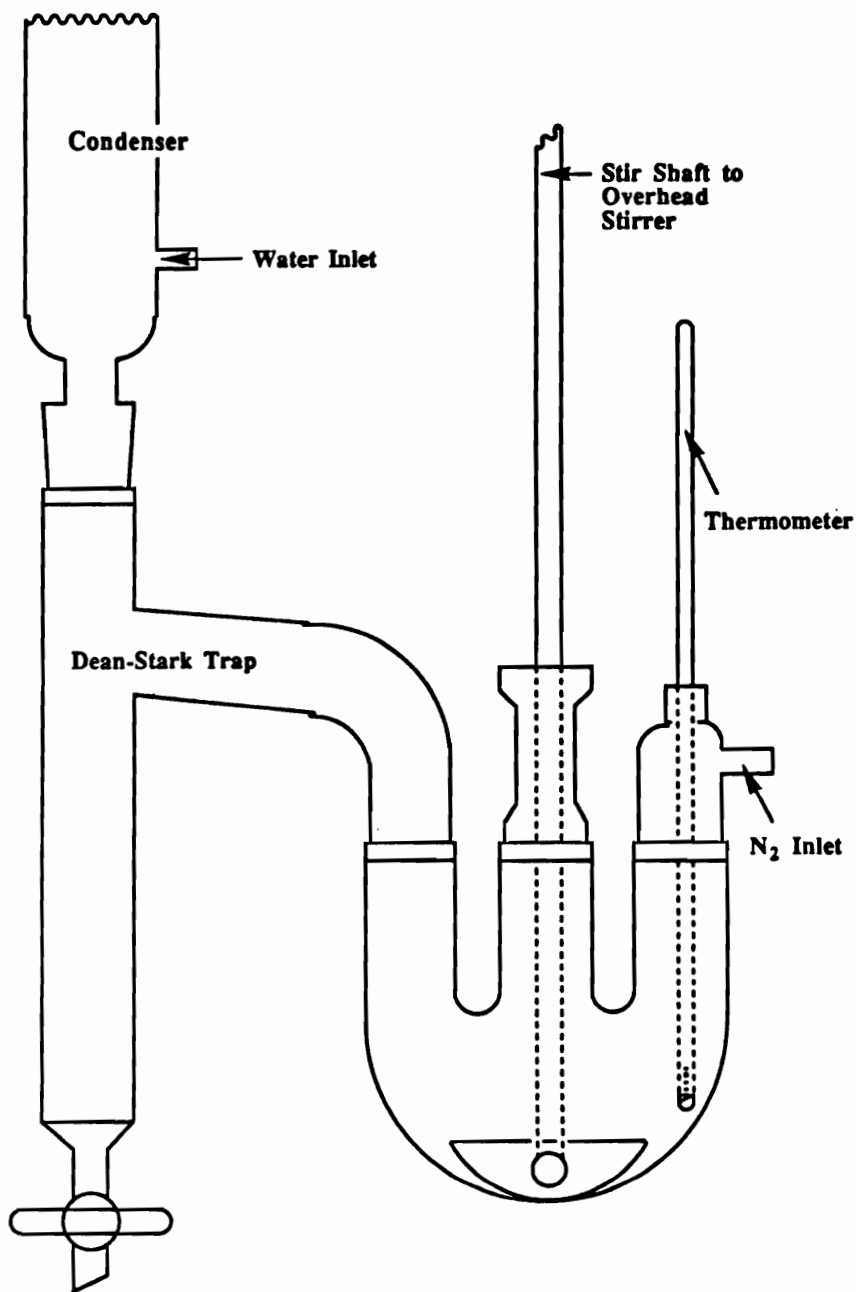


Figure 3.4. Reaction vessel used in the cyclization of poly(hydroxy amide)s.

3.4. Analysis of Oligomers and Polymers

3.4.1. Intrinsic Viscosity Determinations

Intrinsic viscosities or the limiting viscosity number of polymers were determined using Cannon-Ubbelohde viscometers with bore sizes ranging from 50 to 200. The temperature at which the measurements were made was thermostatically controlled using a large water bath. Initial polymer solutions were typically composed of 0.200 g of polymer in 20 mL of a suitable HPLC grade solvent. Eight milliliters of the filtered solution were pipetted into a viscometer, the temperature equilibrated at 25°C and flow times recorded until 3 consecutive flow times with a variance in time of 0.20 seconds or less was obtained. The solution was then diluted with 4 mL of solvent and the procedure repeated. A total of 3 concentrations were required to obtain reliable data. In addition to the polymer solutions, the control flow time of pure solvent was also determined.

To calculate the intrinsic viscosity ($[\eta]$), the relative viscosity (η_{rel}), specific viscosity (η_{sp}), inherent viscosity (η_{inh}) and reduced viscosity (η_{red}) has to be determined. The data used to determine each of these viscosities comes from the average of 3 consecutive retention times (t) at each polymer concentration (c) and the

average solvent retention time (t_0). Typically, at least three different polymer concentrations are used, but four is suggested for higher precision. The following relationships were used to calculate the viscosities:

$$\eta_{rel} = t/t_0$$

$$\eta_{sp} = (t-t_0)/t_0$$

$$\eta_{inh} = (\ln \eta_{rel})/c$$

$$\eta_{red} = \eta_{sp}/c.$$

Intrinsic viscosity is determined by plotting the η_{red} and the η_{inh} versus concentration, extrapolating both lines to zero concentration and averaging the zero concentration values of η_{red} and η_{inh} .

3.4.2. Nuclear Magnetic Resonance Spectroscopy (NMR)

NMR measurements were made on a Varian 400 MHz spectrometer at 24°C. Samples were run as solutions, dissolved in either deuterated chloroform or deuterated dimethyl sulfoxide or some nondeuterated solvent which was spiked with one of the above mentioned deuterated solvents. In some cases the spectra were referenced to tetramethylsilane, but in most cases the spectra were referenced to the deuterated solvent. Shifts are reported in ppms.

3.4.3. Fourier Transform Infrared Spectroscopy (FT-IR)

Fourier transformed infrared spectra collected on monomers and polymers were made on a Nicolet MX-1 Spectrometer which had been upgraded to a 10-DX instrument. The spectra were gathered at room temperature with a sweep width of 400-4000 cm^{-1} and a resolution of 4 cm^{-1} . Monomer samples were prepared in the form of KBr pellets and polymer samples were analyzed as thin films or as KBr pellets.

3.4.4. Differential Scanning Calorimetry (DSC)

Differential scanning calorimetry was used to monitor thermal transitions, such as glass transitions, melting points, crystallization behavior or cure profiles. Data was obtained on a DuPont 912 (dual head) differential scanning calorimeter (DSC) coupled with a DuPont Thermal Analyst 2100 microprocessor. Experiments were conducted with sample sizes of approximately 15 mg, and at a scan rate of 10°C per minute. Glass transition temperatures (T_g 's) were obtained from the second scan and calculated using the half-height method. Melting transitions or cure temperatures were reported as the maximum in the respective endotherm or exotherm.

3.4.5. Dynamic Mechanical Thermal Analysis (DMTA)

Dynamic mechanical thermal analysis was used in conjunction with DSC to monitor thermal transitions in some of the polymer samples. The instrument used to make these measurements was a Seiko Model 200 DMS. Measurements were made on thin films measuring approximately 1 cm by 3 cm, at a frequency of 1 Hz and a scan rate of 10° per minute.

3.4.6. Dynamic Thermal Gravimetric Analysis (TGA)

Dynamic thermal gravimetric analysis was used as a screening tool to identify polymers which displayed outstanding thermo-oxidative stability in aggressive environments. The instrument used to perform this task was a DuPont 915 Thermogravimetric Analyzer equipped with a DuPont Thermal Analyst 2100 microprocessor. Samples were either in the form of films or powders with initial weights ranging from 5-15 mg, depending on sample form. Most of the experiments were performed in an atmosphere of air (N₂ was used occasionally) at a heating rate of 10°C per minute, with a temperature range of 30-750°C.

3.4.7. Isothermal Thermal Gravimetric Analysis (TGA)

To complement the thermo-oxidative stability data obtained from dynamic TGA, isothermal thermo-oxidative stability data was also collected. Preliminary isothermal data was collected on a Perkin-Elmer TGA7 Thermogravimetric Analyzer using film samples of approximately 5 mils in thickness. Data was collected over a 24 hour period at 371°C in an air atmosphere. In addition to using a TGA head to collect thermal stability data, a Big Blue conventional forced air oven was used. Films measuring approximately 4 inches by 6 inches by ~2-5 mil in thickness were placed in aluminum pans and loaded into the oven which had been preheated to 371°C. Air flow was approximately 0.5 psi (25 cf/hour) and samples were weighed periodically via an exterior toploading balance.

3.4.8. Thermal Gravimetric Analysis - Mass Spectrometry (TGA-MS)

Thermal gravimetric analysis coupled mass spectrometry data was used to monitor the percent cyclization in the polybenzoxazoles. The TGA-MS data was obtained on Perkin-Elmer TGS-2 thermogravimetric analyzer equipped with a Hewlett-Packard 5971A mass selective detector, working in the electron impact

ionization mode. After a 10 minute purge with helium, thin film samples were subjected to a heating rate of 40°C per minute in a helium carrier gas. The mass selective detector was configured to scan the 15-300 m/z region, completing 0.7 scans per second.

3.4.9. Hot Stage Optical Analysis

Optical micrographs of crystalline polybenzoxazoles containing fluorinated linkages were obtained using a Zeiss Axioplan polarized optical microscope equipped with a Zeiss camera and Linkam hot stage. Samples were prepared by casting films from polymer solutions (1% solids (w/v)) and removing the the solvent in a vacuum oven. Analysis of the polymers was done in a nitrogen atmosphere and at a heating rate of 5°C/minute.

3.4.10. Stress-Strain Measurements

Tensile properties of solution cast thin films were determined using an INSTRON tensile tester, model 1123. Dogbone shaped specimens were cut from unoriented films (1-10 mils thick) using a steel rule die (ASTM-6381V). Samples measuring 10 mm in length and 2.76 mm in width were clamped between pneumatic clamps and elongated at a rate of 0.50 inches per minute at room temperature.

The modulus was determined by drawing a tangent to the initial slope of the stress-strain curve. The results were reported as an average of at least four measurements. In all cases, an extensometer was employed during the measurement.

3.4.11. Titration Methods

A number of aminophenol monomers synthesized were analyzed for amine functionality using titration methods. The acid-base titration's were carried out using an MCI GT 05 Automatic Titrator fitted with a standard glass combination pH electrode with Ag/AgCl reference as an endpoint detector. The HBr in methanol titrant (~0.020 molar) was standardized using potassium hydrogen phthalate in 65 ml of a 1:2.5 (v/v) glacial acetic acid/tetrahydrofuran solvent system. The glacial acetic acid/THF solvent system was also employed in the titration of the amines. During the titration, a change in potential was observed as a function of titrant volume added. The endpoint volume was determined from the maximum in the 1st derivative curve of the titrant volume versus potential plot. Determination of molecular weight from titration was based on the following formula:

$$\text{Molecular Weight} = W \times \frac{N}{C \times (V - V_b)},$$

where W is the mass of monomer or polymer, N is the number of functional groups per molecule, C is the titrant molarity, V is the titrant volume at the endpoint and V_b is the volume of titrant required to titrate a solvent blank.

3.4.12. Melting Point Determinations

Melting points were determined on a Laboratory Devices Mel-Temp II melting point apparatus at a heating rate of 2°C/minute. Melting points are quoted uncorrected.

2.4.13. Gel Permeation Chromatography

GPC measurements were performed on a Waters 150-CAL/GPC equipped with a viscosity and refractive index detectors. $\langle M_n \rangle$ and $\langle M_w \rangle / \langle M_n \rangle$ values for the polybenzoxazoles were determined using universal calibration techniques [201].

Chapter 4

RESULTS AND DISCUSSION

4.1. Introduction

The state of the art technology for generating polybenzoxazoles is based on the early work of Iwakura, Arnold and Wolfe [17,89,106]. This synthetic procedure utilizes a polyphosphoric acid/ P_2O_5 reaction medium to generate wholly aromatic, liquid crystalline polymers which exhibit phenomenal thermal and mechanical properties [110]. In fact, fibers generated from liquid crystalline dopes have been shown to be some of the most thermo-oxidatively stable polymers known to date. Unfortunately, as with most polymers, a trade off in processing and/or mechanical properties is

required to obtain these excellent properties and polybenzoxazoles are no exception.

The major drawbacks associated with these materials are low transverse tensile strengths and less than favorable processing conditions. The problem of low transverse tensile strengths is related to the high degree of ordering which takes place in the liquid crystalline state, in addition to the low interchain secondary bonding interactions. The completely aromatic nature and absence of acidic sites along the polymer backbone prevents polybenzoxazoles from displaying strong secondary bonding forces such as H-bonding or dipole-dipole interactions. This lack of interchain cohesion is believed to be responsible for the low transverse tensile and compressive strengths observed [18].

Reduction of the ordering within a particular system is a viable option for enhancing transverse mechanical properties, but unfortunately the desirable mechanical properties in the machine direction are also compromised when isotropic systems are employed. The drawbacks associated with processing these wholly aromatic polymer systems are also quite formidable.

Polybenzoxazole fibers are spun directly from the polyphosphoric acid/ P_2O_5 polymerization solvent, through a procedure known as dry-wet spinning [105]. Other processing solvents include sulfuric acid and methanesulfonic acid. Use of such solvent renders film casting, solvent removal, and polymer purification extremely difficult. In addition, use of these environmentally unattractive

solvents significantly limits the scope of applicability for these materials.

Many investigations have been conducted in an attempt to broaden the scope of utility for these materials. A number of synthetic methodologies have been developed to generate polybenzoxazoles which exhibit solubility in common organic solvents, but retain a majority of the thermo-oxidative properties of the wholly aromatic polymers [8,123,126,136]. The most common method of enhancing solubility has been through the incorporation of fluorine containing monomers, such as 2,2-bis(3-amino-4-hydroxyphenyl)hexafluoropropane or via copolymerization [146,156]. Research efforts reported herein are also aimed at synthesizing soluble polybenzoxazoles using commercially available or easily synthesized monomers as well as industrially acceptable solvents.

This chapter will describe results and progress made toward the goal of processible high performance polybenzoxazoles. It begins with a discussion of the synthesis and characterization of a number of bis(*o*-aminophenol) and diacid chloride monomers used in the polymerizations. The second section will address some of the apparent misconceptions reported in the literature relative to low temperature poly(hydroxy amide) reactions, in addition to presenting experimental evidence supporting our new conclusions. Thirdly, cyclization techniques used in the generation of fully cyclized polybenzoxazoles will be introduced and discussed relative to the effect of catalyst type and concentration, as well as the

influence of reaction conditions on percent cyclization, amide hydrolysis and molecular weight. Finally, the synthesis and characterization of poly(hydroxy amide)s and polybenzoxazoles based on nonfluorinated and some related fluorinated monomers will be discussed in detail.

4.2. Synthesis of 2,2-Bis(3-amino-4-hydroxyphenyl)propane (bAAP)

The first monomer synthesized and investigated in this thesis project was 2,2-bis(3-amino-4-hydroxyphenyl)propane, a potentially inexpensive bis(*o*-aminophenol). The precursor dinitro compound to 2,2-bis(3-amino-4-hydroxyphenyl)propane has been synthesized by a number of different methods with yields around 75% [191,202,203]. The most direct synthesis involves nitration of 2,2-bis(4-hydroxyphenyl)propane (bisphenol A) with nitric acid in an acetic acid/benzene mixture at 0-5°C. One drawback to this synthetic procedure was the formation of mono-, di-, tri- and tetranitro derivatives. However, through the use of stoichiometric amounts of nitric acid, the dinitro derivative is the major product. Sulzberg and Cotter [203] reported the use of AgNO₃ as a nitrating agent when the dichloroformate of bisphenol A is employed. Yields of the desired bis(*o*-nitrophenol) were reported as high as 80% after recrystallization.

The approach taken in this research to synthesize bAAP (Figure 4.1) involves direct nitration of bisphenol A by dripping dilute nitric acid (in acetic acid) into a slurry of bisphenol A and acetic acid. Care was taken to avoid the various nitro derivatives by conducting the reaction below 15°C. Yields of 60-70% were realized after recrystallization from ethanol or acetic acid. Transformation of the dinitro compound to 2,2-bis(3-amino-4-hydroxyphenyl)propane involved catalytic hydrogenation in an aqueous medium. Formation of the potassium phenolate allowed for smooth reduction of the nitro groups in water. After neutralization with acetic acid, quantitative yields of bis(*o*-aminophenol) were realized. Molecular weight was determined by titration with HBr; calculated: 258.3 g/mole, titrated: 260.4 g/mole. The molecular structure was confirmed by FT-IR (Figure 4.2) and ¹H NMR (Figure 4.3). The infrared peak frequencies and their assignments are listed in Table 4.1.

4.3. Synthesis of 1,1,1-Triaryl-2,2,2-trifluoroethane Monomers

Hexafluoropropane linkages have been incorporated into a number of different polymers to achieve important improvements in various polymer properties [6]. In particular, these include an increase in glass transition temperatures, enhancements in solubility and an

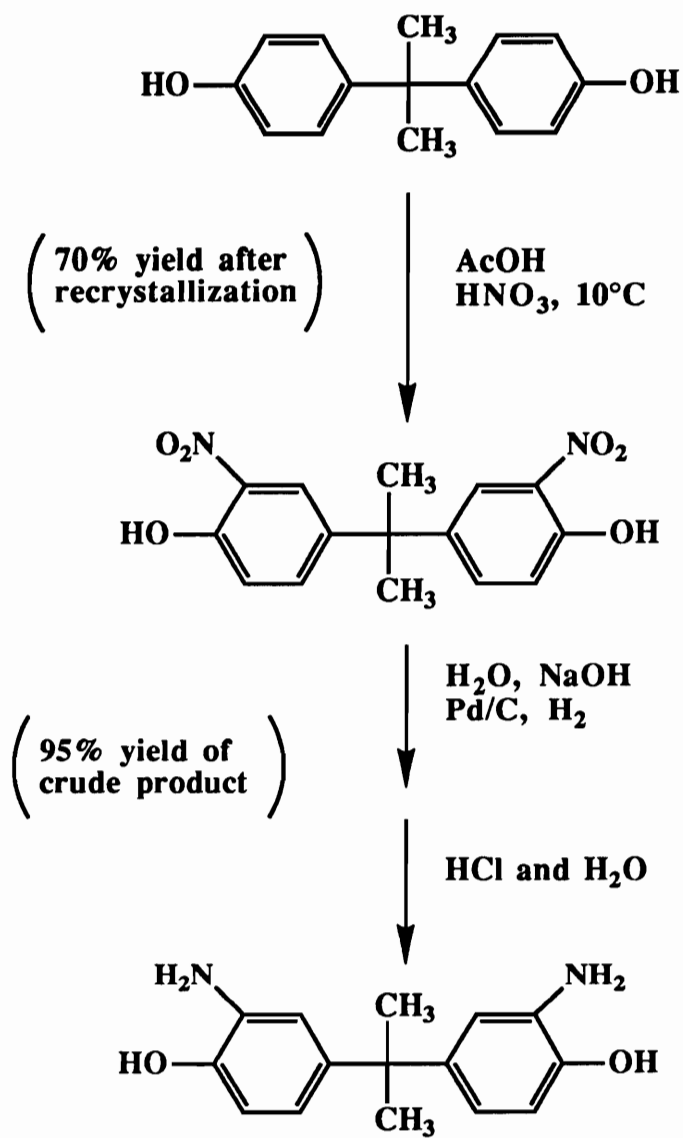


Figure 4.1. Synthesis of 2,2-bis(3-amino-4-hydroxyphenyl)propane (bAAP).

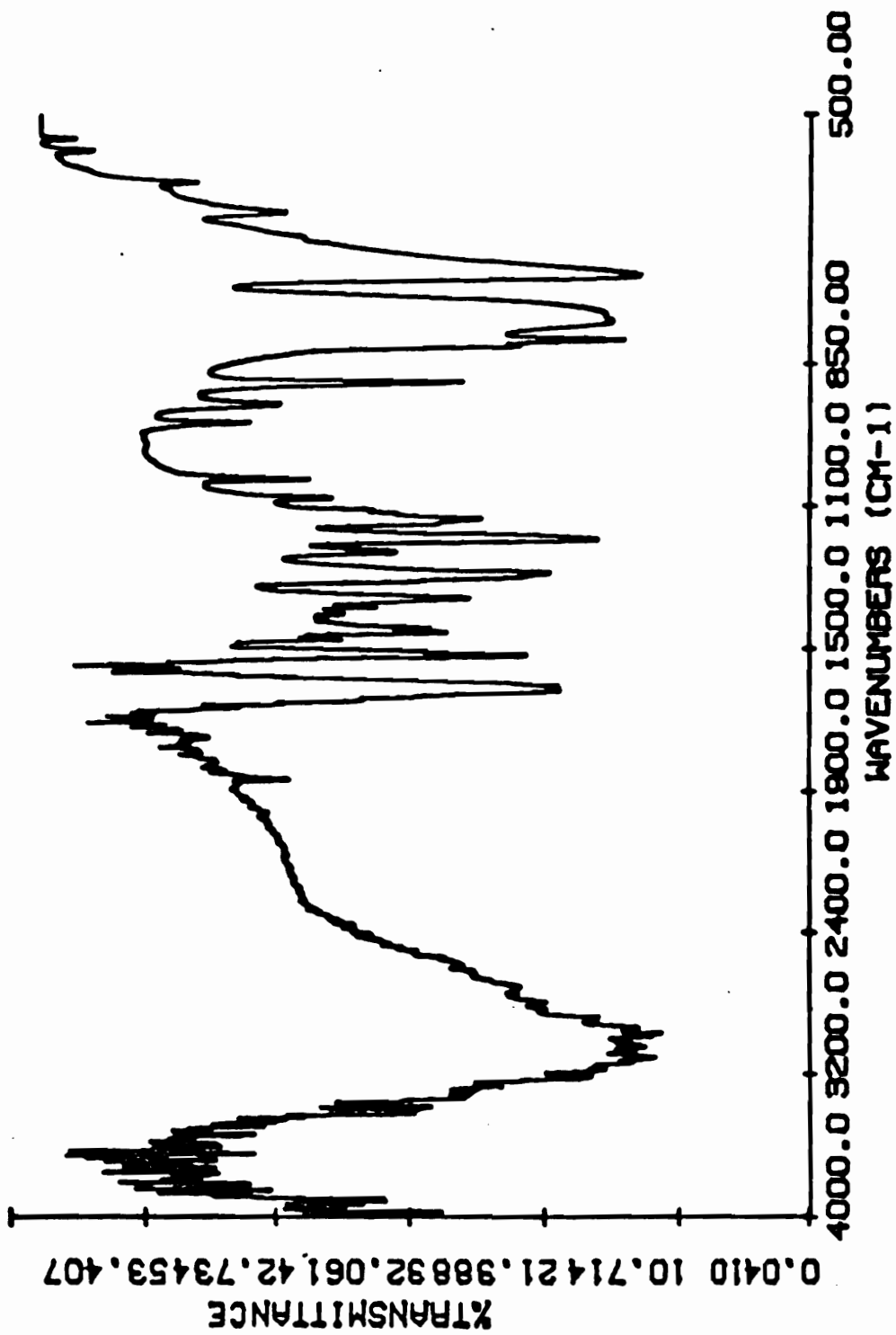


Figure 4.2. FT-IR spectrum of 2,2-bis(3-amino-hydroxyphenyl)propane (bAAP).

Table 4.1. FT-IR spectral assignments for 2,2-Bis(3-amino-4-hydroxyphenyl)propane (bAAP).

<u>Assignment</u>	<u>Frequency (cm⁻¹)</u>
-NH stretch	3460-3280
OH stretch	3350-3250
NH ₂ deformation	1618
Aromatic stretch (C=C)	1520
CH ₃ antisym. deformation	1450
CH ₃ symmetric deformation	1363
C-OH in plane bend	1290
Aromatic CH in plane bend	1195, 1145

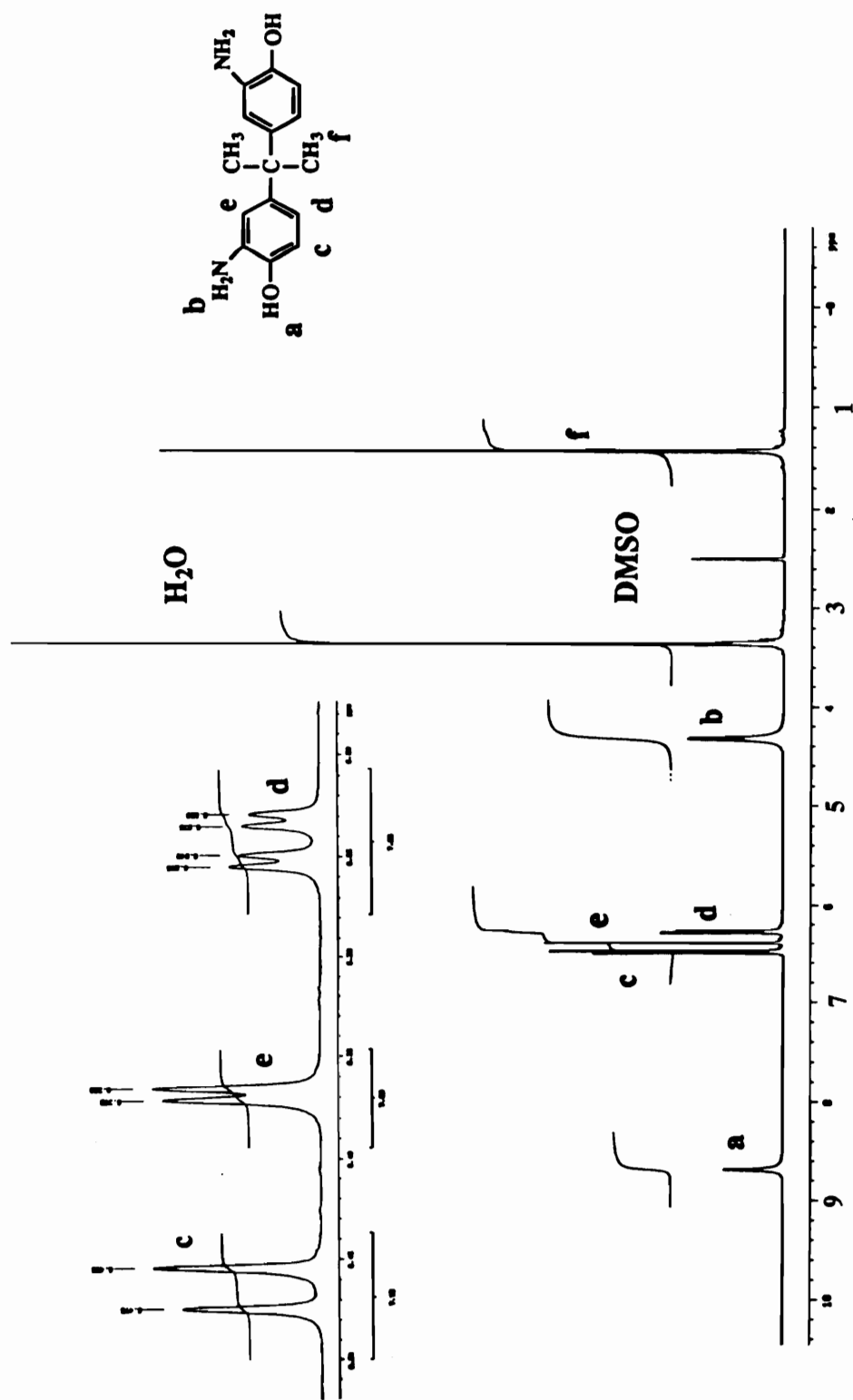


Figure 4.3. ^1H NMR spectrum of 2,2-Bis(3-amino-4-hydroxyphenyl)propane (bAAP).

increase in thermo-oxidative stabilities relative to nonfluorinated analogs. Replacement of one of the trifluoromethyl groups with a phenyl group also results in improved polymer properties, in addition to enhancing polymer solubilities due to the introduction of asymmetry. Investigations conducted with poly(arylene ethers) [204] and polyimides [205,206] confirm several of these features and also suggest that the trifluoromethyl groups may be more thermally labile when bonded to an sp^3 carbon bearing 3 phenyl rings, relative to an sp^3 carbon with 2 phenyl rings and an additional trifluoromethyl group. The effect of incorporating phenyltrifluoroethane linkages on solubility and thermal stability of polybenzoxazoles was investigated by synthesizing new macromolecules based on a novel bis(*o*-aminophenol) and diacid chlorides. The syntheses of these two compounds are outlined in Figures 4.4 and 4.5.

The first attempt to synthesize triaryl substituted trifluoroethane materials appears to have been made by Korshak [207] in 1968. The focus of this work included synthesis of a novel bisphenol which contained the phenyltrifluoroethane linkage and preparation of polyarylates of satisfactory molecular weights. Unfortunately the reaction conditions utilized to generate this novel bisphenol weren't easily applicable to industrial or laboratory use. It wasn't until 1977, when Kray and coworkers [208] described the synthesis of a number of 1,1,1-triaryl-2,2,2-trifluoroethane derivatives, that mention was made in the literature regarding the

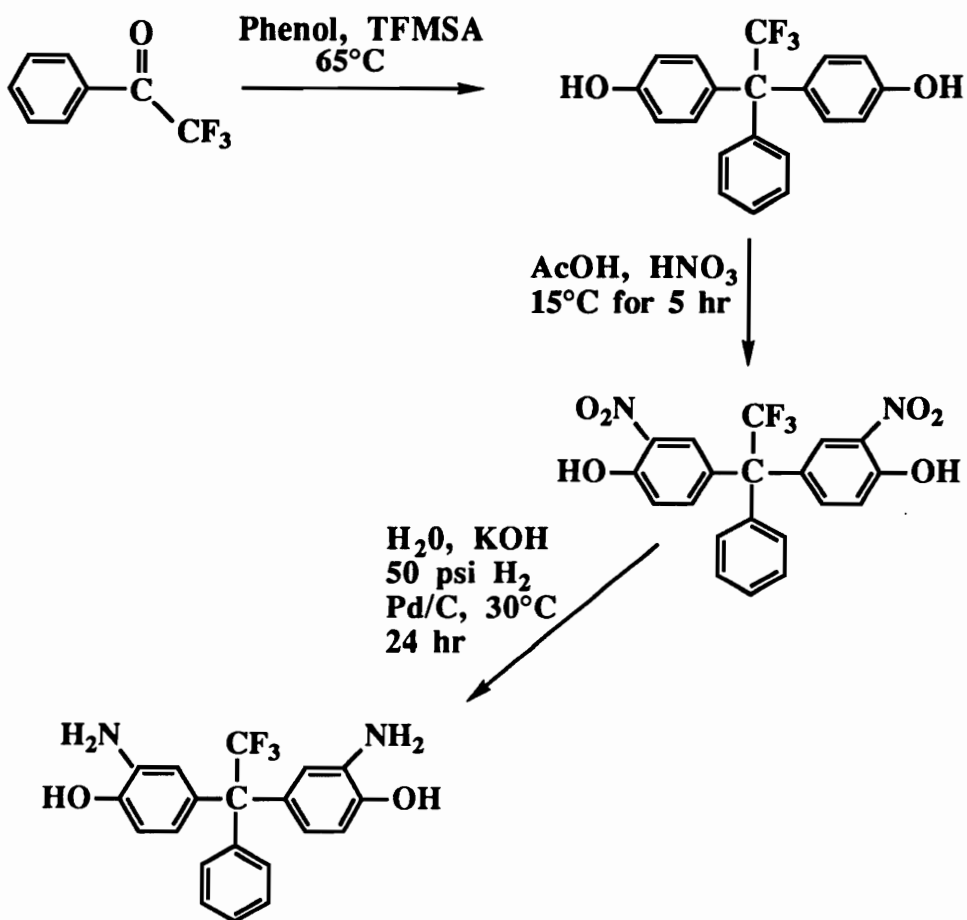


Figure 4.4. Synthesis of 1,1-bis(3-amino-4-hydroxyphenyl)-1-phenyl-2,2,2-trifluoroethane (3FAP).

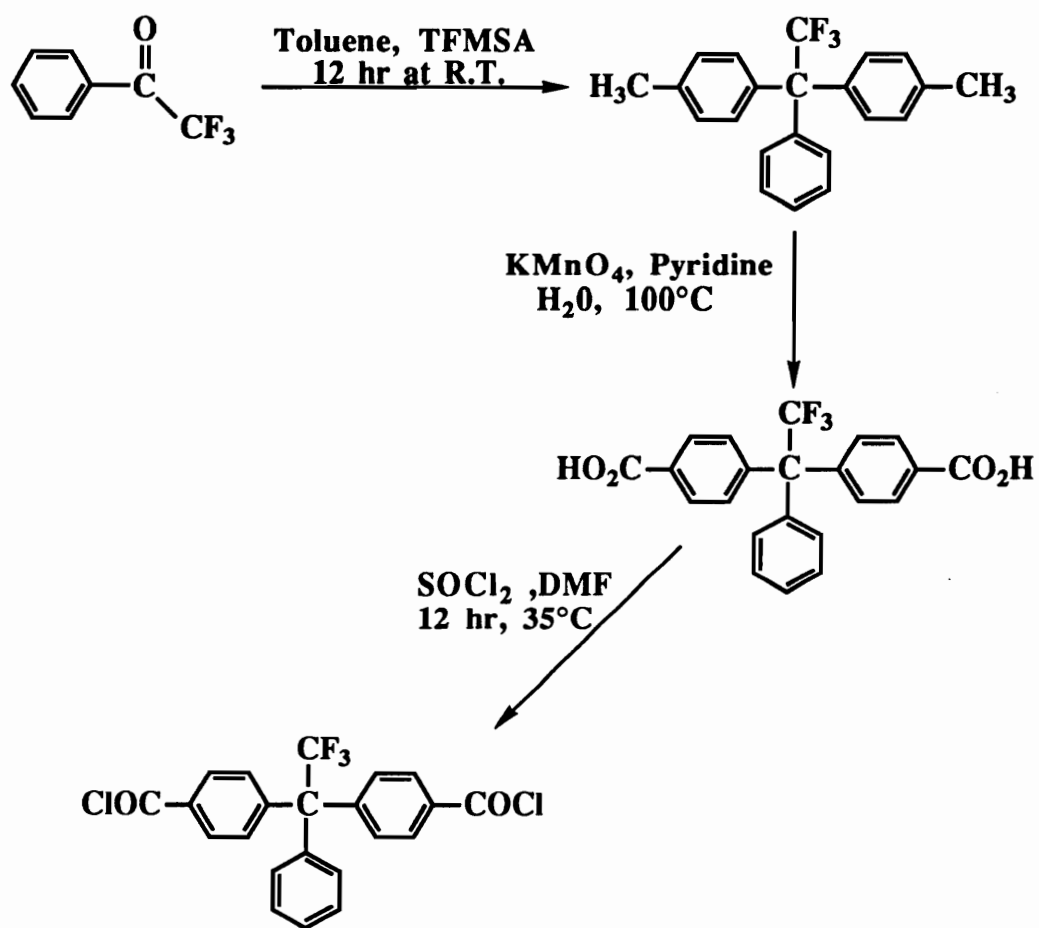


Figure 4.5. Synthesis of 1,1-bis(4-chlorocarbonylphenyl)-1-phenyl-2,2,2-trifluoroethane (3FAC).

incorporation of this linking group into high performance monomers. Since that time, a number of patents [209,210] were issued regarding the synthesis of 1,1,1-triaryl-2,2,2-trifluoroethane derivatives. The synthetic methodology for the diacid chloride, while alluded to in the patents, was not described in detail. In addition, the idea of generating a bis(*o*-aminophenol) containing the phenyltrifluoroethane linkage has not been previously described.

Synthesis of 1,1-bis(3-amino-4-hydroxyphenyl)-1-phenyl-2,2,2-trifluoroethane required the generation of 1,1-bis(4-hydroxyphenyl)-1-phenyl-2,2,2-trifluoroethane via the acid catalyzed condensation of phenol with trifluoroacetophenone (211).

Purification of this compound with a simple methylene chloride wash, followed by nitration with HNO₃ in acetic acid resulted in 1,1-bis(4-hydroxy-3-nitrophenyl)-1-phenyl-2,2,2-trifluoroethane in a 95% yield. If desired, monomer grade material could be afforded with two recrystallizations from ethanol. The identity of this material was confirmed by ¹H NMR (Figure 4.6) and melting point comparison. Conversion of the dinitro compound to the bis(*o*-aminophenol) followed along the same lines as the reduction of 2,2-bis(4-hydroxy-3-nitrophenyl)propane. The reduction was carried out in water utilizing the phenolate intermediate, hydrogen and a palladium on charcoal catalyst. Elucidation of the chemical structure was accomplished via FT-IR (Figure 4.7), ¹H NMR (Figure 4.8) and elemental analysis. The FT-IR peak assignments for this compound can be found in Table 4.2.

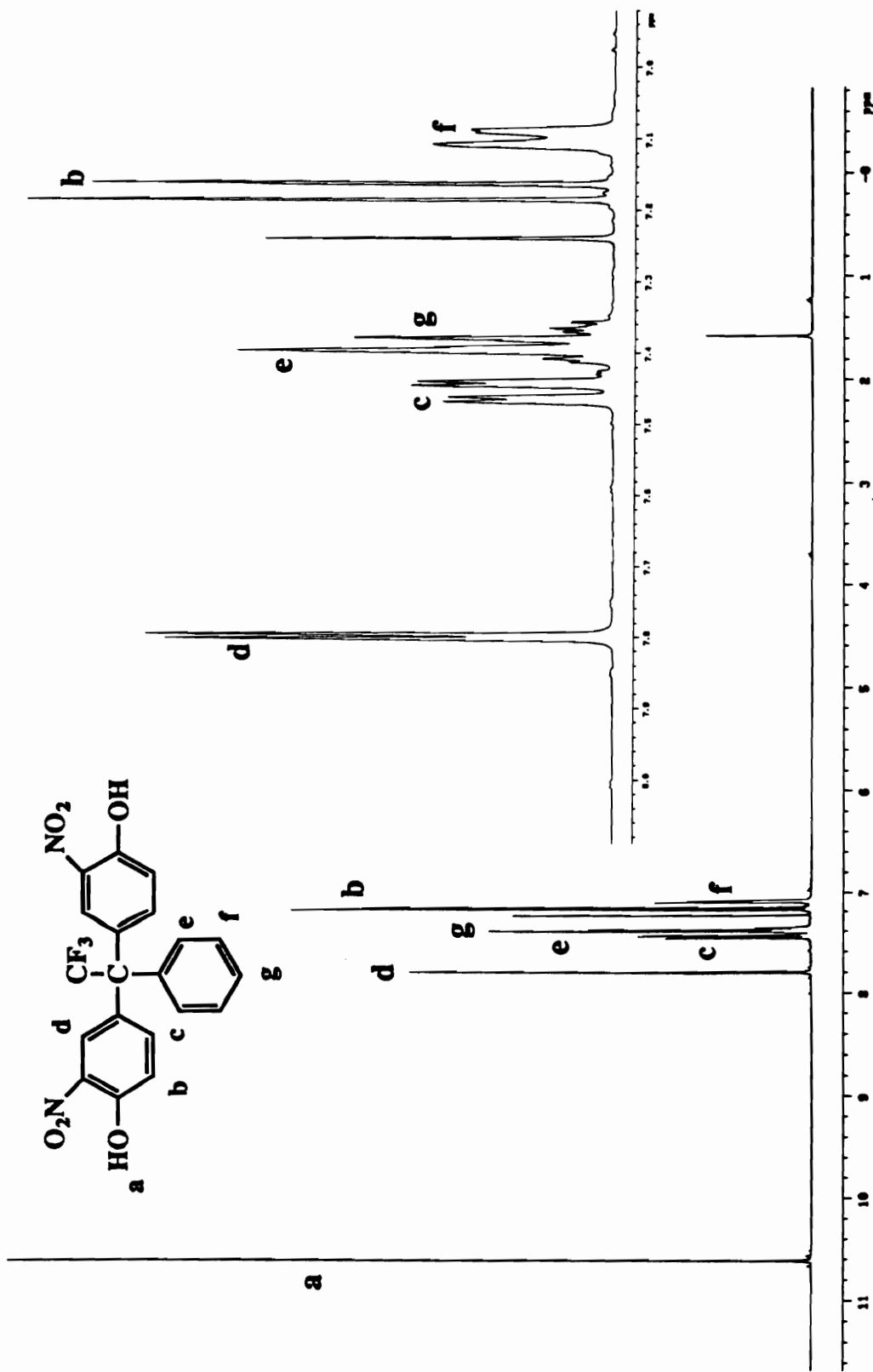


Figure 4.6. ¹H NMR spectrum of 1,1-bis(4-hydroxy-3-nitrophenyl)-1-phenyl-2,2,2-trifluoroethane.

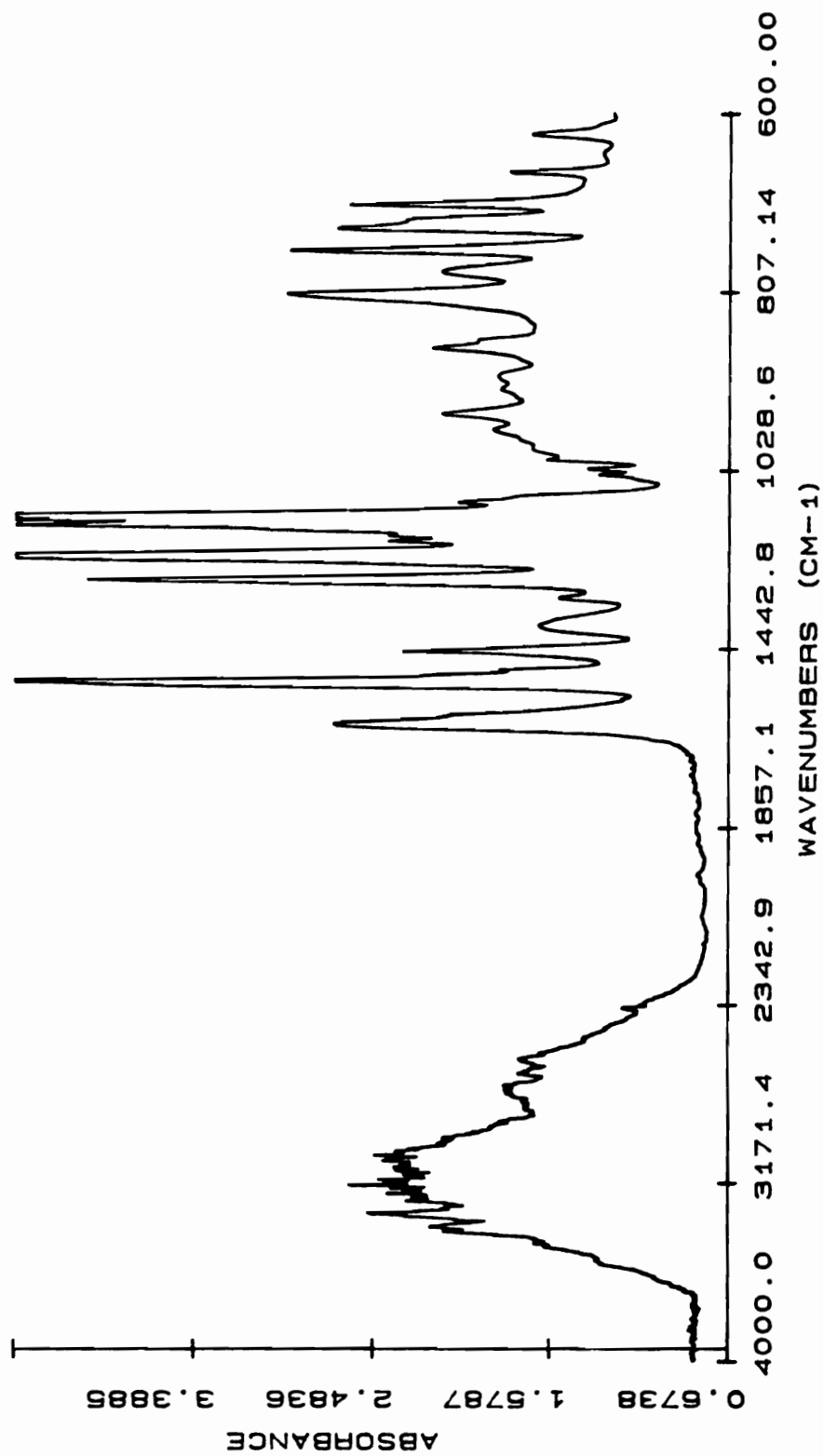


Figure 4.7. FT-IR spectrum of 1,1-bis(3-amino-4-hydroxyphenyl)-2,2,2-trifluoroethane (3FAP).

Table 4.2. FT-IR spectral assignments for 1,1-bis(3-amino-4-hydroxyphenyl)-1-phenyl-2,2,2-trifluoroethane (3FAP).

<u>Assignment</u>	<u>Frequency (cm⁻¹)</u>
-NH stretch	3460-3280
OH stretch	3350-3250
NH ₂ deformation	1616
Aromatic stretch (C=C)	1516
C-OH in plane bend	1277
CF ₃ stretch	1224
<u>Aromatic CH in plane bend</u>	<u>1151, 1131</u>

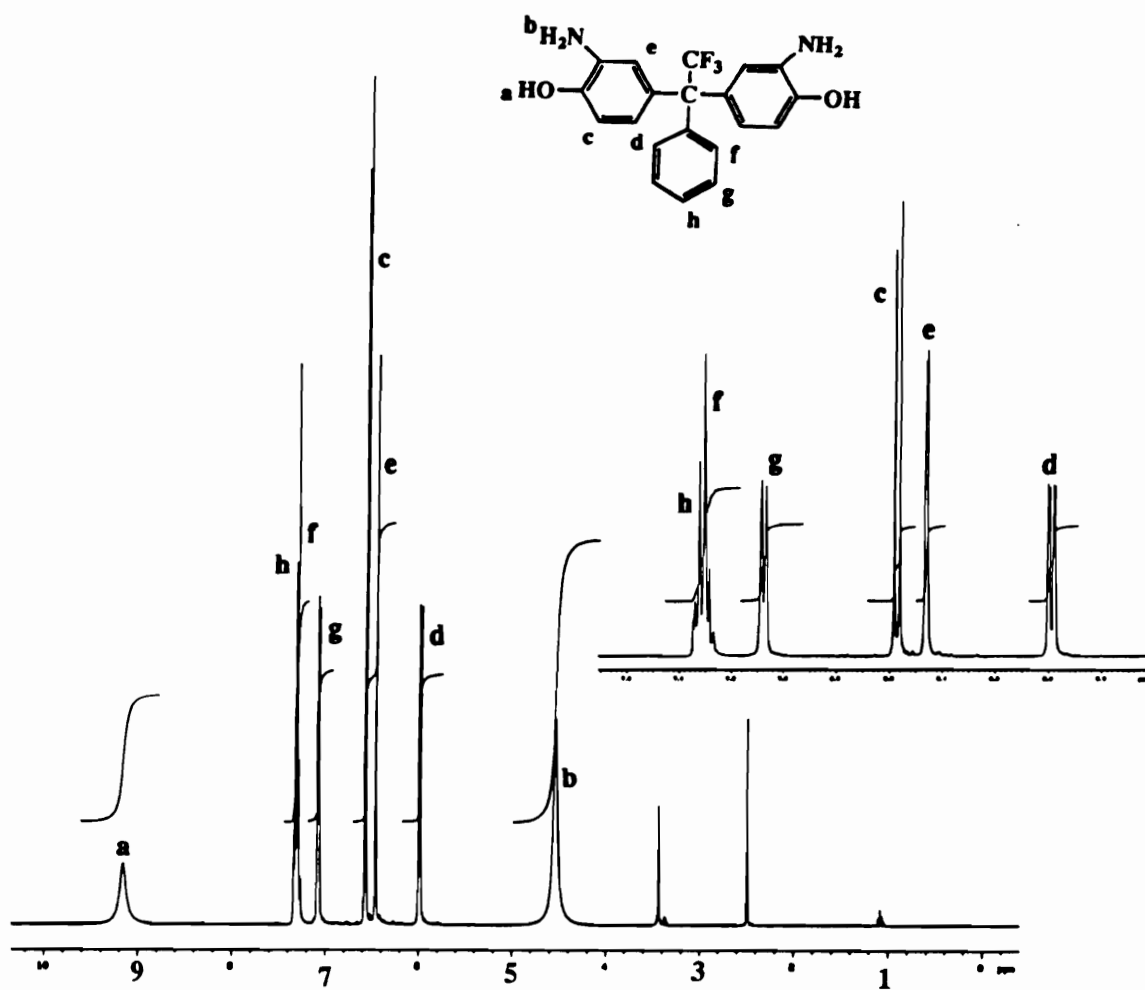


Figure 4.8. ¹H NMR spectrum of 1,1-bis(3-amino-4-hydroxyphenyl)-1-phenyl-2,2,2-trifluoroethane (3FAP).

Synthesis of 1,1-bis(4-chloroformylphenyl)-1-phenyl-2,2,2-trifluoroethane (Figure 4.5) was accomplished using the bistolyl precursor described by Kray and Rosser [209]. Oxidation of this intermediate with a two-step KMnO_4 oxidation resulted in the dicarboxylic acid. Chlorination of the diacid with thionyl chloride/DMF afforded quantitative yields of the desired acid chloride. Confirmation of the product structure was provided by FT-IR (Figure 4.9), $^1\text{H-NMR}$ (Figure 4.10) and elemental analysis. The FT-IR peak assignments for the acid chloride can be found in Table 4.3.

4.4. Synthesis of Bis(4-chlorocarbonylphenyl) phenylphosphine Oxide

The synthesis of monomers containing an alkyl or aryl diphenylphosphine oxide moiety have received considerable attention in the past twenty years due to their inherent fire retardancy characteristics. Traditional methods of incorporating fire retardancy into polymers include incorporation of halogenated monomers or the compounding of various fire retardants into polymers during manufacturing. With halogenated compounds are constantly under fire from environmental agencies, efforts have made to replace or diminish the use of halogenated compounds in the fire retardancy arena in favor of more environmentally sound

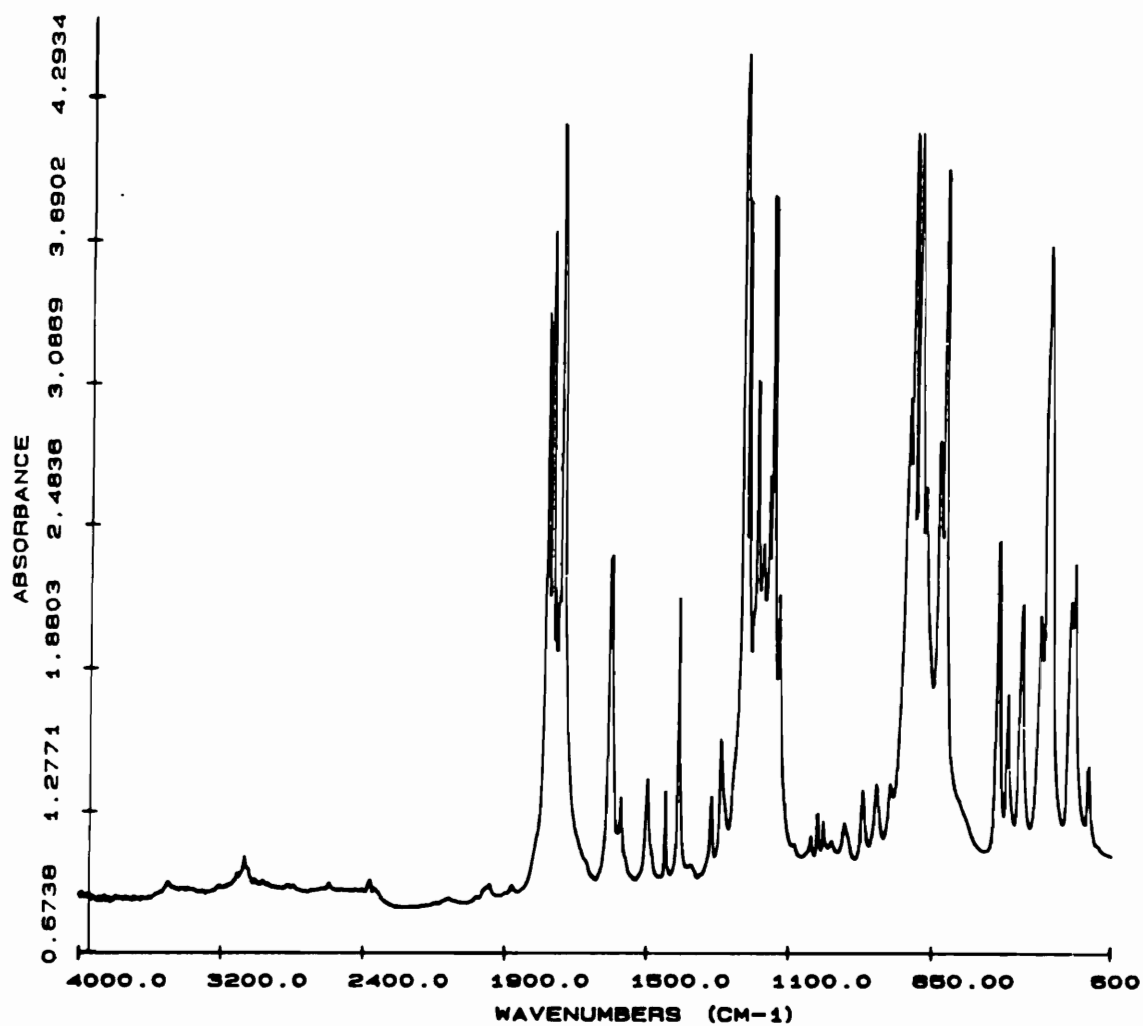


Figure 4.9. FT-IR spectrum of 1,1-bis(4-chlorocarbonylphenyl)-1-phenyl-2,2,2-trifluoroethane (3FAC).

Table 4.3. FT-IR spectral assignments for 1,1-bis(4-chlorocarbonylphenyl)-1-phenyl-2,2,2-trifluoroethane (3FAC).

<u>Assignment</u>	<u>Frequency (cm⁻¹)</u>
Aromatic CH stretch	3070
C=O stretch	1782,1742
Aromatic stretch (C=C)	1602
CF ₃ stretch	1231
C-C stretch (Ar-C)	885
C-Cl stretch	865
Aromatic ring deformation	686

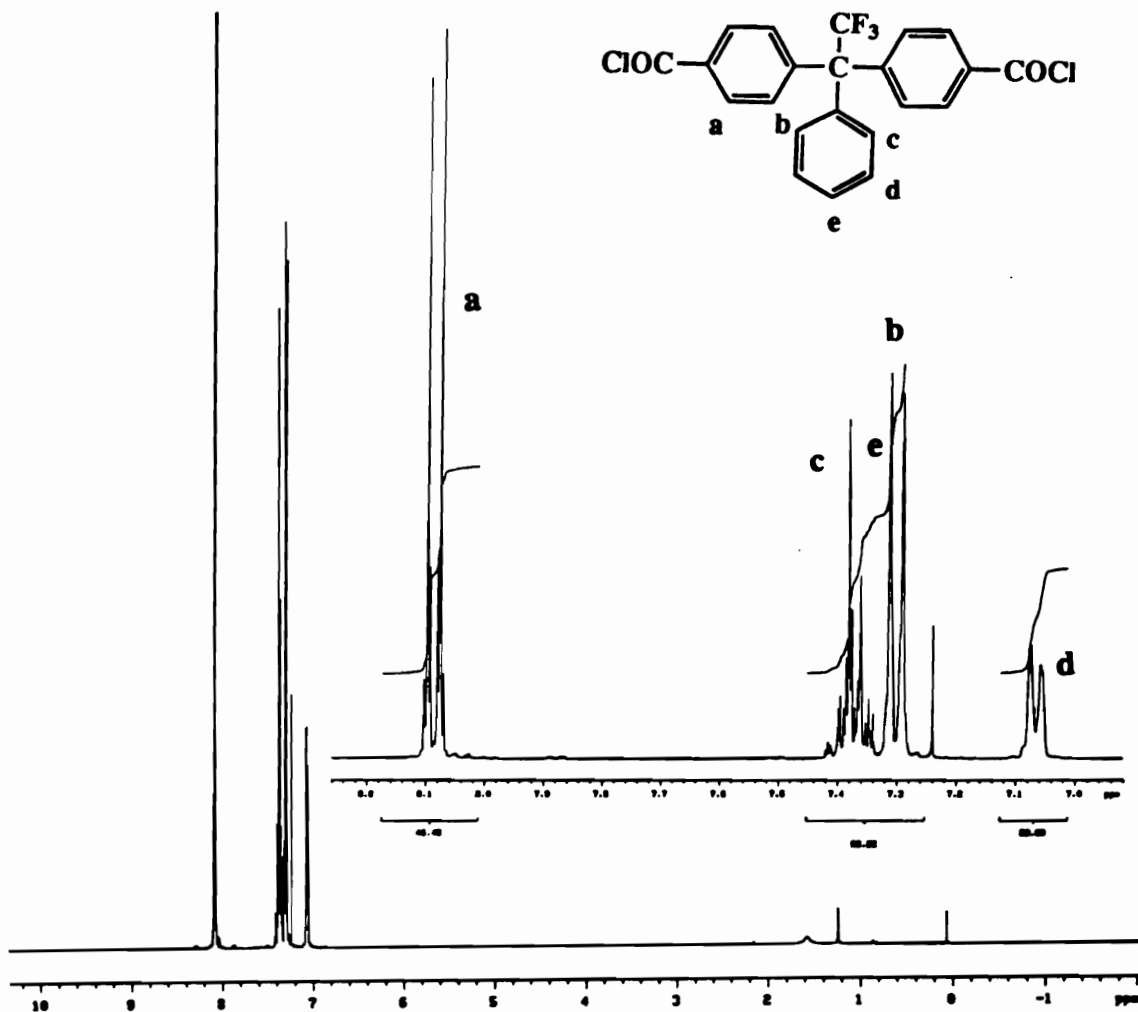


Figure 4.10. ^1H NMR spectrum of 1,1-bis(4-chlorocarbonylphenyl)-1-phenyl-2,2,2-trifluoroethane (3FAC).

alternatives. One such alternative is the incorporation of phosphorus [212]. A number of different monomers have been synthesized and incorporated into various high performance polymers [213-215]. Fire retardancy was investigated in some of these systems and in all cases, an improvement was evident. It should be pointed out that in a number of these reports, only low molecular weight polymers were achieved. A number of other reasons for incorporating phenylphosphine oxide linkages into polymeric systems include enhanced solubility, improved thermo-oxidative stability and dramatically improved atomic oxygen resistance. Consequently it is quite understandable why so much effort has been concentrated on the synthesis of new and improved phosphorus containing monomers and polymers.

For these reasons, research was initiated in an attempt to synthesize bis(4-chlorocarbonylphenyl)phenylphosphine oxide (PPOAc) and incorporate it into polybenzoxazoles. It was hypothesized that by incorporating PPOAc into polybenzoxazole backbones, solubility might be enhanced to a point where solution polymerizations and solution processibility would be viable processes. Initial literature reports regarding the synthesis of triaryl phosphine oxide derivatives suggested the cleanest and easiest synthetic methodology to the bistolyl precursor was via the Grignard route [216]. Reacting excess aryl magnesium bromides with phenylphosphine oxide dichloride in ether solvents resulted in triphenylphosphine oxide derivatives in good yields. Synthesis of

the diacid chloride would involve subsequent oxidation of a the tolyl derivative, followed by chlorination with SOCl_2 (Figure 4.11).

A more industrially acceptable Friedel-Crafts method (Figure 4.12) was proposed in a 1986 patent [217], whereby phenylphosphine sulfide dichloride was reacted with an excess of toluene in the presence of AlCl_3 to generate the sulfide version of bis-*p*-tolylphenylphosphine oxide. A number of other aryl radicals were also mentioned as possible electrophiles. Subsequent conversion of the tolyl sulfide to the diacid oxide can be accomplished in a two step procedure where the sulfide is converted to the oxide with 30% aqueous H_2O_2 in acetic acid and the methyl groups are oxidized to the acid using standard KMnO_4 oxidation conditions. Chlorination of the diacid with thionyl chloride or phosphorus pentachloride has been reported to result in good yields of bis(4-chlorocarbonyl-phenyl)phenylphosphine oxide. Due to the practicality of the Freidel-Crafts route, it was the synthetic procedure of choice.

An interesting feature of the chlorination reaction is the apparent chlorination of the $\text{P}=\text{O}$ bond if the reaction is allowed to progress after the acid moieties have been converted to the acid chlorides. While the synthesis of PPOAc has been reported [218], the experimental procedure has not been adequately described. Under typical reaction conditions, the diacid was stirred with an excess of thionyl chloride and a few drops of DMSO at 35-40°C until the solution cleared. FT-IR analysis of the reaction mixture at this point indicated complete chlorination by disappearance of the COOH

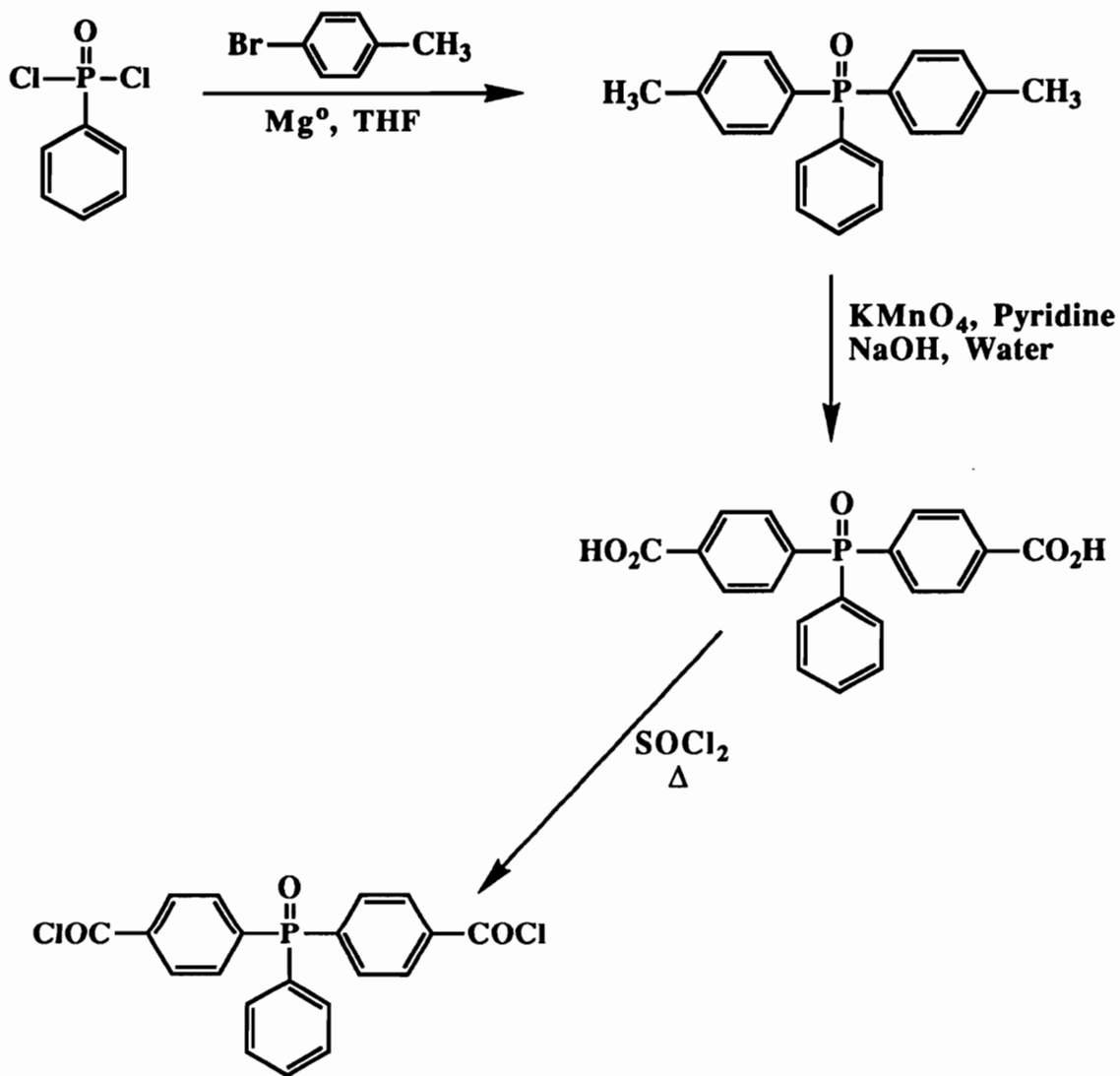


Figure 4.11. Synthesis of bis(4-chlorocarbonylphenyl)-phenylphosphine oxide via Grignard chemistry.

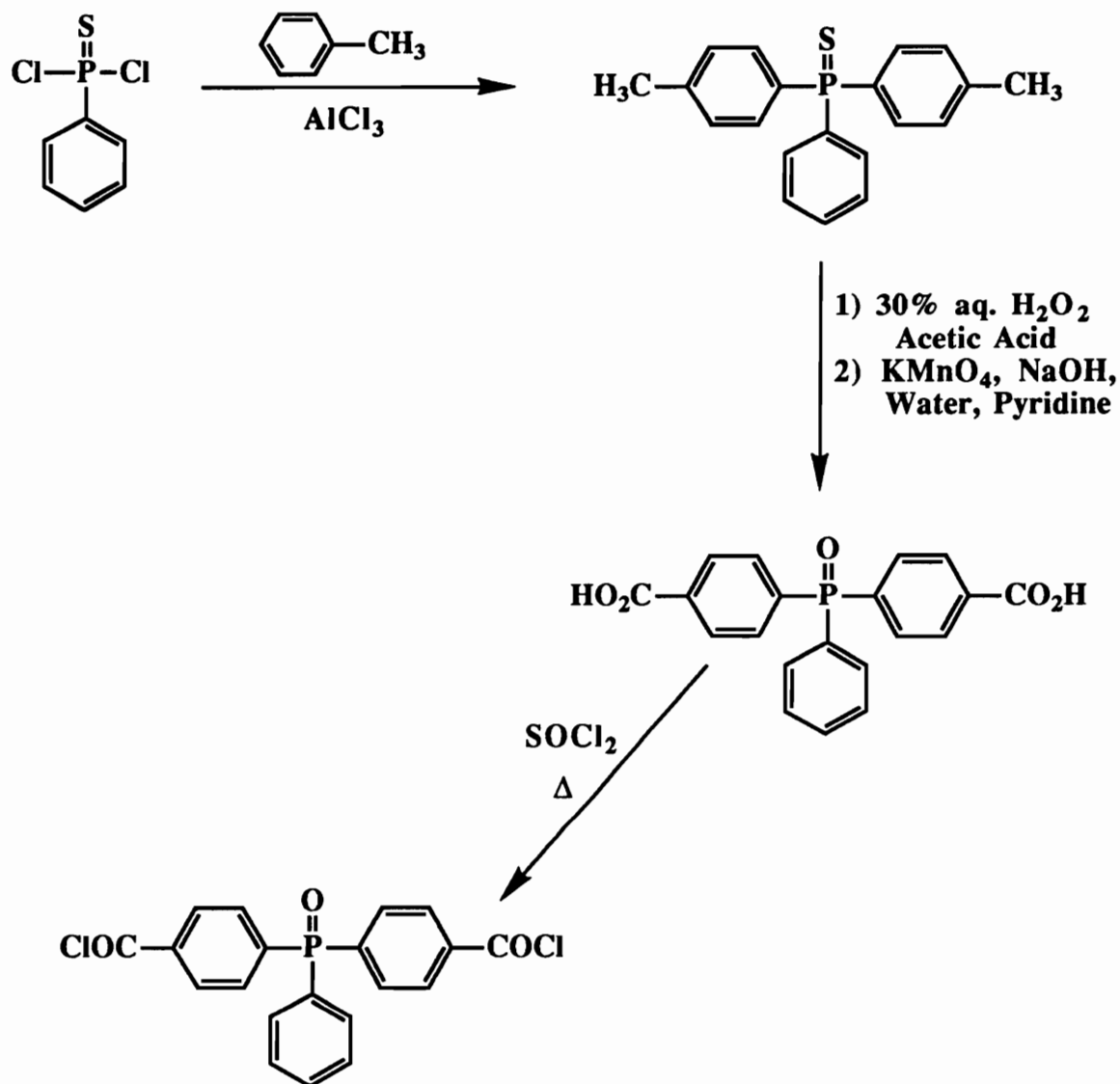


Figure 4.12. Synthesis of bis(4-chlorocarbonylphenyl)-phenylphosphine oxide via Friedel-Crafts chemistry.

groups ($\nu=3000-3400\text{ cm}^{-1}$, Figure 4.13). Prolonged reaction times and higher reaction temperatures also result in carboxy free FT-IR spectra; however, ^1H NMR analysis and melting points indicate a difference in products. Purified PPOAc, obtained from short-term, low temperature chlorination reactions, displays the expected ^1H NMR spectrum (Figure 4.14) and has a rather narrow melting point. On the other hand, the PPOAc's generated under higher reaction temperatures and prolonged exposure to SOCl_2 display polymorphic behavior and unusual ^1H NMR spectra. In fact the post-reaction can be easily followed by ^1H NMR (Figure 4.15).

A possible explanation for this post-reaction is chlorination of the $\text{P}=\text{O}$ bond. It has been reported [219] that chlorinating agents (e.g. SOCl_2 , oxalyl chloride, etc.) will chlorinate the $\text{P}=\text{O}$ double bond generating the dichloride, in addition to carbon monoxide and carbon dioxide byproducts. Similarly, it has been reported [220] that the synthesis of high molecular weight polycarbonates is impossible under interfacial phosgenation conditions with the bis(4-hydroxyphenyl)phenylphosphine oxide. In this case it is believed that phosgene causes a competitive chlorination reaction in addition to polymerization. If one draws an analogy with these systems and the PPOAc system, the formation of phosphorus dichloride as a side reaction during the synthesis of PPOAc appears reasonable. A proposed mechanism for this reaction is shown in Figure 4.16. Verification of the results postulated herein by FT-IR, ^{31}P -NMR, elemental analysis and model compound studies are warranted.

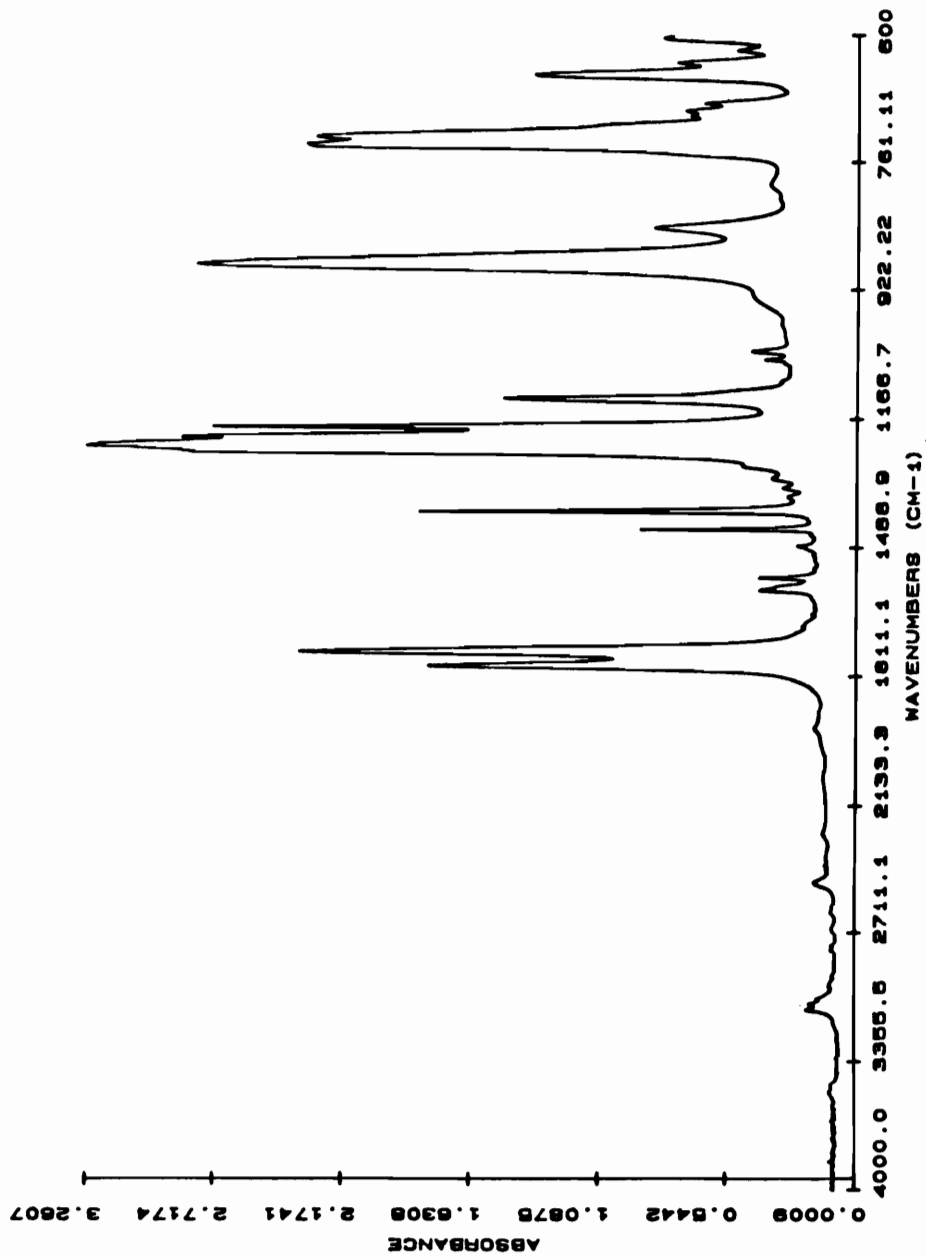


Figure 4.13. FT-IR spectrum of PPOAc chlorination mixture.

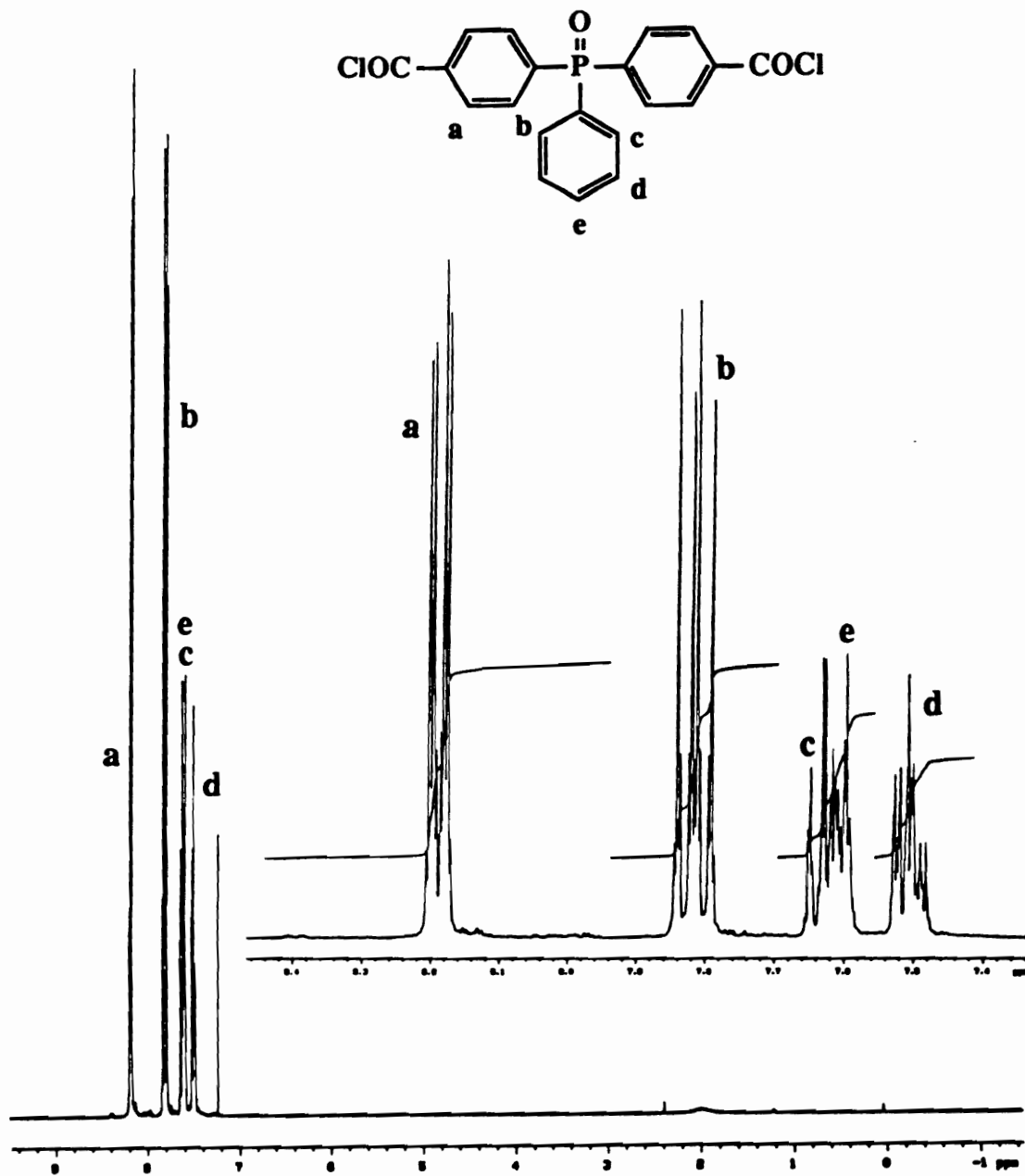


Figure 4.14. ^1H NMR spectrum of bis(4-chlorocarbonylphenyl) phenylphosphine oxide (PPOAc).

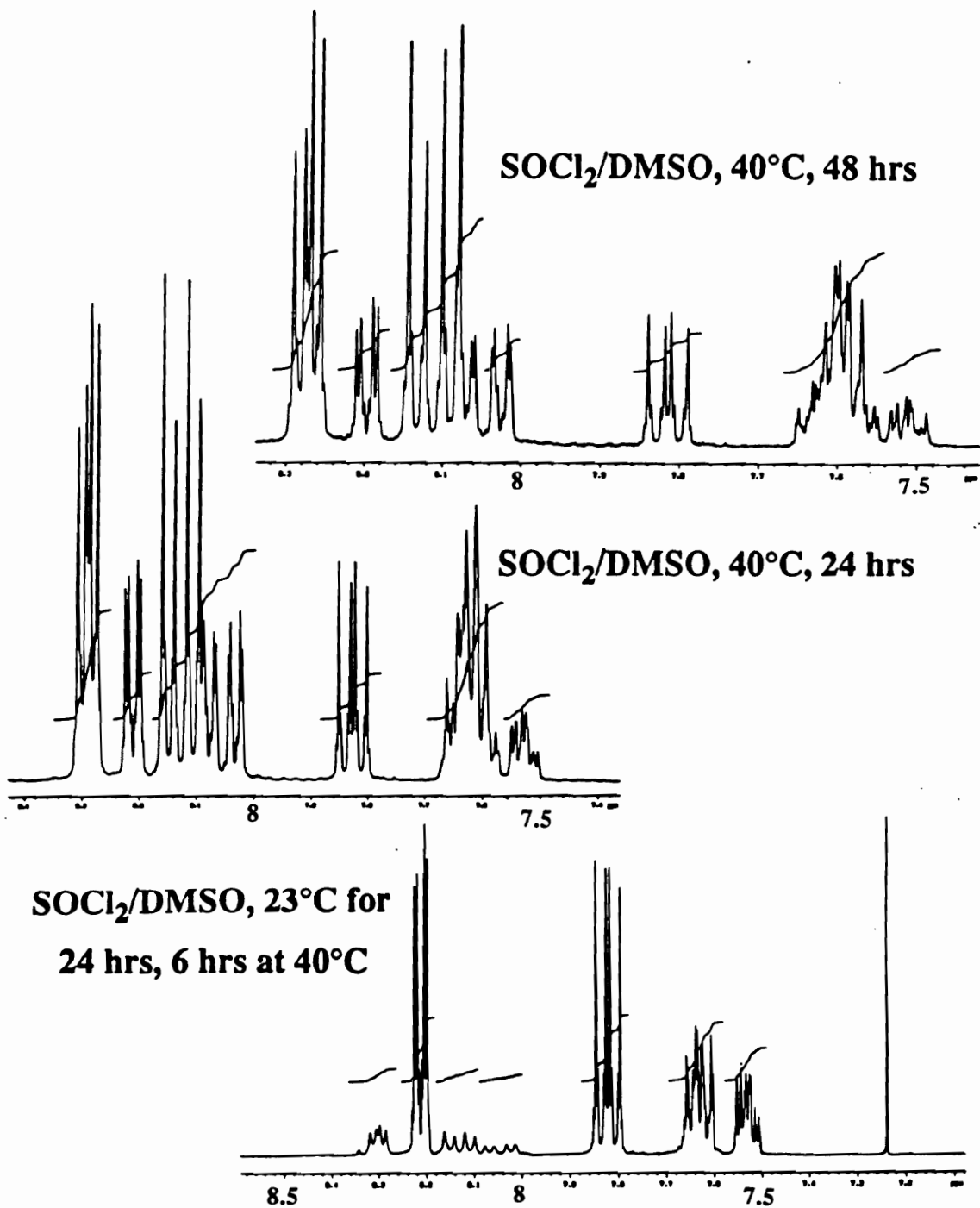


Figure 4.15. ¹H NMR spectra of PPOAc post-reaction with time.

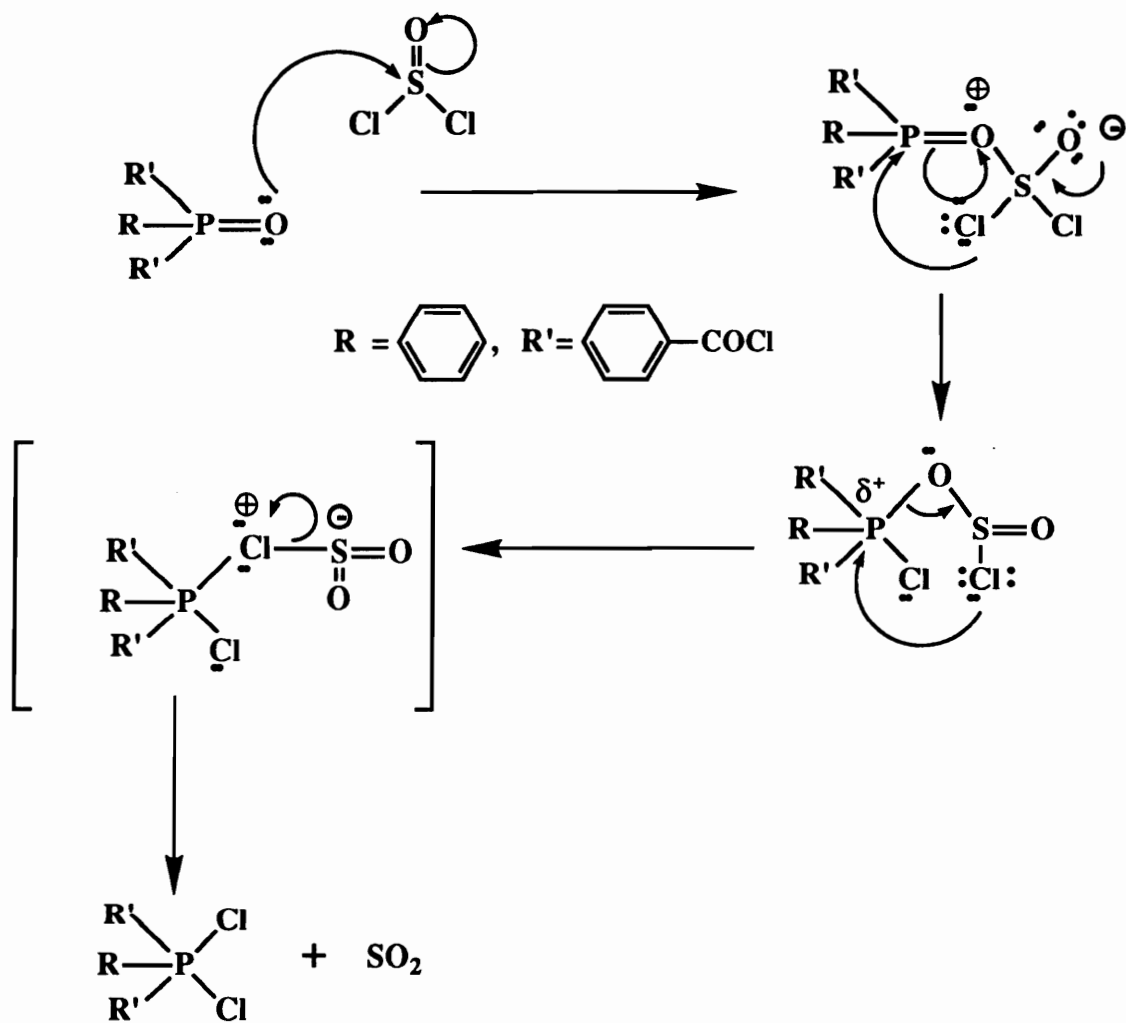


Figure 4.16. Proposed mechanism for the chlorination of PPOAc.

4.5. Synthesis of 4-(Phenylethynyl)benzoyl Chloride (PEBC)

In the latter section of this thesis, the synthesis of polybenzoxazoles which exhibit excellent solubility in common solvents such as THF and CHCl_3 will be addressed. While one of the goals of this research was to generate soluble PBO's, another goal was to achieve solvent resistant materials. One way to accomplish these seemingly contradictory objectives is to incorporate thermally activate functional groups into the polymer backbone. Therefore, polymers can be processed in melts or common solvents and then rendered solvent resistant via crosslinking or aromatization post-reactions.

Phenylethynylbenzoyl chloride is a monofunctional, substituted acetylene containing monomer which has the potential both to control molecular weight in PBO polymerizations and to serve as a high temperature crosslinking site for the resulting thermoplastics. The phenylethynyl endcapper was synthesized according to the methods of Stephens and Castro [199] with modifications of Vollemin and Goussu [221], using palladium coupling chemistry. The particular steps involved in the synthesis are depicted in Figure 4.17. Esterification of commercial *p*-iodobenzoic acid with catalytic amounts of H_2SO_4 in methanol resulted in the protected iodo starting material. Aryl iodides are preferred for the palladium catalyzed coupling reaction due to their enhanced rate of reactivity

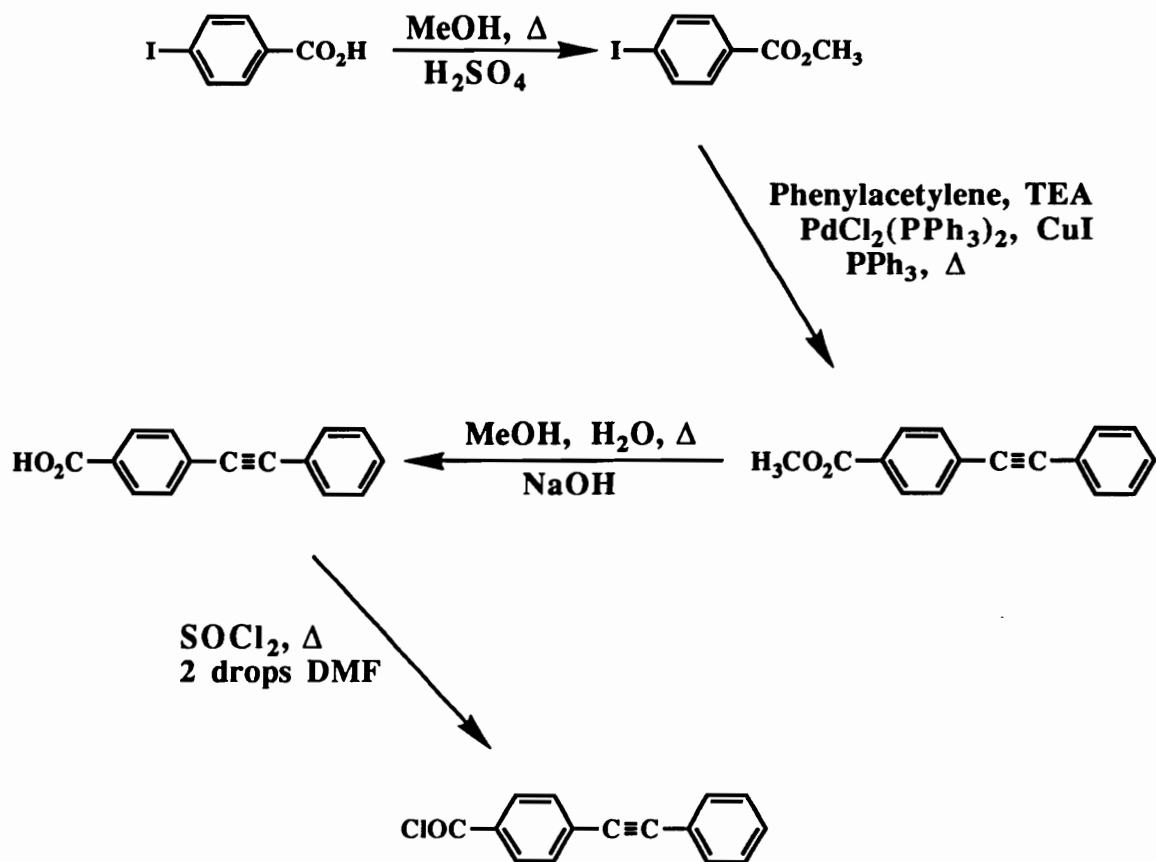


Figure 4.17. Synthesis of phenylethynylbenzoyl chloride.

relative to other halides and their superior yields. Therefore, methyl, 4-iodobenzoate was reacted with phenylacetylene in the presence of palladium for 12 hours to afford the phenylethynyl substituted ester. Hydrolysis of the ester with base, followed by chlorination with SOCl_2 , generated the endcapper in ~80% overall yield. Identification and characterization of the product, as well as each intermediate, was accomplished using ^1H NMR (Figure 4.18) and melting points. Incorporation of *p*-phenylethynylbenzoyl chloride into polybenzoxazoles and its effect on thermal and mechanical properties will be discussed in Section 4.11.

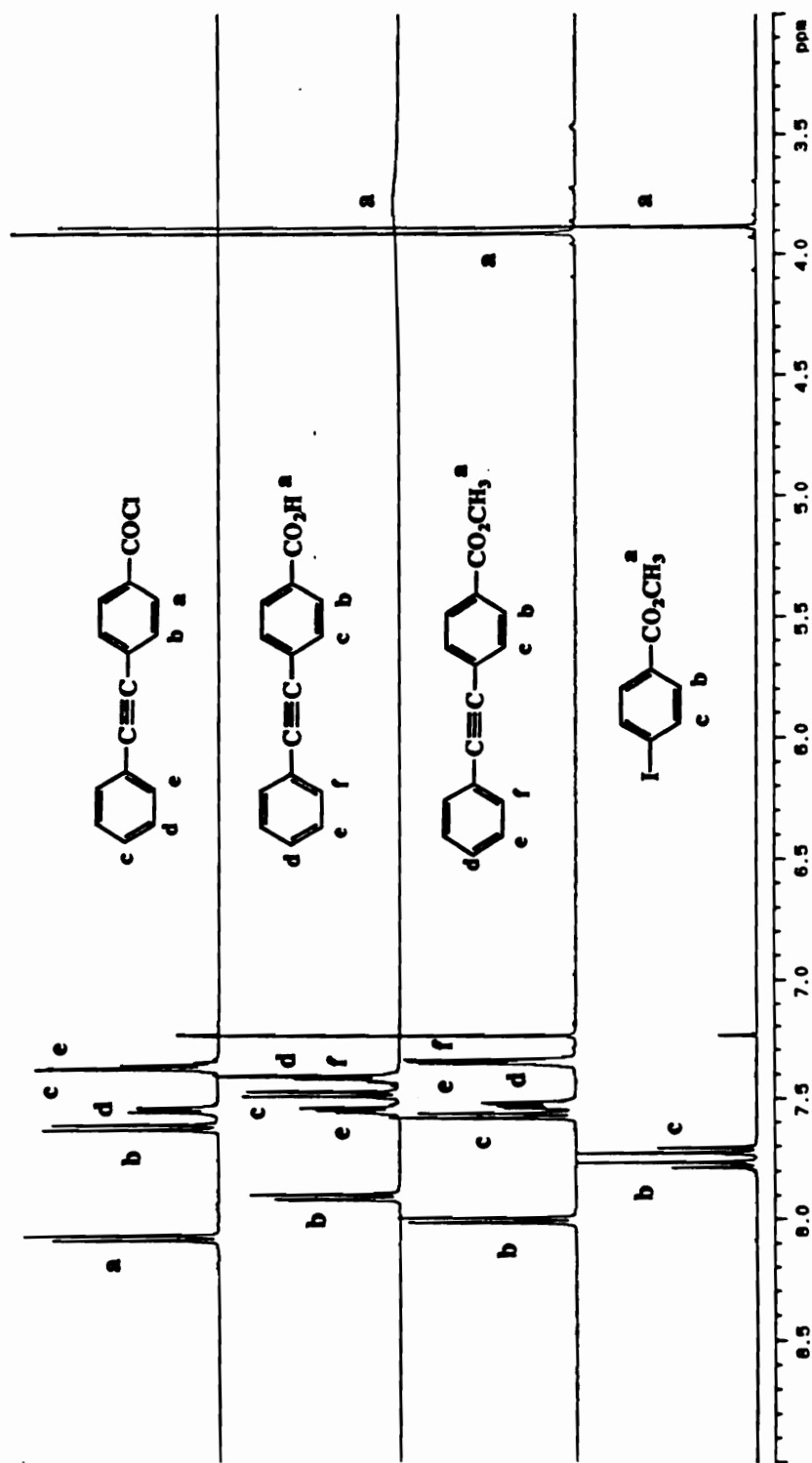


Figure 4.18. ^1H NMR spectra of phenylethynebenzoyl chloride and precursors involved in its synthesis.

4.6. Parameters Affecting the Formation of High Molecular Weight Poly(hydroxy amide)s

4.6.1. Introduction

Wholly aromatic polyamides (polyaramide)s can be polymerized to high molecular weights using low temperature techniques [222]. Typical reaction conditions involve a polar aprotic solvent, a salt, such as calcium oxides, for solubility purposes and an acid scavenging base, such as pyridine. These same types of polymerization techniques, without the salt, have also been utilized to generate poly(amide ester)s with varying degrees of success. [223-225]. Considering the fact that both esters and amides can be generated via this method, it seems reasonable to hypothesize that poly(hydroxy amide)s can also be polymerized via this method (Figure 4.19). Numerous publications have appeared in the literature related to the synthesis of poly(hydroxy amide)s via low temperature polymerization techniques [12,26,30]. A large number of bis(*o*-aminophenol)s and acid chlorides have been investigated and one important conclusion from this research is the fact that bis(*o*-aminophenol)s which possess electron-withdrawing linking groups between the aromatic nuclei result in lower molecular weight polymers. More recently, the hexafluoroisopropylidene (6F) linkage has been incorporated into bis(*o*-aminophenol)s, attracting considerable attention in the literature for its expected electronic

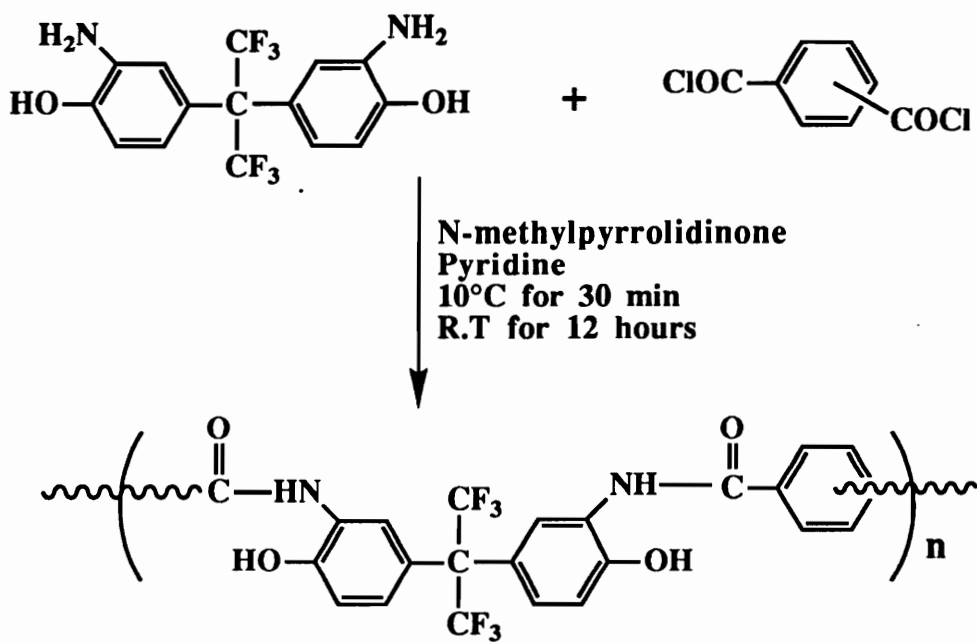
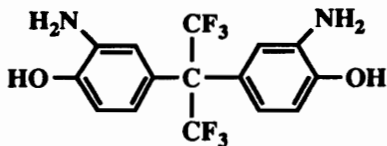


Figure 4.19. Polymerization of poly(hydroxy amide)s via low temperature, base-catalyzed solution techniques.

and thermal properties [7,55,137]. Unfortunately, the 6F linkage is also an electron-withdrawing group and much like the other electron



deficient monomers, resists formation of high molecular weight polymers when polymerized via low temperature techniques. With this in mind, investigations were initiated in an attempt to understand the phenomena exhibited by electron-withdrawing bis(*o*-aminophenols) and, if possible, correct the problem. To accomplish this task, 6FAP was selected as the model electron-withdrawing monomer due to its availability and expected favorable solubility properties.

The fact that high molecular weight polymers have not been achieved using 2,2-bis(3-amino-4-hydroxyphenyl)hexafluoropropane (6FAP) via low temperature methods has prompted a number of research groups to investigate alternate synthetic methodologies to enhance molecular weight. Reinhardt [8] opted to use a trimethylsilyl substituted phosphate catalyst in *o*-dichlorobenzene to achieve high molecular weight polymer, while Imai [7] resorted to activating 6FAP through silylation of the amines and hydroxyls. Imai, among others, has postulated that an electron withdrawing linkage between the aromatic moieties of bis(*o*-aminophenols) deactivates the amines toward nucleophilic attack [28]. Therefore

it's claimed that silylation of the amine enhances reactivity and affords higher molecular weight material.

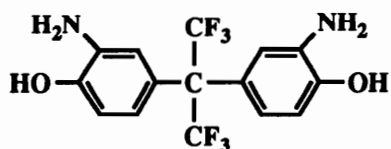
While the premise of amine deactivation may be pertinent, it does not explain observations made in the current research relative to the generation of 6FAP containing polymers. Indeed, the research discussed herein will show that the amine reactivity is more than adequate to generate high molecular weight material and the likely limiting feature relative to the formation of high molecular weight poly(hydroxy amide)s is an ester side reaction. It should be pointed out that this hypothesis is consistent with the observations made by Imai and Yakobovich [7,28,33]. Prior to expanding on the reasoning behind this assumption, it would be informative to list the observations which support the aforementioned postulate. The following observations were made using the polymerization procedure outlined in Figure 4.19 and discussed in Section 3.3.1.

Experimental Observations

- Polymerization of 6FAP with dianhydrides results in high molecular weight polyimides with pendent hydroxyl groups.
- Employing a base stronger than pyridine results in more observable gel formation early in the polymerization.
- Conducting the polymerization in the absence of pyridine results in absolutely no gelation.

- Polymerization of 6FAP with excess acid chloride in the presence of base results in more observable gel and in some cases, gross gelation.
- During the addition of a solution of acid chlorides dissolved in NMP to a solution of 6FAP in NMP and pyridine, gel is formed on the side of the reactor where insufficient stirring allows excess acid chloride to accumulate.
- Polymerization of 6FAP under comparable conditions with electron-rich acid chlorides (e.g., 4,4'-oxydibenzoyl chloride) results in poly(hydroxy amide)s with high molecular weight, while polymerizations carried out using electron-deficient acid chlorides (e.g., isophthaloyl and terephthaloyl chloride) result in low molecular weight materials.
- Bis(*o*-aminophenol)s linked by electron-donating groups generate high molecular weight poly(hydroxy amide)s regardless of the electronic nature of the acid chloride.
- ¹H NMR spectra of poly(hydroxy amide)s generated with a base indicate the presence of residual bis(*o*-aminophenol) groups as well as two different type of protons *ortho* to carbonyls. Spectra of poly(hydroxy amide)s generated without base show only one type of proton *ortho* to the carbonyls and minimal residual bis(*o*-aminophenol) resonances.
- Infrared analysis of poly(hydroxy amide)s generated with base indicates the presence of an ester stretch at 1724 cm⁻¹.

Evidence supporting the hypothesis of ester forming side reactions will now be presented. The issue of possible insufficient amine reactivity will be discussed first. Structural features influencing the reactivity of the amines and hydroxyls include the



substitution pattern on the aryl radical relative to the hexafluoroisopropylidene group and the distance (number of carbon bonds) between the functional groups and the hexafluoro (6F) group. Because the trifluoromethyl groups are not connected directly to the aromatic ring, resonance arguments fall short in explaining amine or hydroxyl reactivity. Inductive or field effect arguments may explain the decreased amine reactivity, but due to the large distance between the functional groups (amines and hydroxyls) and the trifluoro groups (>4 carbon chain), these effects are usually considered minimal. Consequently, based on electronic arguments, the idea of insufficient amine reactivity being responsible for suppressing molecular weight formation is not very convincing. Reviews [226,227] on substitution effects substantiate these resonance arguments.

The fact that high molecular weight polyimides can be generated from the 3F and 6F bis(*o*-aminophenols), further substantiates the claim that the amines are sufficiently reactive. Polymerization of

6FAP and 3FAP with 2,2-bis(4-phthalic anhydride)hexafluoropropane (6FDA), under established polyimide reaction conditions [1,55,228], (Figure 4.20) affords polyimides with $[\eta]^{25^\circ\text{C}}$'s (NMP) >0.70 dl/g. If one accepts the premise that anhydrides are less reactive than acid chlorides, then one is easily convinced that the amines in 6FAP are sufficiently nucleophilic to readily undergo an amidation reactions with an acid chloride. Therefore, based on electronic arguments and the fact that 6FAP is sufficiently reactive to form high molecular weight polyimides, it is concluded that the amines on 6FAP are reactive enough to undergo acylation with acid chlorides and form high molecular weight poly(hydroxy amide)s.

Having established this first point (e.g., adequate amine reactivity), one must propose alternate reasons for the incomplete amide conversion in the poly(hydroxy amide) systems. Monomer purity and stoichiometry offset were immediately ruled out due to scrupulous purification and quantitative weighing techniques. However, the idea of side reactions is a viable assumption. The ester side reaction becomes an obvious choice in light of the gelling observations discussed previously. To adequately discuss the effect of each reaction parameter on the ester side reaction or achievement of high molecular weight poly(hydroxy amide)s, it requires that each parameter be discussed separately. It should also be pointed out that throughout this discussion, intrinsic viscosity ($[\eta]$) or inherent viscosity (η_{inh}) values will be used as indicators of molecular weight.

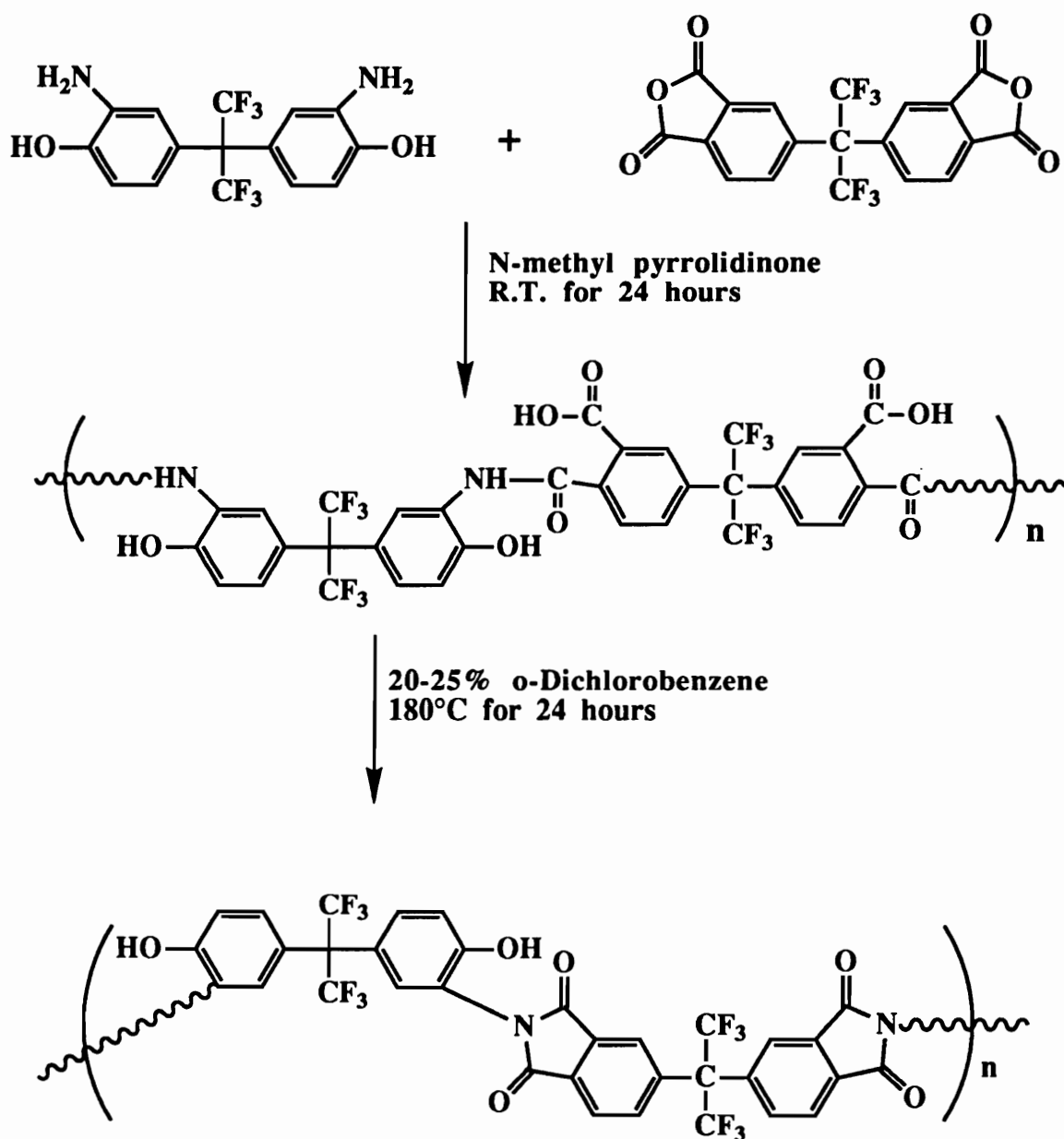


Figure 4.20. Synthesis of 6FAP-6FDA polyimide using recently developed solution cyclization techniques.

4.6.2. Effect of Base

The synthesis of polyamides, as well as polyesters, usually requires the use of an acid scavenger to synthesize high molecular weight polymers. This requirement is necessary for two reasons, 1) base catalyzes esterification and amidation reactions through the formation of an acylium intermediate and 2) the base acts as an acid scavenger to trap the HCl by-product. Without the use of base, amines present in the polyamide polymerization would trap the HCl by-product, thus forming amine hydrochloride, offsetting stoichiometry and rendering the amine functional groups unreactive towards acid chlorides. Because the poly(hydroxy amide) synthesis is a simple variation on the polyamide synthesis, stoichiometric amounts of base are considered to be required.

A discussion of esterification and amidation reactions are required in this section due to the fact that both reactions are base-catalyzed and possible during the polymerization of poly(hydroxy amide)s. Therefore the type and quantity of base employed in the polymerization will dictate, to some extent, how the reaction proceeds. Under most circumstances, it is assumed that amines are more reactive than the hydroxyl groups towards acid chlorides and it is this premise which allows low temperature polycondensation reactions to be used in the generation of poly(hydroxy amide)s. However, for quantitative organic reactions such as step growth polymerizations, certain conditions can exist (e.g., deactivated

amines and strong bases) which allow amine and hydroxyl reactivity to become competitive. If this occurs, clearly the functionality of the bis(*o*-aminophenol)s becomes greater than 2. This increase in functionality allows gelation via the formation of three dimensional networks. It is well known [189,229] that gelation will occur when the average functionality of all reactants in solution becomes greater than 2. If it is assumed that hydroxyl reactivity can become competitive with amine reactivity in electron deficient bis(*o*-aminophenol)s (e.g., 6FAP) and that the magnitude of competition is dictated by reaction conditions (base strength, co-reactants, solvent, temperature, etc.), then the extent of amidation and esterification can be altered by varying reaction conditions.

Table 4.4 demonstrates the effect on $[\eta]$ of varying base strength for the reaction of 6FAP with terephthaloyl (TC) or isophthaloyl chloride (IC) in NMP. Note that when triethylamine (TEA) was used as the base, the $[\eta]$'s are all low. The use of pyridine enhances the $[\eta]$'s, but not to the point of achieving high molecular weight polymer. If no base is used, the intrinsic viscosities are similar to the pyridine values. It should be pointed out that in most cases where a base was used, some form of gelation was evident in the reaction flask. These results can be related to the strength of the base and the influence of base strength on esterification and amidation. When no base is used, the intrinsic viscosities are relatively low due to formation of the amine hydrochloride alluded to earlier. Pyridine ($p_a = 5.25$, pK_a based on the conjugate acid of

pyridine), on the other hand, is more basic than the aromatic amines; consequently it scavenges the HCl formed during the polymerization and results in enhanced $[\eta]$'s. It is proposed that optimum molecular

Table 4.4. Effect of base on intrinsic viscosity.
(5°C for 30 minutes, 20°C for 24 hours).

Polymer	% Solids	Solvent	Acid^{a,b} Acceptor	$[\eta]^{25^\circ\text{C}}$ (dl/g)^c
6FAP-TC	10	DMAc	TEA	0.12 ^d
6FAP-TC	20	NMP	TEA	0.10
6FAP-TC-IC	18	DMAc	TEA	0.13
6FAP-TC	15	NMP	Pyridine	0.36
6FAP-TC	20	NMP	Pyridine	0.39
6FAP-TC-IC	18	DMAc	Pyridine	0.30 ^d
6FAP-TC	15	NMP	No Base	0.28
6FAP-TC	20	NMP	No Base	0.27
6FAP-TC ^e	20	NMP	Lutidine	Gel

^a pK_a of conjugate acids of pyridine, lutidine and triethylamine 5.25, 6.99, 10.01, respectively

^bMolar ratio of base to acid chloride = 2.2

^cIntrinsic viscosities run in NMP

^dIntrinsic viscosities run in DMAc

^e50% molar excess of TC employed

weights are not achieved due to a small amount of ester side reaction. Triethylamine is also more basic than the aromatic amines and consequently it also traps HCl; however, due to its higher basicity (pK_a of conjugate acid = 11.0) relative to pyridine, it is proposed that triethylamine promotes more ester side reaction.

This increase in esterification is just enough to decrease amide conversion and reduce molecular weight (lower $[\eta]$'s) without reaching the gel point. Molecular weight in these arguments is based on the concept of a linear polyamide and therefore a small amount of branching resulting from esterification would not produce an increase in molecular weight. However, branching would offset stoichiometry, reduce linear molecular weight and reduce the observed intrinsic viscosity of the polymer. Other work-up procedures (e.g., the fact that polymer samples are filtered prior to $[\eta]$ determinations) may remove any gelled particles and result in lower $[\eta]$'s. Consequently changing from pyridine to TEA reduces intrinsic viscosities due to an increase in gelling (lower sol fraction) or branching. Offsetting the stoichiometry in favor of the acid chloride and using a relatively strong base (lutidine, $pK_a = 6.99$) results in competitive esterification and gelation of the reaction flask. To review, the majority of these observations were made for the step polymerization of 6FAP with terephthaloyl and isophthaloyl chloride.

Considering the fact that base type influences molecular weight, it should also be expected that base concentration would be important. To test this hypothesis, a number of polymerizations were conducted in NMP at 15% solids, with the base concentration changed over a wide range of concentrations. Pyridine was selected due to the favorable results obtained in the previous study. The results of these polymerizations are shown in Table 4.5. It appears

from these results that a 40% excess of base results in the most favorable intrinsic viscosity. It was also found in other polymerizations that a 40% excess of pyridine tended to yield the best results.

Table 4.5. Effect of base concentration on intrinsic viscosity. (Reactions conducted in NMP (15% solids) at 20°C for 24 hr at)

Polymer	Base/TC Mole Ratio	[η]^{25°C} (dl/g)^a
6FAP-TC	2.2	0.25
6FAP-TC	2.8	0.39
6FAP-TC	3.0	0.23
6FAP-TC	3.7	0.20

^aIntrinsic viscosities run in NMP

4.6.3. Effect of Stir Rate

While no systematic study was made regarding the rate of stirring, a few observations need to be discussed. First, the rate of stirring has to be steadily increased during the addition of acid chloride solutions. If the stirring rate is not increased, gel begins to form in the vicinity of addition and spreads throughout the flask. The buildup of acid chloride concentration within localized areas in the reaction vessel are believed to be responsible for gel initiation. Once gelation is started, monomer dispersion becomes more

difficult, and as a result, more acid chloride groups become available to react with hydroxyl groups and a substantial increase in gelation is observed. It is assumed that esterification becomes more prominent in the gelled regions. Consequently very efficient stirring is required to prevent monomer concentration gradients and excessive crosslinking. Under the reaction conditions employed above for the base catalyzed 6FAP-TC systems (molar ratio of base/acid chloride > 2), it was observed that no amount of stirring could stop the formation of at least a small portion of gel, regardless of the base identity.

4.6.4. Effect of Addition Methods

The method or order of monomer addition also plays a role in the ability to generate high molecular weight polymer. In most cases the bis(*o*-aminophenol) was dissolved in NMP, pyridine added, solution cooled to 5°C and the acid chloride (acid chloride dissolved in NMP or THF) dripped into the reaction mixture slowly. Attempts were made to add the acid chloride as a solid, but excessive gelation around the acid chloride particles prohibited complete dissolution of the acid chloride even after 24 hours at room temperature. Even finely powdered acid chloride tended to cause gross gelation in the reaction mixture. Rapid addition of the acid chloride solution has the same effect as adding the acid chloride as a solid. Reversing the

method of addition also resulted in unsatisfactory results. It is believed that by adding the acid chloride as a solution, the monomer is quickly dispersed throughout the reaction mixture, resulting in predominantly amide formation. Efforts to dissolve both monomers in NMP and then add excess pyridine also resulted in low molecular weight material.

4.6.5. Effect of Temperature

A number of preliminary studies were made to ascertain the effect of temperature on the generation of high molecular weight polymer. Polymerizations were conducted at various temperatures without the use of pyridine and the results (Figure 4.21) indicate that optimal reaction temperature to be 0-5°C. Holding the reaction mixture at this temperature for 68 hours resulted in little or no change in the intrinsic viscosity with time and it appears as though the reaction has reached some form of equilibrium after 3-5 hours (Figure 4.22). Although similar systematic studies were not made with an acid acceptor, experimental observation of such systems indicate comparable results. That is, low temperatures tend to generate higher intrinsic viscosities while elevated temperatures result in lower intrinsic viscosities. Again, it should be pointed out that these results were achieved with the 6FAP-TC system and

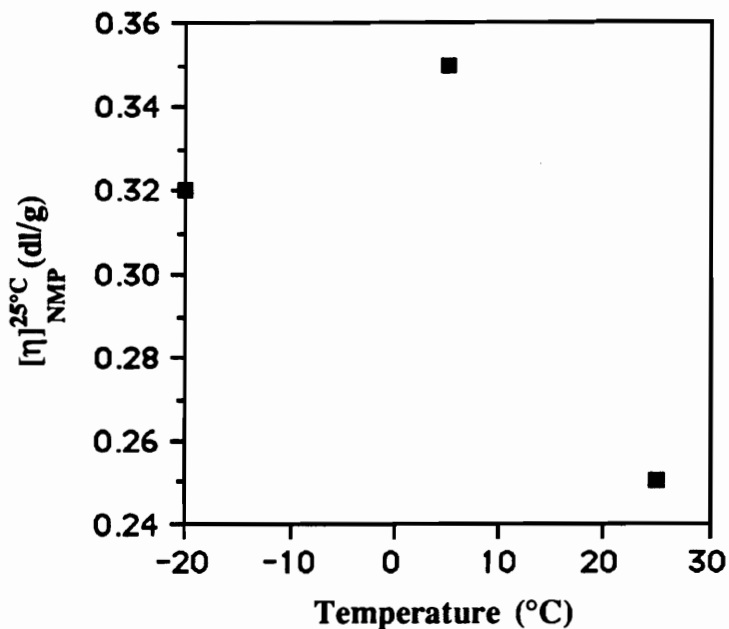


Figure 4.21. Effect of reaction temperature on intrinsic viscosity for 6FAP and TC polymerizations carried out in NMP (20% solids) for 24 hours with no base.

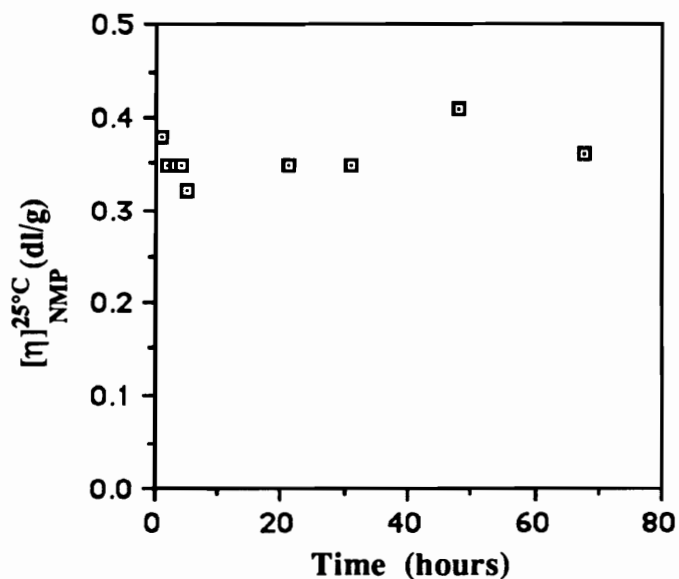


Figure 4.22. Intrinsic viscosity as a function of time for 6FAP-TC polymerizations carried out at 5°C in NMP (20% Solids) without base.

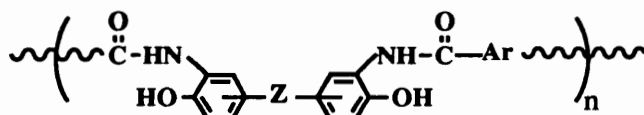
while they are not very impressive, other optimized systems (Section 4.8-4.11) did show favorable results.

4.6.6. Effect of Linking Groups in the Aminophenols

In the previous paragraph, reference was made to optimized systems which exhibit high intrinsic viscosities. Table 4.6 summarizes the results from a number of polymerizations where the linking group between the aminophenols and acid chlorides has been systematically varied. Note that the systems with appreciable viscosities have electron donating or electron neutral linking groups between the aromatic moieties. Bis(*o*-aminophenol)s containing electron donating linkages *para* or *meta* to the amine generate high molecular weight PHA's regardless of the type of acid chloride. This fact would seem to conclude that electron-rich aminophenols undergo rapid amidation under this set of reaction conditions. On the other hand, electron-deficient aminophenols may undergo competitive acylation reactions depending on the reaction conditions.

Comparison of amine ¹H NMR shifts from a select number of aminophenols (Table 3.7) reveals no real difference in the electron density at the amines relative to the type or orientation of the linkage (*m-meta* to linkage, *p-para* to linkage). While the proton shifts for the amine protons vary only 0.3 ppm, they vary as much as

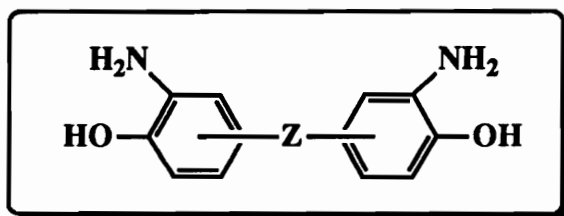
Table 4.6. Effect of acid chloride and aminophenol linking group on the intrinsic viscosity of various poly(hydroxy amide)s.



Z Composition	Ar Composition	PHA $[\eta]_{\text{NMP}}^{25^\circ\text{C}}$ (dl/g)
$\begin{array}{c} \text{CH}_3 \\ \\ -\text{C}- \\ \\ \text{CH}_3 \\ \\ \text{CH}_3 \\ \\ -\text{C}- \\ \\ \text{CH}_3 \end{array}$		0.67
$\begin{array}{c} \text{CH}_3 \\ \\ -\text{C}- \\ \\ \text{CH}_3 \end{array}$		0.71
-		1.30
-		Insoluble
-		1.11*
-		0.77
$\begin{array}{c} \text{CF}_3 \\ \\ -\text{C}- \\ \\ \text{CF}_3 \end{array}$		0.88
$\begin{array}{c} \text{CF}_3 \\ \\ -\text{C}- \\ \\ \text{CF}_3 \end{array}$		~0.35
$\begin{array}{c} \text{CF}_3 \\ \\ -\text{C}- \\ \\ \text{CF}_3 \end{array}$		~0.39
$\begin{array}{c} \text{CF}_3 \\ \\ -\text{C}- \\ \\ \text{CF}_3 \end{array}$		~0.30
$\begin{array}{c} \text{CF}_3 \\ \\ -\text{C}- \\ \\ \text{C}_6\text{H}_5 \end{array}$		

*Inherent viscosity run in NMP at 25°C (0.5%)

Table 4.7. ^1H NMR^a shifts of various bis(*o*-aminophenol)s.



Linking Group (Z)	Hydroxyl Proton (ppm)	Amine Proton (ppm)
$\text{C}(\text{CF}_3)_2$	9.4 (<i>p</i>)	4.6 (<i>m</i>)
$\text{C}(\text{CF}_3)(\text{Ph})$	9.1 (<i>p</i>)	4.5 (<i>m</i>)
$\text{C}(\text{CH}_3)_2$	8.7 (<i>p</i>)	4.3 (<i>m</i>)
nil	9.0 (<i>m</i>)	4.4 (<i>p</i>)

^aExperiments conducted in and referenced to d_6 -DMSO

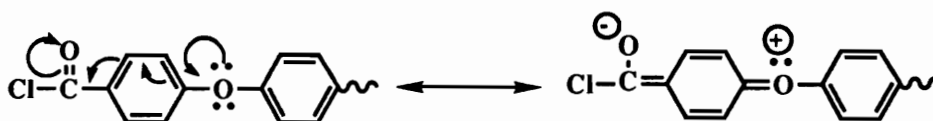
0.7 ppm for the hydroxyl protons, indicating a more significant electronic effect at the hydroxyl groups. Care was taken to minimize the influence of water and monomer concentration on quantitative peak assignment for both the amine and hydroxyl resonances. The electronic effect on proton shift positions can be correlated with the amine and hydroxyl reactivity [230]. In the case of hydroxyl groups, a downfield shift would indicate a more acidic proton (poorer nucleophile) and in the case of amines, a downfield

shift would indicate a less basic amine (poorer nucleophile). Acid chlorides being equal, one would expect both the rate of amidation and esterification to decrease with a downfield shift of the amine and hydroxyl protons for a noncatalyzed reaction system. In the case of amines, it's a well known fact that electron withdrawing groups deactivate amines toward nucleophilic substitution reactions [231]. Similarly, electron withdrawing groups deactivate aryl hydroxyls in most ester and ether forming reactions [2,232,233]. However, evidence generated from the synthesis of polyesters through low temperature, base catalyzed solution techniques tends to contradict the above mentioned trends [234-237]. That is, more acidic phenols appear to have enhanced reactivity under low temperature, base-catalyzed reactions conditions. In the case of bis(*o*-aminophenol)s, this phenomenon would suggest an increase in hydroxyl reactivity with a simultaneous decrease in amine reactivity when an electron withdrawing linking group is incorporated into bis(*o*-aminophenol). In other words, a situation is set up where competitive amidation and esterification is possible. Depending on the details of the reaction (i.e., base strength, type of acid chloride, temperature etc.), esterification can become more competitive. One could also argue that the closer proximity of the amine to the bridging group, relative to the hydroxyl group, deactivates the amines more than the hydroxyl groups and therefore esterification becomes more competitive. However, if this were the case, one would expect to

see a larger variation in the amine proton shifts with respect to bridging group identity. Irrespective of the rationale one uses to explain the effect of bridging group identity on reaction pathway, clearly, if enough esterification takes place to offset stoichiometry, molecular weight is compromised and gelation is possible. It is proposed that these rationales are useful in explaining the effect of bridging groups on the inherent viscosity (molecular weight) of poly(hydroxy amide)s.

4.6.7. Effect of Linking Groups in the Acid Chloride

The results in Table 4.6 demonstrate that 6FAP will polymerize to high molecular weights when 4,4'-oxydibenzoyl chloride (ODBC) is the acid chloride. The only obvious difference between this acid chloride and all others listed is that an electron donating oxygen linkage is present between the benzoyl chloride portions of the molecule. The effect of having an electron-donating substituent *para* to a carbonyl group during an acylation reaction is to decrease the reactivity of the carbonyl group towards nucleophiles. This reduction in reactivity can be attributed to an enhancement of electron density about the carbonyl carbon as a result of electron donation through resonance from the oxygen linkage. Consequently,



the acid chloride becomes less reactive and the competitive reaction pathway shifts in favor of the stronger amine nucleophile. As a result, little or no esterification takes place and much higher inherent viscosities are observed. If the acid chloride contains electron withdrawing groups, the reaction pathway is less selective and the ester reaction may become competitive. The fact that high molecular weight polymer can be achieved using electron rich acid chlorides also reaffirms the fact that 6FAP has adequate amine reactivity to undergo nucleophilic attack and that amine deactivation due to electron-withdrawing linkages is not responsible for the generation of low molecular weight polymers.

4.6.8. Effect of Monomer Concentration

Monomer concentration or final polymer concentration also has an effect on the ability to achieve high molecular weight polymer. This concentration effect was noticed in both base catalyzed and uncatalyzed systems. In general it was found that higher percent solids tended to generate higher intrinsic viscosities (Figure 4.23). Unfortunately this has practical limitations on polymer systems which achieve high molecular weight due to excessive viscosity buildup. Consequently, 15-20% solids are recommended for these solution step polymerizations and clearly can result in high molecular weight polymer in optimized systems.

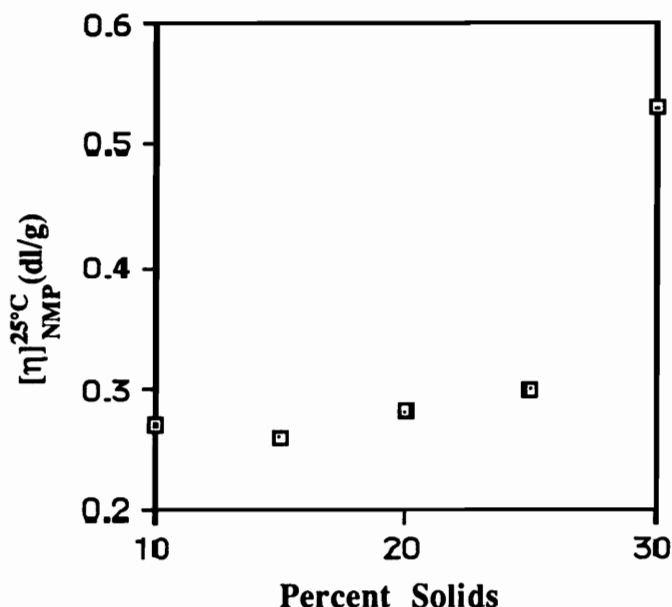


Figure 4.23. Effect of solids content on intrinsic viscosity for a 6FAP-TC polymerization carried out in NMP for 20 hours at 25°C, without base.

4.6.9. Effect of Solvent

The major requirements of the solvent in these polycondensation reactions are threefold; 1) the ability to solubilize the poly(hydroxy amide) as well as the polybenzoxazole, 2) high thermal stability and 3) ease in removal. The solvents which meet these criteria best are represented by high boiling polar, aprotic solvents such as N-methylpyrrolidinone and N,N-dimethylacetamide. The majority of the reactions were conducted in these solvents and little if any difference was noticed between these regarding achievable

molecular weight. In a number of cases THF was used as the acid chloride addition solvent, simply because THF can be scrupulously dried and is less hydrophilic than NMP or DMAc. *o*-Dichlorobenzene was investigated as a cosolvent in an attempt to moderate the reaction solvent polarity and promote amidation over esterification. Unfortunately no significant improvements were observed (Figure 4.24). In general it was found that NMP and DMAc are suitable solvents for the generation of high molecular weight polymers when conditions were optimized. A number of azeotroping solvents for

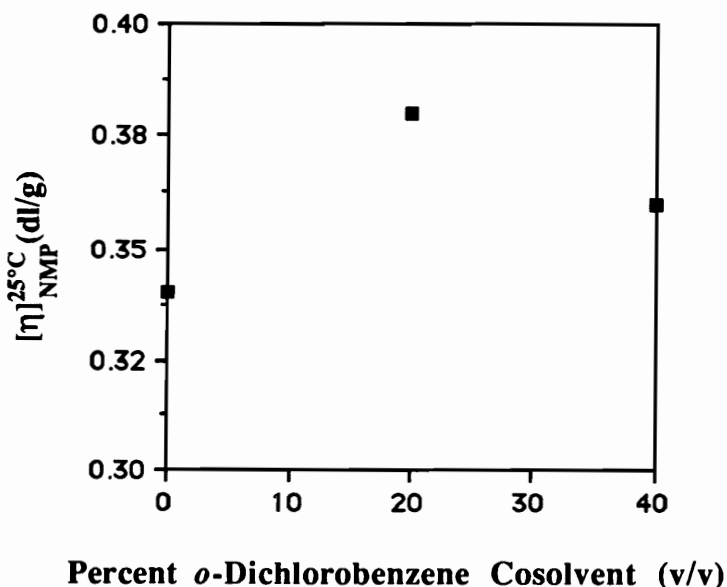
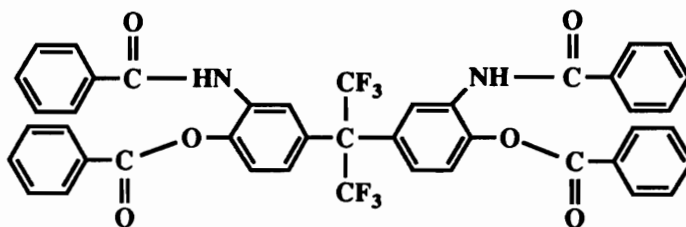


Figure 4.24. Effect of cosolvent concentration on intrinsic viscosity for the polymerization of 6FAP-TC run in NMP (15% solids) at 23°C for 24 hours. THF was used as the acid chloride addition solvent and a 2.2 molar ratio of pyridine/TC was employed.

the cyclodehydration step were also investigated and these will be discussed in the section 4.7

4.6.9. Spectroscopic Evidence for an Ester Side Reaction

Experimental observations described earlier were consistent with the presence of a small, but significant amount of ester side reaction. However, spectroscopic analysis of these materials was required to provide real evidence to confirm or disprove the presence of a molecular weight limiting ester side reaction. FT-IR and ^1H NMR spectroscopic analysis of model compounds and 6FAP-TC poly(hydroxy amide)s made with and without a base catalyst were initiated to accomplish this task. The interpretation of the spectra, as well as the conclusions reached, follow. Figure 4.25 is a stacked plot of various ^1H NMR spectra which correspond to the structures shown below. Spectrum I corresponds to the model diester-diamide prepared by condensing 6FAP and 4 moles of benzoyl chloride (Compound 1). Resonances of interest include the amide proton at



Compound 1

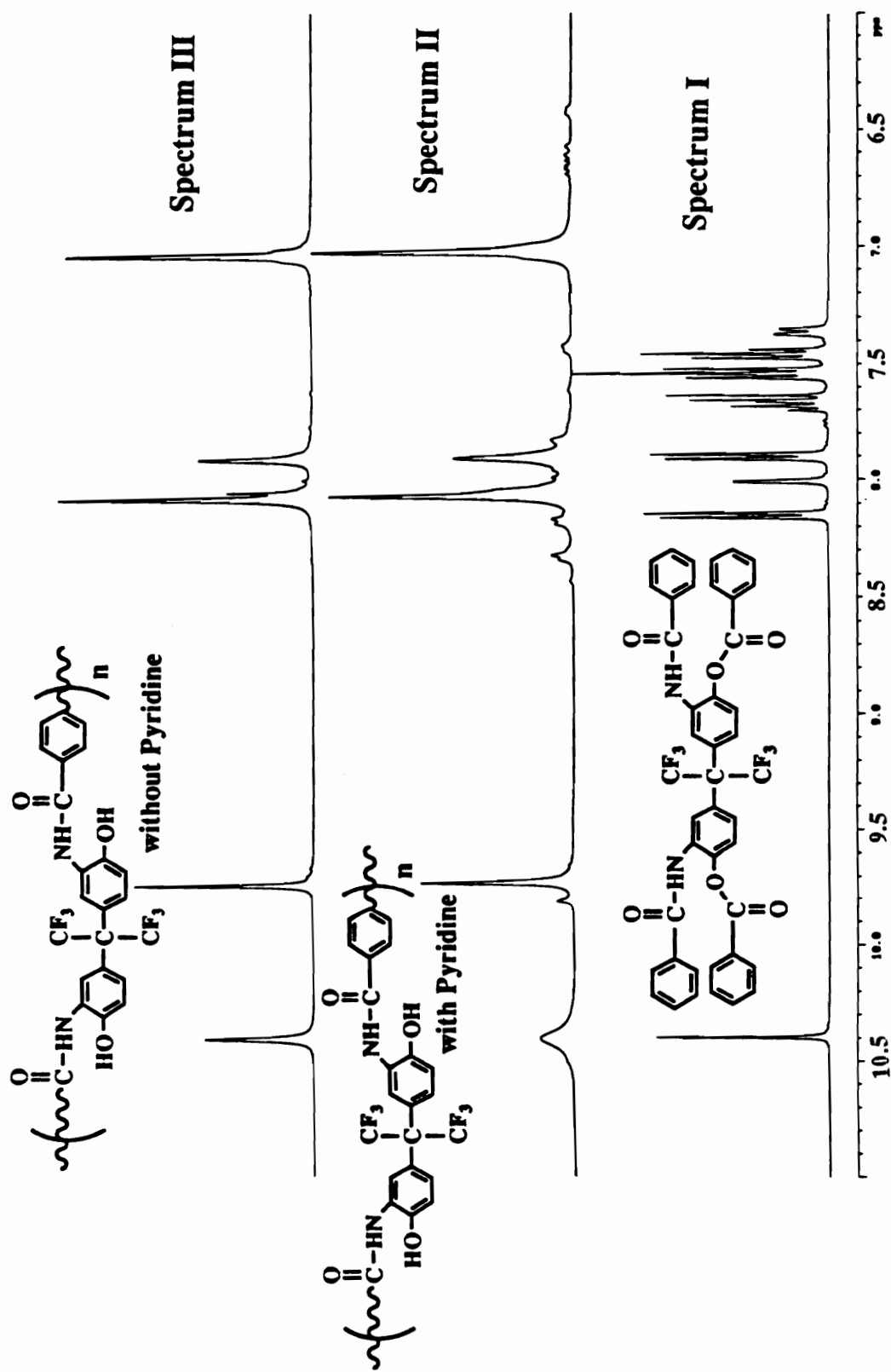
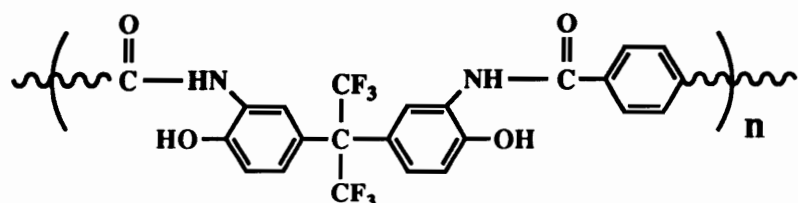


Figure 4.25. ^1H NMR spectra of compounds 1, 2, 3.

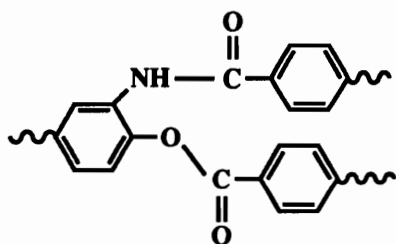
$\delta=10.4$ ppm and the protons *ortho* to the ester and the amide at $\delta=8.15$ and $\delta=7.9$ ppm respectively. Spectrum II and III represent the poly(hydroxy amide)s generated with and without a base catalyst (Compound 2 and 3, respectively). Peaks of importance include the hydroxyl peak ($\delta=10.5$), amide peak ($\delta=9.67$), terephthaloyl protons



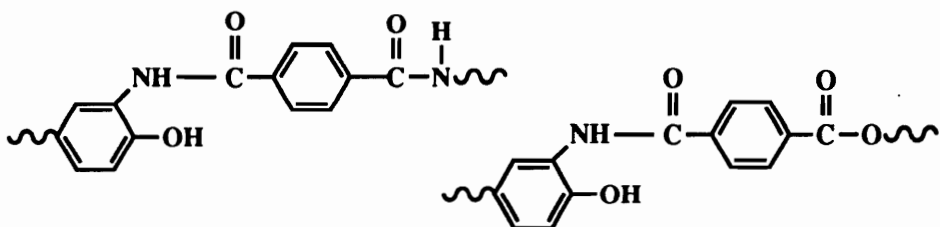
Compound 2 (with base) and Compound 3 (without base)

($\delta=8.1$) and the aminophenol proton resonances at $\delta=7.0$ and $\delta=7.9$ ppm. It should also be noted that an extra amide peak ($\delta=9.8$) as well as peaks potentially attributable to protons *ortho* to an ester and/or an amide ($\delta=8.2$ and 8.4) and starting material ($\delta=6.5-6.7$) are present in spectrum II, while they are not present in spectrum III.

Inspection of this data indicates that a side reaction is occurring during the base-catalyzed polymerization as evident by the extra signals in spectrum II. The downfield shoulder ($\sim\delta=9.8$) on the amide resonance of spectrum II indicates a second type of amide is present in the polymer made with a base catalyst. Considering the fact that an amide flanked by an ester has a proton shift of $\delta=10.4$ in model compounds (spectrum I), it is logical to conclude that the second amide signal is caused by a change in functionality

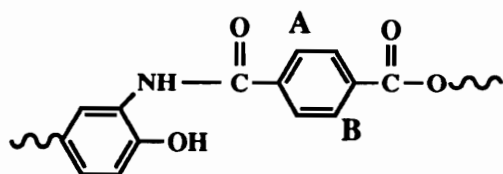


para to the amide carbonyl. Only two functional groups are possible in this case, an amide and an ester. The proton shift from an amide



para to an amide is known from spectrum III, consequently the small downfield amide peak is being assigned to an amide *para* to an ester group. Electronic effects caused by substitution on the other aminophenol ring, through the hexafluoroisopropylidene linkage, will of course influence peak positions. However, due to the symmetry of the system, these features should lead to the same conclusion. Slight broadening of the hydroxyl peak ($\delta=10.4$) in spectrum II is also consistent with the possibility that some amides are flanked by esters (similar to compound 1 (spectrum I)). If the second amide peak in spectrum II is due to an amide *para* to an ester, then explanation of the observed two small downfield doublets ($\delta=8.15$ and 8.3 ppm) should be straightforward.

The relationship between these two doublets was verified by performing a 2D ^1H NMR decoupling experiment on the polymer synthesized with base. Figure 4.26 displays the spectroscopic results of this experiment. It is quite clear that the set of doublets are coupled to one another as illustrated by the off diagonal correlation. The fact that the peaks are shifted downfield from the protons *ortho* to an amide-amide linkage indicates the protons are affected by an electron-withdrawing group stronger than an amide carbonyl, such as an ester carbonyl. Due to the relative size of each peak and the splitting pattern, one can conclude that these protons are equivalent in quantity and occupy a position *ortho* to one another. Based on this evidence and the fact that the aminophenol protons all display resonances below $\delta=8.0$ ppm, these two signals are assigned to protons *ortho* to an amide ($\delta=8.15$ (A)) and *ortho* to an ester ($\delta=8.3$ (B)), where the amide is *para* to an ester.



For the sake of argument, one could argue that these proton shifts are simply due to residual carboxylic acid groups which didn't react during the polymerization. Evidence contrary to this assumption can be found in Figure 4.27. All three spectra are from compound 2 above, the bottom spectrum is from a polymer made without base, the central spectrum is from polymer made with base

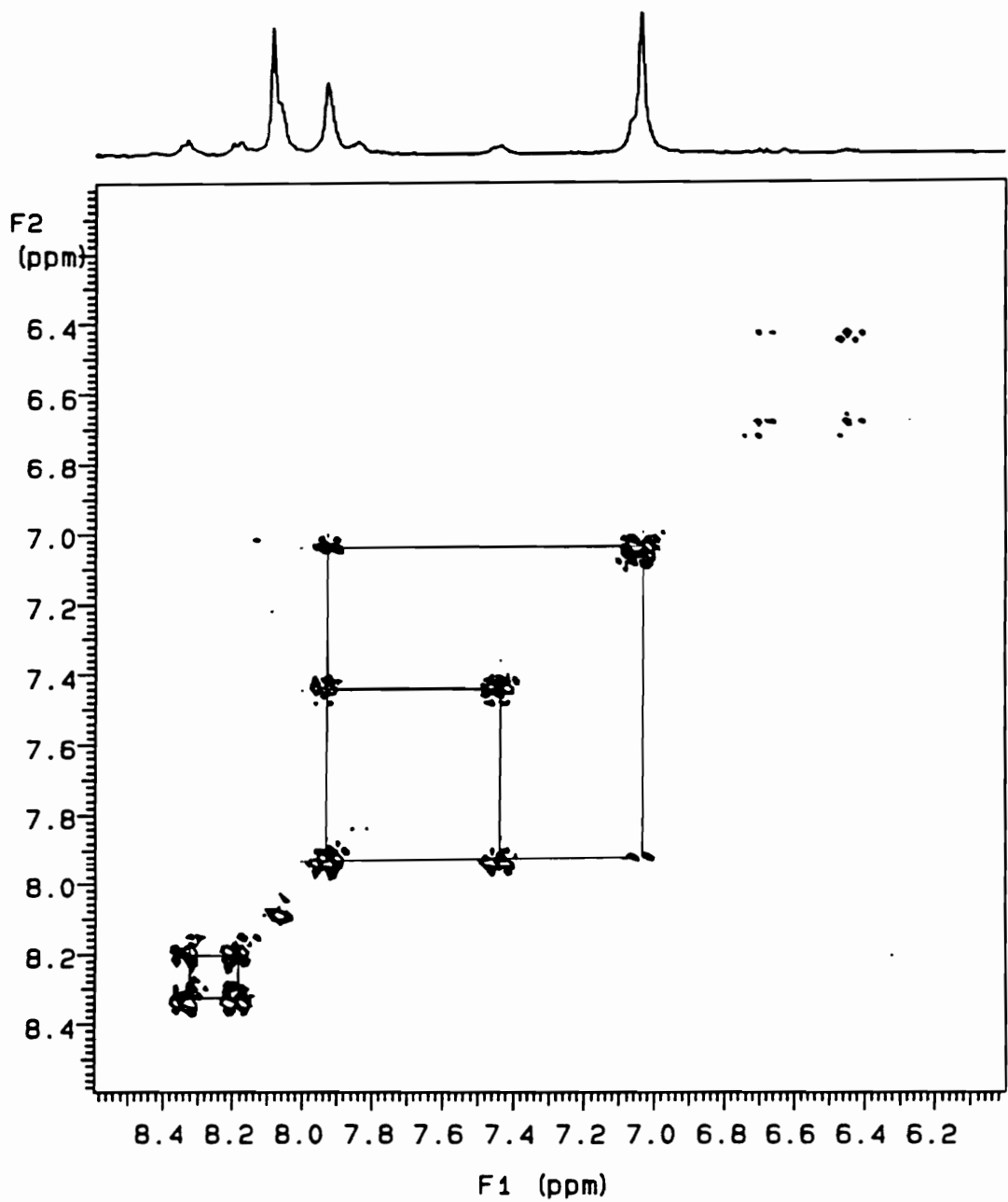


Figure 4.26. 2D ^1H NMR spectrum of base generated 6FAP-TC poly(hydroxy amide).

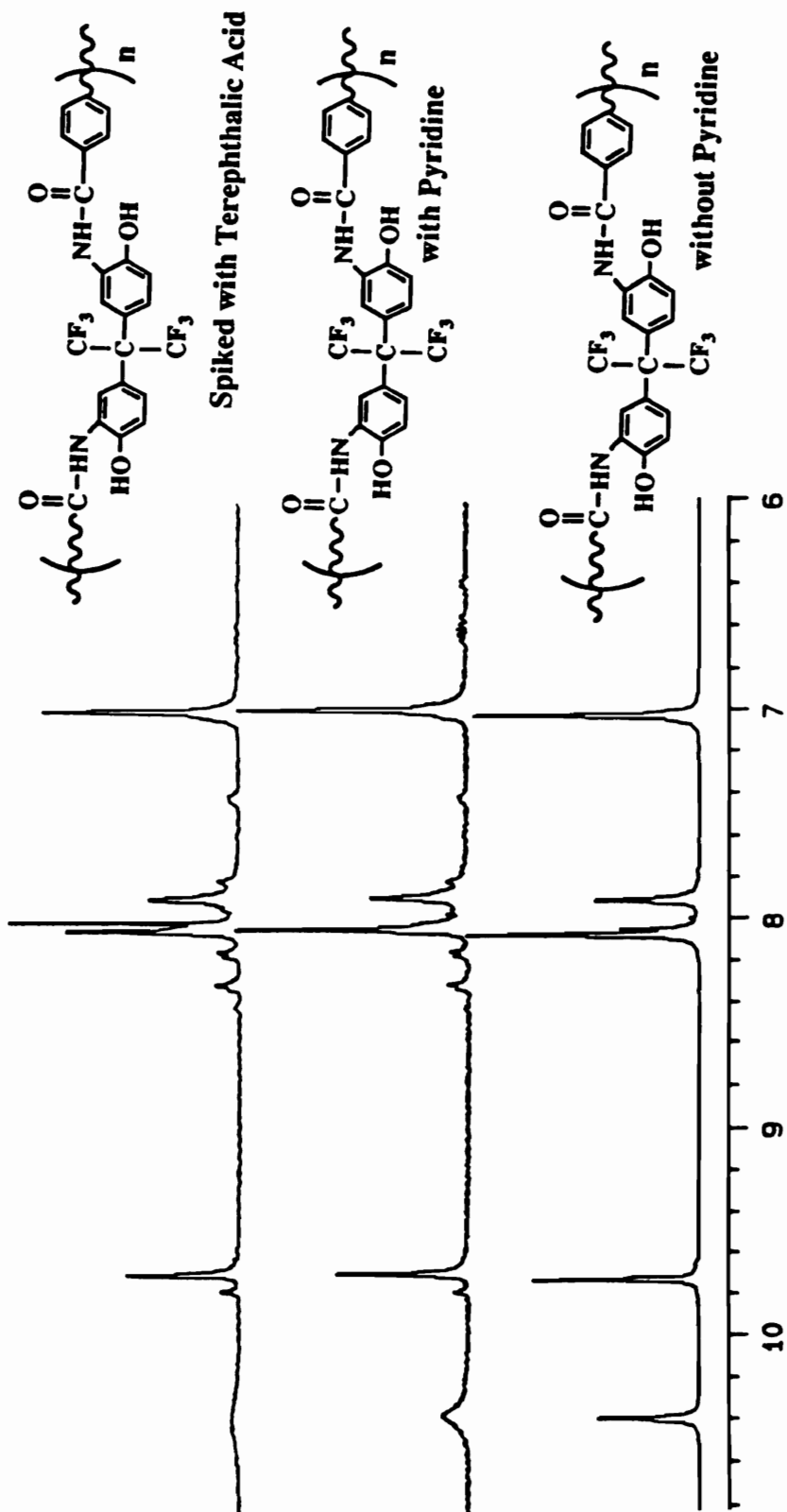
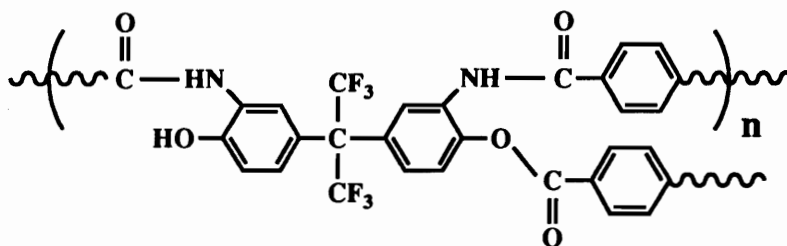


Figure 4.27. ^1H NMR spectra of 6FAP-TC poly(hydroxy amide)s synthesized and analyzed under various conditions.

and the top spectrum is from a polymer made with base, but spiked with terephthalic acid. It is obvious from these results that the resonances at $\delta=8.15$ and 8.3 ppm can't be residual acid groups because they are not present at or near the terephthalic acid proton resonance ($\delta=8.05$). In addition, if these shifts were due to residual acid groups, they should appear in the spectra of the PHA's generated with and without base. It is important to recall that both of the polymers are low molecular weight as judged by their respective intrinsic viscosities.

Infrared analysis of the above structures also supports ester formation. Figure 4.28 is a stack plot of the FT-IR spectra obtained from compounds 1 and 2 above and compound 4 shown below. Stretches of major significance are the ester stretches at 1749 and 1724 cm^{-1} and the amide stretches at 1684 and 1650 cm^{-1} . Spectrum I corresponds to a completely acylated 6FAP monomer (compound 1), therefore only one type of ester stretch should be present (1749 cm^{-1}). Spectrum II (compound 3) represents the reaction product of 1 mole of 6FAP and 1.25 moles of TC, reacted



Compound 3

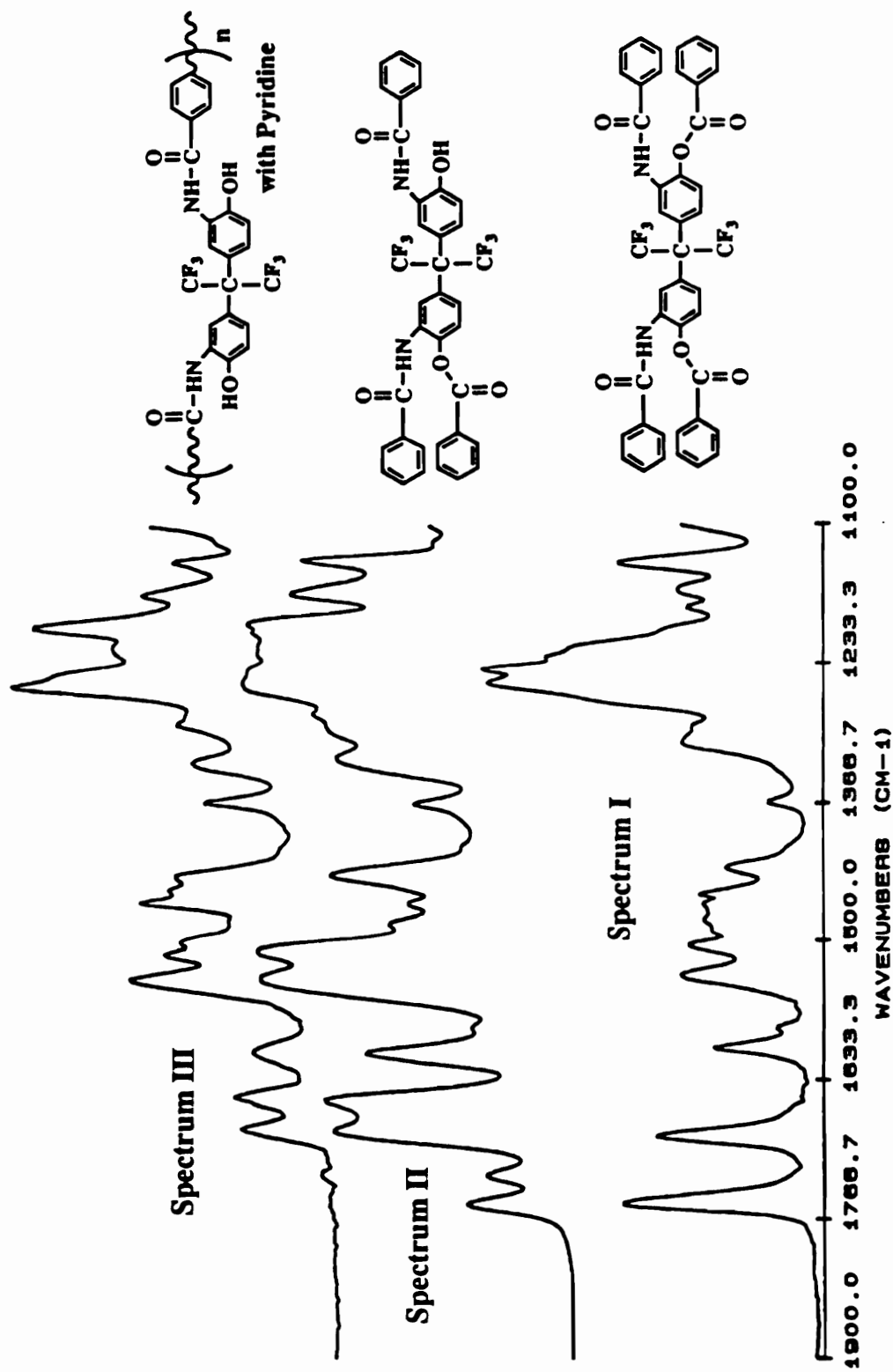


Figure 4.28. FT-IR spectra of 6FAP-TC poly(hydroxy amide) and 6FAP model compounds.

in the presence of base. Excess terephthaloyl chloride allows for the formation of ester-ester, ester-amide and amide-amide compounds. The infrared bands at 1749 cm^{-1} and 1724 cm^{-1} correspond to the different types of ester functionalities, while the amide peaks are once again visible below 1690 cm^{-1} . The amide stretches are also much larger relative to the ester stretches, indicating that a majority of the carbonyls are amides. Spectrum III represents the IR spectrum of a poly(hydroxy amide) generated under "normal" base catalyzed polymerization conditions (compound 2). Note that the ester bands have not completely disappeared, suggesting an ester forming side reaction is taking place. The fact that esters can be detected by FT-IR, correlates very well with ^1H NMR data.

The last observation which must be addressed is the fact that a gel forms upon the addition of a slight excess of terephthaloyl chloride in a matter of minutes when the reaction temperature is raised to room temperature, but over the course of time, the gel disintegrates. Subsequent disintegration of the gel could be explained by an acyl exchange reaction between unreacted amines and esters, resulting in amides and phenols. It is expected that an increase in TC content would result in a permanent amide-ester gel. In fact when lutidine was used in place pyridine and a 50% molar excess of terephthaloyl chloride was employed, the entire contents of the flask gelled in matter of minutes at room temperature. This gel was stable even after heating for 8 hours at 165°C .

Generation of high molecular weight poly(hydroxy amide)s via low temperature techniques has been utilized just short of thirty years [11] and over this time period, a large portion of the research has been delegated towards the synthesis of high molecular weight PHA's with electron-withdrawing linkages between the aminophenol portion of the polymer [7,29,30]. While much of this work has focused on enhancing the reactivity of the amines toward nucleophilic addition, it should be clearly understood that amine reactivity is not the molecular weight limiting feature. The fact that 6FAP can be polymerized to high molecular weights when an electron rich acid chloride is used is further evidence to contradict the assumption of inadequate amine reactivity.

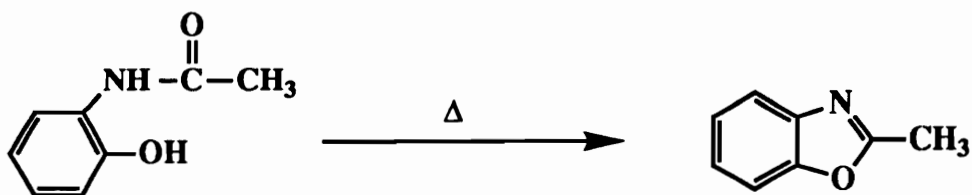
Spectroscopic and other evidence described herein indicates that molecular weight is lowered by an ester side reaction. Immediate gelation in the case of either inadequate mixing, strong base or high concentrations of acid chloride can be easily explained by an ester forming side reaction. Polymerizations carried out in the absence of base exhibit no gelling behavior, indicating that the base is acting as a catalyst for the ester reaction; as it is well known to do in poly(arylate) syntheses [222]. Finally spectroscopic evidence, both ^1H NMR and FT-IR, confirms the formation of amide-esters during the polymerization process.

4.7. Methods of Cyclization

4.7.1. Poly(hydroxy amide) Cyclization Studies

The "Research Objectives" section mentioned the goal of generating fully cyclized polybenzoxazoles in solution. Synthesis of completely cyclized polymers allows one to avoid the lengthy thermal cyclization process and the disadvantages associated with it (e.g., morphological differences, shrinkage, etc.). As alluded to in the "Literature Review," the polyphosphoric acid reaction mixture does accomplish solution cyclization, but at the expense of using a undesirable solvent. Reinhardt [8] demonstrated that fluorinated PBO's can be prepared in situ using a PPSE catalyst in *o*-dichlorobenzene; unfortunately stoichiometric amounts of PPSE are required and removal of this catalyst is difficult. The approach employed herein is to perform the actual polymerization at a low temperature and then catalytically cyclize the poly(hydroxy amide) to the polybenzoxazole. Efforts made to identify suitable cyclization conditions will be addressed in the following section.

Reports in the literature [238], suggest *o*-hydroxyacetanilide will undergo spontaneous intramolecular cyclization/aromatization upon heating to form 2-methylbenzoxazole in high yields. Similar reports suggest 2-phenylbenzoxazole can also be generated in this fashion, albeit at higher reaction temperatures [239,240]. There-



fore efforts were undertaken to use this approach to cyclize poly(hydroxy amide)s to polybenzoxazoles. Unfortunately, research carried out by the Russians [241] and experiments conducted in our labs indicated elevated temperatures alone are inadequate to facilitate rapid cyclization. In addition, appreciable reduction in molecular weight was observed; probably due to hydrolysis of the amide bond (Figure 4.29). Efforts to enhance the rate of cyclization by using an acid catalyst resulted in highly cyclized materials, but degradation of molecular weight was still a problem. Due to the apparently competitive rate of hydrolysis, it was postulated that efficient removal of water (generated in the cyclization process, Figure 4.30) from the reaction system would suppress the rate of hydrolysis and maintain molecular weight. This would certainly agree with our recent research on solution imidization [228].

A series of reactions were carried out using various reaction conditions, different acid catalysts and various temperatures to test this hypothesis. 6FAP-ODBC poly(hydroxy amide) was the polymer of choice for these experiments since high molecular weight PHA's could be generated. The reaction scheme and polymer structures are illustrated in Figure 4.31. Dehydration of the reaction mixture was achieved using several solvents at various

azeotroping temperatures. For example, toluene is effective at removing water in the temperature range of 150-170°C, while

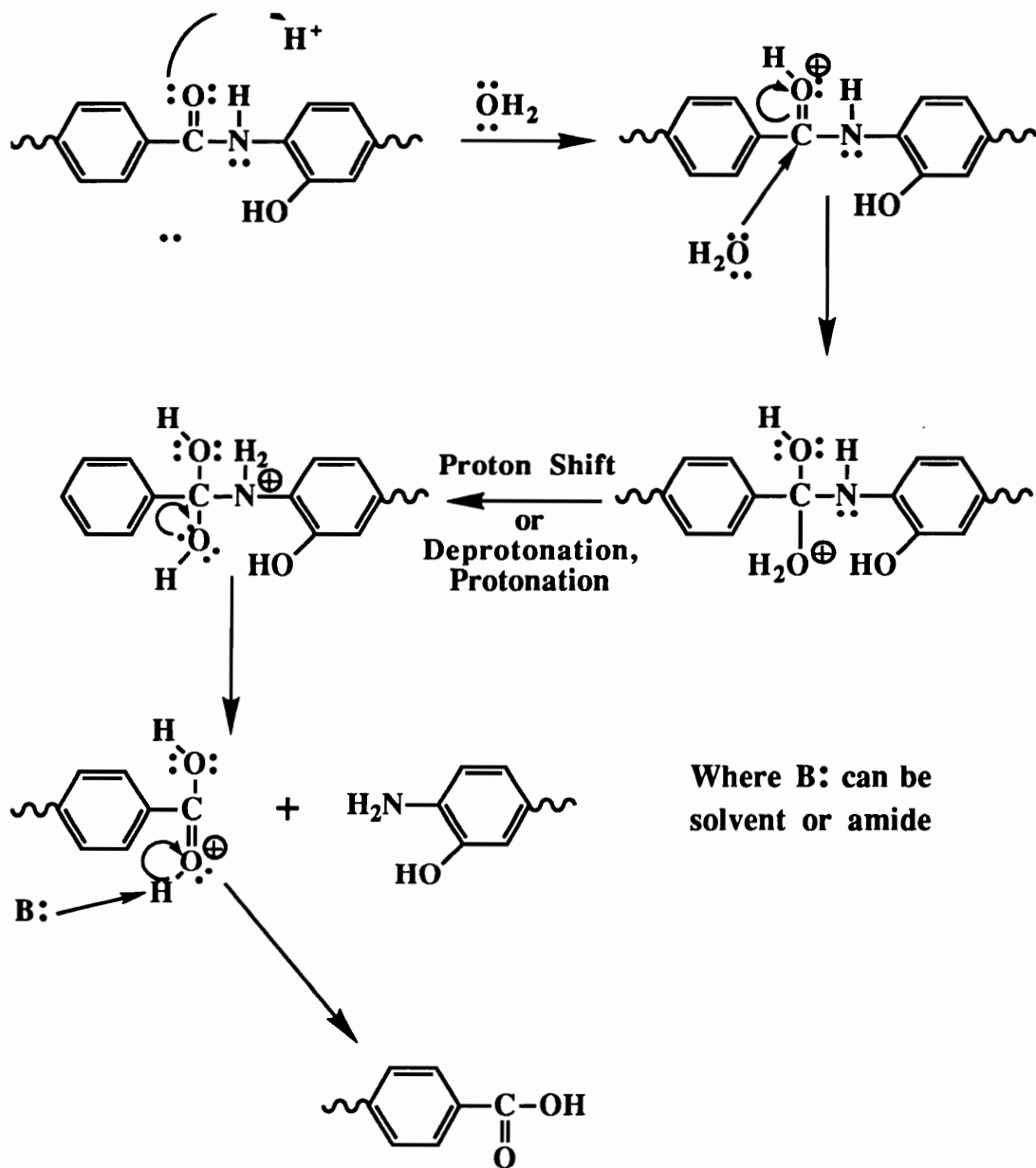


Figure 4.29. A proposed mechanism for the acid catalyzed hydrolysis of an amide bond in poly(hydroxy amide)s.

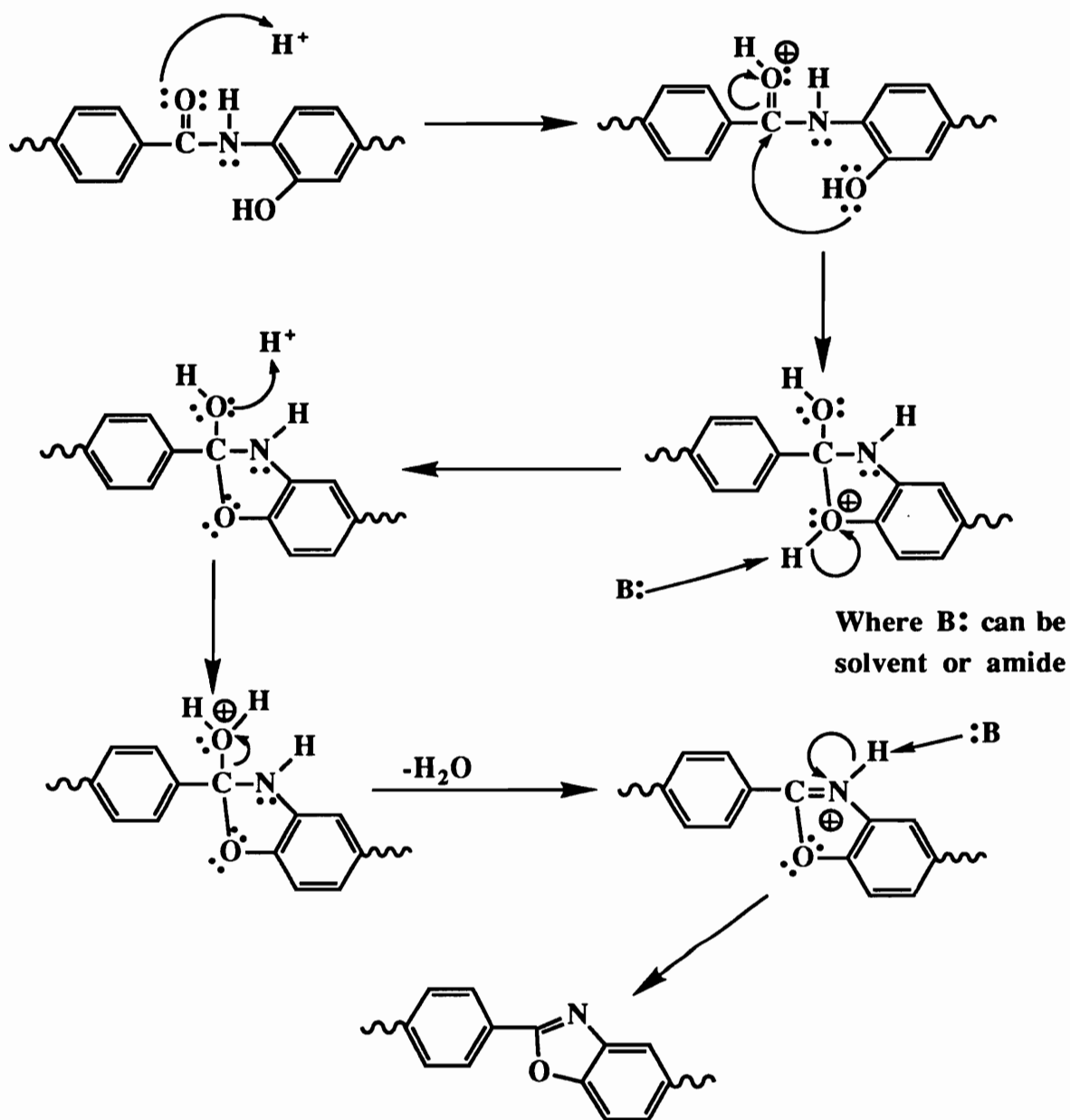


Figure 4.30. Proposed mechanism for the acid catalyzed cyclization of poly(hydroxy amide) to polybenzoxazole.

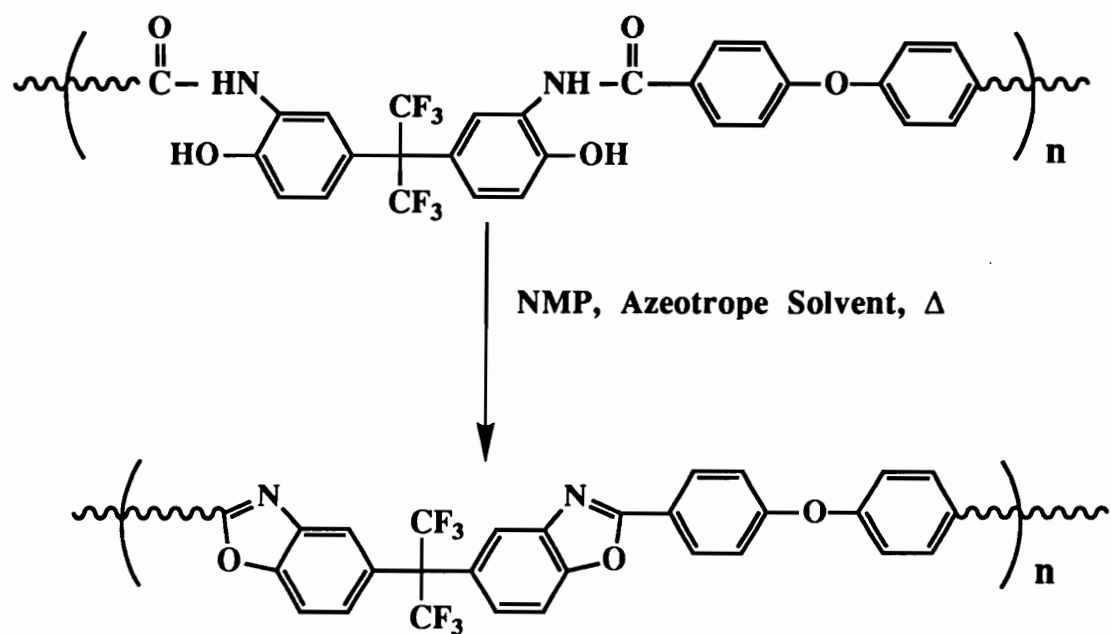


Figure 4.31. General poly(hydroxy amide) cyclization reaction.

o-dichlorobenzene (DCB) is effective at temperatures around 185°C. For higher temperature reactions, *N*-cyclohexylpyrrolidinone (CHP) was used as the solvent and the azeotrope solvent. Typical reaction procedures entailed dissolving the polymer in NMP, adding judicious quantities of azeotrope solvent and heating at the azeotroping temperature until cyclization was complete.

Percent cyclization was determined using the aromatic portion of the ^1H NMR spectra (Figure 3.32). Aliquots of the reaction mixture were sampled at various times throughout the reaction. Dividing the integral for the two peaks at $\delta=7.8$ ppm by the combined integrals from the peaks at $\delta=7.8$ and $\delta=7.05$ ppm and multiplying by 100 results in the percent polybenzoxazole formed at a specific time, or conversely, the percent poly(hydroxy amide) remaining. It should be pointed out that no attempt was made to identify spectral shifts due to intermediates, nor was any consideration of intermediates made in the calculation of percent cyclization. Figure 4.32 demonstrates quite clearly that complete cyclization has occurred and that monitoring the cyclization by ^1H NMR is very reliable.

Initial attempts to cyclize the poly(hydroxy amide) without an acid catalyst resulted in less than 1% conversion over a 5 hour period and an appreciable amount of polymer hydrolysis. Therefore pyridine hydrochloride was investigated as a catalyst to enhance the rate of cyclization. Pyridine hydrochloride was initially selected

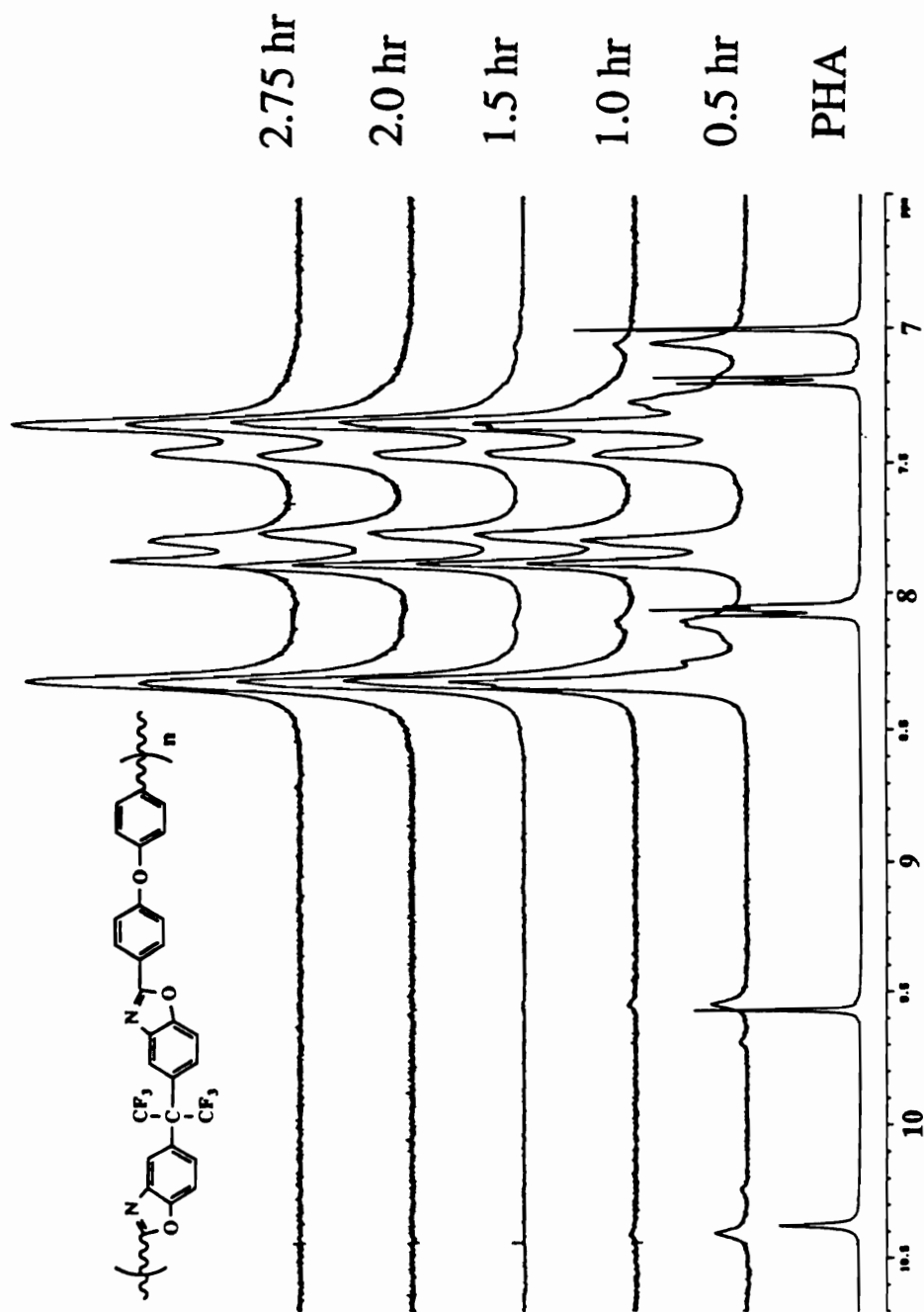


Figure 4.32. Change in ^1H NMR spectra with time for conversion of 6FAP-ODBC PHA to polybenzoxazole at 185°C (80/20 NMP/DCB, 15% solids, 10% p-toluenesulfonic acid).

because it is a byproduct of the initial step polymerization. Since stoichiometric quantities of pyridine hydrochloride were generated in the polycondensation, stoichiometric quantities were used in the cyclization studies. By varying the azeotrope solvent composition, the azeotroping temperature or reaction temperature, percent cyclization could be systematically studied.

The influence of reaction temperature on percent cyclization is shown in Figure 3.34. As indicated, pyridine hydrochloride is a very effective catalyst over the entire temperature range investigated. At lower reaction temperatures, cyclization progresses at a slower rate, but complete conversion could be achieved in as little as 12 hours at 165°C. Unfortunately, the use of pyridine hydrochloride as a catalyst is complicated, especially at higher reaction temperatures, by its volatility. At cyclization temperatures above 165°C, pyridine hydrochloride is a very effective catalyst during the initial stages of the reaction, but as the reaction progresses, pyridine hydrochloride disassociates, distills from the system and the rate of cyclization decreases dramatically. If more pyridine hydrochloride is added to the system, the rate of cyclization will again increase, but only as long as pyridine hydrochloride remains in the system. The plateauing effect of the 185°C curve (Figure 4.33) is the result of this phenomenon. At lower reaction temperatures, disassociation of pyridine hydrochloride and subsequent distillation from the system is minimized, therefore conversion of poly(hydroxy amide) to polybenzoxazole follows a smooth continuous curve.

Unfortunately, lower cyclization temperatures also lead to more amide hydrolysis in this particular case. Alternate catalysts were explored due to these undesirable effects.

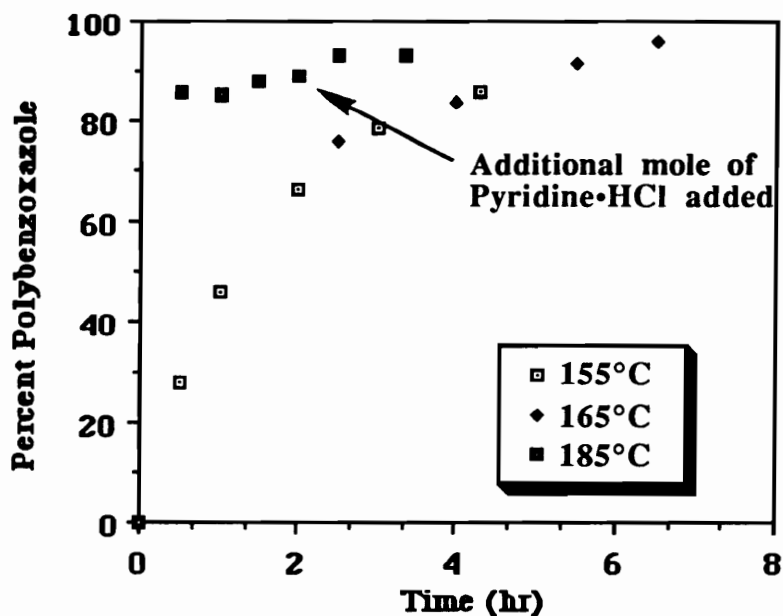


Figure 4.33. Conversion of 6FAP-ODBC PHA to PBO as a function of reaction temperature with stoichiometric amounts of pyridine hydrochloride [NMP/DCB (80/20), 15% solids].

p-Toluenesulfonic acid monohydrate (*p*-TSA) is a solid at room temperature and unlike pyridine hydrochloride, displays minimal volatility at high reaction temperatures. Therefore, a steady conversion of poly(hydroxy amide) to polybenzoxazole is realized. Analogous to the pyridine hydrochloride reaction conditions, higher reaction temperatures were found to enhance the rate of cyclization. In an attempt to optimize the cyclization conditions

with respect to catalyst concentration and reaction temperature, a series of experiments were conducted with various quantities of *p*-toluenesulfonic acid monohydrate. Catalyst concentrations are reported as a mole percent of the hydroxyl groups, assuming 2 hydroxyl groups per repeat unit.

The results of the study are depicted in Figure 4.34. In all cases, *p*-toluenesulfonic acid was found to dramatically increase the rate of the cyclization, even with as little as 1% catalyst. In general, the rate of cyclization was directly dependent on reaction temperature and catalyst concentration. Increasing the reaction temperature or increasing the catalyst concentration results in enhanced rates of cyclization. Reactions at 185°C with 10% *p*-toluenesulfonic acid were found to be completely cyclized in as little as 2.5 hours. An interesting feature of the lower reaction temperatures and lower catalyst concentrations is an apparent 2 stage cyclization profile. In all the reactions, percent conversion rose quickly in the first few hours, but then dramatically tailed off towards the end of the reaction. A possible explanation for this phenomenon is a decrease in functional group concentration with time. With fewer functional groups to react, the catalyst is less efficient and the rate of cyclization decreases. Therefore, increasing the catalyst concentration should depress this tailing and it does, within expected limits. An increase in solution viscosity with percent conversion would also be expected to

decrease functional group and catalyst mobility, further contributing to a reduction in cyclization rate.

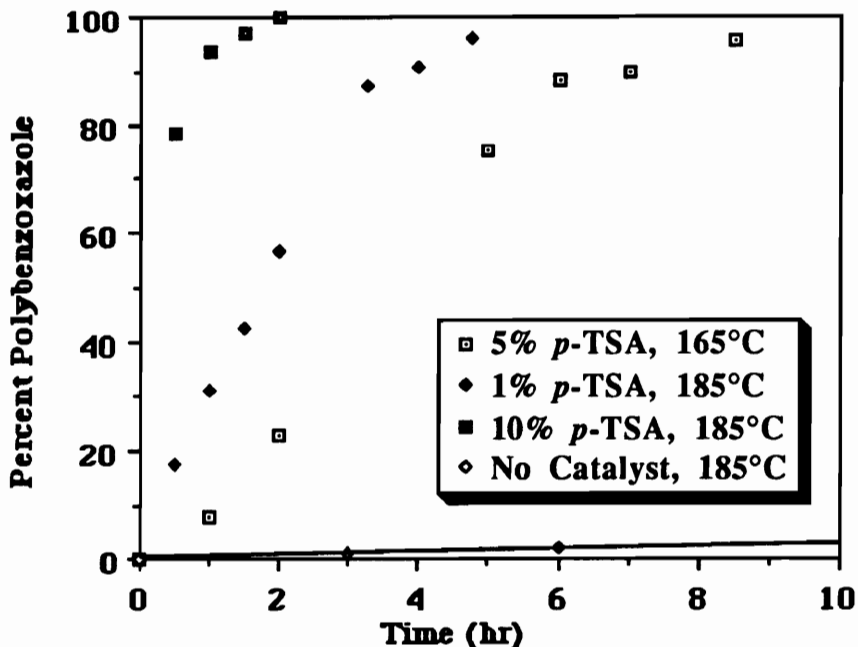


Figure 4.34. Conversion of 6FAP-ODBC poly(hydroxy amide) to PBO as a function of reaction temperature and *p*-TSA concentration (15% Solids, NMP, toluene or *o*-dichlorobenzene).

One drawback associated with using *p*-toluenesulfonic acid is the required isolation of the precursor poly(hydroxy amide)s and removal of the pyridine hydrochloride by-product. Efforts to avoid this rather tedious step were investigated by using combinations of pyridine hydrochloride and *p*-toluenesulfonic acid in the cyclization step. It was expected that pyridine hydrochloride would enhance the rate of cyclization in the initial stages of the reaction and *p*-toluenesulfonic acid would erase the plateauing effect and lead to a

steady continuation of the process at longer reaction times. The results of this study are shown in Figure 4.35. Addition of 10% *p*-toluenesulfonic acid to stoichiometric amounts of pyridine hydrochloride resulted in the same curve as using 10% *p*-toluenesulfonic acid alone. Adding 1% *p*-toluenesulfonic acid to stoichiometric amounts of pyridine hydrochloride reduces the rate of cyclization relative the 10% *p*-TSA addition, but like adding 10% *p*-TSA, erases the plateauing effect exhibited by pyridine hydrochloride alone. Also note that combinations of pyridine hydrochloride and *p*-toluenesulfonic acid result in a dramatic

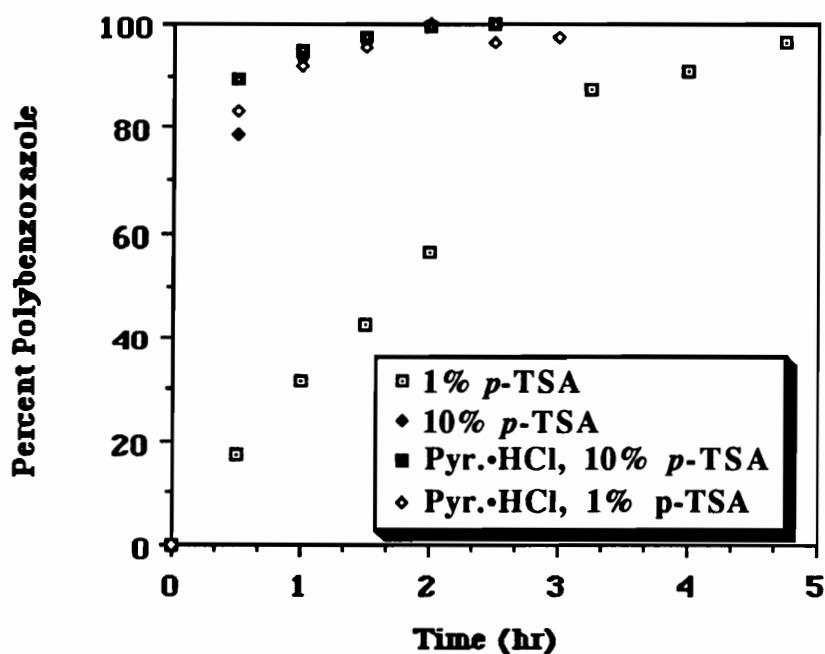


Figure 4.35. Conversion of 6FAP-ODBC poly(hydroxy amide) to PBO as a function of catalyst composition and catalyst concentration (NMP, 15% solids, DCB azeotrope, 185°C).

increase in the rate of cyclization relative to 1% *p*-toluenesulfonic acid alone. It is obvious from this study that catalyst combinations can be used, but the real test of catalyst viability lies in the effect of reaction conditions on molecular weight.

The effect of reaction conditions on molecular weight (inherent viscosity) were investigated by measuring the inherent viscosities of the precursor poly(hydroxy amide)s and the resulting polybenzoxazoles. Comparison of the PHA and PBO η_{inh} 's for each set of reaction conditions would, in principle, allow for the determination of optimum reaction conditions. While it is understood that solubility parameters and Mark-Houwink parameters are not equal for poly(hydroxy amide)s and polybenzoxazoles, it is believed that an increase or stabilization of η_{inh} 's throughout the cyclization process is a positive sign that molecular weight is not deteriorating to any appreciable extent. An increase in the η_{inh} 's could be attributed to a number of different factors. Some of these include an increase in chain stiffness due to the formation of aromatic rings during cyclization, an increase in molecular weight after cyclization due to chain extension or simply a change in polymer-solvent interaction parameter. A drawback of using this technique is that one can only compare the effect of different catalysts and temperatures in relative terms and not in absolute terms. Gel permeation chromatography can in principle determine the quantitative influence of reaction conditions on molecular weight.

The influence of reaction conditions on inherent viscosities for the pyridine hydrochloride reactions are shown in Table 4.8. These results imply that higher reaction temperatures produce more favorable results. However, in all cases the PBO η_{inh} 's have dropped below those of the precursor poly(hydroxy amide). These decreases in the η_{inh} 's are being attributed to chain cleavage. The marked

Table 4.8. Summary of cyclization conditions for reactions catalyzed with pyridine hydrochloride.

Polymer/ Cosolvents	Catalyst	Temp. (°C)	Reaction Time (hr)	η_{inh}^a (dl/g)	η_{inh}^b (dl/g)
Poly(hydroxy amide)				0.70	0.92
NMP/Tol.	100% PyrHCl	160	7.50	----	0.33 ^c
NMP/Tol.	100% PyrHCl	170	7.50	----	0.39 ^c
<u>NMP/DCB</u>	<u>100% PyrHCl</u>	<u>185</u>	<u>5.00</u>	<u>----</u>	<u>0.69</u>

^aMeasured in tetrahydrofuran (0.5 g/dl, 25°C)

^bMeasured in NMP (0.5 g/dl, 25°C)

^cIncomplete cyclization

reduction of η_{inh} 's at lower reaction temperatures could be the result of incomplete pyridine hydrochloride disassociation and thus a reduction in catalysis. As a result, amide hydrolysis becomes a more competitive reaction and molecular weight is reduced.

Table 4.9 summarizes the effect of cyclization conditions on molecular weight (inherent viscosity) for the *p*-toluenesulfonic acid

and combined catalyst systems. Note that all the η_{inh} 's have increased relative to the PHA η_{inh} and the above mentioned pyridine hydrochloride results. As in Table 4.8, higher reaction temperatures, shorter reaction times and lower catalyst concentrations resulted in higher inherent viscosities. It is

Table 4.9. Summary of cyclization conditions and inherent viscosities using *p*-toluenesulfonic acid and pyridine hydrochloride.

Polymer/ Cosolvents	Catalyst	Temp. (°C)	Reaction Time (hr)	η_{inh}^a (dl/g)	η_{inh}^b (dl/g)
Poly(hydroxy amide)		---	---	0.70	0.92
NMP/DCB	1% <i>p</i> -TSA	185	4.75	0.92	Insol.
NMP/Tol.	5% <i>p</i> -TSA	165	12.00	0.88	Insol.
NMP/DCB	10% <i>p</i> -TSA	185	2.00	0.83	0.61 ^c
CHP	10% <i>p</i> -TSA	195	3.00	1.45 ^d	Insol.
NMP/DCB	100% PyrHCl				
	& 10% <i>p</i> -TSA	185	2.75	0.76	Insol.
NMP/DCB	100% PyrHCl				
	& 1% <i>p</i> -TSA	185	3.00	0.61	Insol

¹ Measured in tetrahydrofuran (0.5g/dl, 25°C)

² Measured in NMP (0.5g/dl, 25°C)

³ η_{inh} measured on soluble fraction

⁴ Measured in CHCl₃ (0.5g/dl, 25°C)

especially satisfying to see the dramatic increase in the η_{inh} using CHP as the azeotrope/reaction solvent. Moreover, note the η_{inh} 's

were analyzed in THF, due to the insolubility of the PBO's in NMP. This is another indication of appreciable molecular weight and high degrees of cyclization. The use of catalyst combinations resulted in shorter reaction times and increased percent cyclizations relative to using pyridine hydrochloride alone, but η_{inh} 's indicate these catalyst systems to be less attractive than the *p*-toluenesulfonic acid systems. Nevertheless, the combined catalyst systems resulted in higher η_{inh} 's in all cases relative to pyridine hydrochloride alone.

In summary, reaction conditions necessary to generate fully cyclized, soluble polybenzoxazoles which possess high molecular weights have been elucidated. A simple spectroscopic method has been developed to follow the cyclization process and determine percent conversion to polybenzoxazole. A variety of different catalyst systems were studied and results indicate *p*-toluenesulfonic acid is the favored acid catalyst and while combinations of pyridine hydrochloride and *p*-toluenesulfonic acid or pyridine hydrochloride alone are highly desirable, they appear to still induce hydrolysis, which limits molecular weight. Nevertheless, molecular weight is not being dramatically affected by cyclization under optimum conditions and the best results were obtained using 10% *p*-TSA at 190-195°C in CHP for 3 hours, as shown in Table 4.9.

4.7.2. Alternate Cyclization Techniques

Earlier discussions (Section 4.6) mentioned the difficulty in achieving high molecular weight poly(hydroxy amide)s when electron-deficient bis(*o*-aminophenol)s and electron-deficient acid chlorides were employed. Efforts made to rectify this situation included investigations into alternate bases and varying base concentration. Another approach considered was to react bis(*o*-aminoanisole)s with acid chlorides in an attempt to generate poly(methoxy amide)s. It was expected that by protecting the hydroxyl group, one could eliminate the competitive ester reaction and generate high molecular weight polymers. If this is possible, the obvious question becomes, how does one deprotect the hydroxyl group, cyclize the oxazole ring and avoid amide degradation? It was assumed that generation of bis(*o*-aminoanisole)s would be a relatively simple task, so research efforts were concentrated on finding suitable reaction conditions to carry out the deprotection, cyclization reaction.

Investigations into this problem were initiated using 2,2-bis(3-amino-4-methoxyphenyl)propane and benzoyl chloride. The bis(*o*-aminoanisole) was synthesized by methylating Bisphenol A in acetone, nitrating with HNO₃ and finally reducing with 10% Pd/C in methanol (Figure 4.36). Subsequent condensation with benzoyl chloride resulted in the desired methoxy substituted bisbenzanilide (Figure 4.37). The product was confirmed by ¹H NMR. Traditional

aryl methyl ether cleavage conditions were attempted because of their similarity to the previously mentioned cyclization conditions and their favorable success in general. Following a report by Gates [242] and research performed in our labs, pyridine hydrochloride and sodium cyanide in DMSO were selected as cleavage reagents. It was realized that NaCN is not the most desirable reagent, but literature reports [243] indicate it to be quite successful in cleaving aryl methyl ethers in the presence of amide groups.

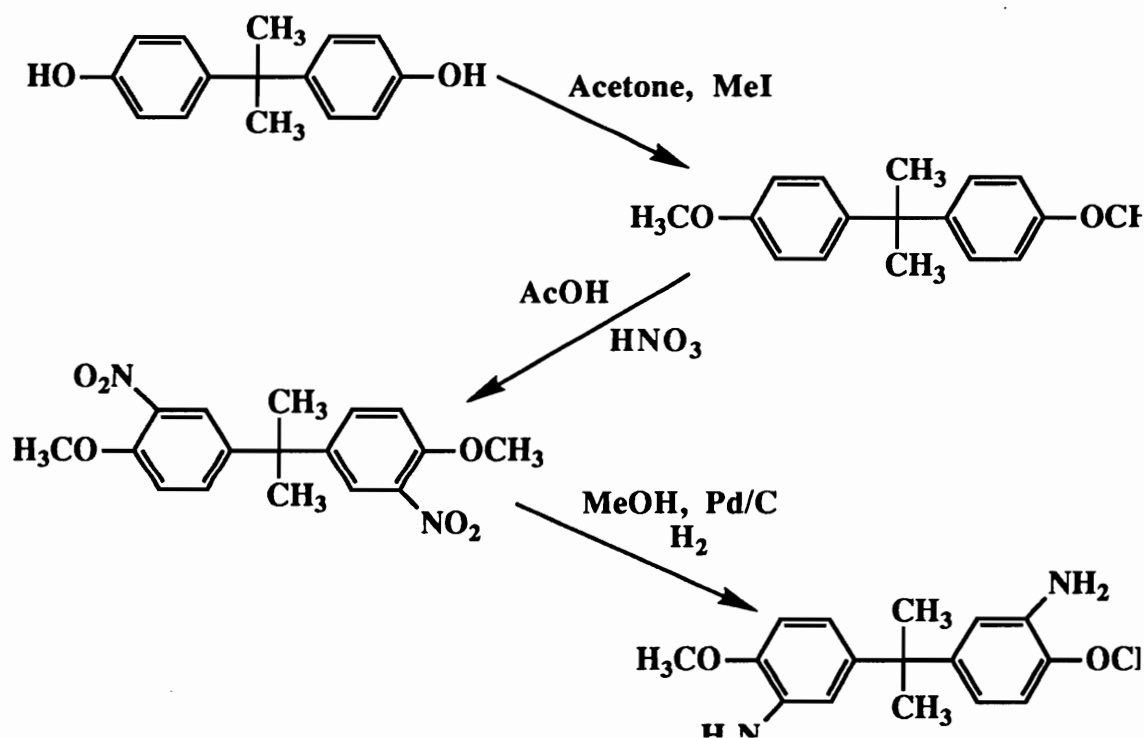


Figure 4.36. Synthesis of 2,2-bis(3-amino-4-methoxyphenyl)propane.

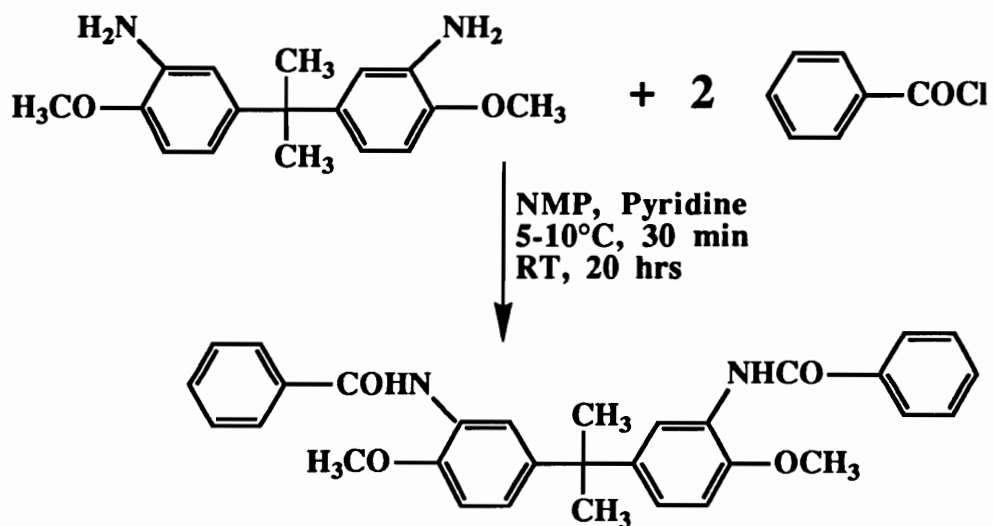


Figure 4.37. Synthesis of 2,2-bis(4-methoxy-3-benzoylamino)propane.

The reaction conditions used in the cleavage/cyclization reactions were as follows:

NMP/DCB Experiment - 15% solids (w/v), 80/20 (vol/vol) NMP/DCB, 2.05 moles of pyridine hydrochloride, 180-185°C for 23 hours

NMP Experiment - 15% solids (w/v) in NMP, 2.05 moles of pyridine hydrochloride, 185-190°C for 48 hours

NaCN Experiment - 15% solids (w/v) in DMSO, 5 moles of NaCN, 180°C for 48 hours.

To monitor the percent cleavage, aliquots of the reaction mixture were removed periodically and analyzed via ^1H NMR. Ratioing the methoxy methyl protons ($\delta=3.78$) to the isopropylidene methyl protons ($\delta=1.61$), an accurate assessment of aryl methyl ether

cleavage could be obtained (Figure 4.38). Splitting of the methoxy singlet to a doublet and the isopropylidene singlet to a triplet, indicates the methoxy groups are being cleaved in a random fashion and that cleaved, monomethoxy and dimethoxy compounds exist in solution simultaneously.

Results of these studies indicate long reaction times (excess of 24 hours), high temperatures and at least stoichiometric quantities of catalyst are required (Figure 4.39). Furthermore, reactions using pyridine hydrochloride as the catalyst resulted in amide cleavage in as little as 12 hours, while the NaCN reaction appeared to leave the amide linkages intact. Assessment of percent cyclization was not performed due to the unfavorable results obtained from the cleavage reactions. In summary, generation of methoxy substituted bisbenzanilides is possible, but subsequent successful cleavage of the aryl methyl ether moiety without detrimental effects on the amide linkage is difficult. Long reaction times, high temperatures, unfavorable catalysts and incomplete cleavage render this approach at generating polybenzoxazoles unattractive.

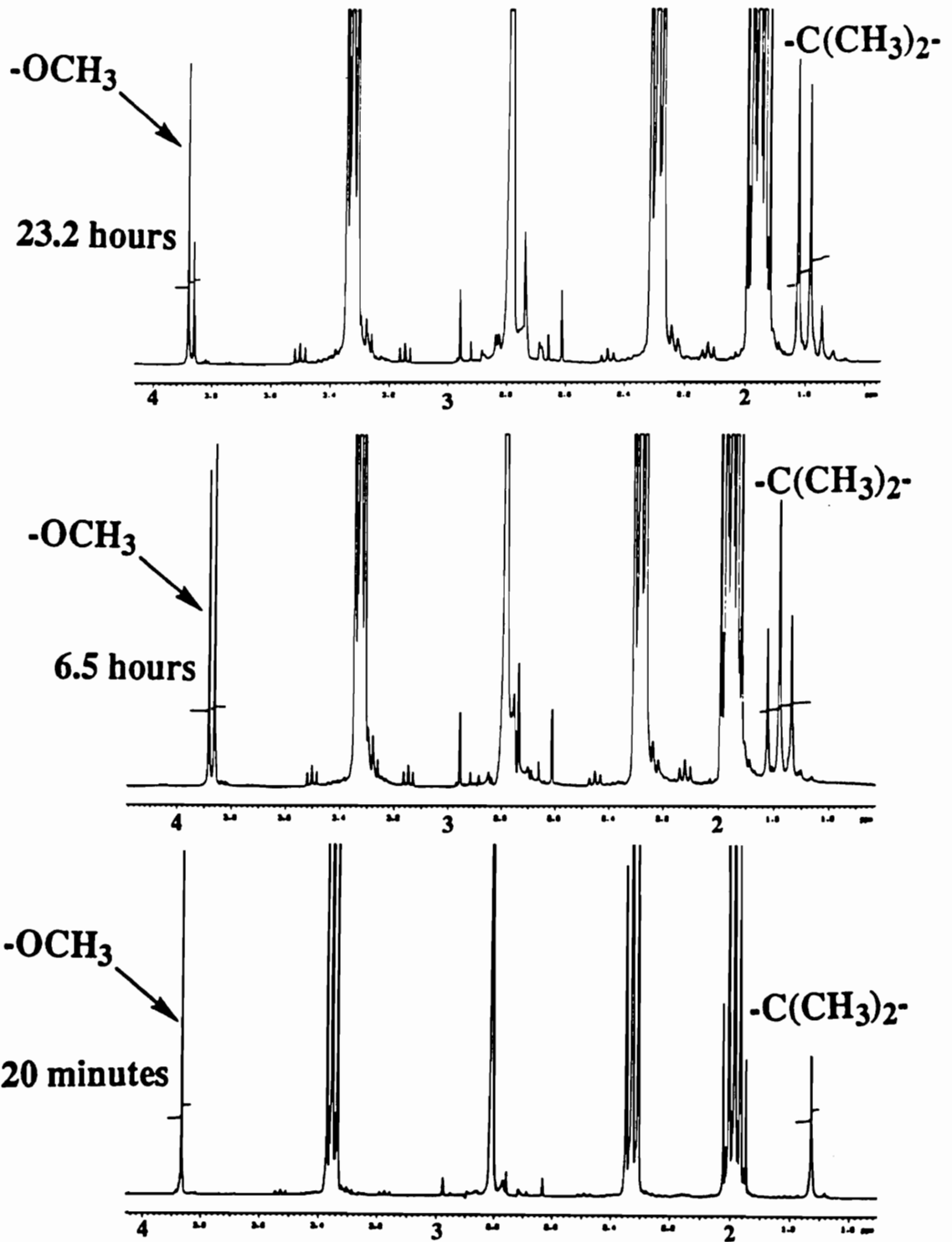


Figure 4.38. ^1H NMR spectra of methoxy cleavage reaction mixture at various times.

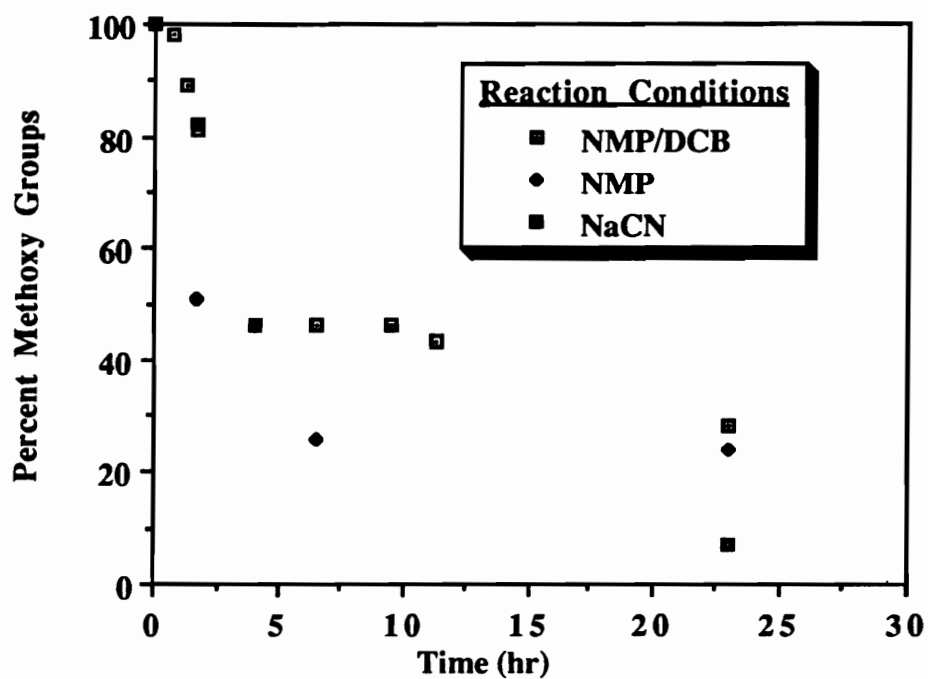
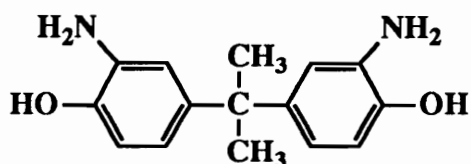


Figure 4.39. Percent methoxy groups remaining as a function of time under various reaction conditions.

4.8. Polymers Based on 2,2-Bis(3-amino-4-hydroxyphenyl)propane

It was already mentioned in the previous sections that difficulty was encountered during attempted polymerizations of electron-withdrawing bis(*o*-aminophenols) and various acid chlorides. To overcome this problem and determine if solution polymerization, as well solution cyclization was a viable synthetic procedure, 2,2-bis(3-amino-4-hydroxyphenyl)propane (bAAP), an electron-rich bis(*o*-aminophenol) was selected for investigation. In addition,



many of the commercially available engineering thermoplastics (polycarbonates, polysulfones, poly(arylene ether)s, etc.) are based on the bisphenol-A building block, consequently an adequate data base available to aid in predicting structure-property relationships. It was expected that many of the desirable characteristics attributed to the bis-A linkage (e.g., good solubility, toughness, thermo-oxidative stability and melt processability) could be extended to polybenzoxazole systems. Synthesis of the bAAP monomer as well as purification of the various acid chlorides have already been discussed; therefore the polymerization conditions and

resulting polymer properties will be discussed in the following paragraphs.

Initial research efforts focused on the generation bAAP-TC polymers using the polymerization methods discussed previously (Figure 4.40). Generation of high molecular weight (based on adequate $[\eta]$'s) poly(hydroxy amide)s was accomplished quite easily, but conversion to the polybenzoxazoles was much less successful. Premature precipitation of the bAAP-TC polybenzoxazole was observed during initial cyclization efforts. Based on previous experience, it was concluded that high molecular weight was causing precipitation and effective molecular weight control would result in a homogeneous reaction mixture. Unfortunately, this assumption was incorrect as premature precipitation occurred even when molecular weight was controlled. Thermal and WAXS analysis of the reaction products indicated the presence of crystallinity, which was certainly the main alternative consideration. Differential scanning calorimetry detected a T_g of 312°C and a crystalline melting point around 380°C after thermal cyclization and annealing (Figure 4.41). WAXS, also displayed 2 rather broad peaks overlaying the amorphous halo (Figure 4.42). As expected, the resulting polymer was insoluble in all organic solvents. Although this is attractive in terms of achieving solvent resistance, the major thrust of the research was to develop more soluble systems.

An examination of the effect positional isomers had on crystallinity and solubility was conducted in an attempt to

overcome the this solubility issue. It was rationalized that incorporation of isophthaloyl linkages into the polymer backbone would decrease crystallinity and increase solubility. Using the polymerization conditions outlined in Figure 4.40, the series of isomeric PBO's listed in Table 4.10 were generated. All the polybenzoxazoles, except the bAAP-TC system, stayed in solution during cyclization; therefore lending credence to the concept of

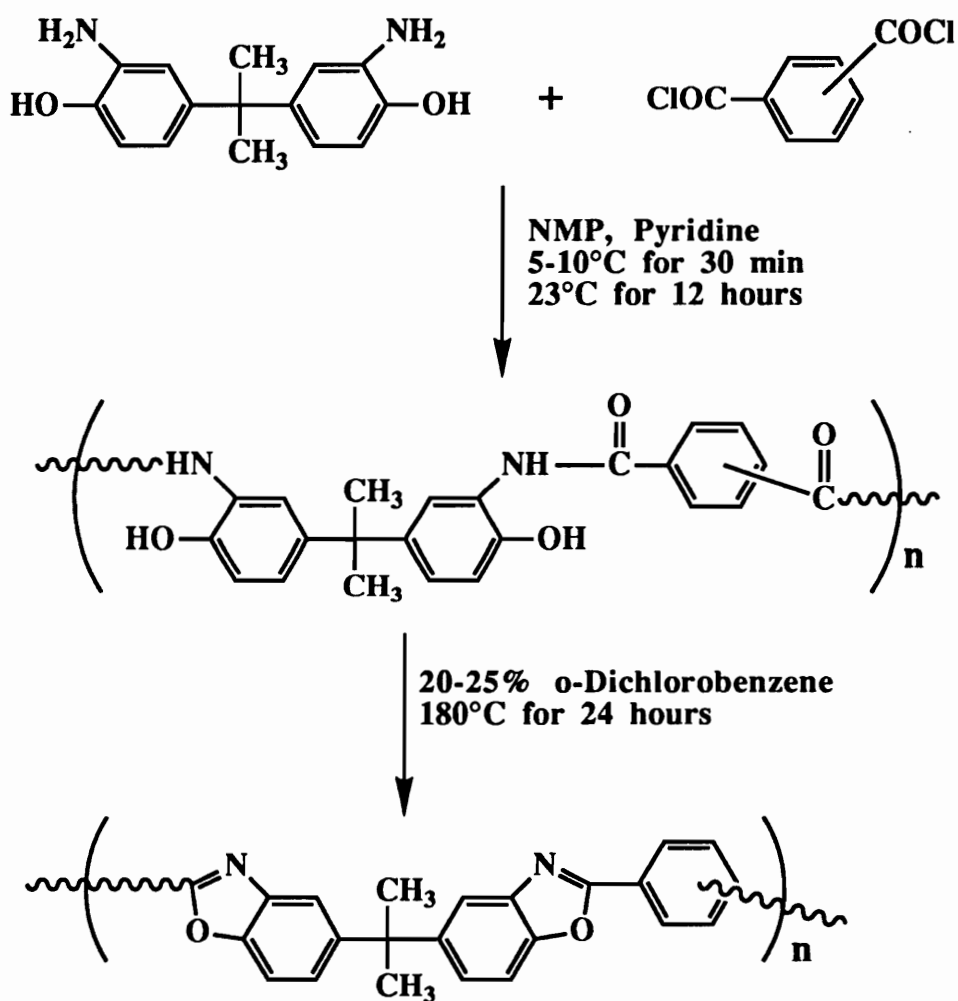


Figure 4.40. Low temperature polymerization of bAAP based poly(hydroxy amide)s and polybenzoxazoles.

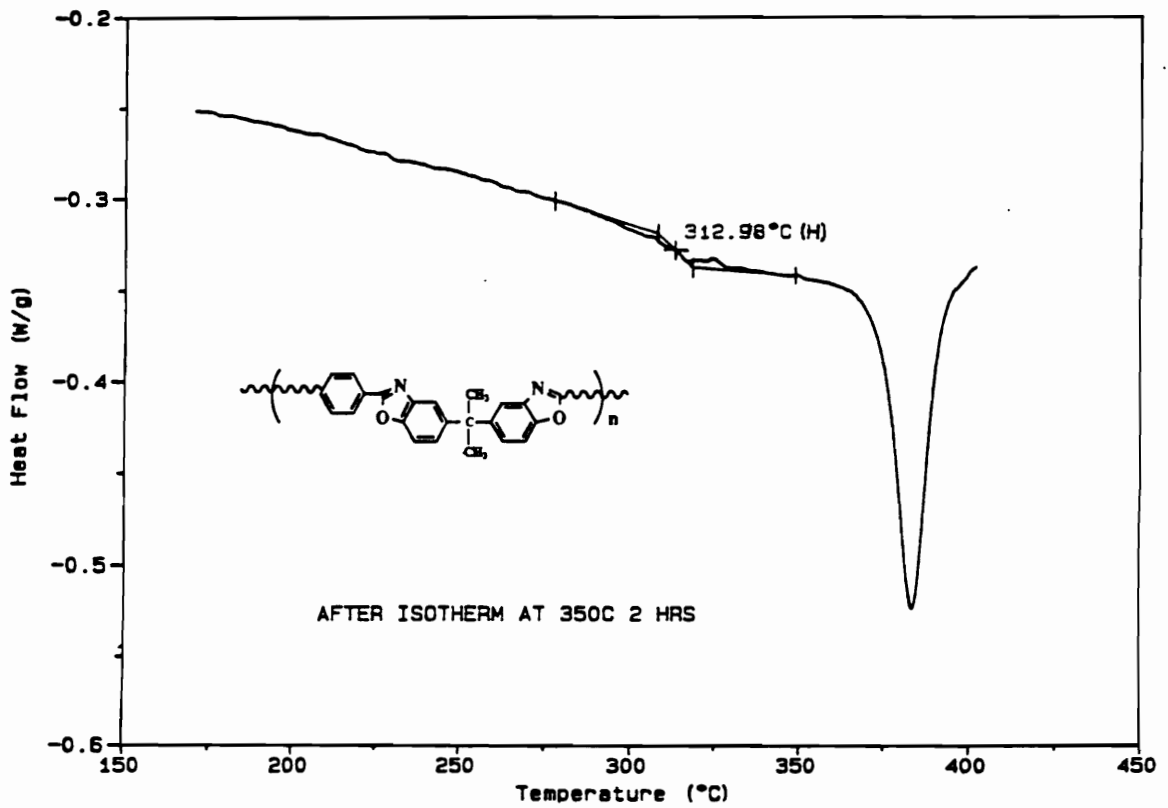


Figure 4.41. Differential scanning calorimetry thermogram of bAAP-TC polybenzoxazole (10°C/min in N₂).

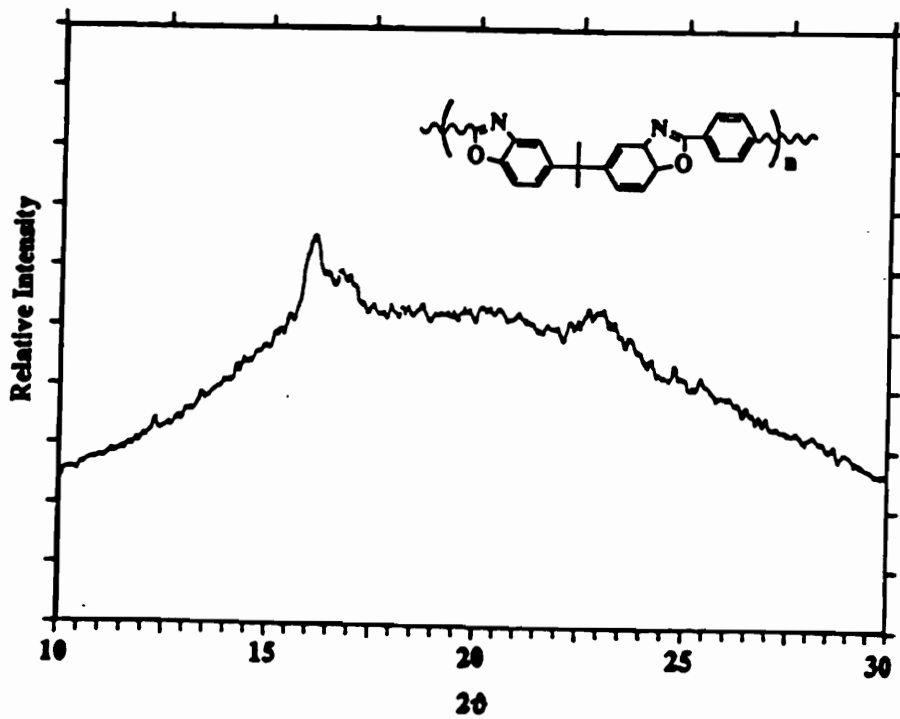


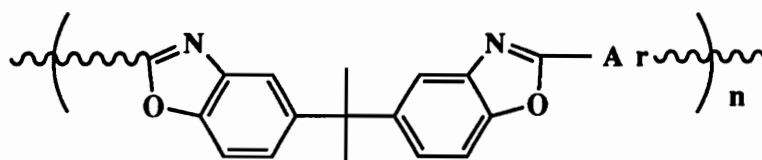
Figure 4.42. Wide angle X-ray scattering pattern of bAAP-TC polybenzoxazole (Courtesy of Prof. Herve Marand).

premature precipitation due to crystallinity.

Verification of complete cyclization was investigated by FT-IR, TGA and TGA-MS, as well as ^1H NMR and ^{13}C NMR spectroscopy. Infrared spectroscopy of the polybenzoxazoles showed complete disappearance of the amide and hydroxy stretches ($3000\text{-}3300\text{ cm}^{-1}$) and the carbonyl stretch (1650cm^{-1}) (upper spectrum, Figure 4.43), along with the appearance of a characteristic oxazole stretch and vibration at 1620 cm^{-1} and 1060cm^{-1} (lower spectrum, Figure 4.43). The poly(hydroxy amide) shows a distinct two-step degradation profile for the poly(hydroxy amide), where the weight loss at $\sim 350^\circ\text{C}$ is the expulsion of water due to cyclization and the weight loss around 480°C is thermo-oxidative degradation of the polymer backbone. The polybenzoxazole spectrum on the other hand displays no water loss at 350°C , indicating complete cyclization. The major weight loss at 480°C is backbone degradation as in the poly(hydroxy amide) case.

TGA-MS generates similar data, but has the added benefit of being able to identify weight losses. Investigation of ring closure by TGA-MS. showed no detectable water loss for the polymers until backbone decomposition was initiated around 480°C (Figure 4.45). Decarboxylation was noticed around 380°C and is attributed to the loss of acid end groups. Attempts were also made to ascertain percent cyclization via solid state ^{13}C NMR and ^1H NMR spectroscopy, but due to the broad character of the ^{13}C resonances and the insolubility of the polybenzoxazoles in deuterated solvents, inconclusive results were obtained.

Table 4.10. Aromatic composition and solution properties of isomeric bAAP poly(hydroxy amide)s and polybenzoxazoles.



Aromatic Composition		$[\eta]^a$	$[\eta]^b$
TC	IC	(dl/g)	(dl/g)
100	0	0.67	---
80	20	0.63	1.16
60	40	0.61	0.81
50	50	0.49 ^c	0.73
40	60	0.67	0.72
20	80	0.71	0.73
0	100	0.34 ^d	0.57

^a $[\eta]^{25^\circ\text{C}}$ of PHA measured in NMP

^cM.W. controlled to 20K

^b $[\eta]^{25^\circ\text{C}}$ of PBO measured in *m*-cresol

^dPrecipitated PHA at 150°C

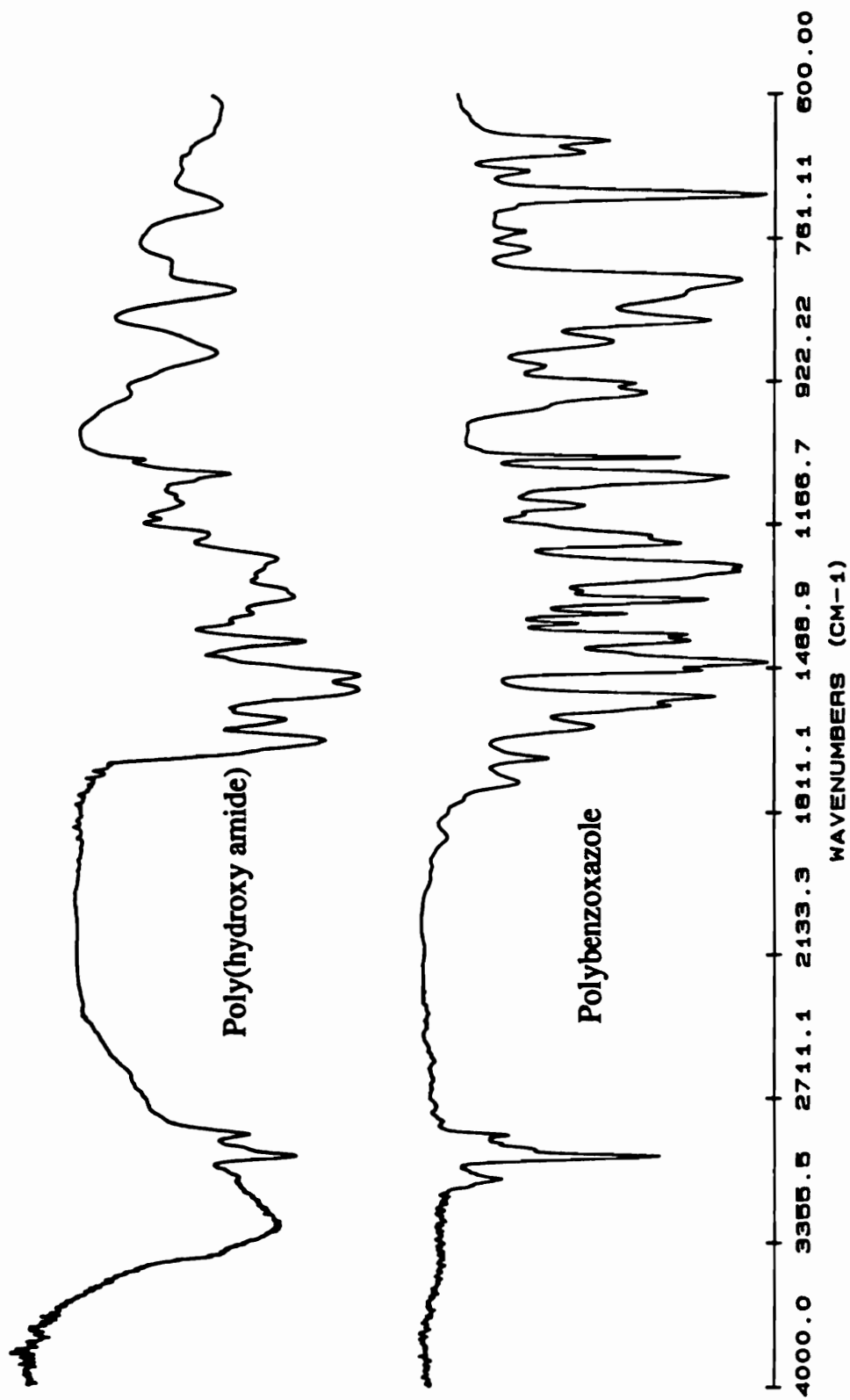


Figure 4.43. FT-IR spectra of bAAP poly(hydroxy amide) (upper) and polybenzoxazole (lower).

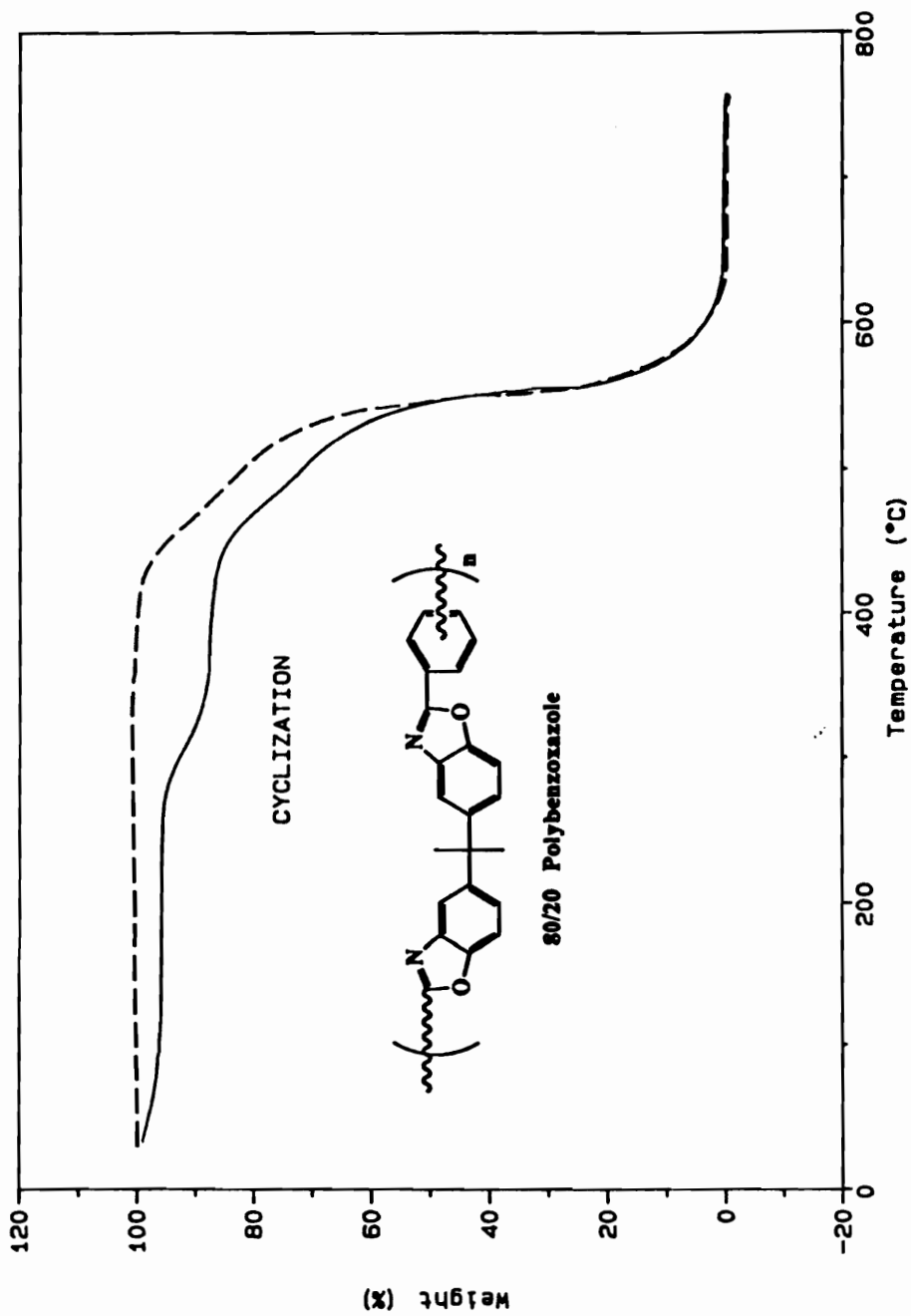


Figure 4.44. TGA thermogram (10°C/min in air) of bAAP poly(hydroxy amide) (—) and polybenzoxazole (---).

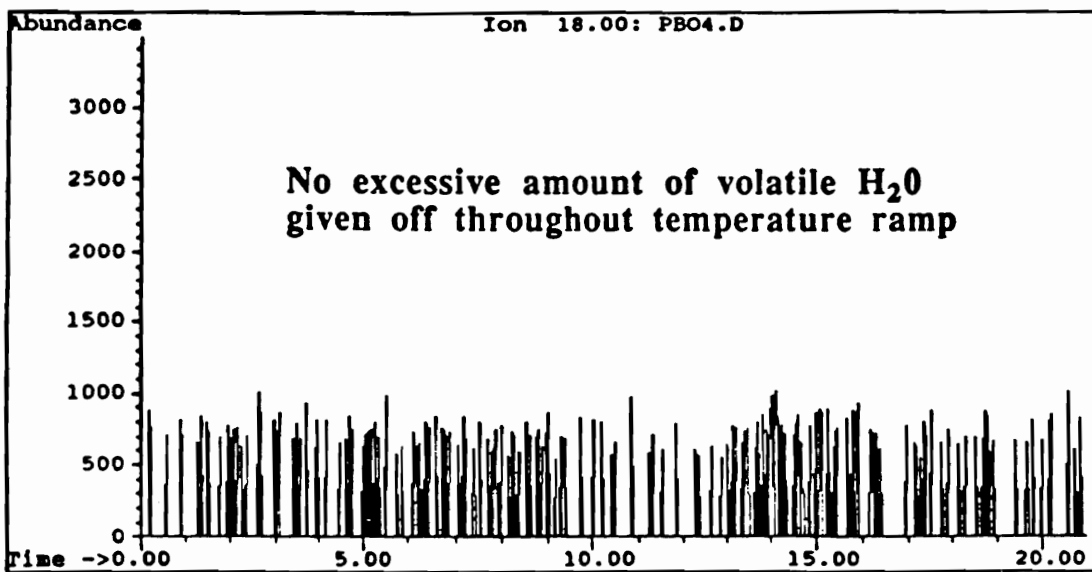
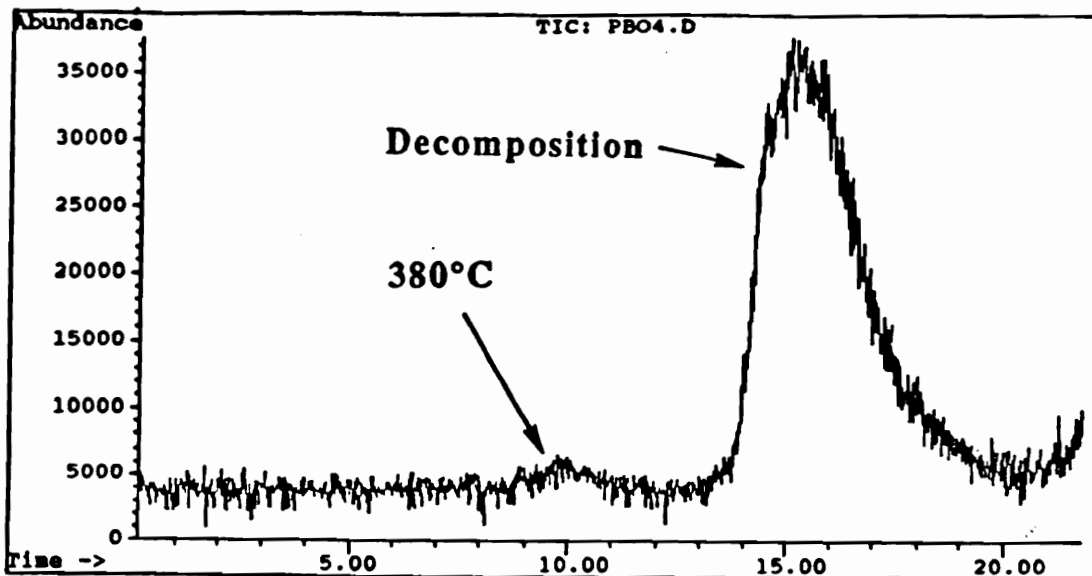
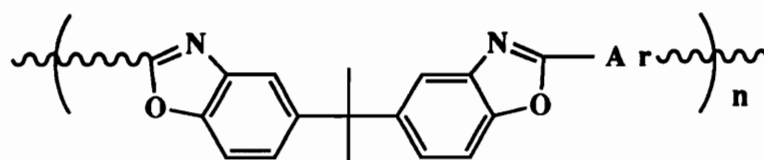


Figure 4.45. Total ion (upper) and selective ion count (lower) TGA-MS spectra of bAAP polybenzoxazole (40°C/min in He).

Solution and thermal properties of the poly(hydroxy amide)s and polybenzoxazoles were monitored by intrinsic viscosity measurements and differential scanning calorimetry (DSC). Results of these experiments (Table 4.10 and 4.11) indicate positional isomers have a much larger effect on the PBO solution properties than on PHA solution properties. Intrinsic viscosities of PHA's remained relatively constant with incorporation of isophthaloyl linkages, while PBO's showed a marked decrease in $[\eta]$'s in going from 100% *para*-linked systems to 60/40 *para/meta* linked systems. Assuming constant molecular weight, these decreases in $[\eta]$'s would be expected due to the removal of conformational constraints in going from a 100% *para*-linked system to the less linear isomeric systems. One would also expect a steady decrease in glass transition temperatures as the number of *meta* linkages is increased. As Table 4.11 indicates, this trend is also observed. Thermal stabilities, as measured by dynamic TGA in air, were as expected and resulted in 5% weight losses around 490°C. No obvious trends in thermal stability were observed relative to positional isomer content (Table 4.11).

Alteration of crystallinity and solubility was the major goal of this work and as noted in Table 4.11, a complete loss of crystallinity was observed in going from 100% terephthaloyl chloride to an 80/20 (TC/IC) isomeric ratio. Crystallinity was only detected by DSC after annealing the samples ~50°C above their T_g 's for 2 hours. Optical microscopy (OM) on the other hand showed no

Table 4.11. Thermal and morphological properties of isomeric bAAP poly(hydroxy amide)s and polybenzoxazoles.



Ar Composition		T _g (°C)	5% Wt. Loss (°C)	Crystallinity by	
TC	IC			DSC ^a	OM ^b
100	0	313	492	Yes	No
80	20	307	489	No	No
60	40	296	489	No	No
50	50	287	477	No	No
40	60	283	493	No	No
20	80	278	498	No	No
0	100	267	486	No	No

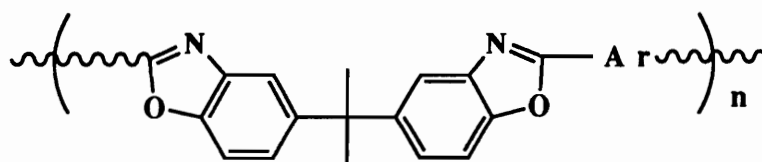
^aHeating rate of 10°C/minute in N₂

^bOM = Optical Microscopy

anomalies in any of the polymer systems investigated, even after annealing above their respective T_g 's for 2 hours.

Solubility of the resulting isomeric polybenzoxazoles was also changed relative to the 100% TC system (Table 4.12). While highly *para*-linked systems displayed absolutely no solubility in any of the solvents tested, the highly *meta*-linked systems showed various degrees of solubility in hot N-methylpyrrolidinone (NMP), *o*-dichlorobenzene (DCB) and even chloroform. This increase in solubility can be attributed to the above mentioned increase in the number of positional conformations available to the copolymers with an increase in *meta* links along the polymer backbone. It must be pointed out however that solubility (3-5% solids) was only achieved in boiling solvents and precipitation occurred immediately upon cooling, except in the case of *m*-cresol. All solution cyclized PBO systems were soluble in warm *m*-cresol, while the thermally cyclized bAAP-TC PBO was insoluble in hot *m*-cresol. It is interesting to note that all solution cyclized copolymers remained soluble in a 80/20 (NMP/DCB) reaction mixture (15% solids), but once precipitated and dried, their solubility was greatly reduced. The ability of the solvent mixture to solubilize the polybenzoxazoles during cyclization is attributed to the acidic nature of the reaction media. It is hypothesized that the HCl liberated during the degradation of pyridine hydrochloride protonates some of the oxazole rings and enhances solubility. Upon precipitation and isolation, the protonated species are eliminated

Table 4.12. Solubility of isomeric bAAP polybenzoxazoles in various solvents (3-5% solids)



Ar Composition		Solvents ^a					
TC	IC	DMAc	DCB	NMP	THF	<i>m</i> -cresol ^b	CHCl ₃
100	0	I	I	I	I	S	I
80	20	I	I	I	I	S	I
60	40	I	SS	I	I	S	I
40	60	I	SC ^c	SC ^c	I	S	SS
20	80	I	SS	SC ^c	I	S	SS
0	100	I	SS	SC ^c	I	S	I

^aRefluxing solvents

^bSoluble at room temperature

S-Soluble, I-Insoluble, SS-Slightly Soluble

c-clouds upon cooling

and therefore polymer solubilities decrease.

The previous data confirm that the synthesis of bAAP based polybenzoxazoles via an acid catalyzed solution cyclization method is a viable synthetic strategy and little if any difficulty was encountered during the synthesis of poly(hydroxy amide)s with appreciable molecular weight. A semi-crystalline morphology was observed for the 100% para linked system, but incorporation of small amounts of isomeric linkages resulted in amorphous materials with slightly improved solubilities. Excellent solvent resistance was observed for all solvents tested, with the exception of *m*-cresol. High molecular weight poly(hydroxy amide)s were achieved, evident from the solution viscosities and retention of molecular weight during cyclization is believed to have occurred. The thermo-oxidative stability of these materials was in the range expected and glass transition temperatures increased with percent incorporation of terephthaloyl linkages. Unfortunately, poor solubility, unfavorable thermo-oxidative stability and the tendency to degrade during melt processing render the polymers unacceptable as candidates for high performance applications. Nevertheless, the methods used in the synthesis of bAAP based polybenzoxazoles demonstrate the viability of the synthetic approach and allow for extension to alternate systems.

4.9. Synthesis of Fluorinated Poly(hydroxy amide)s and Polybenzoxazoles

Based on the impressive results obtained in the bAAP systems, efforts were undertaken to extend the methodology to polybenzoxazole systems which have the potential to exhibit enhanced thermo-oxidative stability and improved processability. The two step polymerization process was investigated with a series of fluorinated and/or kinked monomers. Unfortunately, when the bAAP reaction conditions were applied to fluorinated systems, high molecular weights were not achieved. The problems discussed in Section 4.3 and hydrolysis of amide linkages during cyclization were encountered. Consequently a systematic study of the cyclization conditions was conducted by varying the catalyst type and concentration, solvent system and temperature in an effort to determine the optimum reaction conditions. The results of these studies have been addressed previously in Section 4.4. Using the optimal conditions, a series of fluorinated polybenzoxazoles based on 2,2-bis(3-amino-4-hydroxyphenyl)-1,1,1-3,3,3-hexafluoropropane (6FAP) and 2,2-bis(3-amino-4-hydroxyphenyl)-2-phenyl-1,1,1-trifluoroethane (3FAP) and various fluorinated and nonfluorinated aromatic acid chlorides were synthesized and characterized. The molecular structures and acronyms of the bis(*o*-aminophenyl)s and diacid chlorides are depicted in Figure 4.47.

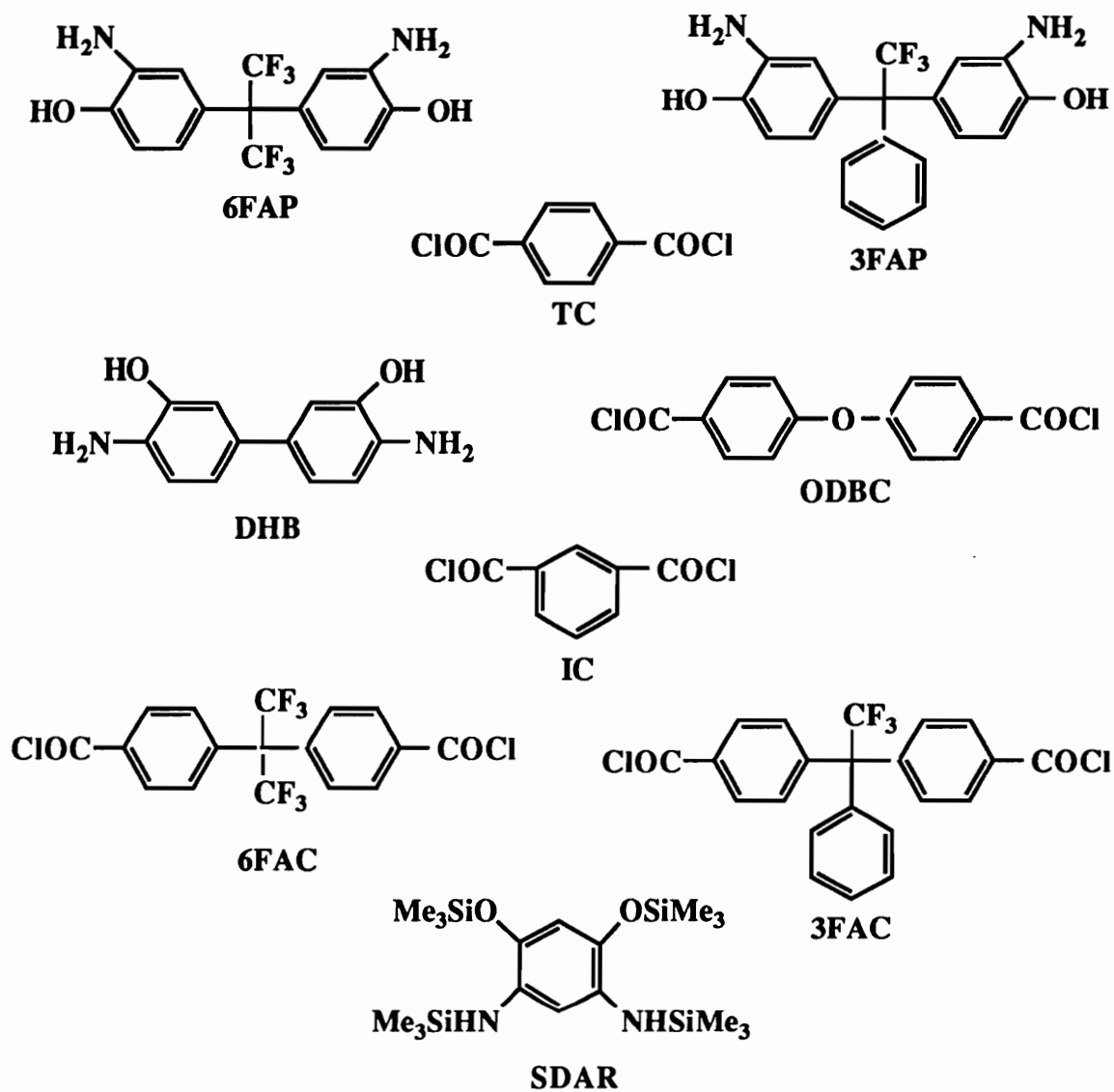
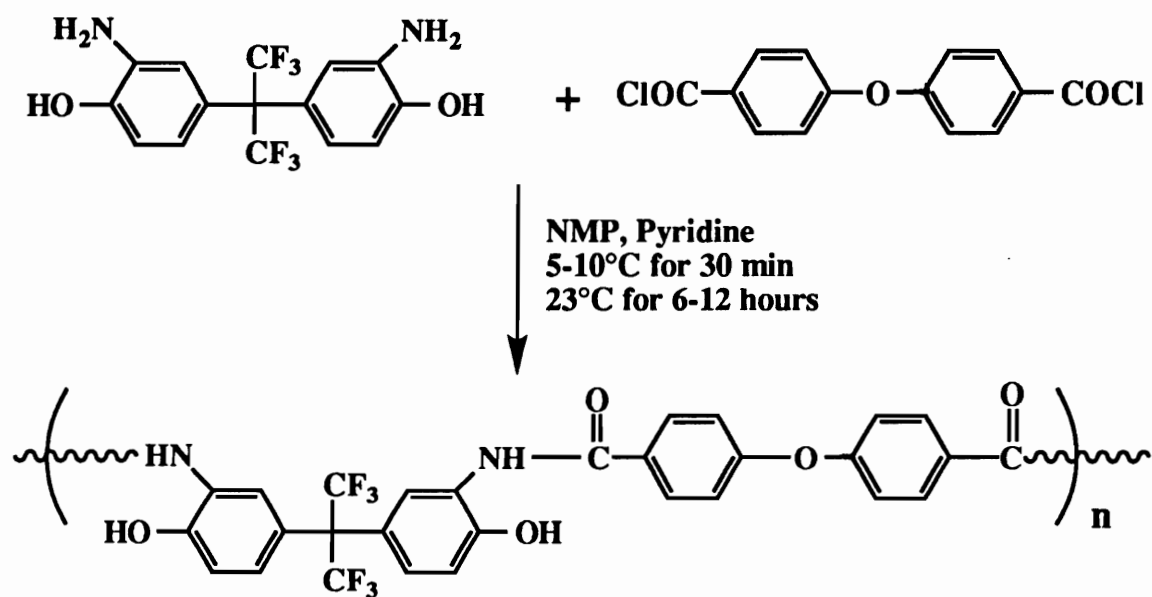


Figure 4.46. Acronyms and structures of various bis(*o*-amino-phenols) and acid chlorides

The poly(hydroxy amide)s were formed via the same low temperature base catalyzed reaction (Figure 4.47) discussed earlier. Consequently, some of the drawbacks associated with this synthetic procedure manifested themselves in these systems, namely competitive esterification. For purposes of comparison, the polymers have been divided into 3 different groups based on the bis(*o*-aminophenol) identity. Therefore, the polymers will be discussed as the 6FAP series, the 3FAP series and the 2,2'-dihydroxybenzidine (DHB) series. In some instances, the diaminoresorcinol polymer will be included in the DHB series. ¹H NMR spectroscopy (Figure 4.48-4.50) clearly identifies the polymers as poly(hydroxy amide)s, evident by the hydroxyl proton signals at $\sim\delta=10.3-10.4$ and the amide proton signals at $\sim\delta=9.5-9.8$. Variation in the exact location of these signals is expected due to different electronic environments. The assignments associated with the aromatic peaks are indicated on each respective spectra. It's noteworthy to point out the fact that the ¹H NMR spectra display many similarities to previously mentioned ¹H NMR spectra (Section 4.6). The extraneous downfield doublets, splitting of the amide protons and residual monomer signals are all assumed to be attributable to esterification. It's also interesting to note that these aberrations tend to decrease with electron-donating acid chlorides and electron-donating aminophenols, similar to results previously discussed. Prior to conducting cyclization, the poly(hydroxy amide)s were isolated from the polymerization



Scheme 4.47. Low temperature polymerization of 6FAP-ODBC poly(hydroxy amide).

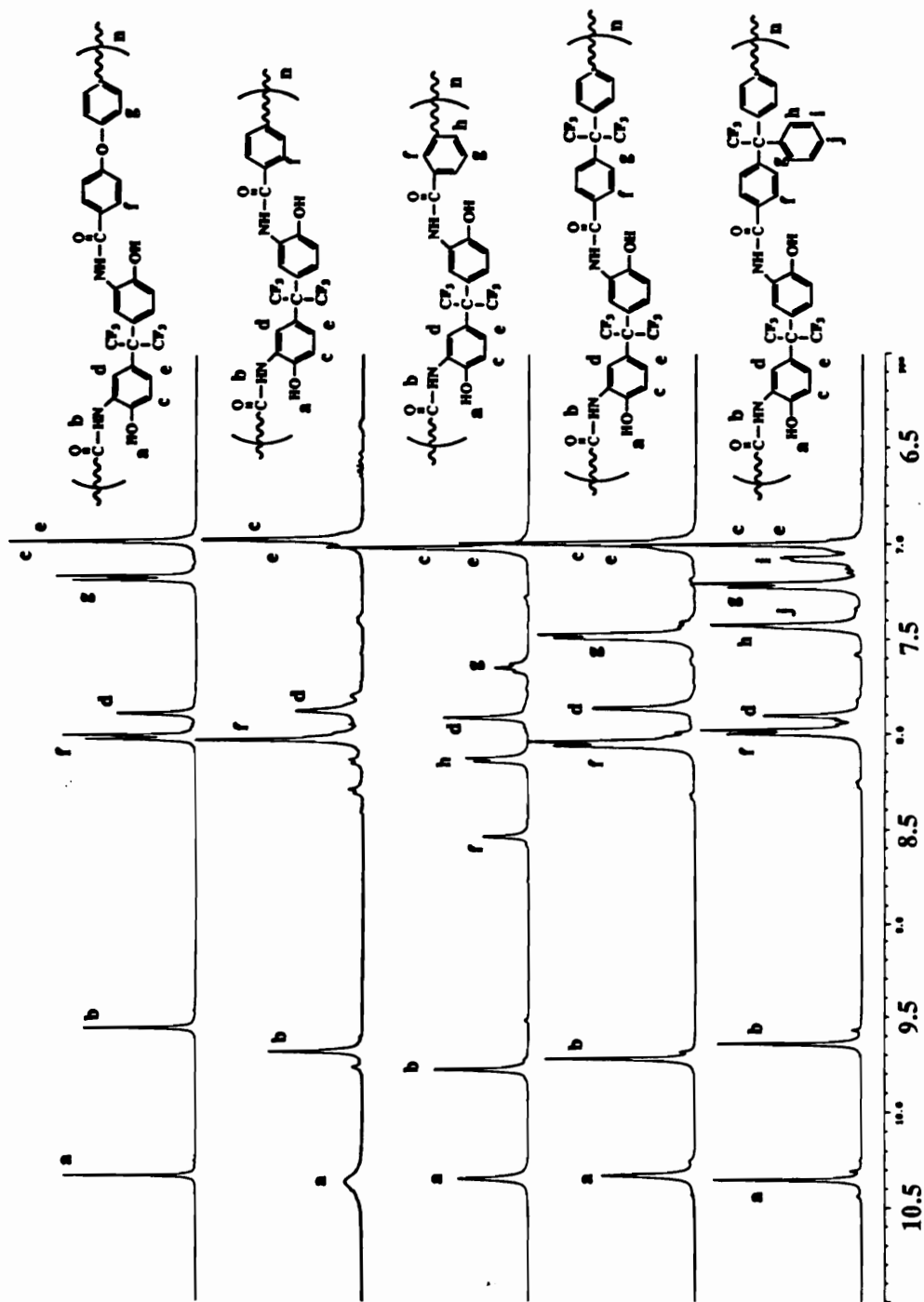


Figure 4.48. ^1H NMR spectra of 6FAP containing poly(hydroxy amide)s.

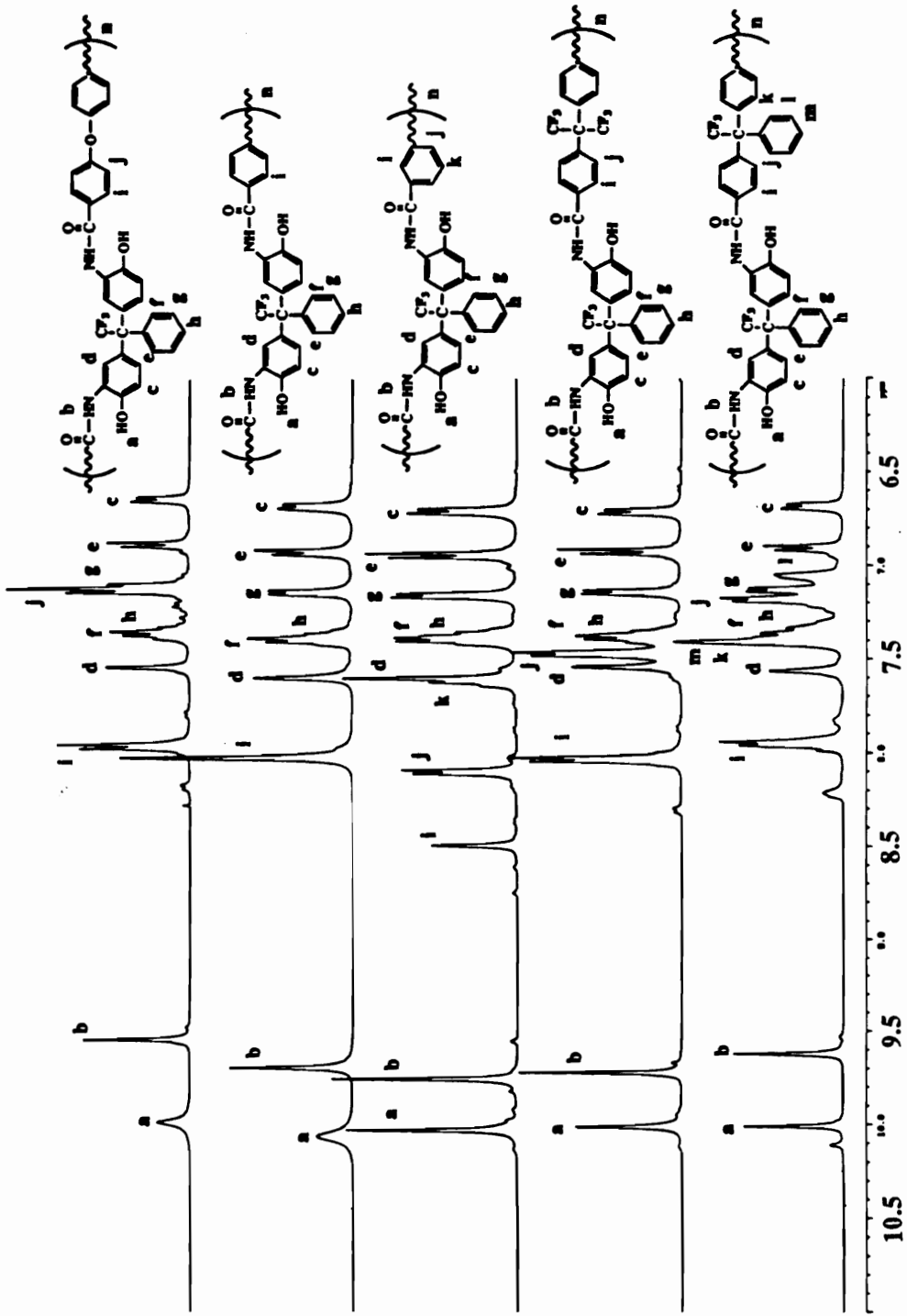


Figure 4.49. ^1H NMR spectra of 3FAP containing poly(hydroxy amide)s.

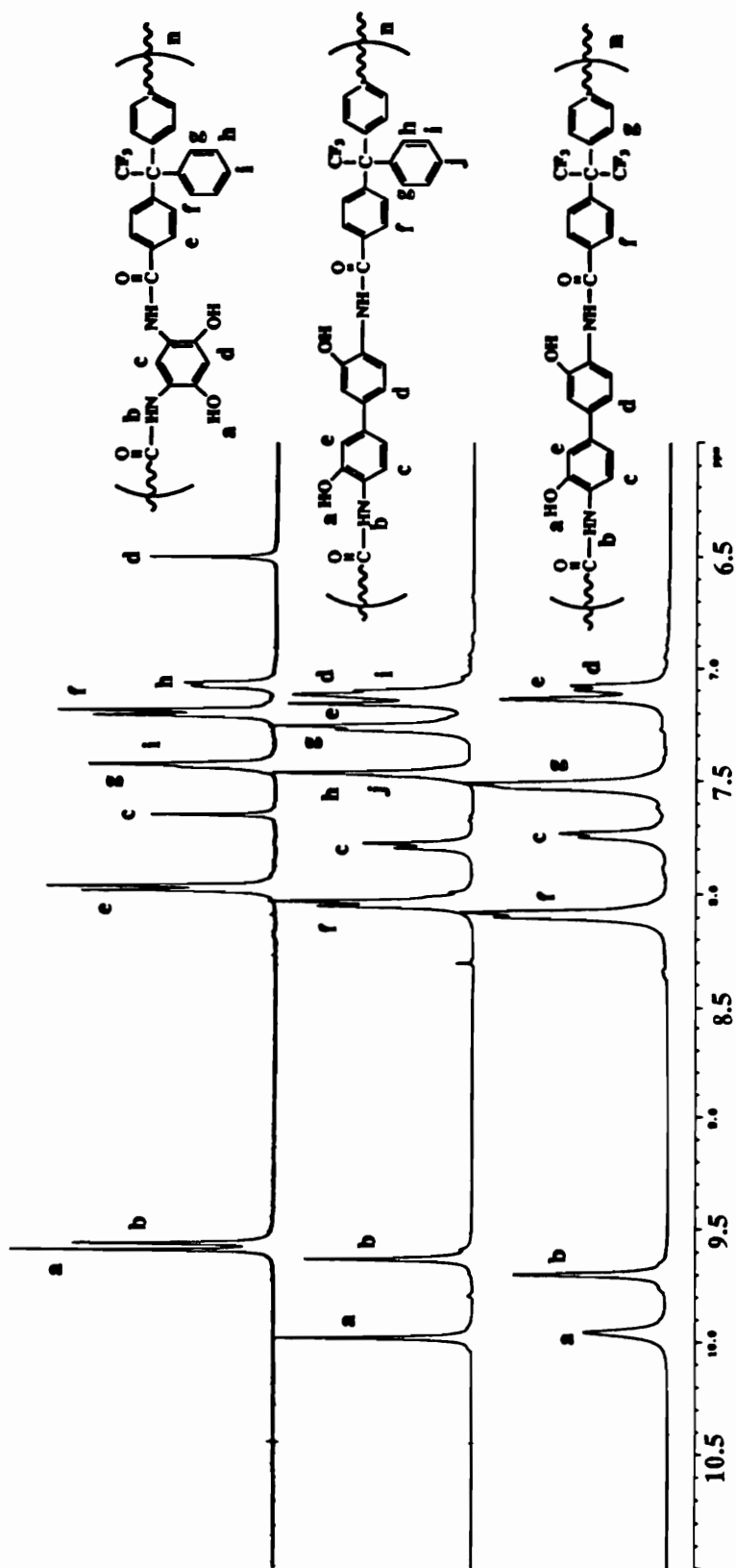


Figure 4.50. ^1H NMR spectra of DHB and DAR containing poly(hydroxy amide)s.

reaction mixture via precipitation, washed with copious amounts of water and dried under vacuum to insure efficient removal of residual pyridine hydrochloride and water.

The poly(hydroxy amide)s were cyclized by dissolving in CHP, adding 10% mole percent *p*-toluenesulfonic acid monohydrate and heating at 190-200°C for 4 hours (Figure 3.51). In nearly all cases the PBO's remained in solution throughout the cyclization reaction. Exceptions to this trend were found in PBO's containing the terephthaloyl and isophthaloyl linkages. But even in these cases, only slight clouding of the reaction mixtures were observed and not complete precipitation. Unlike cyclization conditions reported earlier, the CHP reaction mixture displayed an enhanced solution viscosity during cyclization and in some cases required dilution. Since intrinsic viscosities (Table 4.13) suggest only a negligible increase in molecular weight, the exact nature of this viscosity increase is unclear, but it is quite probably related to the solvent-polymer interaction parameter.

Confirmation of ring closure was achieved with TGA, TGA-MS and infrared spectroscopy. A representative TGA thermogram is displayed in Figure 4.52. Note the absence of any type of weight loss at ~350°C (dehydration of residual uncyclized poly(hydroxy amide)). TGA-MS also confirmed this finding by identifying only the casting solvent as a volatile (Figure 4.53). The peaks at 28, 32 and 44 mass/charge ratios represent the atmospheric gases, nitrogen, oxygen and carbon dioxide. Infrared spectroscopy provides further

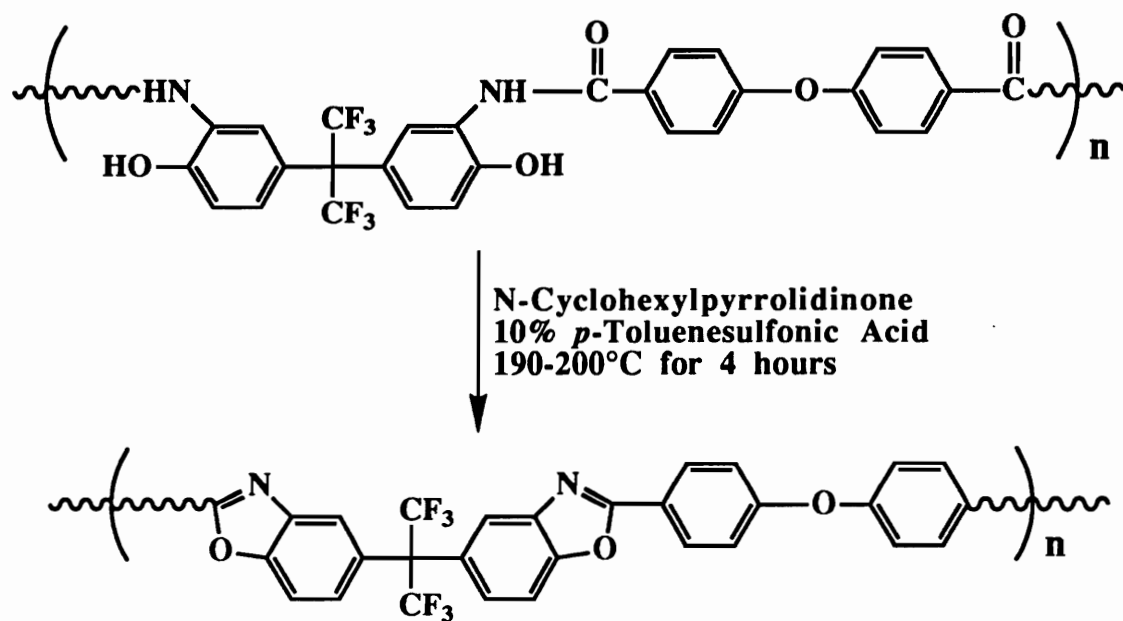


Figure 4.51. Solution cyclization of 6FAP-ODBC poly(hydroxy amide) to polybenzoxazole.

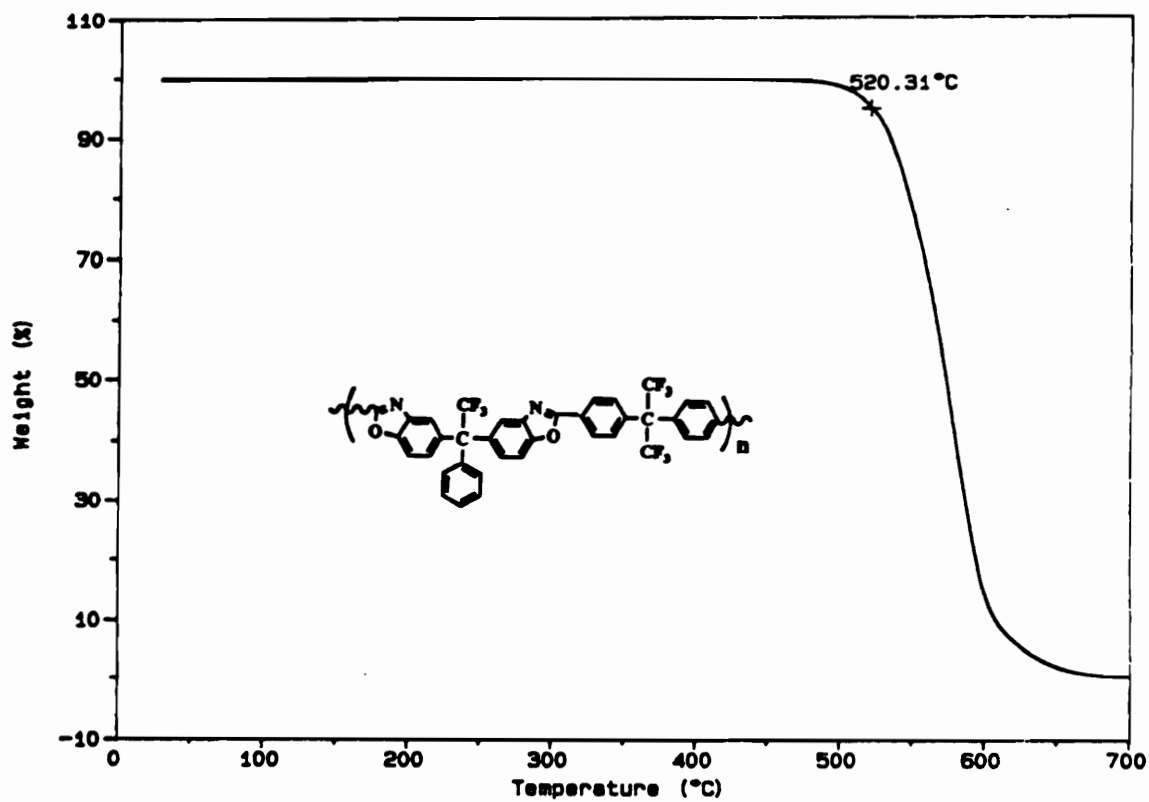


Figure 4.52. Dynamic thermogravimetric thermogram of 3FAP-6FAC polybenzoxazole (10°C/min in air).

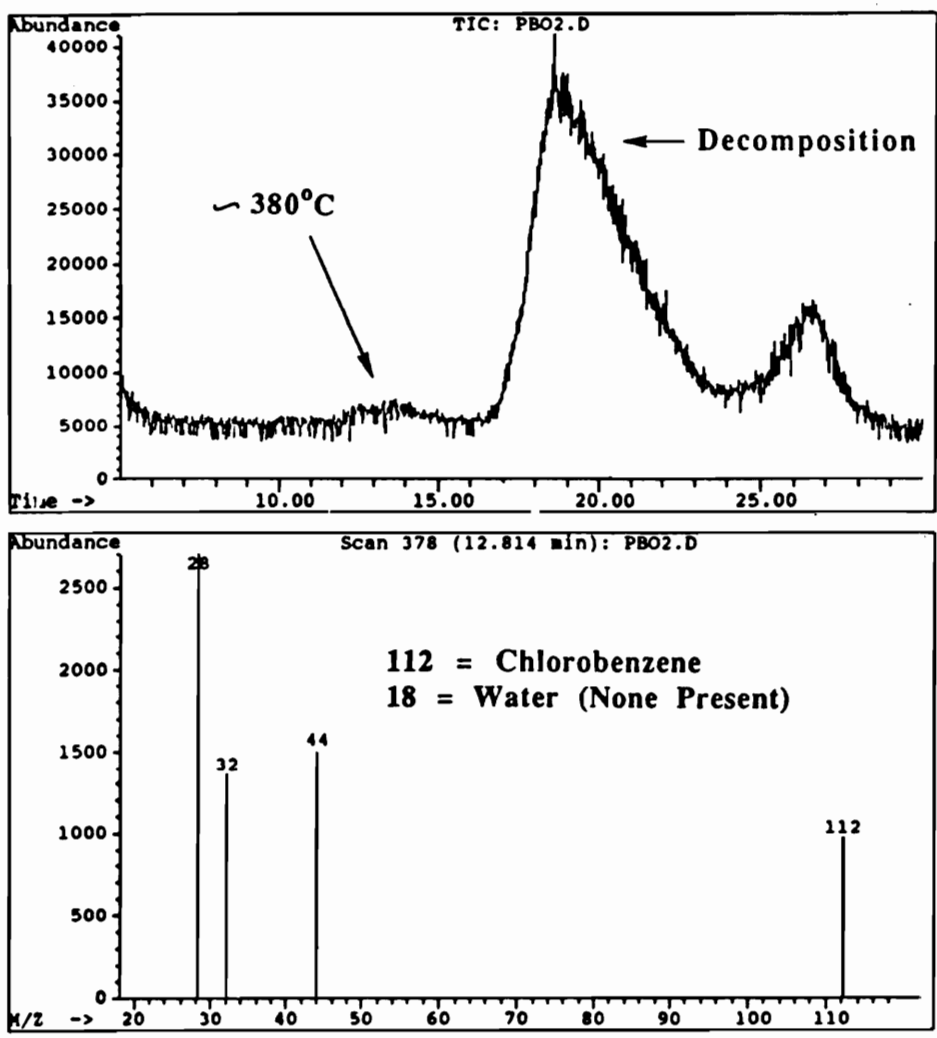


Figure 4.53. Total ion (upper) and selective ion count (lower) TGA-MS spectra of 3FAP-TC polybenzoxazole (40°C/min in He).

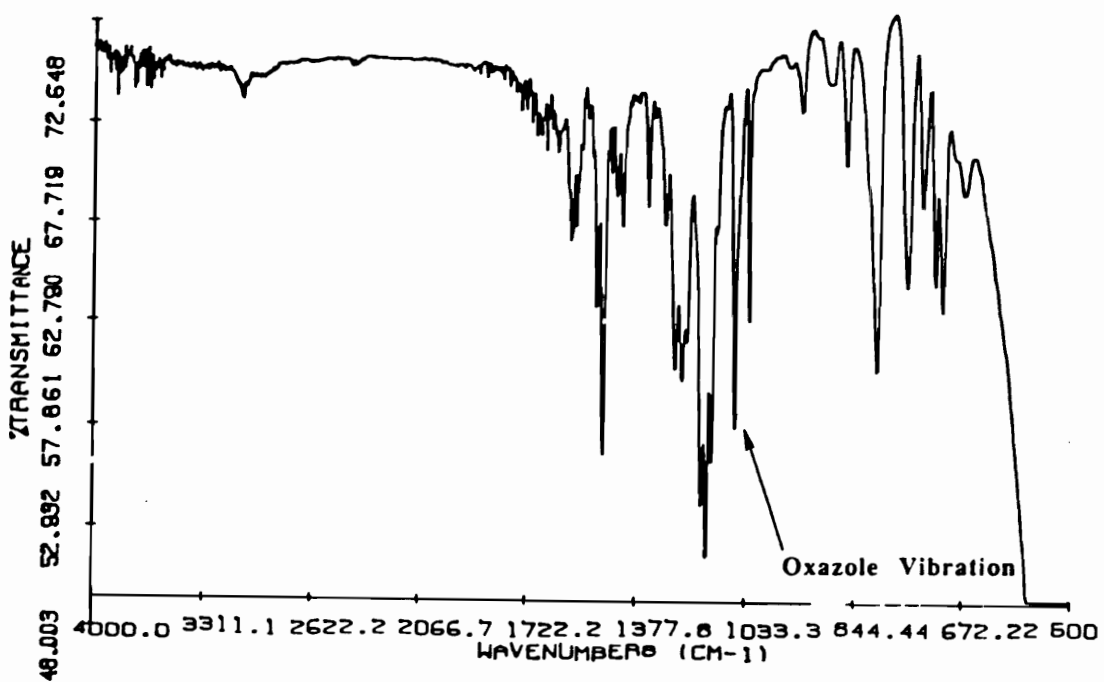
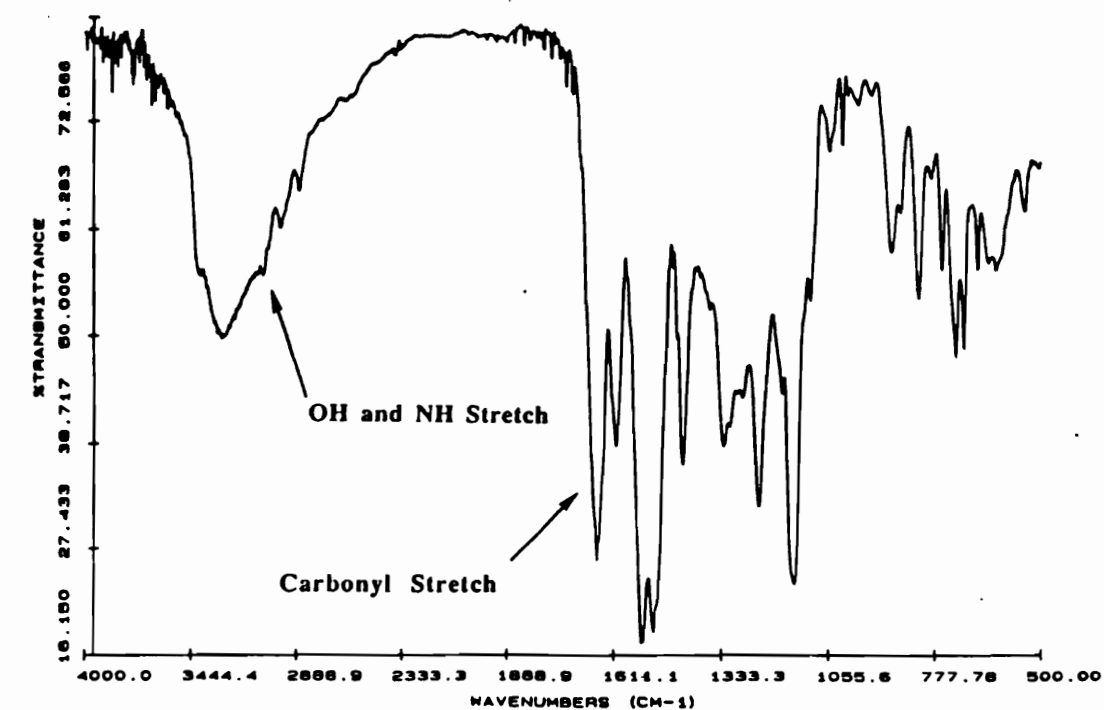


Figure 4.54. Fourier transformed infrared spectra of 3FAP-TC poly(hydroxy amide) (upper) and polybenzoxazole (lower).

evidence of complete cyclization. Figure 4.54 displays the FT-IR spectra of a 3FAP-TC poly(hydroxy amide) and polybenzoxazole (top and bottom, respectively). Disappearance of the hydroxyl and amide stretches at $\sim 3000\text{-}3400\text{ cm}^{-1}$ and the carbonyl stretch at $\sim 1650\text{ cm}^{-1}$, along with the appearance of an oxazole stretch ($\sim 1620\text{ cm}^{-1}$) and vibration ($\sim 1060\text{ cm}^{-1}$) indicates complete cyclization. FT-IR stack plots (Figures 4.55-4.57) of each series of polybenzoxazoles indicate similar spectroscopic characteristics. In some cases residual amide solvent is exhibiting the amide stretches.

Thermal transitions (Table 4.13) clearly demonstrate the influence of various connecting groups. Polybenzoxazoles possessing flexible linking groups exhibit T_g 's around 280°C and rigid linkages raise T_g 's to around 370°C . Perhaps the most interesting effect on glass transition temperatures is the similarity of a trifluoro- (3F) linking group and a hexafluoro- (6F) linkage. In most cases T_g 's are only slightly influenced by altering these linkages, for example, 6FAP-TC and 3FAP-TC, 6FAP-IC and 3FAP-IC and DHB-6FAC and DHB-3FAC have nearly the same T_g 's. On the other hand, the two polybenzoxazoles (6FAP-3FAC, 3FAP-3FAC) have T_g 's some 20°C apart. The reason why substitution changes should alter glass transition temperatures for one system and not another is unclear at this time. However, molecular weight is known to dramatically alter glass transition temperatures and this effect may be significant in some of these systems.

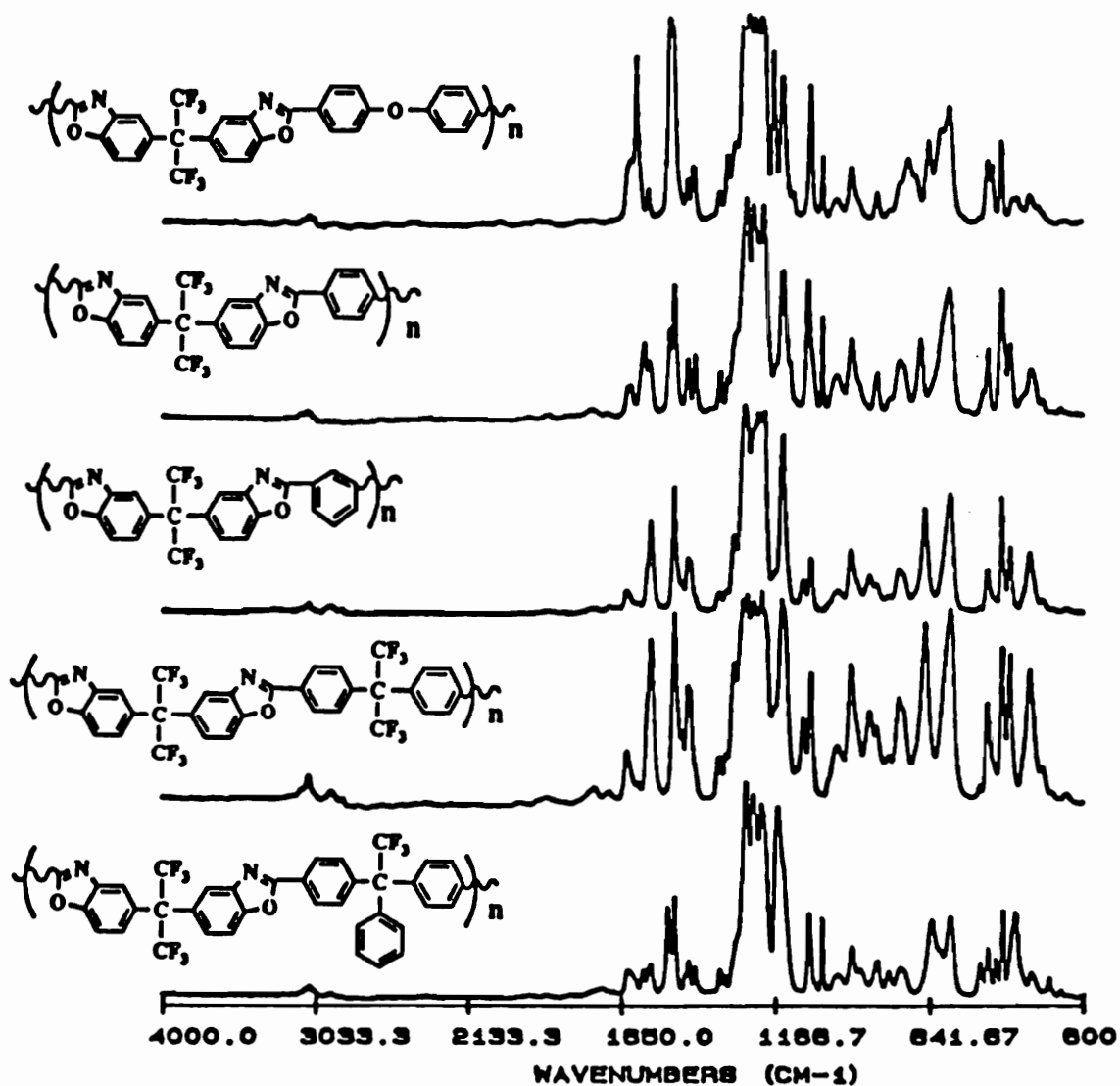


Figure 4.55. Fourier transform infrared spectra of various 6FAP containing polybenzoxazoles.

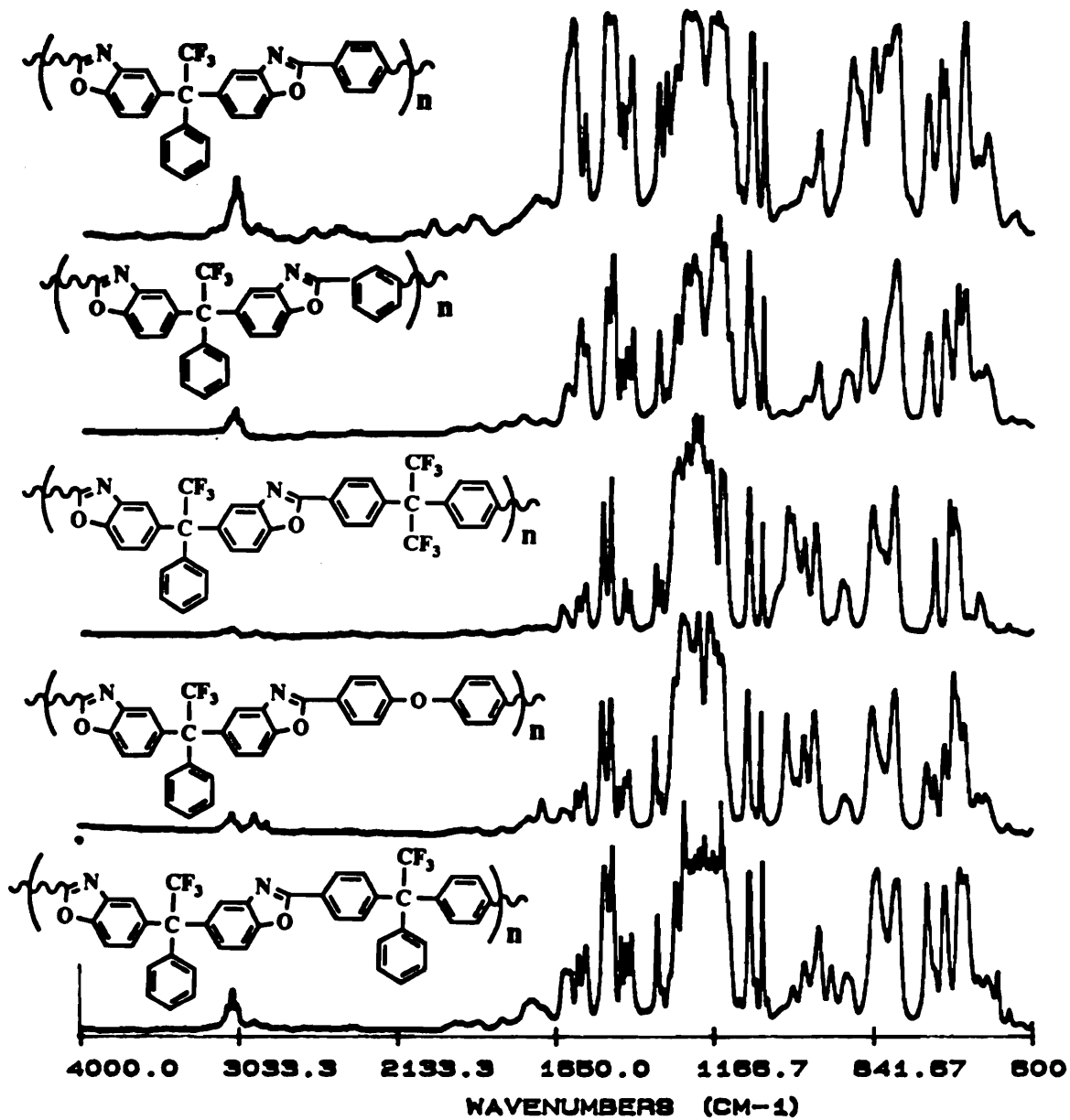


Figure 4.56. Fourier transform infrared spectra of various 3FAP containing polybenzoxazoles.

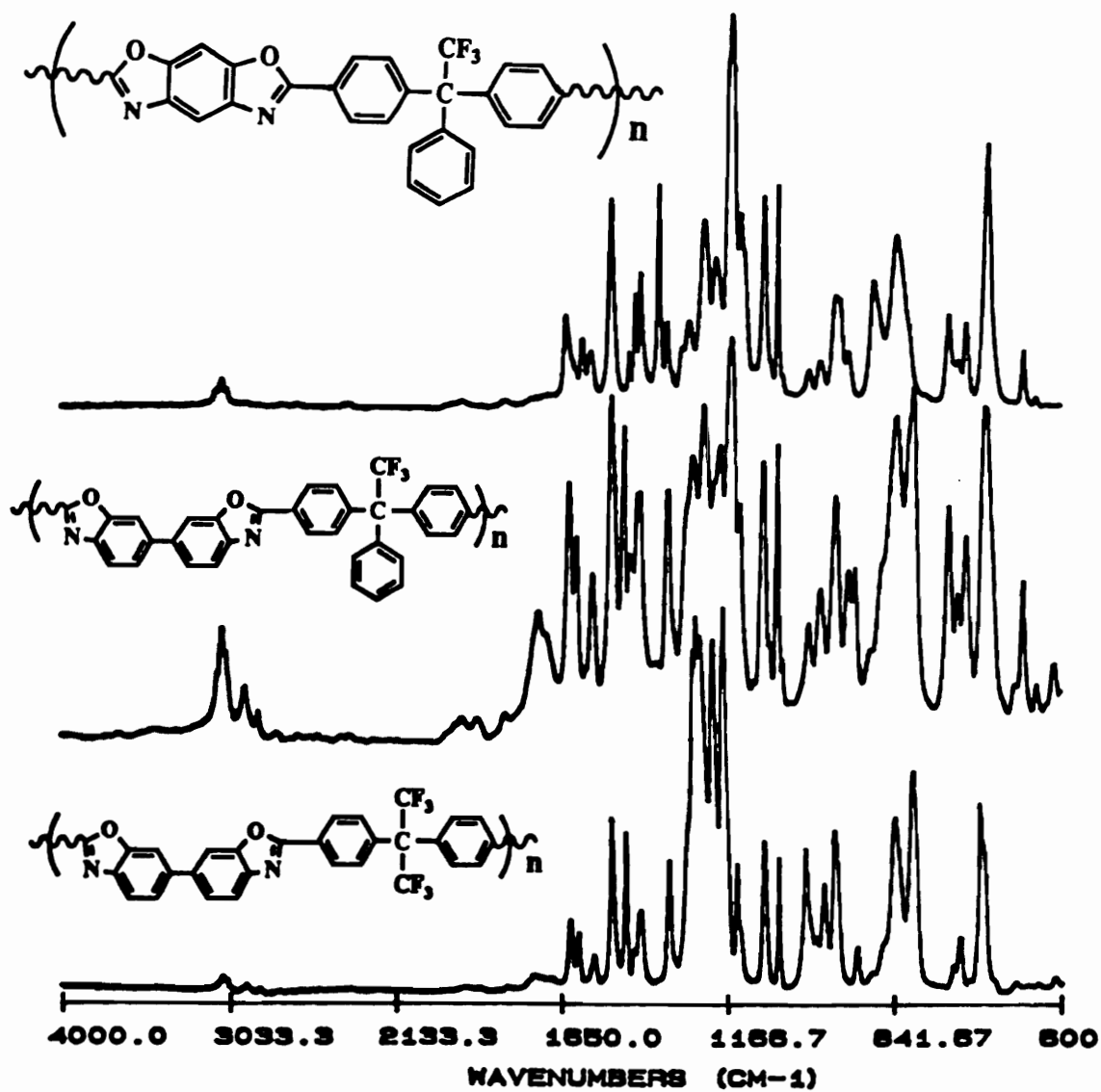


Figure 4.57. Fourier transform infrared spectra of various DHB and DAR containing polybenzoxazoles.

The effect of linking group on thermo-oxidative stability was measured using dynamic thermogravimetric analysis in an atmosphere of air and a heating rate of 10°C/minute. Five percent weight losses (Table 4.14) appear to be indifferent to backbone structure, with all values exceeding 500°C and onsets of weight loss starting just short of 500°C. Isothermal aging studies carried out on solvent cast films of 6FAP-TC and 3FAP-TC PBO indicated the 6F linkage to be more stable. Initially, the 3FAP-TC PBO was aged at 371°C under an atmosphere of air in a TGA cell and results of these tests indicated the material to be extremely stable (Figure 4.58, upper). However, isothermal aging of both 3FAP-TC and 6FAP-TC films in a large convection oven with an air flow of 5 psi, resulted in less impressive results. As can be seen from Figure 4.58 (lower), the 6FAP-TC PBO lost 16% of its mass over a 150 hour period, while the 3FAP-TC PBO lost 16% of its mass in less than 50 hours. One can conclude from this data that the hexafluoro- linkage is more thermo-oxidatively stable than the corresponding phenyltrifluoromethyl- linkage. Further work should be conducted to verify these conclusions.

For comparison, the solution properties exhibited by these materials are summarized in Table 4.14. The η_{inh} and $[\eta]$ data suggests that 6FAP polybenzoxazoles are of higher molecular weight relative to their 3FAP counterparts. This observation also carries through in the formation of higher quality 6FAP films. Monomer purity may have played a role in the inability to achieve high

Table 4.13. Solution and thermal properties of various fluorine containing polybenzoxazoles.

Polymer	[η]^a (dl/g)	T_g^b (°C)	5% Weight Loss^c (°C)
6FAP-ODBC	1.08	280	534
3F-ODBC	0.29	299	547
6FAP-3FAC	0.48	310	529
3FAP-3FAC	0.27	330	514
6FAP-IC	0.54*	296	512
3FAP-IC	0.26	301	524
6FAP-TC	0.45*	361	531
3FAP-TC	0.20	369	536
6FAP-6FAC	0.41*	336	531
3FAP-6FAC	0.26	334	520
DHB-6FAC	0.52	345	534
DHB-3FAC	0.45	350	509

^aMeasure in NMP at 25°C, unless starred

^bMeasured in nitrogen, 10°/minute

^cMeasured in air, 10°C/minute

*Measured in m-cresol at 25°C

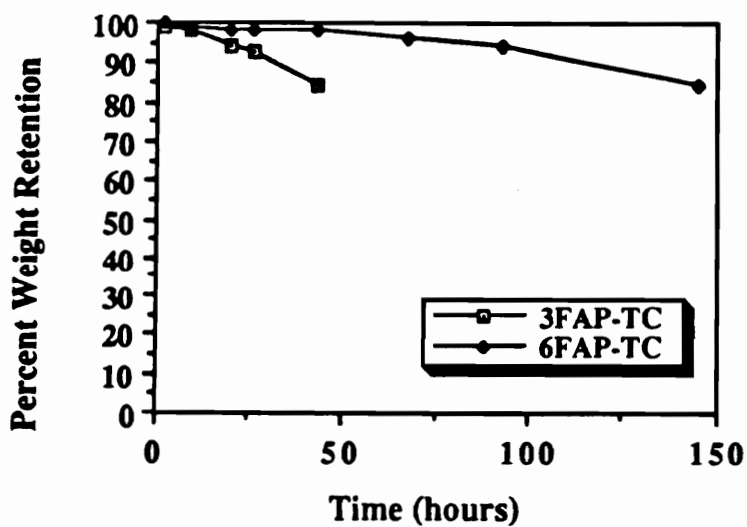
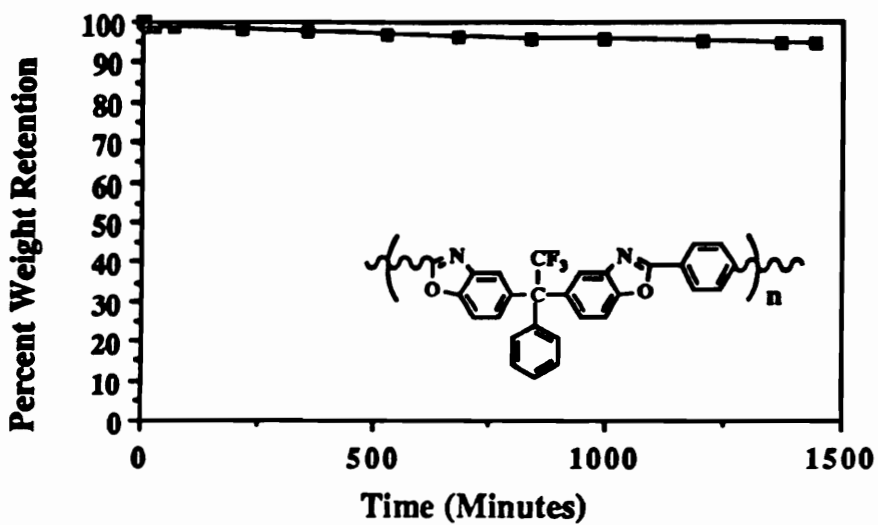


Figure 4.58. Isothermal weight retention data for 3FAP-TC polybenzoxazole aged in TGA head in air at 371°C (upper) and isothermal weight retention data for 3FAP-TC and 6FAP-TC polybenzoxazole aged in conventional oven at 371°C (air).

Table 4.14. Solution properties of various fluorine containing poly(hydroxy amide)s and polybenzoxazoles.

Polymer	PHA η_{inh}^a (dl/g)	PBO $[\eta]^b$ (dl/g)
6FAP-ODBC	0.92	1.08*
3F-ODBC	0.48	0.29
6FAP-3FAC	0.44	0.48
3FAP-3FAC	0.29	0.27
6FAP-IC	0.62	0.54*
3FAP-IC	0.31	0.26
6FAP-TC	0.65	0.45*
3FAP-TC	0.37	0.20*
6FAP-6FAC	0.56	0.41*
3FAP-6FAC	0.27	0.26
DHB-6FAC	0.61	0.52
DHB-3FAC	0.73	0.45

^aMeasured in NMP at 25°C (0.5 g/dl)

^bMeasured in NMP at 25°C unless starred

*Measured in *m*-cresol at 25°C

molecular weight polymers in the 3FAP series. With respect to maintaining molecular weight during cyclization, it appears that the observations made in the model cyclization reactions may not apply in general. The intrinsic viscosities of the PBO's were lower than the inherent viscosities of the precursor poly(hydroxy amide)s in nearly all cases. It is understood that inherent viscosity and intrinsic viscosity are not directly comparable, and that poly(hydroxy amide)s and polybenzoxazoles have different solvent-polymer interaction parameters. Nevertheless, the drop in viscosity suggests chain degradation could be occurring during the cyclization process. It is obvious that direct molecular weight measurements (GPC, light scattering or vapor phase osmometry) on the poly(hydroxy amide)s and polybenzoxazoles need to be conducted to validate or contradict the assumptions made herein.

Preliminary GPC results (Figure 4.59) on a select number of THF soluble PBO's display a bimodal distribution and very broad molecular weight distributions (~10-20). Number average molecular weights (absolute) ranged from 3000-6000 g/mole , while $\langle M_w \rangle$'s varied from 60,000-70,000 g/mole. This evidence suggests the formation of both high and low molecular weight species during the polymerization and may explain why films could be formed from such apparently low molecular weight materials (as indicated by intrinsic viscosities). Further studies need to be conducted to elucidate the mechanism responsible for the formation of low molecular weight species during the polymerization.

Solubility differences between the 3FAP and 6FAP polymers were noted and in general, the 3FAP polybenzoxazoles were more soluble than the 6FAP PBO's (Table 4.15). However, variation in molecular weight between the two series of polymers may also be influencing solubility. Polybenzoxazoles synthesized from nonfluorinated, rigid aminophenols (DHB) exhibited a much higher

Table 4.15. Solubility characteristics of various fluorinated polybenzoxazoles at room temperature (10% Solids (w/v)).

Polymer Composition	Solvent				
	CHCl ₃	THF	NMP	<i>o</i> -DCB	<i>m</i> -Cresol
6FAP-ODBC	S	S	S	S	S
3F-ODBC	SS	S	S	S	S
6FAP-3FAC	S	S	S	S	S
3FAP-3FAC	S	S	S	S	S
6FAP-IC	SS	I	I	SS	S
3FAP-IC	SS	I	SS	S	S
6FAP-TC	SS	I	I	I	S
3FAP-TC	SS	I	I	S	S
6FAP-6FAC	SS	I	S	I	S
3FAP-6FAC	S	S	S	S	S
DHB-6FAC	I	I	I	I	S
DHB-3FAC	SS	I	S	S	S

S - Soluble, I - Insoluble, SS - Slightly Soluble

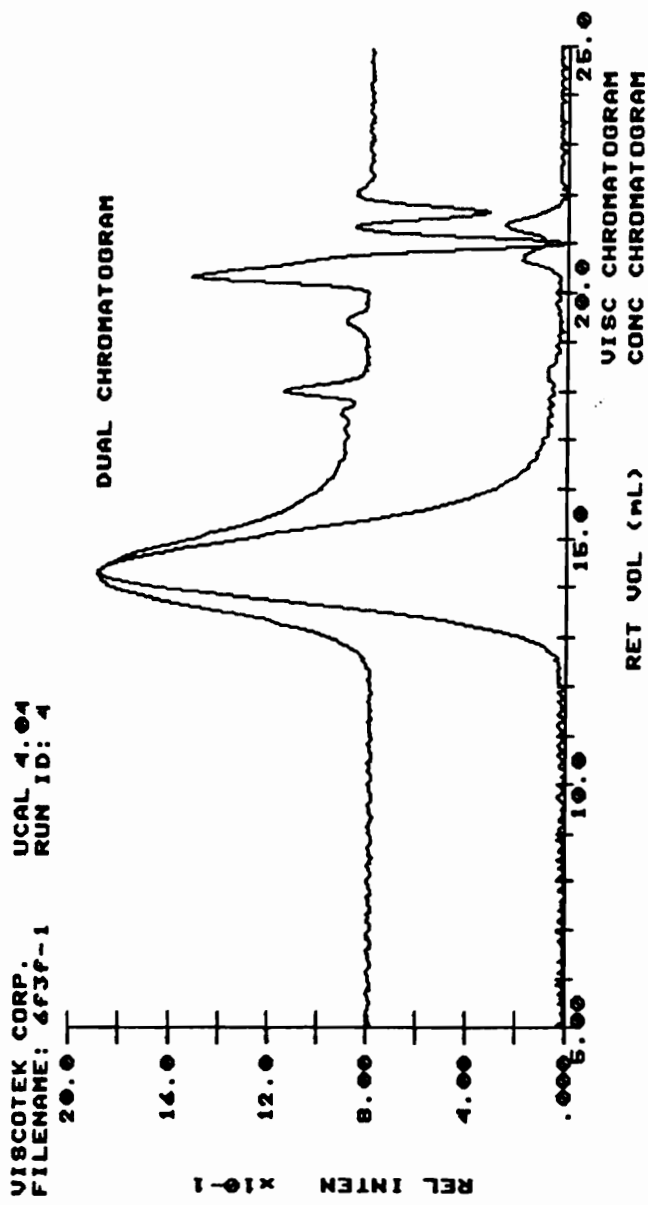


Figure 4.59. Absolute gel permeation chromatogram of 6FAP-3FAC polybenzoxazole (THF, $\langle M_n \rangle = 6470$ g/mol, $\langle M_w \rangle = 66,400$ g/mol).

level of solvent resistance and in general were only soluble in hot CHP and *m*-cresol. The poly(hydroxy amide)s on the other hand showed no real differences in their solubilities.

Preliminary stress-strain results (Table 4.16) from a limited number of polybenzoxazoles indicate mechanical properties are similar to polyimide type materials [1] and compare favorably with quoted literature values for similar polybenzoxazoles [7]. In general, tensile moduli ranged from 2.3 GPa to 4.2 GPa, tensile strengths ranged from 107 MPa to 158 MPa and percent elongation to break varied from 5-9%. While these data are limited, the general trend is incorporation of bulky groups into the polymer backbone results in elevated moduli, decreased tensile strength and reduced elongations to break.

Observations made during the synthesis and film casting procedures suggest the presence of order in some of the fluorinated systems. For example, clouding of the reaction mixtures during cyclization of the terephthaloyl and isophthaloyl based systems and preferential solubility in various solvents for certain polymer systems may point to some type of ordering. These observations may only be the inability of certain solvents to solvate the polybenzoxazoles, but evidence supporting crystallinity has been generated for some of these systems. Optical micrographs of the 6FAP-TC and 6FAP-IC polybenzoxazole films, cast from CHCl_3 and *o*-dichlorobenzene, respectively, indicate the presence of crystallinity in both systems. The spherulitic texture of the 6FAP-

TC PBO could only be obtained by casting films from chloroform. Attempts to anneal in crystallinity were unsuccessful. While

Table 4.16. Thin film tensile properties of various fluorinated polybenzoxazoles.^a

Polymer	[η]^b (dl/g)	Tensile Modulus (GPa)	Tensile Strength (MPa)	Percent Elong. to Break
6FAP-3FAC	0.48	4.2 (0.4)	149 (10)	7.(1)
6FAP-ODBC	1.08 ^c	2.3 (0.3)	116 (8)	9 (1)
3FAP-6FAC	0.26	3.2 (0.2)	107 (4)	5 (1)
3FAP-ODBC	0.29	3.0 (0.3)	114 (5)	8 (1)
DHB-3FAC	0.45	3.6 (0.1)	158 (2)	9 (1)

^aMeasurements made on thin films (1-5 mils) cast from CHCl₃ or *o*-dichlorobenzene and reported values are an average of at least 4 test specimens (strain rate = 0.5 in/min, 23°C.). Standard deviation in parentheses.

^bMeasured in NMP at 25°C

^cMeasured in *m*-cresol at 25°C

optical microscopy clearly identifies crystallinity, WAXS analysis indicates only low levels of crystallinity (~5%). No further attempts were made to analyze the 6FAP-IC polybenzoxazole. It should be pointed that hazing of polymer films and crystallization only occurs when the polymers are cast from chloroform or dichlorobenzene. While crystallinity is being observed in these particular systems, one should be careful to extend the notion of crystallinity over the entire molecular weight range. It is a well

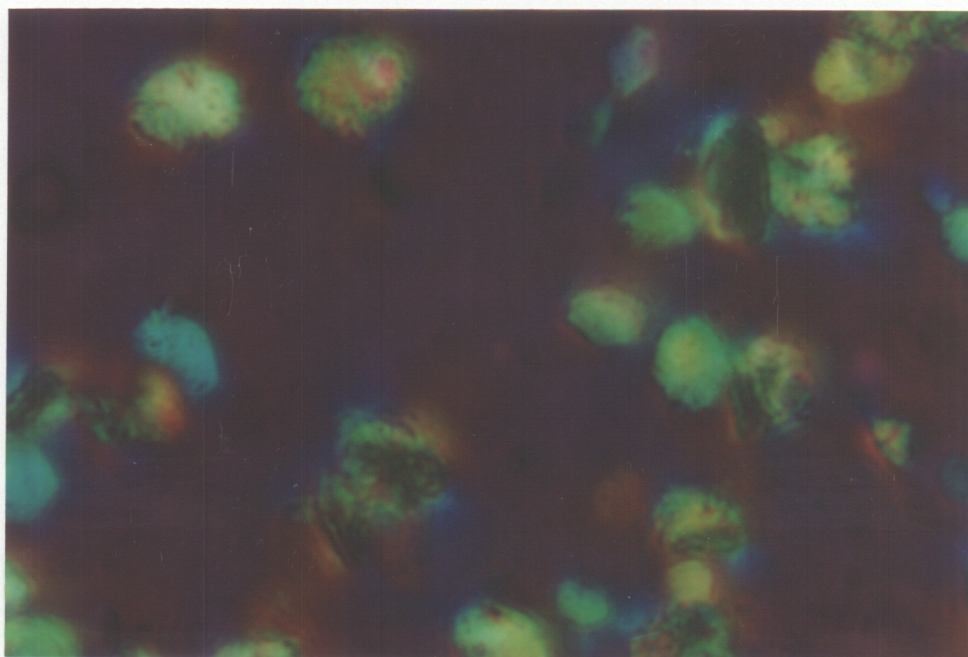
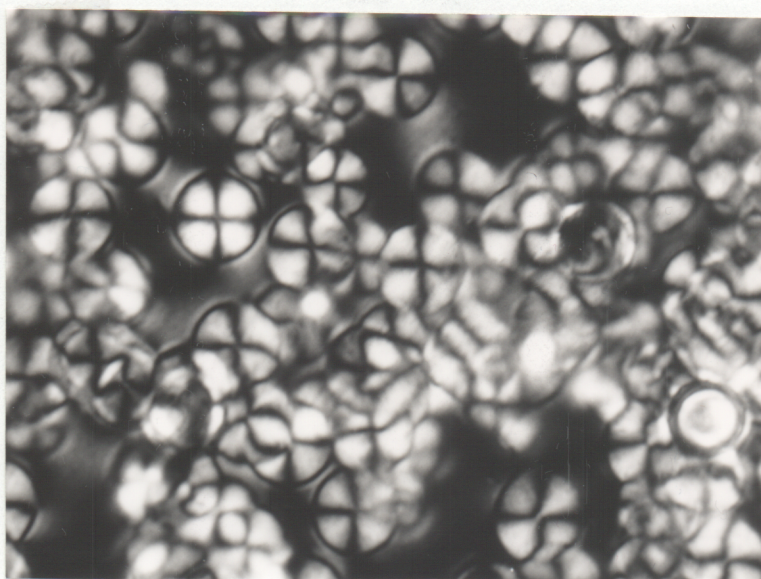


Figure 4.60. Optical micrographs of 6FAP-TC at 420°C (upper, 17 mm = 50 μ m) and 6FAP-IC at 23°C (lower, 53 mm = 50 μ m) polybenzoxazoles. Polymers were cast from chloroform and *o*-dichlorobenzene, respectively and observed with crossed polars.

known fact that lower molecular weight polymers have a greater propensity to order.

In summary, a number of novel fluorinated polymers have been generated using a "two-step" polymerization/cyclization technique. Based upon model studies carried out on 6FAP-ODBC PBO's, optimum cyclization conditions were achieved when 10% *p*-toluenesulfonic acid was used as the catalyst in CHP at 195°C for 4 hours. Unfortunately, the use of these cyclization conditions on a variety of fluorinated poly(hydroxy amide)s resulted in poor results. Nevertheless, numerous novel fluorine containing poly(hydroxy amide)s and polybenzoxazoles have been synthesized and characterized with respect to solution, thermal and mechanical properties. Spectroscopic evidence indicates the formation of PHA's and polybenzoxazoles as well as complete cyclization of the oxazole ring system. Glass transition temperatures ranged between 280 and 370°C. Polybenzoxazoles with analogous structure, except for the nature of the fluorinated linkage, exhibited similar T_g 's with few exceptions. Dynamic thermo-oxidative stability proved to be quite good, with the onset of weight loss typically around 480-490°C. In general polybenzoxazoles containing the 3F linkage displayed enhanced solubility relative to their 6F counterparts, mechanical properties were on par with similar thermoplastic polymers and some degree of crystallinity was observed in certain systems.

4.10. Polymers Based on 4,6-Diaminoresorcinol

Research was undertaken to incorporate as much aromaticity into a polymer backbone as possible, while simultaneously maintaining processibility in an effort to synthesize processible polybenzoxazoles which exhibit outstanding thermo-oxidative stability and very high glass transition temperatures. To accomplish this goal, 4,6-diaminoresorcinol (provided by Dow Chemical Company) was selected as the bis(*o*-aminophenol) and 1,1-bis(4-chlorocarbonyl-phenyl)-1-phenyl-2,2,2-trifluoroethane (3FAC) or bis(4-chloro-carbonylphenyl)phenylphosphine oxide (PPOAc) were chosen as the acid chlorides (Figure 4.61). The impetus for using these monomers came from analogous polyimide work where incorporation of related monomers into the polyimide backbone enhanced solubility and pushed T_g 's well over the 400°C mark [207]. Therefore similar results were expected in the case of polybenzoxazoles.

Major drawbacks associated with using these monomers include the oxidative instability of diaminoresorcinol and the fact that both acid chlorides have to be synthesized. The oxidative instability of diaminoresorcinol can be circumvented through the use of its dihydrochloride salt. Preliminary efforts to generate polybenzoxazoles took advantage of the dihydrochloride salt in a low temperature, base-catalyzed amidation reaction. Unfortunately, incomplete dehydrochlorination and amidation resulted in low

molecular weight powders and excessive quantities of triethylamine hydrochloride. Due to these discouraging results, the reaction conditions were modified to allow for the use of N,N',O,O'-tetrakis(trimethylsilyl)diaminoresorcinol (SDAR), a less stable protected diaminoresorcinol, but a more reactive monomer. Synthesis of SDAR involved a base catalyzed silylation reaction where both amines and hydroxyls were substituted with trimethylsilyl groups (Figure 4.62). Monomer grade material could be achieved via repeated vacuum distillations. The acid chloride syntheses have been discussed previously and will not be elaborated on.

The synthetic methodology employed to polymerize the silyl protected diaminoresorcinol utilizes a low temperature condensation reaction between silylamines and acid chlorides,

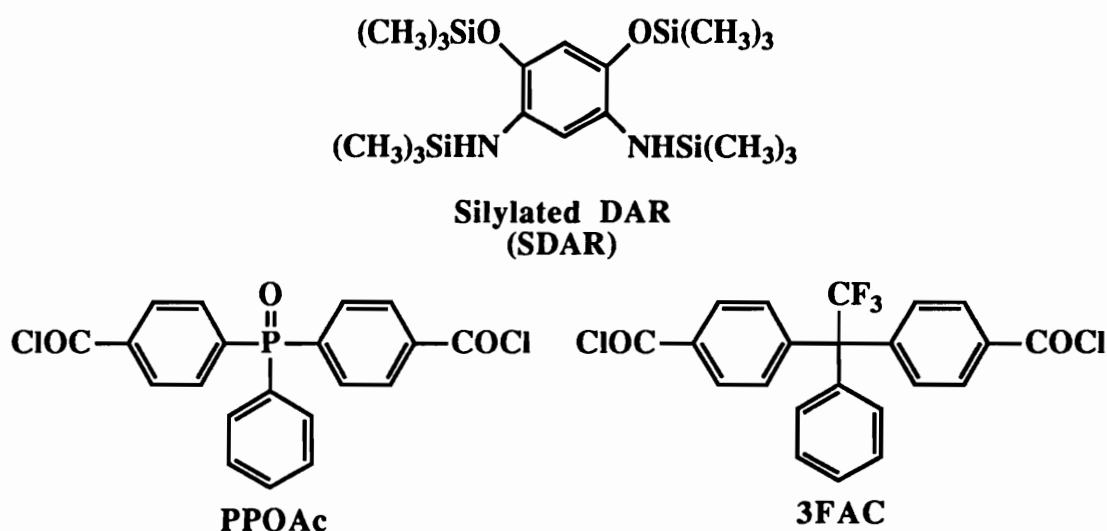
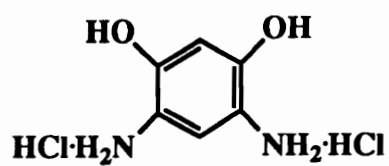
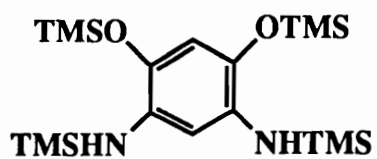


Figure 4.61. Monomers and acronyms for high performance polymers.



THF, TEA
(CH₃)₃SiCl
25°C for 2 hrs
Reflux for 8 hrs
Filter off Salt



60% Yield After 1st Distillation
b. p. = 115-120°C (0.5 torr)

Figure 4.62. Synthesis of N,N',O,O'-tetrakis(trimethylsilyl)-diaminoresorcinol.

followed by high temperature, azeotropic cyclodehydration (Figure 4.63). A calculated amount of silylated DAR was dissolved in NMP, the temperature lowered to -15°C and the acid chloride added as a solid. Total percent solids was 20% (w/v). After complete dissolution of the acid chloride, the temperature was increased to 0°C and maintained for 6 hours. An increase in solution viscosity was noticed immediately. After an additional 6 hours at room temperature, the product was precipitated into MeOH, filtered, washed with MeOH/H₂O and dried at 120° for 12 hours.

Cyclodehydration of the poly(hydroxy amide) was accomplished using an NMP/*o*-dichlorobenzene azeotrope mixture (80/20) and 2 moles of pyridine hydrochloride as catalyst. Three hours at 175°C resulted in a fully cyclized PBO as determined by FT-IR. Table 4.17 summarizes the reaction conditions attempted in an effort to synthesize high molecular weight polymers.

Table 4.17 alludes to the fact that polymerization mixtures instantly gelled when SDAR was treated with a solid form of PPOAc, but gave high polymer when treated with solid 3FAC. Two explanations for this phenomena are possible; 1) PPOAc generates poly(hydroxy amide)s of such high molecular weight that they appear to gel or 2) some sort of side reaction is taking place. In light of the limited success in achieving high molecular weight polymers, explanation 1 would be difficult to rationalize. Explanation 2 is more consistent with experimental observations considering the difficulty encountered during the chlorination of bis(4-carboxy-

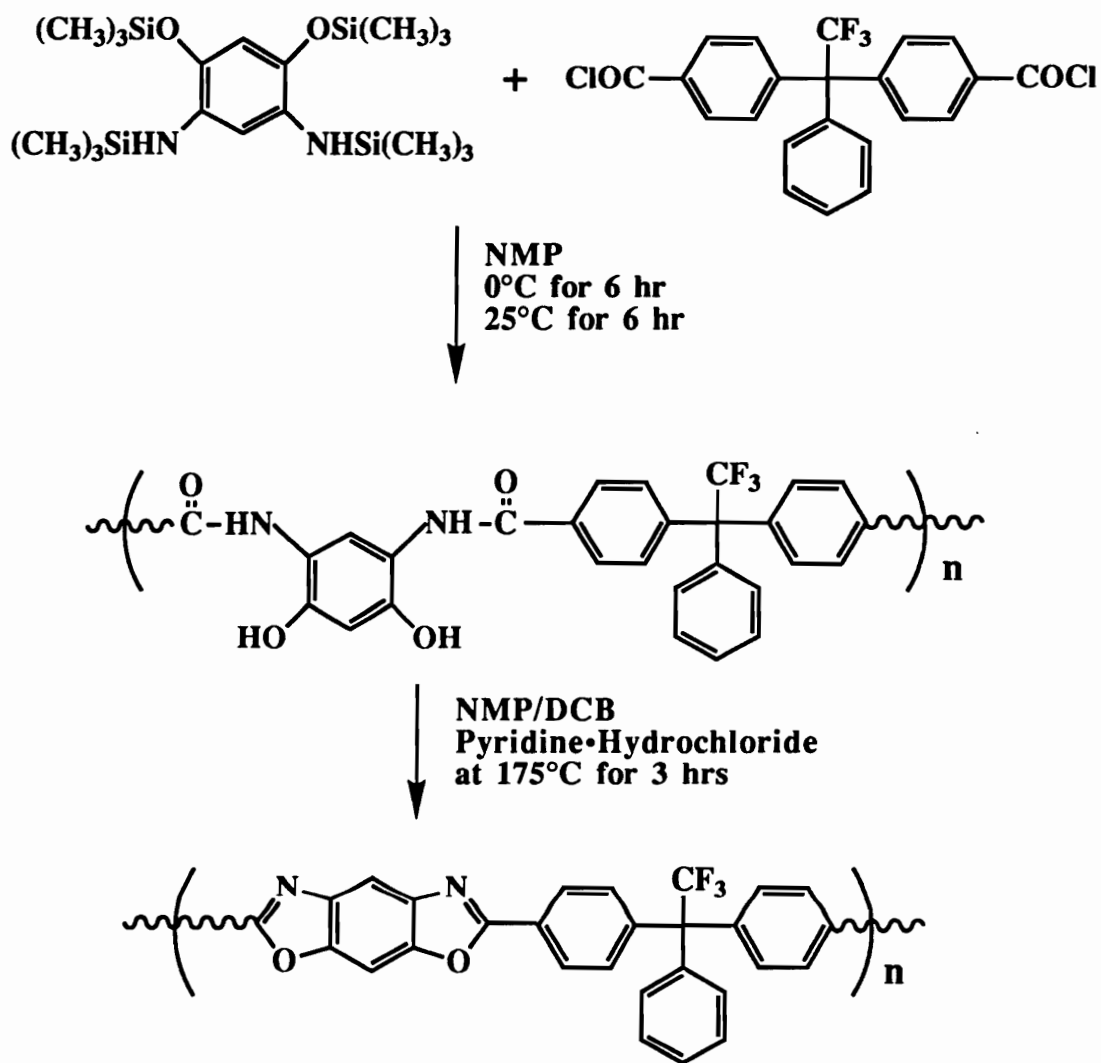


Figure 4.63. Polymerization and cyclization of DAR-3FAC poly(hydroxy amide). Polymerization conducted in NMP, 20% solids.

phenyl)phenylphosphine oxide. Nevertheless, formation of high molecular weight polymer using SDAR as the bis(*o*-amino-phenol)

Table 4.17. Summary of SDAR polymerization conditions.
(20% Solids)

<u>Monomers</u>	<u>Conditions</u>	<u>Results</u>
PPOAc/DAR·2HCl Powder	AC ^a added as NMP solution TEA used as base (4 moles) at 10°C, then 12 hrs at 25°C	Fine
PPOAc/SDAR	Add AC as a solid at -15°C, 6 hrs at 0°C and 6 hrs at 25°C	Gel
PPOAc/SDAR	Add AC as a solid at -30°C, 6 hrs at 0°C and 6 hrs at 25°C	Gel
PPOAc/SDAR	Add AC as a soln in NMP at 10°C, 12 hrs at 25°C	Insoluble PHA
3FAC/SDAR	Add AC as a solid at -15°C, 6 hrs at 0°C and 6 hrs at 25°C	High M.W. Polymer

AC - Acid Chloride

is possible as demonstrated by the formation of high molecular weight DAR-3FAC PBO.

Characterization of the polymer consisted of dilute solution viscometry on both the poly(hydroxy amide) and the polybenzoxazole,

DMA on thermally and solution cyclized materials, ^1H NMR, FTIR spectroscopy and dynamic as well as isothermal thermogravimetric analysis. Evidence supporting the attainment of high molecular weight polymer can be found in the ^1H NMR spectrum of the poly(hydroxy amide) (Figure 4.50), as well as the PHA's $[\eta]^{25^\circ\text{C}}$ of 1.00 dl/g (NMP) and the PBO's $[\eta]^{25^\circ\text{C}}$ of 0.74 dl/g (*m*-cresol). Films formed by casting NMP solutions of the poly(hydroxy amide), followed by thermal cyclodehydration, were noticeably more brittle than films formed from casting *m*-cresol solutions of cyclized polybenzoxazoles. It is suggested that the increase in brittleness found in the thermally cyclized film is due to intermolecular crosslinks. It should also be mentioned that the thermally cyclized film showed more solvent resistance relative to its solution cyclized counterpart. Evidence to support complete ring closure can be found in Figure 4.64. The infrared spectrum indicates complete cyclization has occurred by the disappearance of the broad OH and amide bands ($3000\text{-}3400\text{ cm}^{-1}$) and the carbonyl stretch at 1650 cm^{-1} and the appearance of a 1630 cm^{-1} oxazole stretch and 1056 cm^{-1} oxazole vibration.

Thermal analysis of these materials required the use of dynamic mechanical analysis due to the extremely high glass transition temperatures. Unfortunately, even with this technique, accurate determination of the T_g was impossible due to mechanical failure at higher temperatures. However, it certainly appears that the T_g of these materials are above 450°C , as evident by the lack of a

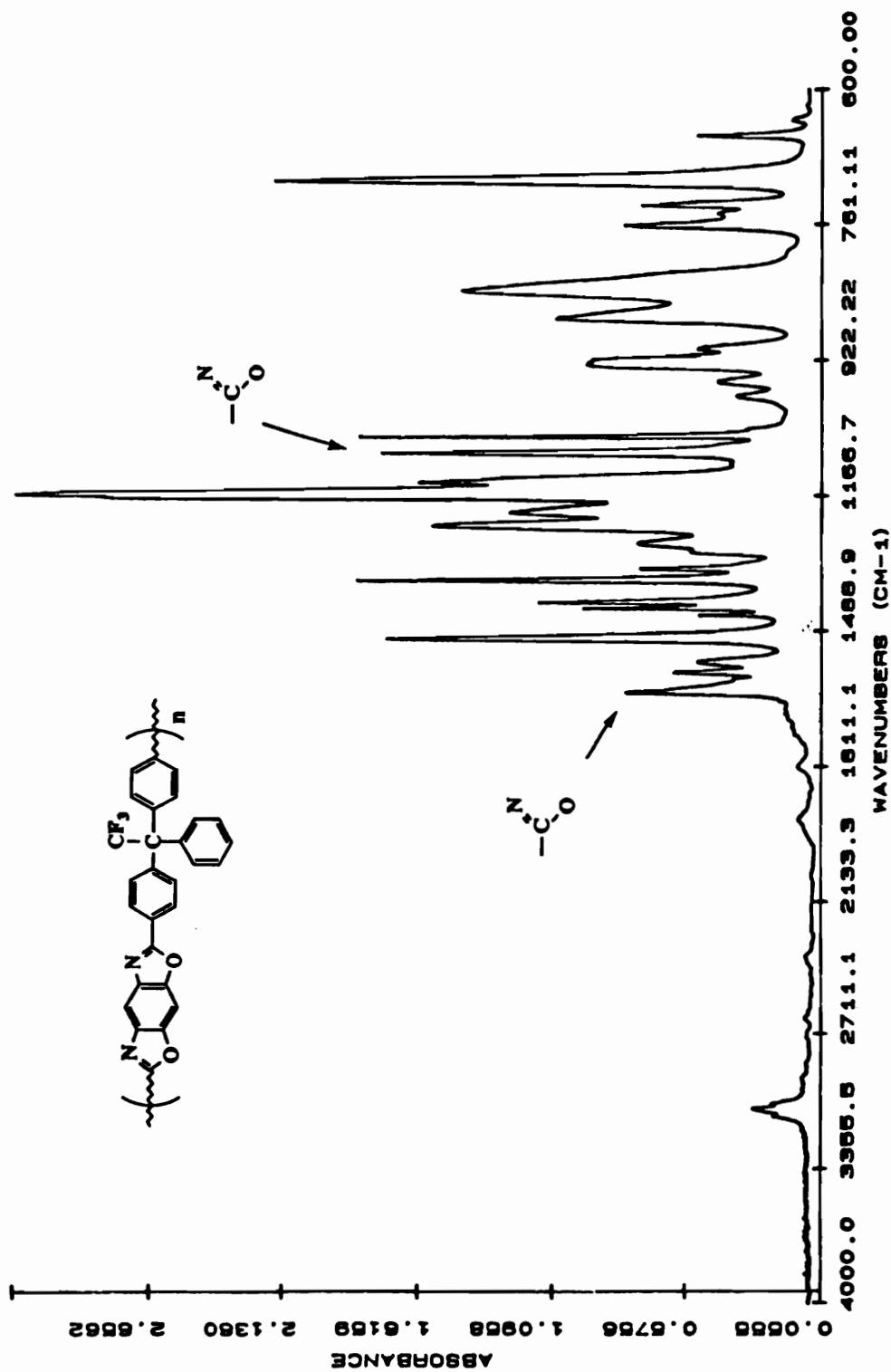


Figure 4.64. Fourier transform infrared spectrum of solution cyclized DAR-3FAC polybenzoxazole.

modulus drop on the modulus-temperature plot (Figure 4.65). It should be pointed out that the thermally cyclized polymer failed at 430°C, while the solution cyclized specimens remained intact. Earlier it was suggested that high T_g materials might perform better under aggressive thermo-oxidative conditions, due to their high aromatic character and their ability to impede the permeation of oxygen into the bulk. Results obtained on this material under dynamic as well as isothermal conditions indicate no significant increase in thermo-oxidative stability. Five percent weight loss in air (10°C/minute) was measured at 527°C (similar to previously mentioned fluorinated PBO's) and films isothermally aged at 371°C for 24 hours in an air atmosphere exhibited an 8% decrease in mass after 24 hours and a 33% mass loss after 50 hours.

In conclusion, polybenzoxazoles containing high aromatic character and select solubilities have been generated and much like similar polyimide materials, possess extremely high glass transition temperatures. Synthesis of these materials required an alternate polymerization methodology, but cyclization followed previously mentioned procedures. While the goal of solubility and high T_g 's was achieved, superior thermo-oxidative resistance was not realized in these initial studies.

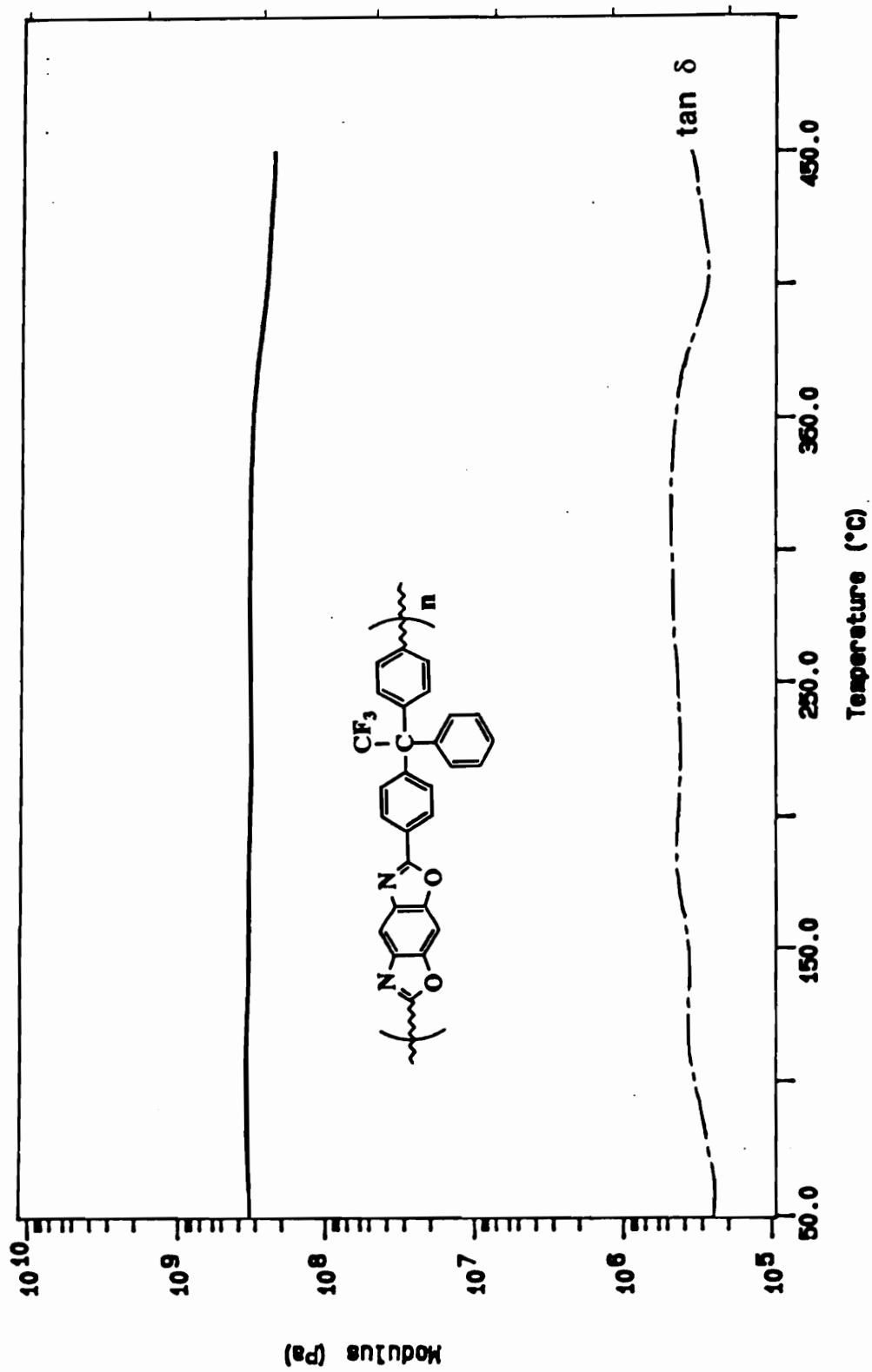


Figure 4.65. DMA trace of solution cyclized DAR-3FAC polybenzoxazole film (10°C/min, 1Hz).

4.11. Phenylethynyl Terminated Polybenzoxazoles

Previous sections have discussed the utility of fluorine containing monomers in the synthesis of processible, thermo-oxidatively stable polybenzoxazoles. In addition, a novel "two-step" polymerization technique has been introduced which results in processible polybenzoxazoles with T_g 's ranging from 280°C to 370°C. To demonstrate further the utility of this synthetic procedure, this section will focus on the generation of controlled molecular weight polybenzoxazoles which can be solution cast from common solvents and subsequently crosslinked into solvent resistant, infusible materials.

A phenylethynyl endcapper was chosen as the crosslinking species, to achieve these objectives. Due to the relatively low cure temperature of acetylene terminated polyimides [244], the phenyl substituted acetylene moiety was selected. Previous investigations conducted on arylene ether [245], polyimide [246], polyquinoxaline [247] and polyamide [248] oligomers supporting internal, terminal or pendent phenylethynyl groups indicated an enhancement of the processing window relative to unsubstituted acetylenes. Cure temperature maximums from calorimetry data ranged from the upper 300's to greater than 400°C. To incorporate the crosslinking functionality, 4-phenylethynylbenzoyl chloride was employed. Using judicious amounts of this acid chloride and solution cyclization techniques, phenylethynyl terminated polybenzoxazoles of various

molecular weights were synthesized. The remainder of this section will discuss the synthetic methodology utilized to prepare these polymers, spectroscopic data substantiating the syntheses as well as thermal and mechanical data demonstrating network formation. The phenylethynyl endcapper was synthesized according to the method of Stephens, Castro and Villemin, using palladium coupling chemistry [199,221]. The particular steps involved in the synthesis are shown in Figure 4.66. Synthesis, purification and characterization of the product, as well as each intermediate, have been discussed in Section 3.2.1.

Polybenzoxazoles containing phenylethynyl functionality and possessing molecular weights ranging between 6,300 to 13,900 g/mole (as determined by ^1H NMR) were generated using the previously outlined "two-step" polymerization procedure (Figure 4.67). 2,2-Bis(3-amino-4-hydroxyphenyl)hexafluoropropane (6FAP) was dissolved in NMP, allowed to react with the monofunctional endcapper at room temperature and then with ODBC at 5°C. The resulting clear viscous solutions were precipitated and the resulting poly(hydroxy amide)s purified via reprecipitation from THF. Extensive washings with water, as well as reprecipitation from THF were carried out to insure complete removal of the pyridine hydrochloride prior to cyclization. It was previously demonstrated that residual pyridine hydrochloride can catalyze the oxazole cyclization reaction and under the right conditions, promote cleavage of the polymer chains.

Conversion of the poly(hydroxy amide)s to polybenzoxazoles was accomplished by dissolving the purified poly(hydroxy amide) in a carefully dehydrated solvent/catalyst system (NMP/toluene/*p*-toluenesulfonic acid) and then subjecting the system to azeotropic distillation (~165°C) for 12-14 hours. A noticeable increase in viscosity was observed in all cases after approximately 3 hours. After the reactions had gone to completion, the viscous solutions were precipitated into methanol, the solid redissolved in THF, filtered and reprecipitated into methanol. Polymer yields for both

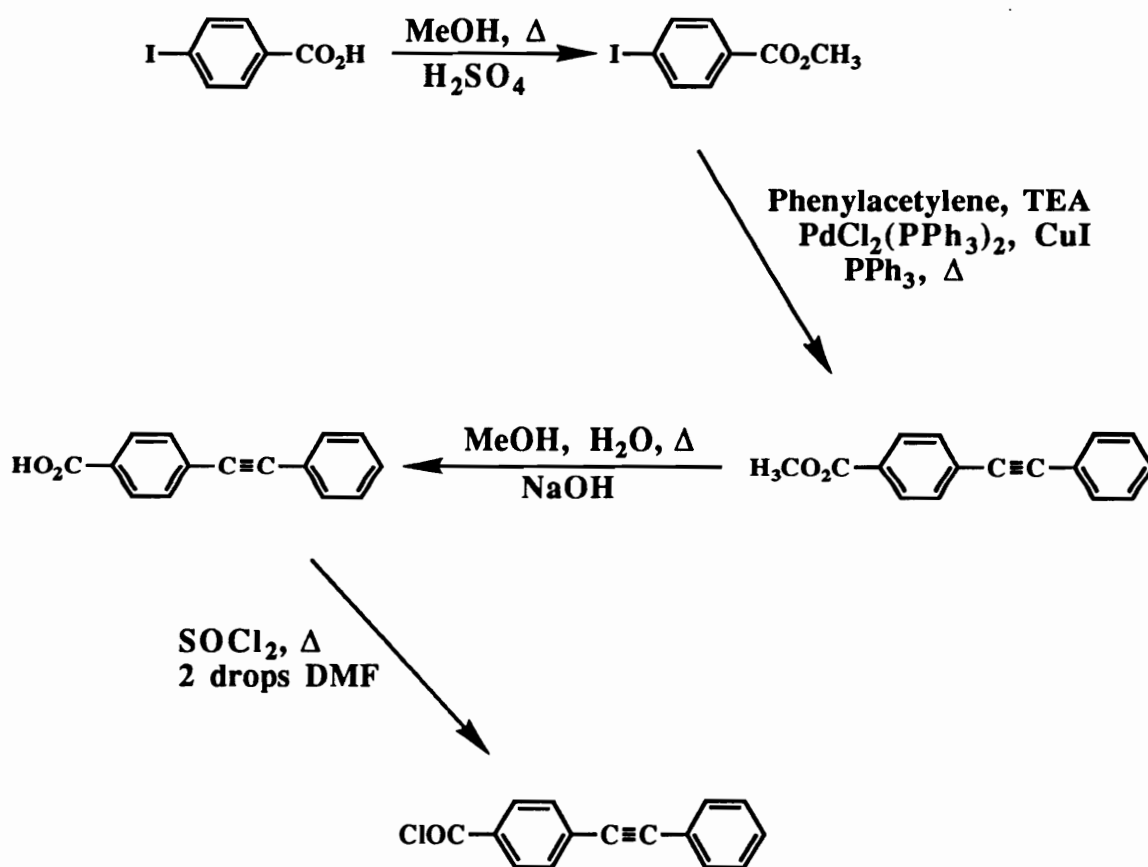


Figure 4.66. Synthesis of 4-(phenylethynyl)benzoyl chloride.

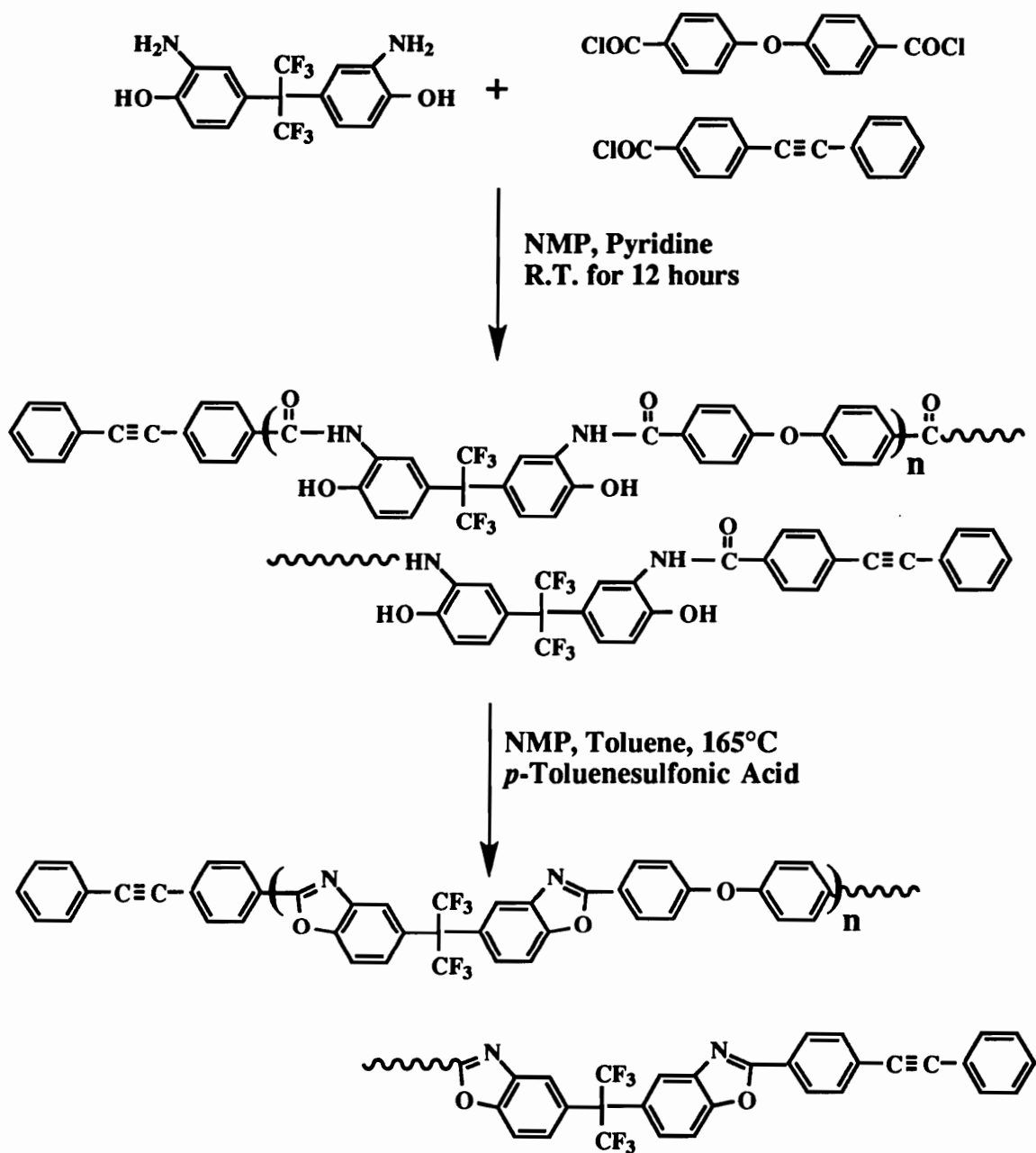


Figure 4.67. Synthesis of controlled molecular weight 6FAP-ODBC poly(hydroxy amide)s and polybenzoxazoles.

steps are shown in Table 4.18. The low polybenzoxazole yields can be attributed to loss of material during the filtration process.

Table 4.18. Yields of controlled molecular weight poly(hydroxy amide)s and polybenzoxazoles.

Theoretical $\langle M_n \rangle$ (kg/mole)	PHA Percent Yield	PBO Percent Yield
5.0	98%	80%
10.0	99%	80%
15.0	99%	90%
Uncontrolled	99%	94%

Spectroscopic evidence supporting complete oxazole formation, incorporation of acetylenic functionality and retention of functionality throughout the cyclization process can be found in Figures 4.68 and 4.69. Note that the poly(hydroxy amide)'s amide and hydroxyl resonances at $\delta=9.55$ and $\delta=10.33$ in Figure 4.68 have completely disappeared in Figure 4.69. Also note that in both Figures 4.68 and 4.69, no extraneous peaks are found in the aromatic regions and the prominent peaks can be easily assigned. Both of these facts indicate complete cyclization has occurred and no apparent side reactions are taking place. In addition, clearly defined endcapper signals, $\delta=7.45$, $\delta=7.6$ and $\delta=7.7$, are present in Figure 4.68 and in Figure 4.69 ($\delta=7.7$). Retention of endcapper signals during the conversion of poly(hydroxy amide)s to poly-

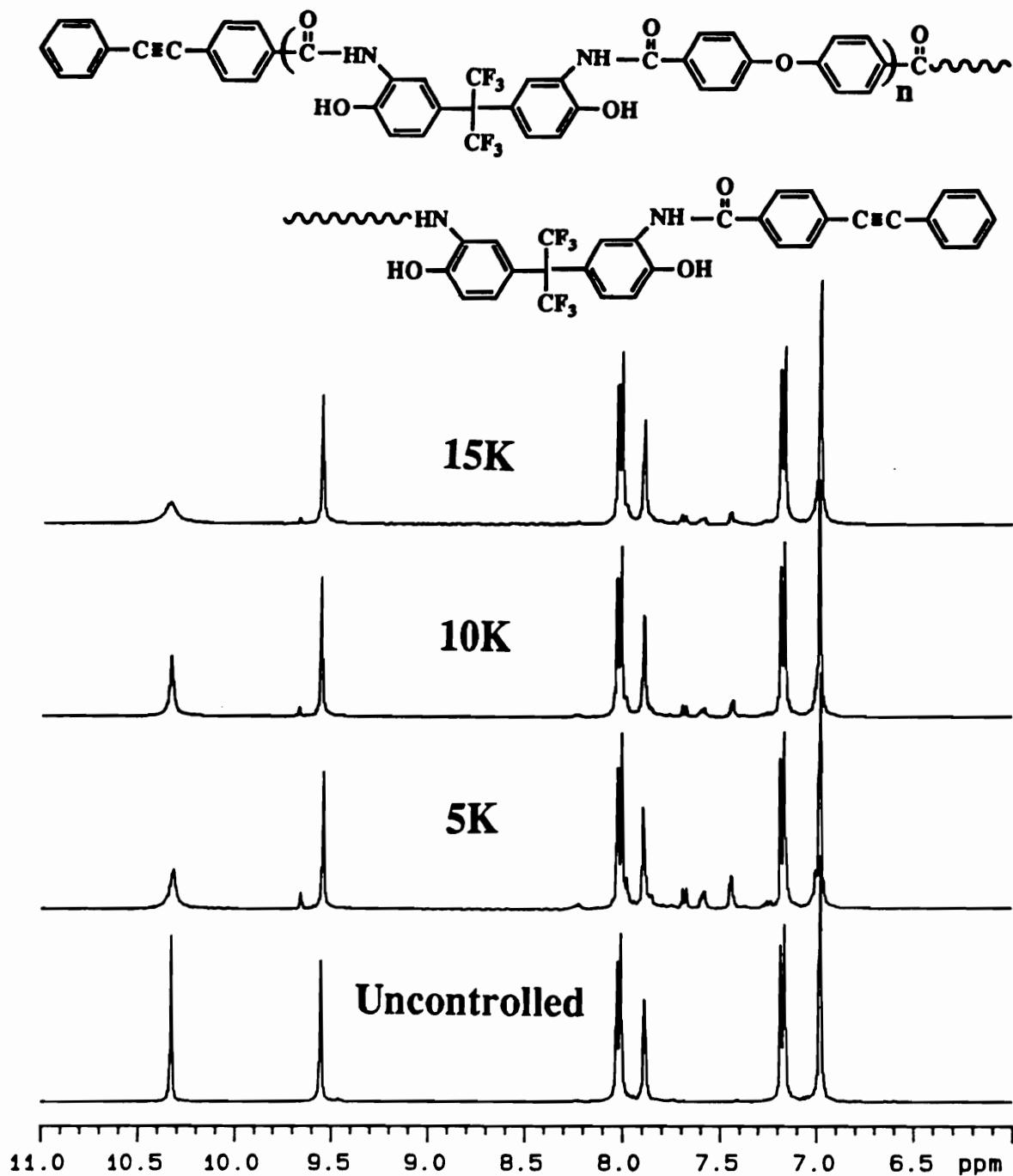


Figure 4.68. ^1H NMR spectra of controlled and uncontrolled molecular weight 6FAP-ODBC poly(hydroxy amide)s.

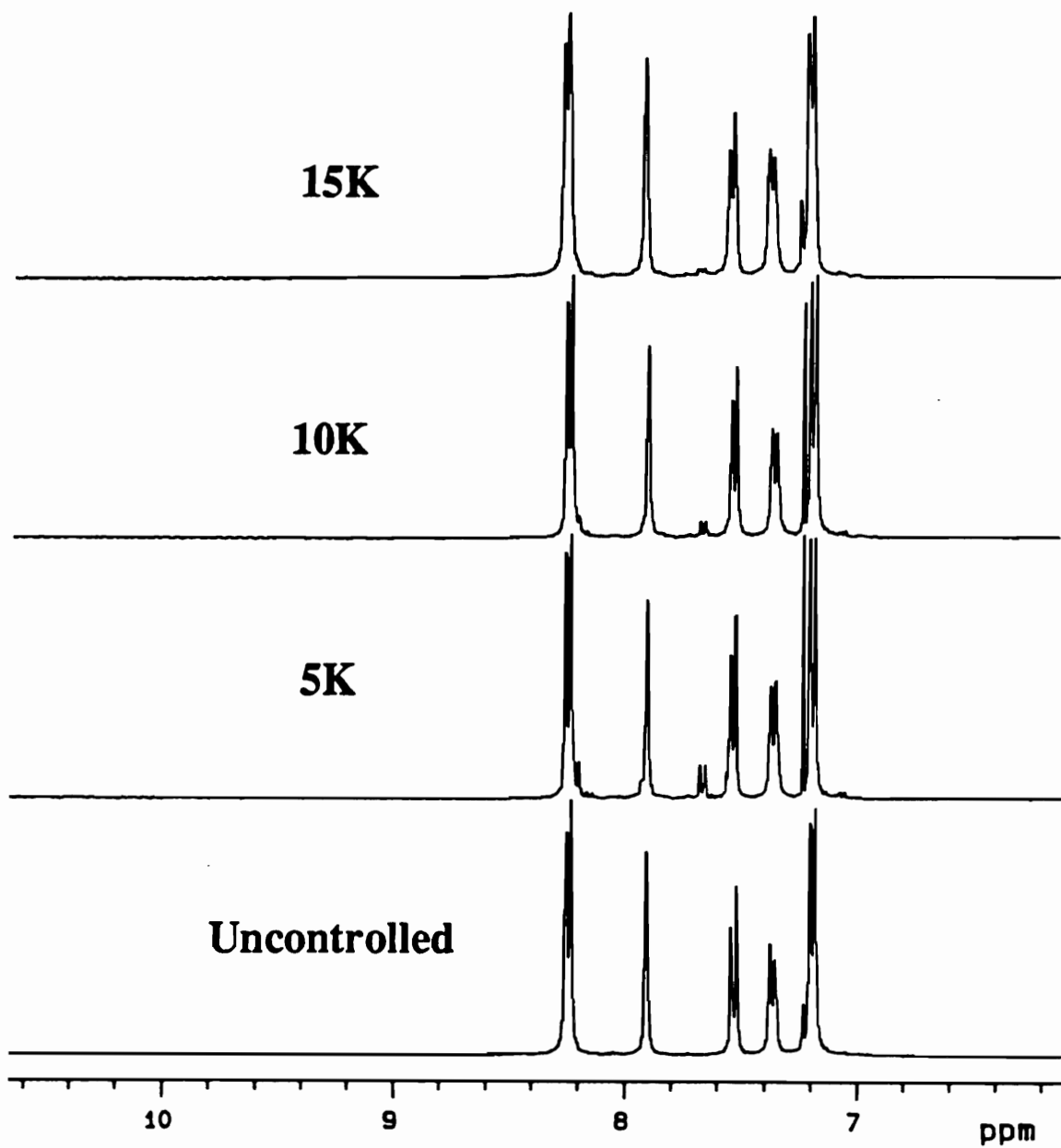


Figure 4.69. ¹H NMR spectra of controlled and uncontrolled molecular weight of 6FAP-ODBC polybenzoxazoles.

benzoxazoles indicates acetylenic functionality is not being altered during the cyclization process.

Verification of molecular weight control was also accomplished using ^1H NMR spectroscopy in addition to intrinsic viscosity measurements. Since the phenylethynyl resonances are clearly separated from the backbone resonances, an approximation of molecular weight was possible by ratioing the integrations of the backbone signals and endgroup signals multiplying by the molecular weight of the repeat unit (equation 1).

$$\langle M_n \rangle = \frac{\frac{\text{Integration of RU Proton}}{\# \text{ of RU Protons}}}{\frac{\text{Integration of EG Protons}}{\# \text{ of EG Protons}}}$$

$$\text{X MW of RU} + (2 \text{ X MW of E.G.}),$$

Equation 1

where RU is the repeat unit, EG is the endgroup and MW represents molecular weight, whether it is the repeat unit molecular weight or endgroup molecular weight. In the case of the poly(hydroxy amide)s, the repeat unit signals at $\delta=7.0$ and $\delta=7.2$ ppm and the phenylethynyl signals at $\delta=7.4$ and $\delta=7.55$ ppm were used to determine molecular weight and in the case of the polybenzoxazoles, the repeat unit signal at $\delta=7.9$ ppm and the endgroup signal at $\delta=7.69$ ppm were used.

The assumption of 2 endgroups per polymer chain and 100% conversion of all functional groups has been made. Results of these calculations, as well as the intrinsic viscosity measurements are summarized in Table 4.19. Note that the experimental molecular weights match quite well with the theoretical molecular weights

Table 4.19. Molecular weight and intrinsic viscosity data for 6FAP-ODBC poly(hydroxy amide)s and polybenzoxazoles.

Theoretical^a	Calc. PHA^a	Calc. PBO^a	PHA^b	PBO^b
<M_n>	<M_n>	<M_n>	[η]	[η]
5.0	5.8	6.3	0.29	0.39
10.0	11.2	10.2	0.63	0.77
15.0	17.4	14.0	---	0.93
Uncontrolled	---	---	1.17	1.52 ^c

^a<M_n> reported in kg/mole

^bIntrinsic viscosity ran in THF at 25°C

^cPBO was insoluble in THF, so [η] was ran in CHCl₃ at 25°C

and the intrinsic viscosities increase with an increase in molecular weight. The increase in intrinsic viscosity during the transformation from poly(hydroxy amide)s to polybenzoxazoles can be explained as an enhancement in chain rigidity due to the loss of rotational degrees of freedom upon oxazole formation. It is of course realized that PHA's and PBO's have different solubility parameters and that this phenomenon will have an effect on the

hydrodynamic volume of polymer chains in solution. Nevertheless, a rise in intrinsic viscosity during cyclization can only be interpreted as a desirable result and it suggests molecular weight was maintained during the cyclization process. From these results it can be concluded that molecular weight control has been achieved and phenylethynyl functionality has been incorporated into the polymers.

Films of the polymers were prepared by dissolving the various molecular weight polymers in chloroform at 10-20% solids (w/v) and spreading the solutions on glass plates with a doctors blade. After evaporation of the solvent at room temperature, the films were dried in a vacuum oven at 100°C for 1 hour, 180°C for 1 hour and finally 250°C for 1 hour. The resulting films were flexible, clear and ranged from water white to gold in color. The 10K polymer exhibited a slight amount of haze. Coloration appeared to increase as the number of phenylethynyl endgroups increased. Half the films were subjected to a post-cure at 350°C for 1 hour in a conventional forced air oven equipped with N₂ purge. The cured films showed little if any loss of clarity and retained their flexibility.

To ascertain the effect of molecular weight on glass transition temperatures, DSC was performed on the samples before and after a 350°C cure. Results of these analyses are detailed in Tables 4.20 and 4.21. Table 4.20 summarizes the thermal characteristics of the

uncured PBO films, while Table 4.21 provides the thermal properties of films cured for 1 hour at 350°C. The columns entitled "Uncured

Table 4.20 Thermal transition data for uncured polybenzoxazoles

Polymer	Uncured T_g (°C)	Cured T_g (°C)	ΔT (°C)	Cure T_{max} (°C)
5K PBO	255	318	63	400
10K PBO	265	310	45	410
15K PBO	284	315	31	399
UNC PBO	311	----	---	----

Table 4.21 Thermal transition data for polybenzoxazoles cured at 350°C for 1 hour.

Polymer	Uncured T_g (°C)	Cured T_g (°C)	ΔT (°C)	5% Wt. Loss (°C)
5K PBO	255	302	47	530
10K PBO	265	303	38	527
15K PBO	284	305	21	527
UNC PBO	311	----	---	527

T_g's" represent the uncured T_g's and as expected, the T_g's increase with an increase in molecular weight; further evidence to support the claim of molecular weight control. The last three columns in Table 4.20 represent the glass transition temperature after

exposure to DSC ramp to 475°C (10°C/min), the difference in uncured and cured glass transition temperatures (ΔT) and the temperature of the maximum cure exotherm (Cure T_{\max}). Note that the cured T_g 's have increased substantially from the uncured values and seemed to have plateaued around 315°C. Slight variations in final T_g 's are expected due to differences in crosslink density as well as molecular weight between crosslinks. The change in glass transition temperature was greatest for the 5K PBO (63°C) and least for the 15K PBO (31°C), in agreement with theory. Figure 4.70 illustrates representative DSC thermograms of a cured and uncured 5K PBO sample. While the cure exotherm is relatively prominent for the 5K material, the 10K and 15K polymers exhibited rather broad and unpronounced exotherms. A consequence of this is great difficulty in assigning a maximum cure temperature for the higher molecular weight polymers.

The last three column headings in Table 4.21 represent the T_g 's after a 1 hour, 350°C cure, the difference between the uncured and cured glass transition temperatures (ΔT) and the 5% weight loss obtained by scanning at a rate of 10°C/min in air. In general, the same trends observed in Table 4.20 are observed in Table 4.21, evident from the low cured T_g 's is the fact that a 350°C cure is inadequate to completely cure the films. However, as indicated in Table 4.20 and Figure 4.70, a post-cure of 475°C does raise the T_g 's and completes the cure. Nevertheless, films exposed to a 350°C

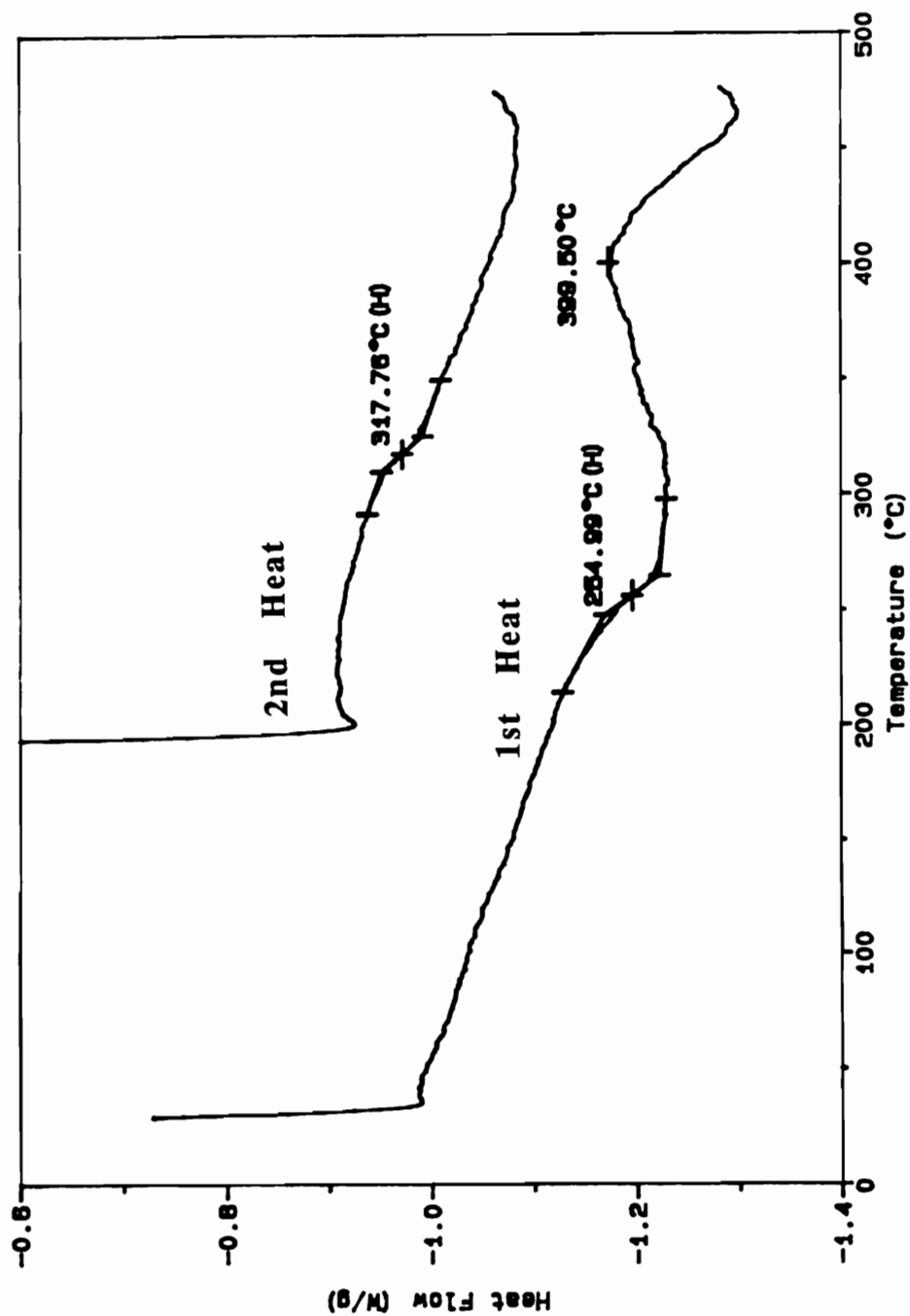


Figure 4.70. DSC thermogram of 5K, phenylethynyl terminated 6FAP-ODBC polybenzoxazole, before and after a 1 hour cure at 475°C (10°C/min).

cure were insoluble and exhibited little if any swelling in THF or CHCl_3 . It should also be pointed out that the T_g of the uncontrolled molecular weight PBO is approximately equal to that of the crosslinked polymers. This fact would suggest that the molecular weight of the uncontrolled PBO is very high. Further studies are currently under way to ascertain an accurate molecular weight for the uncontrolled PBO as well as verify the molecular weights of the controlled polymers.

To determine the effect of molecular weight control on thermo-oxidative stability, thermal gravimetric analysis in air was carried out on the cured samples (Table 4.21). As expected, no difference was noted between the controlled molecular weight samples and the uncontrolled molecular weight sample. In addition, all the polymers demonstrated excellent thermo-oxidative stability. The conclusion from these experiments is that the phenylethynyl terminated PBO's are as thermo-oxidatively stable as the unfunctionalized parent polymer, at least in the short-term, and no apparent instability has been introduced into the cured system by processing at 350°C .

To ascertain the effect of molecular weight and crosslink density on mechanical properties, both the cured and uncured polymers were subjected to thin film stress-strain analysis. The results of these experiments are summarized in Table 4.22. In all cases, the tensile properties are comparable to literature values and an increase in moduli and tensile strengths are noticed in the cured systems relative to the uncured systems. An increase in

tensile modulus is expected due to the incorporation of crosslinks and the lowering of rotational conformations accessible to individual polymer chains. Notice that the tensile strengths, as well as percent elongation, increase with increasing molecular weight between crosslinks. In fact, the higher molecular weight samples, both cured and uncured, exhibited some yielding behavior when exposed to a load.

Table 4.22. Thin film tensile properties of cured and uncured polybenzoxazoles.^a

Polymer	Tensile Modulus GPa (Std. Dev.)	Tensile Strength MPa (Std. Dev.)	Percent Elongation to Break
5K Cured	4.8 (0.3)	202 (9)	9.(2)
10K Cured	6.7 (0.3)	319 (5)	9 (2)
15K Cured	7.7 (1.1)	353 (26)	16 (3)
5K Uncured	3.7 (0.3)	154 (5)	7 (1)
10K Uncured	5.3 (0.6)	241 (8)	13 (3)
15K Uncured	4.1 (0.4)	154 (27)	13 (9)
<u>Uncontrolled</u>	<u>2.3 (0.3)</u>	<u>116 (8)</u>	<u>9 (1)</u>

^aMeasurements made on thin films (1-5 mils) cast from CHCl₃ and reported values are an average of at least 4 test specimens (strain rate = 0.05 in/min.).

The effect of molecular weight on mechanical properties in the uncured systems follows the expected trend, that is, higher

molecular weight affords better mechanical properties. However, the mechanical properties of the uncontrolled molecular weight polymer were inferior to all the controlled molecular weight samples, cured or uncured. A possible explanation for this phenomena can be found by analyzing the GPC data and taking the film casting process into account. Gel permeation data (Figure 4.71) exhibits a bimodal distribution for the controlled molecular weight polymers, one peak showing up at high molecular weights and one at low molecular weights. The $\langle M_n \rangle$ for the 5K material is 3550 g/mol, while the $\langle M_w \rangle$ is 61,300 g/mol. Mechanical properties are directly related to the weight average molecular weight; therefore even though the 5K sample exhibits a $\langle M_n \rangle$ of only 3550, its mechanical properties are behaving like a high molecular weight polymer . Furthermore, during the film casting process the films are exposed to 250°C for 1 hour and undoubtedly some reaction takes place. This may result in some chain extension and/or branching which would enhance mechanical properties. Evidence for this phenomena exists in the fact that after three film castings, the films are no longer soluble in chloroform. Another possible explanation for the lower mechanical properties of the uncontrolled polymer, is film thickness. The INSTRON computer program can only use film thicknesses rounded to the nearest mil, therefore larger errors are incorporated into films of 1 or 2 mils than films of 4 or 5 mils. The uncontrolled polymer was 5 mils, while the controlled polymers were typically around 1 or 2 mils. This differences in film thick-

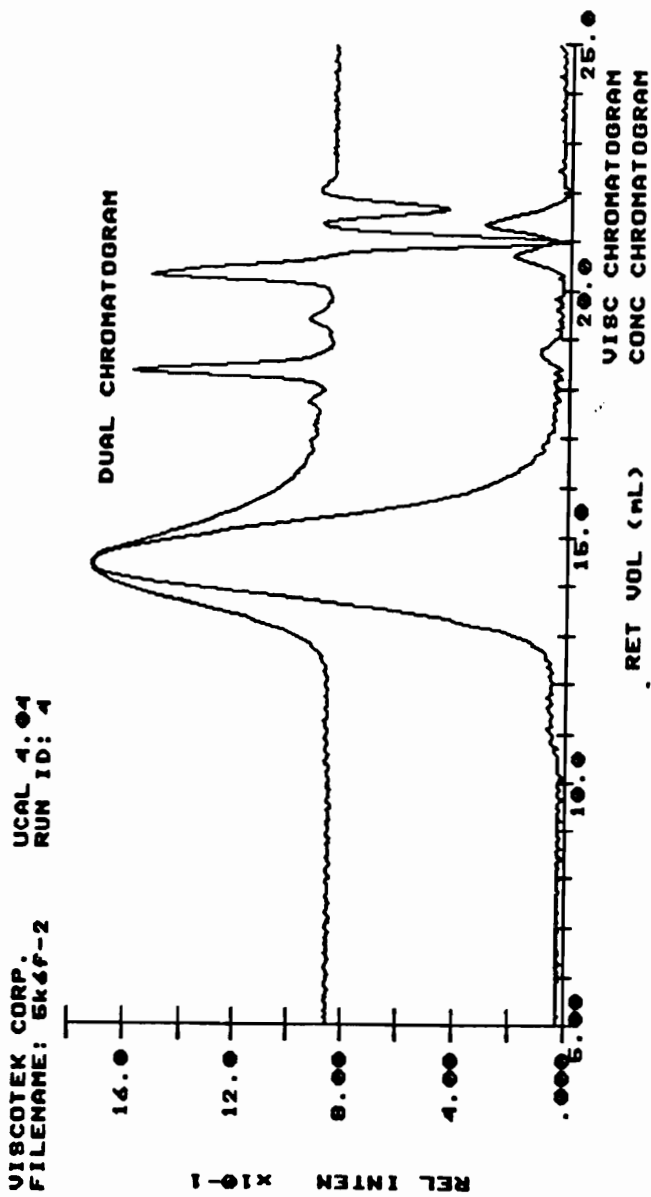


Figure 4.71. Gel permeation chromatogram of 5K 6FAP-ODBC polybenzoxazole (THF, $\langle M_n \rangle = 3.6$ kg/mole, $\langle M_w \rangle = 61.3$ kg/mole).

ness may overestimate the mechanical properties of the controlled molecular weight polymers.

In conclusion, phenylethynyl terminated polybenzoxazoles of various molecular weights have been generated via a "two-step" polycondensation, cyclization process. Endgroup functionality was maintained throughout the cyclization process as was molecular weight. Polymer formation as well as functionalization and molecular weight control was verified by spectroscopic, viscometric, thermal and mechanical analysis. Glass transition temperatures increased with molecular weight for uncured samples, while samples cured at 350°C and 475°C plateaued between 305°C and 315°C respectively. Mechanical properties were significantly enhanced with incorporation of crosslinks and a simultaneous increase in tensile moduli, strengths and percent elongation were noted with an increase in molecular weight for both cured and uncured systems. Chemical resistance in general was dramatically improved, apparently with little loss of ductility.

4.12. Nonfluorinated Homopolymers and Fluorinated Copolymers

A number of nonfluorinated homopolymers and fluorinated copolymers were synthesized during the process of selecting monomers which would impart solubility or thermo-oxidative stability to polybenzoxazoles. In some cases, the polymers were synthesized simply to determine if monomer purity was adequate to obtain high molecular weight polymers, yet in others, copolymers were synthesized to ascertain the effect of monomer composition on crystallinity or solubility. Some of the polymers generated have been reported in the literature previously, but no attempt was made to cyclodehydrate the polymers via solution methods. Therefore the following section describes various homopolymers and copolymers with respect to solution, thermal and morphological properties. In all cases the polymers were synthesized according to the previously mentioned "two-step", one-pot technique where the poly(hydroxy amide)s were generated with a pyridine base in NMP and the cyclization process utilized a pyridine hydrochloride catalyst and an *o*-dichlorobenzene azeotrope solvent.

A summary of the polymers is found in Table 4.23. Notice that in all cases, some percentage of the polymer or copolymer backbone is composed of 3,3'-dihydroxybenzidine and although its not shown, all the polybenzoxazoles precipitated from the reaction mixture during

Table 4.23. Solution and thermal properties of various 2,2'-dihydroxybenzidine containing poly(hydroxy amide)s and polybenzoxazoles.

Z	Ar	PHA $[\eta]_{\text{NMP}}^{25^\circ\text{C}}$ (dl/g)	PBO $[\eta]_{m\text{-cresol}}^{25^\circ\text{C}}$ (dl/g)	T _g ^a (°C)	5% WL Loss ^b (°C)
—		1.30	Insol.	----	532
—		0.47	0.34	345	526
—		----	0.39	357	536
—		Insol.	Insol.	268 (442)	543
—		Insol.	Insol.	----	----
—		1.11*	Insol.	309	496
—		1.10	Insol.	278	527

^aHeating rate = 10°C/min

^bHeating rate = 10°C/min in air

*Inherent viscosity (0.5%)

cyclization. In the examples where combinations of isophthaloyl chloride and 1,1-bis(4-chlorocarbonylphenyl)-1-phenyl-2,2,2-trifluoroethane were employed, the cyclization mixture clouded with the addition of just 5% isophthaloyl chloride, but did not result in gross precipitation like the others. It is suspected that precipitation is being caused by crystallinity. Crystallinity was detected in the DHB-ODBC polybenzoxazole ($T_m=442^\circ\text{C}$) after annealing 100°C above its T_g for an extended period of time (Figure 4.72). Apparently DHB-ODBC or DHB-IC benzoxazole linkages crystallize quite readily and cause precipitation of the polymers. Attempts to keep these polymers in solution by adding flexible comonomers such 3FAC or 6FAP failed in all cases. Its interesting to note that the DHB-ODBC poly(hydroxy amide)s were soluble in NMP during the polycondensation reaction, but upon precipitation and drying, the fibrous polymers lost all solubility in NMP. Efforts to enhance the solubility of this poly(hydroxy amide) by controlling molecular weight to 10K also failed.

Thermal properties of these polymers were very similar to previously mentioned polybenzoxazoles and followed the the normal trends, that being, an increase in glass transition temperature with an increase backbone rigidity. Thermo-oxidative stabilities, as judged by 5% weight loss (heating rate of $10^\circ\text{C}/\text{minute}$ in air), were also similar to previous polymers, ranging from $496\text{-}543^\circ\text{C}$.

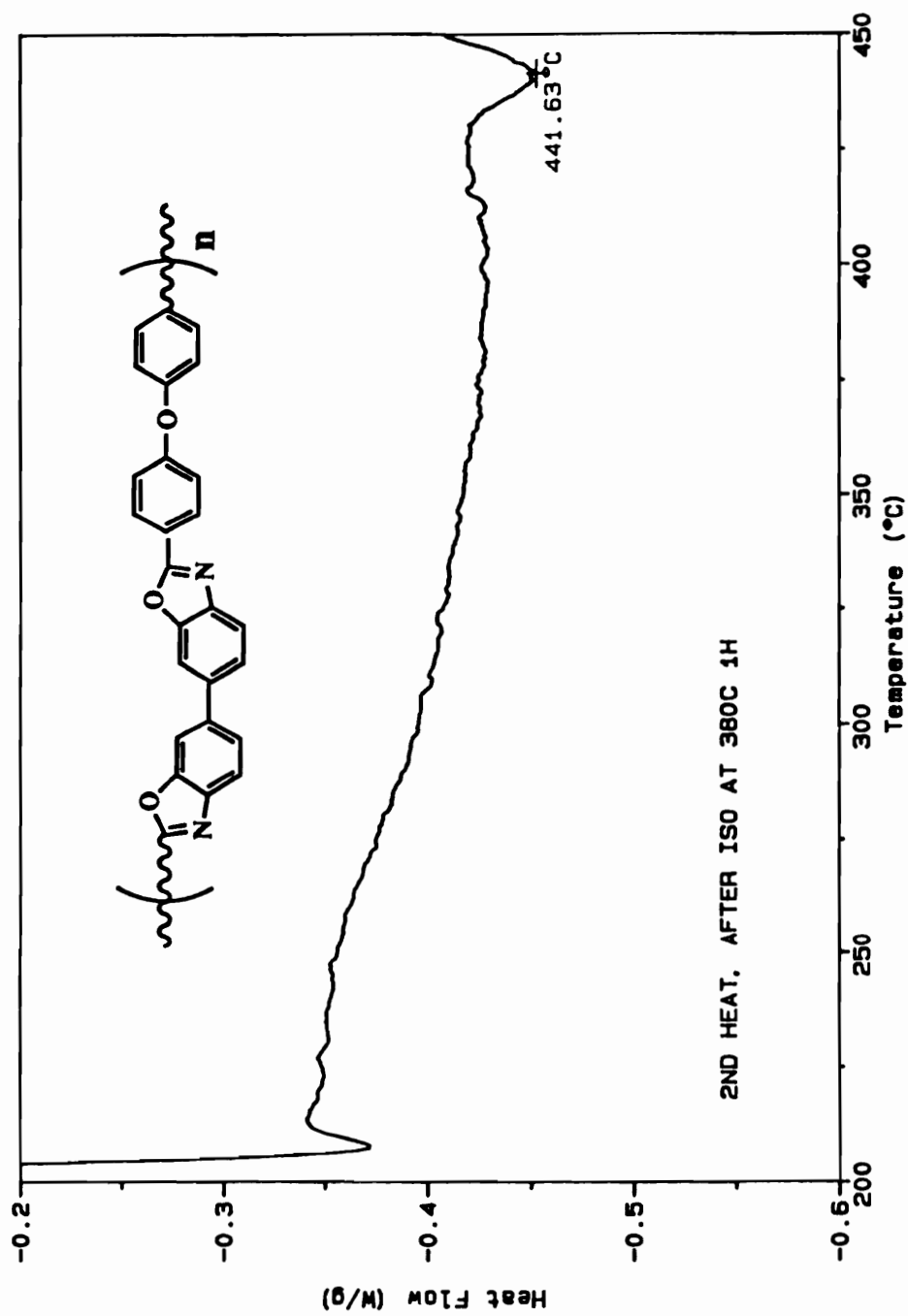


Figure 4.72. DSC thermogram of DHB-ODBC polybenzoxazole (10°C/min in N₂).

Chapter 5

CONCLUSIONS

The low temperature polymerization of bis(*o*-aminophenol)s with aromatic acid chlorides has been investigated in detail to determine the effect of reaction parameters on molecular weight. Results of these studies suggest that amine reactivity is more than adequate to acylate diacid chlorides under the reaction conditions employed. The fact that 2,2-bis(3-amino-4-hydroxy)hexafluoropropane (6FAP) can be polymerized to high molecular weights when an electron rich diacid chloride or dianhydride is employed provides further evidence to support this claim. Spectroscopic and other evidence suggests that molecular weight is limited by an ester side reaction. Immediate gelation in the case of either inadequate mixing or high concentrations of acid

chloride can be easily explained by an ester forming crosslinking reaction. Polymerizations carried out in the absence of base exhibit no gelling behavior, indicating that base is acting as a catalyst for the ester reaction.

Reaction conditions necessary to achieve high molecular weight, fully cyclized, soluble polybenzoxazoles have been elucidated. A simple spectroscopic method has been developed to follow the cyclization process and determine percent conversion to polybenzoxazole. A variety of different catalyst systems were studied and results indicate *p*-toluenesulfonic acid monohydrate is the most effective catalyst and while combinations of pyridine hydrochloride and *p*-toluenesulfonic acid monohydrate or pyridine hydrochloride alone are highly desirable, they appear to induce hydrolysis and degrade molecular weight. Higher cyclization temperatures (180-200°C) not only enhanced the rate of cyclization, but also afforded polymers with substantially higher inherent viscosity values. Results indicate molecular weight is not being dramatically affected by cyclization under optimum conditions and the best results were obtained using 10% *p*-TSA at 190-195°C in CHP for 3 hours, as shown in Table 4.10.

2,2-Bis(3-amino-4-hydroxyphenyl)propane (bAAP) was polymerized with various compositions of isophthaloyl and terephthaloyl chloride under base-catalyzed conditions and subsequently solution cyclized to afford a series of isomeric polybenzoxazoles. A semi-crystalline morphology was observed for

the 100% *para* linked system, but incorporation of small amounts of isomeric linkages resulted in amorphous materials with improved solubilities. Excellent solvent resistance was observed for all solvents tested, with the exception of *m*-cresol. High molecular weight poly(hydroxy amide)s were achieved, evident from the solution viscosities ($[\eta]^{25^{\circ}\text{C}} = 0.60\text{-}1.16$ dl/g (NMP)), and retention of molecular weight during cyclization is believed to have occurred. Incorporation of the aliphatic isopropylidene linkage lowered the thermo-oxidative stability of these materials by approximately 30°, relative to analogous fluorinated materials. Glass transition temperatures ranged from 267° to 313°C, increasing with higher terephthaloyl content. The ability to generate high molecular weight, fully cyclized polybenzoxazoles in the bAAP system demonstrated the viability of the synthetic method and allowed for extension to fluorinated systems.

1,1-Bis(3-amino-4-hydroxyphenyl)-1-phenyl-2,2,2-trifluoroethane (3FAP), a novel bis(*o*-aminophenol), was synthesized by nitrating the requisite bisphenol in acetic acid at low temperatures, followed by aqueous, catalytic reduction of the dinitro precursor. Excellent yields were obtained throughout the synthetic procedure and recrystallization of 3FAP from ethanol/chloroform afforded monomer grade material. Incorporation of 3FAP, along with other fluorinated and nonfluorinated monomers, into polybenzoxazoles using the previously mentioned "two-step"

polymerization/cyclization technique resulted in a series of fluorinated polymers.

The molecular structure of both the poly(hydroxy amide)s and polybenzoxazoles were verified by ^1H NMR and FT-IR spectroscopy. In addition, FT-IR spectroscopic evidence indicated complete cyclization of the oxazole ring systems. Glass transition temperatures ranged from 280°C to greater than 430°C . Curiously, polybenzoxazoles with analogous structure, except for the nature of the fluorinated bridging group, exhibited similar T_g 's with few exceptions. Dynamic thermo-oxidative stability proved to be quite good, with the onset of weight loss typically around $480\text{-}490^\circ\text{C}$ and 5% weight losses averaging $\sim 520^\circ\text{C}$. In general, the polybenzoxazoles containing a trifluoro-linkage (3F) displayed enhanced solubility relative to their 6F counterparts, mechanical properties were on par with similar thermoplastic polymers and some degree of crystallinity was observed in certain systems (6FAP-TC and 6FAP-IC).

Phenylethynyl terminated polybenzoxazoles of various molecular weights have been generated via the above mentioned polycondensation, cyclization process. Endgroup functionality was maintained throughout the cyclization process, as was molecular weight. Polymer formation, as well as functionalization and molecular weight control were monitored via spectroscopic, viscometric, thermal and mechanical analysis. Glass transition temperatures varied from $255\text{-}311^\circ\text{C}$ for the uncured systems

(increasing with molecular weight), while samples cured at 350°C and 475°C plateaued between 305°C and 315°C, respectively.

Mechanical properties were significantly enhanced with incorporation of crosslinks and a simultaneous increase in tensile moduli, strengths and percent elongation were noted with an increase in molecular weight for both cured and uncured systems. Chemical resistance in general was dramatically improved, apparently with little loss of ductility.

Chapter 6

Future Work

Results outlined in previous chapters demonstrated the difficulty in achieving high molecular weight polymer with bis(*o*-aminophenol)s containing electron-withdrawing connecting groups. Unfortunately, all these studies made use of bis(*o*-aminophenol)s possessing hydroxyl groups *para* to the linking groups. Synthesizing bis(*o*-aminophenol) monomers with amine groups *para* to the linking group and polymerizing them with the acid chlorides used herein would help to support or contradict the conclusions reached.

The ability to synthesize controlled molecular weight polybenzoxazoles demonstrates the feasibility of the "two-step" polymerization method and the idea of azeotropically distilling the

water generated during cyclization. Due to the similarities of this synthetic technique to the polyimide polymerization, it is proposed that bis(*o*-aminophenol)s can be incorporated into polyimides at low concentrations to generate polyimides with pendent hydroxyl groups. These pendent hydroxyl groups can be further reacted with molecules susceptible to electrical poling, therefore generating a material for nonlinear optical applications. Studies could be initiated to demonstrate the influence of molecular weight, hydroxyl concentration, chromophore identity, chain rigidity and spacer length on nonlinear optical properties.

References

1. D. Wilson, H. D. Stenzenberger and P. M. Hergenrother, "Polyimides", Chapman Hall, New York, 1990.
2. S. Maiti and B. K. Mandal, *Prog. Polym. Sci.*, **12**, 111 (1986).
3. A. Buckley and G. A. Serad in N. M. Bikales, ed., "Encyclopedia of Polymer Science and Technology", 2nd Ed. Vol. 11, Wiley-Interscience, New York, 1988. p. 572.
4. J. M. Margolis ed., "Advanced Thermoset Composites: Industrial and Commercial Applications," Van Nostrand Reinhold; New York, 1986.
5. M. E. Hunsaker, G. E. Price and S. J. Bai, *Polymer*, **33**, 2128 (1992).
6. P. E. Cassidy, T. M. Aminabhavi and J. M. Farley, *J. Macromol. Sci.: Rev. Macromol. Chem. Phys.*, **C29(2&3)**, 365 (1989).
7. Y. Maruyama, Y. Oishi, M. Kakimoto and Y. Imai, *Macromolecules*, **21**, 2305 (1988).
8. B. A. Reinhardt, *Polymer Comm.*, **31**, 453 (1990).
9. J. G. Hilborn, J. W. Labadie and J. L. Hedrick, *Macromolecules*, **23**, 2854 (1990).
10. J. L. Hedrick, J. G. Hilborn, T. D. Palmer, J. W. Labadie and W. Volksen, *J. Polym. Sci.: Pt. A: Polym Chem.*, **28**, 2255 (1990)
11. K. C. Brinker and I. M. Robinson, US Pat. 2,895,948 (1958).
12. T. Kubota and R. Nakanishi, *J. Polym. Sci.: Polym. Lett.*, **2**, 655 (1964).
13. C. S. Marvel, *Pure and Appl. Chem.*, **16**, 351 (1968).

14. A. H. Frazer, "High Temperature Resistant Polymers", John Wiley, New York, p151, 1968.
15. C. Arnold, Jr. *Macromol. Rev.*, **14**, 265 (1979).
16. P. E. Cassidy, "Thermally Stable Polymers: Synthesis and Properties", Marcel Dekker, Inc., New York, 1980
17. J. F. Wolfe and F. E. Arnold, *Macromolecules*, **14**, 909 (1981).
18. J. F. Wolfe in N. M. Bikales, ed., "Encyclopedia of Polymer Science and Engineering," 2nd ed., Vol 11, Wiley-Interscience, New York, 1986, p. 601.
19. D. C. Martin and E. L. Thomas, *Macromolecules*, **24**, 2450 (1991).
20. S. J. Bai and G. E. Price, *Polymer*, **33**, 2136 (1992).
21. W. W. Moyer, Jr., C. Cole and T. Anyos, *J. Polym. Sci.: Pt. A*, **3**, 2107 (1965).
22. T. Kubota, N. Yoda and R. Nakanishi, *Inter. Symp. Macromol. Chem.*, **9**, (1966).
23. B. M. Culbertson and R. E. Martin, US Pat. 3,389,122 (1965).
24. B. M. Culbertson and R. Murphy, *J. Polym. Sci.: Polym. Lett.*, **4**, 249 (1966).
25. R. M. Gitina, G. I. Braz, V. P. Bazov and A. Ya. Yakubovich, *Polym. Sci., U.S.S.R.*, **A8**, 1691 (1966).
26. G. I. Braz, I. Ye. Kardash, V. S. Yakubovich, B. V. Myasnikova, A. Ya. Ardashnikov, A. F. Oleinik, A. N. Pravednikov and A. Ya. Yakubovich, *Polym. Sci., U.S.S.R.*, **A8**, 295 (1966).
27. I. Ye. Kardash, A. Ya. Ardashnikov, V. S. Yakubovich, G. I. Braz, A. Ya. Yakubovich and A. N. Pravednikov, *Polym. Sci., U.S.S.R.*, **A9**, 2160 (1967).

28. A. Ya. Yakubovich, A. F. Oleinik, G. I. Braz, N. N. Voznesenskaya, V. S. Yakubovich, I. Ye. Kardash and A. Ya. Ardashnikov, *Polym. Sci., U.S.S.R.*, **A9**, 2013, 1967.
29. V. S. Yakubovich, N. N. Voznesenskaya, G. I. Braz, I. Ye. Kardash, A. Ya. Ardashnikov, A. N. Pravednikov and A. Ya. Yakubovich, *Polym. Sci., U.S.S.R.*, **A9**, 2227 (1967).
30. Ya. Yakubovich, N. N. Voznesenskaya, G. I. Braz and V. S. Yakubovich, USSR Pat. 225441 (1968) in ref. 31.
31. V. S. Yakubovich, A. A. Askadskii, G. F. Shalygin, Yu. M. Malinskii, A. I. Mzhel'skii, B. I. Braz, N. N. Voznesenskaya and A. Ya. Yakubovich, *Polym. Sci., U.S.S.R.*, **A12**, 739 (1970).
32. N. N. Voznesenskaya, G. F. Shalygin, G. I. Braz and A. Ya. Yakubovich, *Polym. Sci., U.S.S.R.*, **A12**, 1586 (1970).
33. N. N. Voznesenskaya, G. I. Braz and A. Ya. Yakubovich, *Polym. Sci., U.S.S.R.*, **A14**, 2041 (1972).
34. Toyo Rayon Co., Ltd., GB Pat. 1,059,474 (1967), Chem. Abst. 67:3322a.
35. R. Nakanishi and T. Kubota, JP Pat. 42,009,678 (1967), Chem. Abst. 68:40330t.
36. T. Kubota and R. Nakanishi, JP Pat. 43,002,475 (1968), Chem. Abst. 69:28099n.
37. N. V. Karyakin, I. B. Rabinovich, G. P. Kamelova, A. N. Mochalov, G. M. Tseitlin, V. N. Kulagin and V. V. Korshak, *Polym. Sci., U.S.S.R.*, **A17**, 1127 (1975).
38. V. V. Korshak, V. A. Khomutov, N. S. Zabel'nikov, V. G. Danilov, Yu. Ye. Doroshenko and G. M. Tseitlin, *Polym. Sci., U.S.S.R.*, **A16**, 3111 (1974).
39. H. W. Steinmann, Sparta and E. T. Pollard, US Pat. 3,563,950 (1969).

40. A. B. Berezina, I. A. Serenkova, G. M. Tseitlin, Yu. A. Shlyapnikov and V. V. Korshak, *Polym. Sci., U.S.S.R.*, **A18**, 902 (1976).
41. V. V. Korshak, Russian Authors' Cert. No. 360,353 (1970) in ref. 40.
42. V. P. Yevstaf'ev, V. S. Yakubovich, G. F. Shalygin, V. I. Selikhova, Yu. A. Zubov, G. I. Braz and A. Ya. Yakubovich, *Polym. Sci., U.S.S.R.*, **A14**, 2547 (1972).
43. H. H. Yang, "Aromatic High-Strength Fibers", Wiley Interscience, New York, 1988.
44. N. I. Bekasova, V. V. Korshak, M. A. Surikova and G. M. Tseitlin, *Polym. Sci., U.S.S.R.*, **A16**, 1994 (1974).
45. V. V. Korshak, N. I. Bekasova, M. A. Surikova, Yu. I. Tolchinskii and I. V. Zhuravleva, *Polym. Sci., U.S.S.R.* **A19**, 3198 (1977).
46. G. G. Bellmann, Groult, A. M. and J. H. Arendt, DE Pat. 2,330,452 (1974), Chem. Abst. 83:179909s.
47. B. Despax, N. Paillous, A. Lattes and A. Pallous, *J. Polym. Sci.: Polym. Chem. Ed.*, **18**, 593 (1980).
48. D. A. Bansleben and O. Vogl, *J. Macromol. Sci.; Chem.*, **A14**, 1171 (1980).
49. Y. Imai, M. Kakimoto and Y. Maruyama, GB Pat. 2,188,936 (1987).
50. W. H. Mueller and D. N. Khanna, US Pat. 4,845,183 (1989).
51. W. H. Mueller and K. N. Khanna, EP Pat. 317,942 (1989).
52. T. Yamaoka, N. Nakajima and K. Koseki, *J. Polym. Sci.: Pt. A: Polym. Chem.*, **28**, 2517 (1990).
53. W. D. Joseph, J. C. Abed, R. Mercier and J. E. McGrath, *Amer. Chem. Soc., Polym. Div.; Polym. Prepr.*, **34**(1), 397 (1993).

54. W. D. Joseph, R. Mercier, A. Prasad, H. Marand, A. Brennan and J. E. McGrath, *37th Inter. SAMPE Conf.*, **37**, 654 (1992).
55. D. N. Khanna and W. H. Mueller, *Proc. Photopolymers, Principles, Processes and Materials*, 429 (1988).
56. D. N. Khanna and W. H. Mueller, *3rd Inter. SAMPE Elect. Conf.*, **3**, 905 (1989).
57. D. N. Khanna and W. H. Mueller, *Polym. Eng. Sci.*, **29**, 954 (1989).
58. J. E. McGrath, H. Grubbs, M. E. Rogers, A. Gungor, W. D. Joseph, R. Mercier, D. Rodrigues, G. L. Wilkes and A. Brennan, *23rd Inter. SAMPE Techn. Conf.*, **23**, 119 (1991).
69. V. V. Korshak, G. M. Tseitlin and A. I. Pavlov, *Polym. Sci., U.S.S.R.*, **8**, 1763 (1966).
60. V. V. Korshak, G. M. Tseitlin and A. I. Pavlov, *Polym. Sci., U.S.S.R.*, **A11**, 9 (1969).
61. V. V. Korshak, G. M. Tseiltin, Z. T. Al-Haidar and A. I. Pavlov, *Polym. Sci., U.S.S.R.*, **A13**, 1095 (1971).
62. A. Ya. Yakubovich, A. N. Flerova and V. S. Yakubovich, *Polym. Sci., U.S.S.R.*, **A13**, 1118 (1971).
63. N. Yoda, M. Kurihara, S. Toyama, N. Dogoshi, Y. Hagiwara, M. Itoga, S. Fujita and H. Yamoto, DE Pat. 1,811,588 (1970), Chem. Abst. 73:77843s.
64. N. Dokashi, S. Tohyama, S. Fujita, M. Kurihara and N. Yoda, *J. Polym. Sci.: Pt. A-1*, **8**, 2197 (1970).
65. J. Preston, W. Dewinter and W. B. Black, *J. Polym. Sci.: Pt. A-1*, **10**, 1377 (1972).
66. G. Bellmann and A. Groult, FR Pat. 2,399,454 (1979), Chem. Abst. 91:124216y.

67. H. R. Lubowitz, C. H. Sheppard and R. R. Stephenson, Eur. Pat. 311,735 (1989), Chem. Abst. 111:195633z.
68. D. N. Khanna, *Amer. Chem. Soc., Polym Div.; Polym. Prep.*, **31**(1), 348 (1990).
69. R. A. Sundar and L. J. Mathias, *Amer. Chem. Soc., Polym. Prep.*, **34**(1),505 (1993).
70. K. Shinra, T. Shono, S. Matsumura, N. Asano, M. Eguchi and M. Izumi, JP Pat. 45,018,875 (1970), Chem. Abst. 73:77889m.
71. Y. Yahama, T. Shono, M. Izumi, S. Matsumura and N. Asano, JP Pat. 44,014,945 (1969), Chem. Abst. 73:99409g.
72. C. N. Zellner and H. W. Steinmann, US Pat. 3, 764,581 (1973), Chem. Abst. 80:83892t.
73. L. R. Belhlav and J. R. Costanza, U.S. Pat. 3,479,321 (1966).
74. V. V. Korshak, A. L. Rusanov, D. S. Tugushi, Z. Sh. Dzhaparidze, I. M. Gverdtsiteli, A. Ya. Chernikhov and G. M. Tseitlin, *Polym. Sci., U.S.S.R.*, **A21**, 2051 (1979).
75. G. V. Kazakova, A. Ya. Chernikhov, Ye. A. Selivaerstova, V. A. Isayeva, Yu. I. Kotov, O. V. Kachevskii, A. L. Rusanov and V. V. Korshak, *Polym. Sci., U.S.S.R.* **A27**, 2915, (1985).
76. Y. Miyadera and H. Yokokura, JP 48,017,393 (1973), Chem. Abst. 80:37797t.
77. V. V. Gur'yanova, I. O. Yelin, O. A. Tarakhtunov, A. I. Chechik, V. P. Pshentisyana, L. Ye. Kashtanova, M. S. Akutin and B. M. Kovarshaya, *Polym. Sci., U.S.S.R.* **A14**, 2202 (1972).
78. A. B. Blyumenfel's, A. I. Puzeyev, B. M. Kovarskaya and AM. S. Akutin, *Polym. Sci., U.S.S.R.*, **A15**, 2651 (1973).
79. T. Ueda, S. Yokoyama, M. Watanabe, K. Sanui and N. Ogata, *J. Polym. Sci: Pt. A: Polym. Chem.*, **28**, 3221 (1990).

80. S. Yodkoyama, T. Ueda, M. Watanabe, K. Sanui and N. Ogata, *New Polymeric Mater.*, **2**, 67 (1990).
81. T. Yamaoka, N. Nakajima and K. Koseki, *J. Polym. Sci.: Pt. A: Polym. Chem.*, **28**, 2517 (1990)..
82. E. I. du Pont de Nemours, Brit. 812,798 (1959), Chem. Abst. 53:14581a.
83. V. V. Korshak, G. M. Tseitlin and A. I. Pavlov, *Dokl. Akad. Nauk SSSR*, **163**, 116 (1965), Chem. Abst. 63:13427d.
84. H. Kokelenberg and C. S. Marvel, *J. Polym. Sci., Pt. A-1*, 3235 (1970).
85. L. W. Breed and J. C. Wiley, Jr., *J. Polym. Sci.: Polym. Chem. Ed.*, **14**, 83 (1976).
86. B. Gordon. III, R. J. Kumpf and P. C. Painter, *Amer. Chem. Soc., Polym. Prep.*, **26**(1), 146 (1985).
87. B. Gordon III, R. J. Kumpf and P. C. Painter, *J. Polym. Sci.: Polym. Chem. Ed.*, **26**, 1969 (1988).
88. S. Hideo, Jap. Pat. 7,201,223 (1972), Chem. Abst. 77: 6068q.
89. Y. Imai, I. Taoka, D. Uno and Y. Iwakura, *Makromol. Chemie.*, **83**, 167 (1965).
90. Y. Imai, K. Uno and Y. Iwakura, *Makromol. Chemie.*, **83**, 179 (1965).
91. S. Kon-ya and M. Yokoyama, *Kugakuin Daigaku Kenkyu Gofoto*, **33**, 66 (1973).
92. M. Sato and M. Yokoyama, *Amer. Chem. Soc., Polym. Prep.*, **21**(2), 169 (1980).
93. M. Sato and M. Yokoyama, *J. Polym. Sci.: Chem. Ed.* **19**, 591 (1981).

94. M. Sato and M. Yokoyama, *Eur. Polym. J.*, **16**, 671 (1980).
95. V. V. Korshak, Ye. S. Krongauz, A. L. Rusanov and A. P. Travnikova, *Polym. Sci., U.S.S.R.*, **A16**, 2311 (1974).
96. R. Wolf, M. Okada and C. S. Marvel, *J. Polym. Sci., Pt. A-1*, **6**, 1503 (1968).
97. F. E. Arnold and J. F. Wolfe, US Pat. 4,108,835 (1977).
98. J. Wolfe, B. Loo, F. Arnold, *Amer. Chem. Soc., Polym. Prep.*, **20**, 82 (1979).
99. D. B. Cotts and G. C. Berry, *Amer. Chem. Soc., Polym. Prep.*, **20**(2), 570 (1979).
100. R. C. Evers, F. E. Arnold and T. E. Helminiak, *Amer. Chem. Soc., Polym. Prep.* **21**(1), 88 (1980).
101. R. C. Evers, F. E. Arnold and T. E. Helminiak, *Macromolecules*, **14**, 925 (1981).
102. J. F. Wolfe and F. E. Arnold, *Macromolecules*, **14**, 909 (1981).
103. J. F. Wolfe, B. H. Loo and F. E. Arnold, *Macromolecules*, **14**, 915 (1981).
104. D. B. Cotts and G. C. Berry, *Macromolecules*, **14**, 930 (1981).
105. E. W. Choe and S. N. Kim, *Macromolecules*, **14**, 920 (1981).
106. J. F. Wolfe, P. D. Sybert and J. R. Sybert, US Pat. 4,533, 693 (1982).
107. A. W. Chow, S. P. Bitler, P. E. Penwell, D. J. Osborne and J. F. Wolfe, *Macromolecules*, **22**, 3514 (1989).
108. W. F. Hwang, D. R. Wiff, C. L. Benner and T. E. Helminiak, *J. Macromol. Sci., Phys.*, **B22**, 231 (1983).

109. M. E. Hunsaker, G. E. Price and S. J. Bai, *Polymer*, **33**, 2128 (1992).
110. S. J. Krause, T. B. Haddock, D. L. Vezie, P. G. Lenhert, W. R. Hwang, G. E. Price, T. E. Helminiak, J. B. O'Brien and W. W. Adams, *Polymer*, **29**, 1354 (1988).
111. R. C. Evers and G. J. Moore, *J. Polym. Sci.: Polym Chem.*, **24**, 1863 (1986).
112. R. C. Evers and M. Dotrong, *Mater. Res. Soc.*, **134**, 141 (1988).
113. K. S. Y. Lau and F. E. Arnold, *Org. Prep. and Proc. Int.*, **12**, 327 (1980).
114. T. T. Tsai and F. E. Arnold, *Amer. Chem. Soc., Polym. Prep.*, **27(2)**, 221 (1986).
115. T. T. Tsai and F. E. Arnold, *High Perf. Polym.* **1**, 179 (1989).
116. J. Burkett and F. E. Arnold, *Amer. Chem. Soc., Polym. Prep.*, **28(2)**, 278 (1987).
117. F. E. Arnold, *Mater. Res. Soc.*, **134**, 117 (1988).
118. T. T. Tsai and F. E. Arnold, *Amer. Chem. Soc., Polym. Prep.*, **29(2)**, 324 (1988).
119. T. T. Tsai and F. E. Arnold, US Patent 5,001,217 (1991).
120. J. P. Chen and W. A. Feld, *Amer. Chem. Soc., Polym. Prep.*, **31(2)**, 681 (1990).
121. T. D. Dang, T. G. Archibald, A. A. Malik, R. O. Bonsu, K. Baum, L. S. Tan and F. E. Arnold, *Amer. Chem. Soc., Polym. Prep.* **32(2)**, 199 (1991).
122. J. H. Promislow, E. T. Samulski and J. Preston, *Amer. Chem. Soc., Polym. Prep.*, **32(2)**, 211 (1991).

123. R. F. Hutzler, D. L. Meurer, K. Kinura and P. E. Cassidy, *High Perf. Polym.*, **4**, 161 (1992).
124. Y. Sakaguchi and Y. Kato, *J. Polym. Sci: Polym Chem.*, **31**, 1029 (1993).
125. M. Ueda, H. Sugita and M. Sato, *J. Polym. Sci.: Polym. Chem.*, **24**, 1019 (1986).
126. M. Dotrong, M. H. Dotrong, R. C. Evers and G. J. Moore, *Amer. Chem. Soc., Polym. Prep.*, **31**(2), 675 (1990).
127. L. R. Denny, R. C. Evers, B. A. Reinhardt and M. R. Unroe, *22nd Inter. SAMPE Techn. Conf.*, **22**, 186 (1990).
128. B. A. Reinhardt, US Pat. 4,931,532 (1990).
129. K. Yamamoto and H. Watanabe, *Chem. Lett.* 1225 (1982).
130. T. Imamoto, T. Matsumoto, H. Yokoyama, M. Yokoyama and K. Yamaguchi, *J. Org. Chem.* **49**, 1105 (1984).
131. V. I. Semenov, G. M. Tseitlin, P. M. Valetskii, S. V. Vinogradova, V. V. Korshak, L. B. Sokolov and D. Y. Zhinkin, USSR Pat. 663,699 (1979), Chem. Abst. 91:40349f.
132. Y. Imai, M. Kakimoto, Y. Oishi and Y. Maruyama, UK Pat. 2,191,496 (1987).
133. Y. Maruyama and H. Komoriya, GB Pat. 2,211,193 (1989).
134. Y. Tanaka, Y. Oishi, M. A. Kakimoto and Y. Imai, *J. Polym. Sci.: Pt. A: Polym. Chem.*, **29**, 1941 (1991).
135. K. Okamoto, K. Tanaka, M. Muraoka, H. Kita and Y. Maruyama, *J. Polym. Sci.: Polym. Phys.*, **30**, 1215 (1992).
136. H. R. Kricheldorf and J. Engelhardt, *Makromol. Chem.*, **190**, 2939 (1990).

137. J. W. Labadie, J. L. Hedrick, J. G. Hilborn and R. E. Woodling, *3rd Inter. SAMPE Electr. Conf.* 160 (1989).
138. J. G. Hilborn, J. W. Labadie and J. L. Hedrick, *Polym. Mater. Sci. Eng.*, **60**, 522 (1989).
139. G. Maier, R. Hecht and O. Nuyken, *Amer. Chem. Soc., Polym. Prep.*, **34**(1) 429 (1993).
140. G. Maier, R. Hecht, O. Nuyken, K. Burger and B. Helmreich, *Macromolecules*, **26**, 2583 (1993).
141. a) R. Viswanathan, Ph.D. Thesis, Virginia Polytechnic Institute and State University (1981). b) R. Viswanathan, B. C. Johnson and J. E. McGrath, *Polymer*, **25**, 1827 (1981).
142. J. G. Smith, Jr., J. W. Connell and P. M. Herenrother, *Amer. Chem. Soc., Polym. Prep.*, **32**(1), 646 (1991).
143. J. L. Hedrick, T. P. Russell, J. W. Labadie, J. G. Hilborn and T. D. Palmer, *Polymer*, **31**, 2384 (1990),
144. J. L. Hedrick, J. G. Hilborn and J. W. Labadie, *Amer. Chem. Soc., Polym. Prep.*, **30**(1), 265 (1989).
145. J. L. Hedrick, J. G. Hilborn, J. W. Labadie and W. Volksen, *Polymer Bulletin*, **22**, 47 (1989).
146. J. L. Hedrick, J. G. Hilborn, J. W. Labadie and W. Volksen, *Amer. Chem. Soc., Polym. Prep.*, **31**(1), 446 (1990).
147. F. W. Mercer and M. T. McKenzie, *Amer. Chem. Soc., Polym. Prep.*, **34**(1), 395 (1993),
148. R. A. Sundar and L. J. Mathias, *Amer. Chem. Soc., Polym. Prep.*, **33**(2), 142 (1992).
149. J. Preston, W. R. DeWinter and W. B. Black, *J. Polym. Sci.: Pt. A-1*, **7**, 283 (1969).

150. J. Preston, W. DeWinter, W. B. Black and W. L. Hofferbert, Jr., *J. Polym. Sci.: Pt. A-1*, **7**, 3027 (1969).
151. J. S. Rodia, US Pat. 3,247,165 (1965) and US Pat. 3,389,111 (1968).
152. a) J. Preston and J. W. Carson, Jr., *Amer. Chem. Soc., Polym. Prep.*, **33**(1), 390 (1992)., b) J. Preston and J. W. Carson Jr., *Polymer*, **34**, 830 (1993).
153. J. Preston, *Polym. Eng. Sci.*, **16**, 298 (1976).
154. A. E. Lozano, J. Preston, J. d. Abajo and J. G. de la Campa, *Amer. Chem. Soc., Polym. Prep.*, **34**(1), 517 (1993).
155. R. Hirohashi, Y. Hishiki and S. Ishikawa, *Makromol. Chem.*, 297 (1970).
156. a) H. R. Kricheldorf and S. A. Thomsen, *Makromol. Chem., Rapid Commun.* **14**, 395 (1993)., b) H. R. Kricheldorf and S. A. Thomsen, *J. Polym. Sci.: Polym. Chem.*, **29**, 1751 (1991).
157. U. Caruso, R. Centore, A. Roviello and A. Sirigu, *Macromolecules*, **25**, 2290 (1992).
158. C. P. Reghunadhan Nair, T. V. Sebastian, S. K. Nema and K. V. C. Rao, *J. Polym. Sci.: Polym. Chem.*, **24**, 1109 (1986).
159. H. C. Bach and W. B. Black, *J. Polym. Sci.: Pt. C*, **22**, 799 (1969).
160. H. C. Bach and H. E. Hinderer, *Amer. Chem. Soc., Polym Prep.* **11**(1), 334 (1970).
161. H. Bach, US Pat. 3,598,768 (1969), Chem. Abst 75:152358j.
162. J. Preston, W. F. DeWinter and W. L. Hofferbert, Jr., *J. Heterocyclic Chem.*, **5**, 269 (1968).
163. L. J. Mathias, *Amer. Chem. Soc.; Polym. Prep.*, **24**, 335 (1983).

164. L. J. Mathias, S. U. Ahmed and P. D. Livant in "New Monomers and Polymers", B. Culbertson and C. U. Pittman Jr., Eds.; Plenum Press: New York, 1984, p. 55-65.
165. L. J. Mathias and S. U. Ahmed, *Amer. Chem. Soc., Polym. Prep.*, **25**(2), 47 (1984).
166. L. J. Mathias and S. U. Ahmed, *Polym. Bull.*, **13**, 145 (1985).
167. L. J. Mathias, S. U. Ahmed and P. D. Livant, *Macromolecules*, **18**, 616 (1985).
168. L. J. Mathias and D. Livant, *J. Polym. Sci.: Polym. Chem.*, **25**, 2711 (1987).
169. S. U. Ahmed, P. D. Livant and L. J. Mathias, *Amer. Chem. Soc., Polym. Prep.*, **28**(1), 232 (1987).
170. J. Preston and W. L. Hofferbert, Jr., *J. Polym. Sci.: Polym Symp.* **65**, 13 (1978).
171. C. D. Burton and N. L. Madison, US Pat. 3,560,438 (1968).
172. R. Evers, *Amer. Chem. Soc., Polym. Prep.*, **15**(1), 685 (1974).
173. R. Evers, *J. Polym. Sci.: Polym Chem. Ed.*, **16**, 2817 (1978).
174. C. K. Schoff and J. K. Gillham, *Amer. Chem. Soc., Polym Prep.*, **15**(2), 451 (1974).
175. C. K. Schoff and J. K. Gillham, *Amer. Chem. Soc., Polym. Prep.*, **16**(1), 566 (1975).
176. C. K. Schoff and J. K. Gillham, *J. Appl. Polym. Sci.*, **19**, 2731 (1975).
177. J. K. Gillham and C. K. Schoff, *J. Appl. Polym. Sci.*, **20**, 1875 (1976).
178. R. C. Evers, *J. Polym. Sci.: Polym. Chem. Ed.*, **16**, 2833 (1978).

179. R. C. Evers, T. Abraham and J. L. Burkett, *J. Polym. Sci.: Polym. Chem. Ed.*, **19**, 427 (1981).
180. E. G. Jones and L. J. Goldfarb, *Thermochimica Acta*, **54**, 131 (1982).
181. R. M. Gitina, G. I. Braz, V. P. Bazov and A. Ya. Yakubovich, *Polym. Sci., U.S.S.R.*, **A8**, 1961 (1966).
182. A. Ya. Yakubovich, R. M. Gitina, Ye. L. Zaitseva, G. S. Markova and A. P. Simonov, *Polym. Sci., U.S.S.R.*, **A12**, 2854 (1970).
183. P. J. Lemstra, N. A. J. M. van Aerle and C. W. M. Basteaansen, *Polym. J.*, **19**, 85 (1987).
184. T. L. Cottrell, "The Strength of Chemical Bonds", 2nd ed., Butterworths, London, 1958.
185. P. M. Hergenrother, *SAMPE Q.*, **3**, 1 (1971).
186. P. J. Barham and A. Keller, *J. Mater. Sci.*, **20**, 2281 (1985).
187. H. H. Yang, "Aromatic High-Strength Fibers", John Wiley, 1988.
188. W. H. Carothers, *Trans. Faraday Soc.*, **32**, 39 (1936).
189. G. Odian, "Principles of Polymerization", 3rd Ed., John Wiley, NY (1991).
190. T. Sulzberg and R. J. Cotter, *J. Polym. Sci.; Pt. B. Polym Lett.*, **7**, 185 (1969).
191. Ng. Ph. Buu-Hoi, K. Lavit and Ng. D. Xuang, *J. Chem. Soc.*, 2612 (1953).
192. R. C. Weast, ed., "CRC Handbook of Chemistry and Physics", 67th ed., CRC Press, Boca Raton, FL, 1987.
193. K. S. Y. Lau, A. L. Landis, W. J. Kelleghan and C. D. Beard, *J. Polym. Sci.: Polym Chem. Ed.*, **20**, 2381 (1982).

194. W. D. Kray and R. W. Rosser, US Pat. 4,307,024 (1981).
195. P. W. Morgan and B. C. Herr, *J. Am. Chem. Soc.*, **74**, 4526 (1952).
196. H. Shizunobu, F. Isao, *Kobunshi Kagaku*, **25**, 11 (1968), Chem. Abst. 70:47979m.
197. T. Hattori and K. Akita, JP Pat. 4,268,332 (1992), Chem. Abst. 118:192524y.
198. N. A. Bumagin, A. B. Ponomarev, A. N. Ryabtsev and I. P. Belestskaya, *Izv. Akad. Nauk. SSSR, Ser. Khim.* **3**, 604 (1988), Chem. Abst. 109:230415n.
199. R. D. Stephens and C. E. Castro, *J. Org. Chem.*, **28**, 3313 (1963).
200. Ciba Ltd. FR Pat. 1,547,502 (1968), Chem. Abst. 72:P56714.
201. M. Konas, T. M. Moy, M. E. Rogers, A. R. Shultz, T. C. Ward and J. E. McGrath, *J. Polym. Sci.: Polym. Phys.*, submitted (1993).
202. J. C. Bailar et al., Quarterly Reports to WADC Contract No. AF33(616)-3209 (1958) reported in ref. 203.
203. T. Sulzberg and R. J. Cotter, *J. Polym. Sci.: Polym. Lett.*, **7**, 1968 (1969).
204. J. E. McGrath, H. Grubbs, M. E. Rogers, T. M. Moy, W. D. Joseph, R. Mercier, H. Marand, A. Prasad and A. Brennan, *Proc. 6th Japan-U.S. Conf. Composite Mater.*, June 22-24, 213 (1992).
205. M. E. Rogers, M. H. Brink, A. Brennan and J. E. McGrath, *Polymer*, **34**, 849, 1993.
206. W. B. Alston and R. F. Gratz in "Recent Advance in Polyimide Science and Technology", W. D. Weber and M. R. Gupta, ed., Society of Plastic Eng., New York, 1987, p. 1.

207. V. V. Korshak, S. V. Vinogradova and V. A. Pankratov, *Dokl. Akad. Nauk SSSR*, **181**, 1393 (1968).
208. W. D. Kray and R. W. Rosser, *J. Org. Chem*, **42**, 1186 (1977)
209. W. D. Kray and R. W. Rosser, US Pat. 4,307,024 (1981).
210. W. B. Alston and R. F. Gratz, US Pat. 4,758,380 (1988).
211. H. J. Grubbs, Ph. D. Thesis, Virginia Polytechnic Institute and State University (1993).
212. J. Troitzsch, "International Plastics Flammability Handbook", 2nd Ed. Hanser, Munich, 1990.
213. M. Sato and M. Yokoyama, *Eur. Polym. J.* **15**, 75 (1979).
214. H. Sivriev and G. Borissov, *Eur. Polym. J.* **13**, 25 (1977).
215. M. Sato and M. Yokoyama, *Eur. Polym. J.* **15**, 541 (1979).
216. P. W. Morgan and B. C. Herr, *J. Am. Chem. Soc.*, **74**, 4526 (1952).
217. W. Ude, S. Besecke, A. Riemann and G. Schroeder, DE 3,425, 282 (1986), Chem. Abst. 105:P79895p.
218. V. V. Korshak, S. V. Vinogradova, P. Y. Wu, *Polym. Sci., U.S.S.R.*, **A4**, 968 (1962).
219. M. Masaki and K. Fukui, *Chem. Lett.*, 151 (1977).
220. S. Hashimoto, I. Furukawa and T. Kondo, *J. Polym. Sci.: Polym. Chem. Ed.*, **12**, 2357 (1974).
221. Didier Villemin and Delphine Goussu, *Heterocycles*, **29**, 1255 (1989).
222. P. W. Morgan, "Condensation Polymers by Interfacial and Solution Methods", Interscience, Yew York, 1965.

223. F. Higashi and I. Takahashi, *J. Polym. Sci.: Polym. Chem. Ed.*, **23**, 1369 (1985).
224. Y. Imai, S. Abe and M. Ueda, *J. Polym. Sci.: Polym. Chem. Ed.*, **19**, 3285 (1981).
225. J. Preston, *J. Polym. Sci, A-1*, **8**, 3135 (1970).
226. J. Shorter, "Correlation Analysis in Organic Chemistry", Clarendon Press, Oxford, 1973.
227. O. Exner, "Correlation Analysis of Chemical Data", Plenum Press, New York, 1988.
228. Y. J. Kim, T. E. Glass, G. D. Lyle and J. E. McGrath, *Macromolecules*, **26**, 1344 (1993).
229. P. J. Flory, "Principle of Polymer Chemistry", Cornell University Press, Ithaca, 1953.
230. S. Ando, T. Matsuura and S. Sasaki, *J. Polym. Sci.: Pt. A, Polym. Chem.*, **30**, 2285 (1992).
231. M. I. Bessonov, M. M. Koton, V. V. Kudryavtsev and L. A. Laius, "Polyimides, Thermally Stable Polymers", Consultants Bureau, New York, 1987, Ch. 2.
232. V. V. Korshak, S. V. Vinogradova, P. M. Vasetskii and A. N. Baskakov, *Dokl. Akad. Nauk. SSSR*, **174**, 849 (1967) in ref. 228.
233. Kolesnikov et. al., *Polym. Sci., U.S.S.R.*, **A12**, 449 (1970).
234. E. Turska, L. Pietrzak and R. Jantas, *J. Appl. Polym. Sci.*, **23**, 2409 (1979).
235. V. V. Korshak, S. V. Vinogradova, V. A. Vasnev and A. I. Tarasov, *Polym. Sci., U.S.S.R.*, **A17**, 1388 (1975).
236. V. V. Korshak, E. Turska, A. V. Vassel'ev, M. Sinyarska-Kapustinsda, S. V. Vinogradova and V. A. Vasnev, *Polym. Sci., U.S.S.R.*, **A14**, 1417 (1972).

237. S. V. Vinogradova, V. A. Vasnev, V. V. Korshak and T. I. Mitaishvili, *Polym. Sci., U.S.S.R.*, **A12**, 1252 (1970).
238. Hubner et al., *Ann.*, **210**, 384 (1881)
239. Galatis, *J. Am. Chem. Soc.*, **70**, 1967 (1948).
240. Ladenburg, *Ber.*, **9**, 1524 (1876).
241. G. V. Kazakova, A. Ya. Chernikhov, Ye. A. Seliverstova, V. A. Isayeva, Yu. I. Kotov, O. V. Kachevskii, A. L. Rusanov and V. V. Korshak, *Polym. Sci., U.S.S.R.*, **A27**, 2915 (1985).
242. M. Gates and G. Tschudi, *J. Am. Chem. Soc.*, **78**, 1380 (1956).
243. J. R. McCarthy, J. L. Moore and R. J. Cregge, *Tet. Lett.*, **52**, 5183 (1978).
244. S. Alam, L. D. Kandpal and I. K. Varma, *J. of Macromolecular Science-Rev. Macromol. Chem Phys.*, **C33**(3), 291-320 (1993)
245. a) M. R. Unroe and B. A. Reinhardt, *J. Polym. Sci.: Pt. A: Polym. Chem.*, **28**, 2207 (1990)., b) M. Strukely, M. Paventi and A. S. Hay, *Macromolecules*, **26**, 1777 (1993)., c) R. L. Frenzel and C. S. Marvel, *J. of Polym. Sci.: Polym. Chem. Ed.* **17**, 1073 (1979)., d) R. G. Bryant, B. J. Jensen and P. M. Hergenrother, *Amer. Chem. Soc.; Polymer Preprints*, **33**(1), 910 (1992).
246. a) B. J. Jensen and P. M. Hergenrother, *Polymer*, **34**(3) 630 (1993)., A. L. Landis, N. Bilow, R. H. Boschan, R. E. Lawrence and T. J. Aponyi, *Amer. Chem. Soc.; Polymer Preprints*, **15**(2), 537 (1974)., c) F. W. Harris, A. Pamidimukkala, R. Gupta, S. Das, T. Wu and G. Mock, *J. Macromol. Sci.: Chem.* **A21**(8&9) 1117 (1984).
247. P. M. Hergenrother, *Macromolecules*, **14**(4) 898 (1981).
248. F. Martinez and J. Abajo *Makromol. Chem* **194**, 953 (1993).

Vitae

William Dale Joseph was born to Harold and Dabney Joseph on February 11, 1963 and raised in Glidden, Wisconsin. After graduating from Glidden Public School, he worked 3 years in the lumber industry before enrolling at the University of Wisconsin at Stevens Point. In the fall of 1985, he married Mary Ann Schoch. Four years later he received a Bachelor of Science degree in Chemistry and was accepted into the Ph.D. program at Colorado State under the guidance of Professor John K. Stille. Due to the unfortunate death of Professor Stille in August of 1989, he transferred to Virginia Polytechnic Institute and State University and joined the research group of Professor James E. McGrath. Upon completion of his Ph.D. requirements, William accepted a position with the 3M Company, located in St. Paul, Mn, as a Senior Research Scientist.

A handwritten signature in black ink, appearing to read "William Dale Joseph". The signature is written in a cursive style with a long horizontal line extending to the right.